DOCTORAATSPROEFSCHRIFT

2009 | Faculteit Wetenschappen

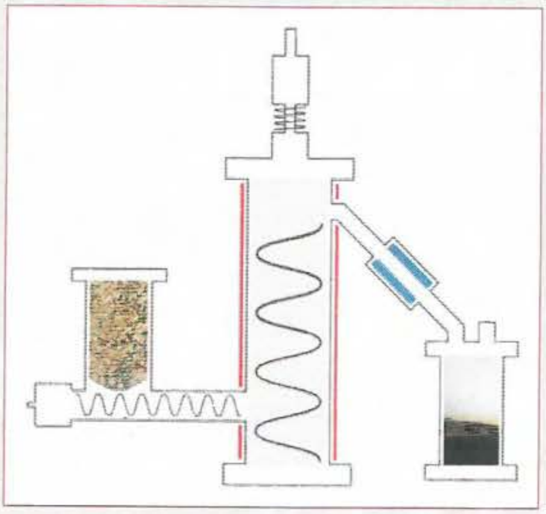

Flash pyrolysis of biomass and co-pyrolysis with biopolymers

Proefschrift voorgelegd tot het behalen van de graad van
Doctor in de Wetenschappen, scheikunde, te verdedigen door:

Tom CORNELISSEN

Promotor: Prof. dr. Jan Yperman
Copromotoren: Prof. dr. Robert Carleer
dr. Sonja Schreurs (XIOS)

universiteit hasselt
CENTRUM
VOOR MILIEUKUNDE

54
CORN
2008

uhasselt

DOCTORAATSPROEFSCHRIFT

2009 | Faculteit Wetenschappen

Flash pyrolysis of biomass and co-pyrolysis with biopolymers

Proefschrift voorgelegd tot het behalen van de graad van
Doctor in de Wetenschappen, scheikunde, te verdedigen door:

Tom CORNELISSEN

Promotor: Prof. dr. Jan Yperman
Copromotoren: Prof. dr. Robert Carleer
dr. Sonja Schreurs (XIOS)

universiteit hasselt
CENTRUM
VOOR MILIEUKUNDE

D/2008/2451/43

xios Hogeschool Limburg

NuTeC
Nucleair Technologisch Centrum

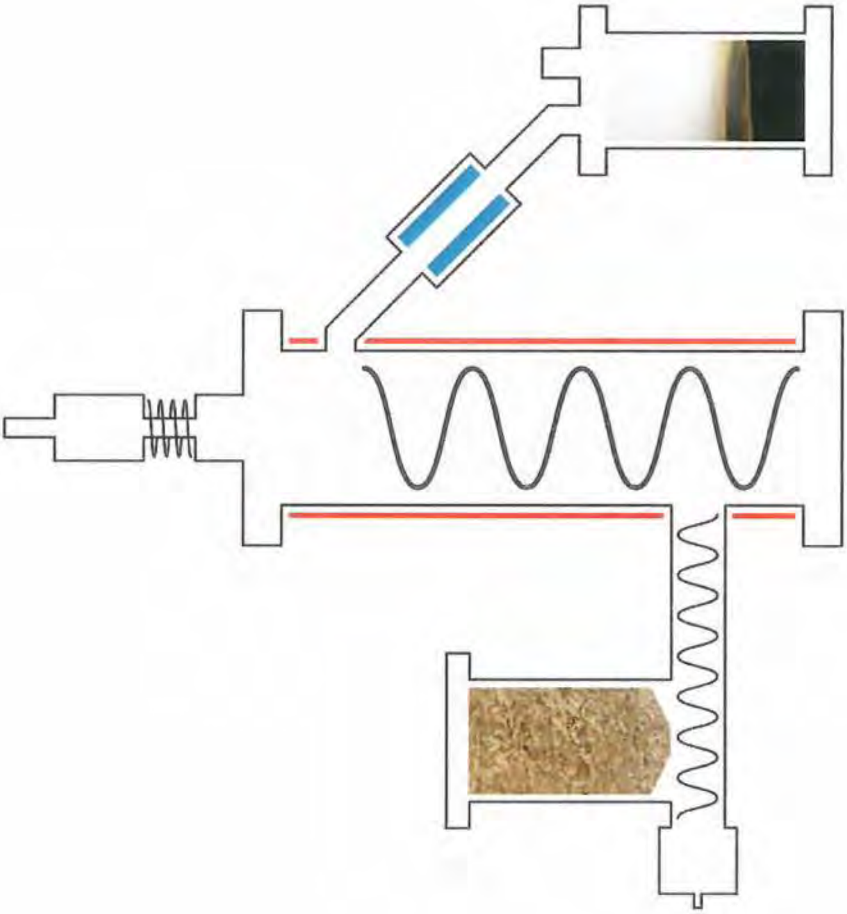

Dankwoord – een muzikaal intermezzo

Saturday, oh Saturday,
How cruel of you to go away
You turn us on and you don't even have
the decency to stay

Soulwax – Saturday, in Much against everyone's advice, 1998

If...

Als alles had verlopen, zoals het had moeten verlopen, dan verdedigde ik 4 jaar na datum mijn doctoraat. Op dat moment zou ik 28 jaar zijn geweest, waarvan de laatste 4 jaren, mijn doctoraatsjaren, 'mijn zaterdag' zouden betekend hebben. Een zaterdag is toch ook één zevende van een week...
Ok, ik heb er 5 jaar en een beetje van gemaakt, maar laat dit de zondagsdienst zijn. Kortom, ondanks de vele mislukkingen, vertragingen, ... heb ik waarlijk genoten van mijn doctoraatsjaren en hiervoor ben ik velen dankbaar. Vandaar dit deel, en geloof mij, ik ga moeite moeten doen om dit niet langer te maken dan mijn feitelijk doctoraatsproefschrift!

Het begint natuurlijk bij mijn promotoren, Sonja, Jan en Robert, of Jan, Robert en Sonja, of ook Robert, Sonja en Jan. Allen betekenden jullie evenveel voor mij en mijn onderzoek, ieder op zijn/haar manier. Ieders bijdrage was/is van uitermate belang, en vandaar dat ik ook mijn dankbaarheid naar jullie en jullie complementariteit wil betuigen. Ondanks dat mijn onderzoek misschien moeilijk van grond geraakte, hebben jullie steeds vertrouwen getoond en mij desbetreffend begeleid.

Een ander persoon die ik eigenlijk meermaals zou moeten bedanken is mijne/onze Jos, de handyman van dienst, maar nu op pensioen... Een verlies voor de UH, maar gelukkig genoeg heb ik met hem kunnen samenwerken. Het was hij die de plannen van onze eigen reactor in werkelijkheid bracht, en jouw bijdrage in het optimaliseren van het proces is naar mijn mening van onschatbare waarde. Samen hebben we vaak gesleuteld, maar ook gevloekt op de nu goed presterende reactor. Jos, je opvolger Tim zal de glasblazerij zeker in ere houden, daar heb ik alvast alle vertrouwen in. En Johan is bereid om ons verder te helpen met de reactor, dat is reeds bewezen tijdens de succesvolle verdubbeling. Ook aan hen: dank.

Zo ook heeft prof. dr. Jan Meuldijk (TU/e en gastprofessor UH) een belangrijk aandeel in het reactorgebeuren. Ik zou hem een "suikeroom" van de reactor kunnen noemen. Je hebt ons in de constructiefase zeer gewillig begeleid om op basis van enkele bestaande pyrolyseprocessen een eigen reactor te vervaardigen die in huis geconstrueerd kon worden op een relatief korte tijd. Eveneens toonde je constant interesse in het verdere verloop van de reactor en mijn doctoraat en stond je steeds klaar voor wijze raad en leuke gesprekken.

Ik kan mezelf ook zéér gelukkig prijzen met de samenwerking met prof. dr. Geert Molenberghs (UH en KUL). Nog steeds ben ik onder de indruk van hoe snel ik jou input, antwoorden, opmerkingen,... ontving. Het was een samenwerking uit de duizend! Statistiek leek soms zo tastbaar. Zelfs tijdens uw vakantieperiode kon ik op jou rekenen. Super! Ik moet er ook bij vertellen dat Amerika harder op me roept dan ooit tevoren, en als ik er ooit geraak laat ik zeker mijn ervaringen weten. Wie weet hoe snel het kan gaan...

Een andere samenwerking waaruit ik veel geleerd heb, is ontstaan dankzij prof. dr. Gerrit Janssens (UH). Jij bracht mij in contact met prof. dr. Hugo Pastijn (KMS), en bleef de evolutie van dichtbij volgen. Prof. dr. Hugo Pastijn zelf verdient allerminst ook een blijk van dank. Onze collaboratie, en vooral je privé-lessen zal ik nooit vergeten... Stond ik even terug met mijn voeten op de grond, maar het was net de eerlijkheid die ik apprecieerde. Eveneens, zou ik graag Frédéric Hallot willen bedanken voor het aanleveren van 'MCDM tool'.

Een ander belangrijk persoon tijdens mijn doctoraat is Rien van Bio-oil Exploitation. Bedankt voor de leuke momenten, vooral de keren dat ik steeds één van je groter wordende reactoren kon komen bewonderen. Succes met de verdere uitbouw! And off course companion Uros, who shared his technical knowledge and showed great interest in my PhD. Good luck with the recently enlarged family.

Ook vanuit de grondvesten van het CMK ('Centrum voor Milieukunde' – UH) is er een soort van samenwerking ontstaan die een meerwaarde zal bieden aan het verrichte onderzoek. Tom Kuppens is namelijk onder begeleiding van prof. dr. Theo Thewys de bekomen resultaten economisch aan het bekijken. Nog veel succes, en hopelijk komen we tot een interessant artikel... Thx.

Tevens dank aan Biomer, Luts Plastic Production, Rodenburg Biopolymers, Biopearls, and Jemaco voor het aanleveren van de biopolymeren.

Finally, my Polish experience... an awesome time, honestly. For that, I first need to thank prof. dr. Grazyna and her partner/colleague dr. Stanislav Gryglewizc. You both helped me in many ways, scientifically and socially. Together with your PhD-students Paulina, Ola, Piotr and Wojtek, and the other members of your team, you made me feel welcome in Wroclaw. According to me, Poland can be proud of its hospitality! Ola, for instance, you and Alec took me and Elke across Poland as if it was normal to do so. But believe me, I am not used to such kindness... I also had the joy to work with both Ola and Paulina in Poland and in Belgium. A wonderful experience. For Paulina I want to add that I will never forget her smile and that I hope she can continue recovering and enjoying her married life. Your husband, Marcin, is a very special man and was so kind to keep me informed during the difficult moments in your lives. May all the luck be with the two of you, because you really deserve it!

Als ik zo terug kijk naar de hulp die ik ontvangen heb van anderen die initieel niets met mijn onderzoek te maken hadden, voel ik mij waarlijk gezegend! Ik zou het zo opnieuw doen, ondanks het soms veel moeite vereiste om bepaalde dingen te begrijpen. Vandaar dat ik de andere leden van het pyrotech-team aanraad om eens verder te kijken dan enkel 'ons labo'. Er is zo veel meer, en er zijn zo veel mensen die open staan voor vakoverschrijdende problemen. Het zijn opportuniteiten die met beide handen gegrepen moeten worden. En ik beloof jullie dat het lonend zal werken. Jullie verdienen trouwens niet alleen "wijze raad" maar ook dank voor de leuke sfeer onderling: Mark a.k.a. 'Spark' omwille van uw droge humor, maar vooral enthousiasme en vriendschappelijke collegialiteit; Niels, of ook 'Mr. Cool', die iedereen weet mee te sleuren in sportievere aangelegenheden, en Koen, 'Mr. Nice guy', voor uw inzet en vooral interesse naar andermans bezigheden. Hopelijk krijg je de andere twee helden nog regelmatig mee op pad tijdens een donderdagse avond. Kenny, die finaal gezien toch niet zonder TOES verder kan. Wees welgekomen! And off course Eva... I really hope that there will be one day that you realise that Belgium is a nice country to live in. By the way, your recent poster is a good start. And finally, Palina, the only PhD-student of TOES that isn't a member of the Pyrotech-team, which makes her even more special. Even though I know that you are performing way above average, good luck with the finalisation of your PhD. And, lets hope that all the problems you encountered made you even stronger. I admire your drive.

Maar TOES is meer dan enkel wat doctoraatstudenten, veel meer zelfs en ik weet eigenlijk niet goed waar te beginnen... Greet, voor mij is het eigenlijk 'Greetje', ik ben trots dat ik één van de weinigen ben die dat mag zeggen tegen jou ☺, maar willen of niet, het verkleinwoordje blijft staan voor mijn liefkozing. "kck kck". Martine, wie gaat er nou nog voor mij zorgen, als jij er niet meer bent Martine (herken *Louise - Clouseau*)? Elsy, man wat heb ik u geplaagd... Maar je kent het gezegde hé "meisjes plagen,..." Jenny, 'Mama Garzelli' omdat jij het moederfiguur bij uitstek bent, alhoewel het soms leek dat jij die bijnaam liever niet had. Je bent wel steeds te vinden om uw aanstekelijke lach te delen en te transfereren naar ons allen, merci, maar nu zit ik wel met een geweldig vrouwelijke lach. Lindake, 'mijn pindake' (waarvoor stond dat weer in het Pools???), ik hoop dat ik nog vele jaren uw speculaasjes mag komen afhalen want die zijn oh zo lekker. Succes nog met het dansen en de andere duizenden activiteiten. Nu lijkt het alsof TOES alleen maar goddelijke dames bevat, maar er is ook heel wat mannelijk geweld beschikbaar. Yvo, de 'snelle Eddy' van TOES, nooit verlegen om een grap of ben jij eigenlijk wel ooit serieus? Voor algemene labo-vragen kon ik steeds bij jou (en trouwens iedereen) terecht, en soms kreeg ik dan ook nog eens een fatsoenlijk antwoord. Er is wel nog één ding, wanneer gaan wij eigenlijk tegen elkaar lopen? De vragende partij wacht af! Guy, je zou denken stil, maar ik denk eerder aan (ondeugende) humor. En 'GC/MS koning' Jan, waar ik nog zo veel van te leren heb... Petje af! Maar ik zou u nog willen spreken ivm een afbetalingsplan, want ik heb het verstoplokaaltje iets te veel gebruikt. Je stuurt de rekening maar, dan zet ik er wel een kostenplaats op. Allen dien ik te bedanken voor hun hulp met allerhande analytische technieken, maar wat voor mij vooral telde is de gezellige TOES-sfeer! Hopelijk kom ik ergens terecht waar men aan jullie kan tippen (hoop doet zege).

Spijtig genoeg is TOES ook al geconfronteerd met enkele verliezen. Eéntje dat nooit verwerkt zal worden is het begrip 'Olga'. De vrolijke meid die mij steeds onder handen wist te nemen o.a. met haar oh zo lange nagels. Wanneer gaan wij nog zo eens op stap als in Krakau... Olga, besef goed dat heel TOES u mist. En last but not least Caroline, of eerder Calorien, die maar al te graag werd uitgedaagd om 10000 calorieën te verliezen. Succes met je carrière bij de noorderburen.

Maar ook buiten TOES zijn er heel wat mensen van de UH die ik uitermate dankbaar ben. Zoals Christel, die veel meer deed dan de bestellingen. Ik hoop dat ik niet al je snoepjes verorbert heb, maar als ze na mijn vertrek niet geledigd worden, bezorg je mij er maar een paar als Kerstcadeau. Naar 't schijnt ken jij één of twee van zijn rendieren... En Magda voor de broodnodige foto-upgrading. Kathleen voor de leuke en vooral lachwekkende gesprekjes in de gang. Peter bedankt voor uw hulp over eigenlijk een breed gamma van mijn onderzoek, gaande van NMR tot zelfs statistische

interpretaties. Nog veel succes trouwens met uwe kameraad Raoul, die ik graag nog eens wil tussen pakken. Wat is de volgende uitdaging? Raoul, ook nog eens bedankt om mijn eerste bedrijfje levende te houden. DSS is always at your service! En Koen V., waarbij ik mij volledig kan laten gaan. Chirohumor is blijkbaar niet aan iedereen gegund, maar al doende leert men. Er is dus nog hoop.
Eveneens zijn er heel wat andere chemisten die toch even vermeld dienen te worden. Veerle, mijn Salsa moves konden u niet imponeren, maar ik heb er toch alleszins van genoten. En als ik Koen zie, verwijs ik hem zeker door... Jan, Wouter, Bert, Arne, Wibren, en Sylvain voor de leuke momenten voetbal, muziek, ... Jullie maakten de sfeer tot bij ons. Tja, Fré, eigenlijk had jij ook in vorig lijstje moeten staan, maar ik wacht nog steeds op een avondje "volkoren". Iris, veel geluk met je dikke buik. Hopelijk lijkt hij/zij op jou. Jimmy, proficiat met je job, maar vergeet niet om je doctoraat af te werken en Eva volwaardig te soigneren. Iemand anders die ik ook nog eens aan zijn doctoraat moet helpen denken is Vespa-lover Jorge. Volgende zomer gaan we eens een fatsoenlijke toer maken! Dan monteren we een side-span op ieders Vespa om onze gedeelde oogappeltjes mee te vervoeren. Waaronder Ineke die maar nooit naar thuis komt om van mijn spaghetti te proeven, Marjoleine die dezelfde weg als mij heeft moeten bevaren en via wie ik in contact ben gekomen met PLA, Nadia die haar vrolijkheid steeds met mij weet te delen, en Ilse die eindelijk geleerd heeft om kranen dicht te draaien. Maar ook de andere organici, anorganici en theoristen. Filipo, please, when will you give me some style advice so that I can leave my rags and run. Eveneens de ex-onderzoekers waarmee ik de leuke jaren aan het LUC heb mogen beleven zoals Lien, Colladetti, Steven, Ineke, Sofie, Anja, en natuurlijk mijn 'over 't spoor' buurvrouw Liesbetje, maar ook Kristof, John, Annick, Dirk en Dirk.
Ten laatste wil ik de dames (en de zeldzame heren) van biologie en het secretariaat met een knipoogje bedanken voor de leuke momenten. Administratief was ik een nachtmerrie, maar het moet ook niet allemaal te gemakkelijk gaan hé... En enkele bioloogjes moet ik misschien meer dan enkel en alleen bedanken. Misschien is er op sommige plaatsen nog wel een verontschuldiging of heel iets anders op zijn plaats, bijvoorbeeld omwille van wilde blind-dates, onopzettelijke beledigingen van wederhelften, nachtelijke uitjes, ... Speciale dank aan Jana en Nele (benoemd tot de 2 liefste meisjes van de Biologie) en Karen S. voor de steun tijdens de afwerkingfase (maar ook voor de snoepjes).

Er zijn ook enkele mensen van de Xios die ik nog zou willen vermelden. Dr. Micheline Breugelmans voor het begeleiden van een speciaal geval. Ondanks de persoonlijke teleurstelling heb ik er toch veel uit geleerd. Pascal, Wouter en Niki voor de momenten dat ik binnen viel op NuTeC en af en toe kwam knoeien met de calorimeter. Maar ook ex-werkneemster Ilse voor een geweldige Reims-reis en al wat daaruit volgde! En zelfs enkele oud-studenten, waaronder ing. en ir. in spe Maarten Jans, die mij, dankzij zijn enorme inzet, heel wat resultaten voor dit proefschrift bezorgde. Ik hoop dat je ooit de weg naar de UH en liefst TOES terug vindt.

Niet alleen mag ik tevreden terug kijken naar mijn werkgerelateerde achtergrond. Sinds mijn allerjongste jaren ben ik bedeeld met mensen die ik ten zeerste apprecieer en die ik hoop mijn hele leven mee te dragen in mijn hart en dus niet alleen in dit dankwoord... De bende van Runkst bij wie ik ben opgegroeid. Kameraden (m/v) als Maati, Kelly, Juveins, Achmed, Willems, ... (ik ga ze niet allemaal op noemen want dan vergeet ik er sowieso) wens ik toe aan iedereen, amusement gegarandeerd. Chiro Runkst is no more, maar de gesmeden vriendschappen zijn solide! Ook hier waag ik mij niet aan een volwaardige lijst, maar sommigen springen toch uit het oog en verdienen een plaatsje in deze toch wel lange lijst. Zo is er mijn "moatje" Jos, Dennis, Danny, Dirk, Claes, en vele vele anderen. Gregor en Sven horen zowat overal en nergens, dus mix ik er jullie helemaal doorheen. Mijn voetbalmakkers, die al een ettelijke tijd er voor zorgen dat ik mezelf regelmatig kan ontladen: Jouri, Erik, Michel J., Bjorn, Michel C., Jens, Fre en Alex. SB Demolder aan de top, alhoewel FC Cambrinus, FC Tunes en de Runkster Rangers ook enkele pluimen verdienen. Jasper en Yves mag ik natuurlijk ook niet vergeten die samen met SB Demolder fetjam_B levende proberen te houden. Ten laatste zijn er enkele die overblijven na de jaren aan het Atheneum, waarvan er twee een uitermate belangrijke bijdrage geleverd hebben. Timothy, die ik oneindig vaak 'dank je wel' zal moeten zeggen voor zijn inspanningen om mijn Engels een beetje op te smukken voor publicatie. En Dr. Geoffrey, die op een artistieke manier weet om te gaan met technische dingen. Ik vind de tekening op de cover echt mooi! (Om maar te zwijgen over de dustjacket.) Hopelijk vind jij hem zelf ook nog steeds goed. En hier horen natuurlijk twee schatten van vrouwen bij, sorry... drie, Hanne, Hanne en Sien.

Allen noem ik 'mijn vrienden', en met ieder van hen heb ik superweekenden meegemaakt en vandaar dat ik weet wat een "zaterdag" betekent in een hele week...

Because we are your friends
You'll never be alone again

Justice – We are your friends, 2006

En zo neig ik langzaam naar het einde van mijn dankwoord, maar toch moeten er hier nog enkele de revue passeren. Zoals bijvoorbeeld mijn familie, waaronder Bompa, Rudi en Carine, Hugo en Marie-Jeanne, Vivianne en Ludo, Eddy, Dianne en Fonny. Maar ook mijn neven en nichten: Greet, Joost, Dries, Sven (welkom op de UH), Wim, Kurt, David en Sigrid. Sommigen van hen dien ik toch even terug aan te halen. Bompa, die mij steeds leuke anekdotes, die af en toe zelfs leerrijk waren voor mijn doctoraat, weet te vertellen op de heen- en terugweg van Antwerpen. Maar vooral Rudi en Carine, die ontzettend veel voor mij hebben betekend en altijd zullen betekenen! Dank je wel voor alles!

Be careful whose advice you buy, but,
Be patient with those who supply it

Baz Luhrman – Everybody's free (to wear sunscreen), 1999
Sunscreen Speech by Mary Schmich in Chicago Tribune, 1997

Ook dank aan mijn zogezegde schoonfamilie die in het allerbegin dacht dat ik aan het opereren was als chirurg. Hopelijk hebben jullie het al verwerkt dat ik geen chirurg ben... Het leven is vol verrassingen, net zoals het moment dat jullie mij in de bloemetjes zetten bij het publiceren van mijn eerste artikel. Ik ga me niet uitspreken over jullie zangtalent, maar toch klasse.

't is moeilijk bescheiden te blijven,
wanneer je zo goed bent als ...

Een parodie op Peter Blanker – 't Is moeilijk bescheiden te blijven, 1981
door Croughs-Dardenne, 21 juli 2007

Zoals elk muzikaal gebeuren draait alles om melodieën, ... om meestal te eindigen met een grandioze climax. En voor mij draait die climax om 4 personen die uitermate veel voor mij betekenen! Allereerst zijn er mijn ouders. Die mij mooie, maar soms ook moeilijke tijden hebben bezorgd. Moeder, alhoewel je liever 'mama' hoort, jij verdient waarlijk een standbeeld! En ondanks het niet altijd gemakkelijk was, hebben Anja en ik onze studies en studies na studies, ... mogen afwerken en heb jij er steeds voor gezorgd dat wij er in september vol goede moed in konden vliegen. Heel wat liedjes zijn over moeders geschreven en ik weet waarom! Maar dit doet mij het meest...

I finally understand
For a woman it ain't easy trying to raise a man
You always was committed
A single mother, tell me how you did it
There's no way I can pay you back
But the plan is to show you that I understand
You are appreciated

2Pac – Dear mama, in Me against the world, 1995

Vervolgens mijn vader a.k.a. 'het paard van Zorro', van wie ik heel wat levenslessen meedraag... Maar er is één dat mij het meest geholpen heeft tijdens mijn doctoraat: bloemen aan de meet! Wat mij volharding, doorzettingsvermogen en vertrouwen gaf als dingen niet naar behoren verliepen. Meermaals werd ik tijdens mijn doctoraat geconfronteerd met tegenslag, maar bleef toch alles optimistisch zien. Hopelijk heb jij, net als ik, veel aan uw leuze...

Want papa, ik lijk steeds meer op jou

Stef Bos – Papa, 1991

En dan mijn zus, Anja, veel te ver verwijderd om continu bij te kunnen dragen aan mijn doctoraat, maar toch meer dan betekenisvol. Misschien vreemd (behalve als je Anja kent) dat een jongere broer zoveel belang hecht aan zijn zus, maar ik ben blij dat wij goed overeenkomen! Naar 't schijnt mag ik u verwelkomen op mijn verdediging, wat meteen van u 'eregast' maakt.
En dan is er iemand die al enkele jaren staat te wachten op dit moment (niet dit doctoraat, maar wel de vermelding erin...), mijn vriendin Elke die allerhande bijnamen draagt gaande van 'keukendeur' tot 'My Needy Girl' (*Chromeo, 2004*). En neen, Elke, je staat er niet omdat ik dit moet van jou, maar wel omdat jij een belangrijke rol hebt gespeeld en zult spelen in de dingen die ik doe en niet doe. Jij hield me soms bij de les (wat trouwens ook de taak is van een leerkracht) en toonde op uw manier interesse voor wat ik deed op die universiteit. Eveneens heb jij een nieuw begrip in mijn leven gebracht: pyliwyse, whatever that may be, maar naar 't schijnt is het heel verwant met pyrolyse, niet?

Nu word ik opnieuw geconfronteerd met iets wat ik al een hele tijd besef: ik moet dankbaar zijn aan velen! En vandaar deze welgemeende gezamenlijke

DANK U WEL!!!!

Tom

En om te eindigen waarmee ik begonnen ben: Soulwax! Net als hen ben ik gelukkig om te constateren dat:

Part of the weekend never dies

Table of content

List of abbreviations

A	ash
AHP	analytic hierarchy process
AISI	American iron and steel institute
BBOT	bis(5-tert-butyl-benzoxazol-2-yl)thiophene
BHT	butylated hydroxy toluene
C	carbon
°C	degrees Celsius
ca.	circa
CAS	chemical abstracts service
CFB	circulating fluidised bed
cfr.	compare with, confront with ("conferatur")
CHP	combined heat and power (cogeneration)
C.R.	consistency ratio
den. d.f.	denominator degrees of freedom
DSC	differential scanning calorimetry
DTG	differential thermogravimetric analysis
d_f	film thickness
e.g.	for example ("exempli gratia")
ESP	electrostatic precipitator
et al.	and others ("et alii")
eV	electron volt
FT-IR	Fourier transform infrared
g	gram
GAIA	graphical analysis for interactive assistance
GC	gas chromatography
GPC	gel permeation chromatography
H	hydrogen
H.H.V.	higher heating value
HPLC	high performance liquid chromatography
i.e.	that is ("id est")
J	Joule
K	Kelvin (=x°C + 273)
kPa	kilopascal
l	liter
LCA	life-cycle assessment
m	meter
max	maximum
MCDA	multi-criteria decision aid
MCDM	multi-criteria decision making
min	minutes
min	minimum
MS	mass spectrometry
m/z	mass-to-charge ratio
N	nitrogen
NIST	national institute of standards and technology

num. d.f.	numerator degrees of freedom	
O	oxygen	
p	preference threshold	
$P_i(a,b)$	preference degree	
PCA	principal component analysis	
PE	polyethylene	
	HDPE	high density polyethylene
	LDPE	low density polyethylene
PET	polyethylene terephthalate	
PHA	polyhydroxyalkanoate	
PHB	polyhydroxybutyrate	
PLA	polylactic acid	
PP	polypropylene	
	aPP	atactic-polypropylene
	iPP	isotactic-polypropylene
PROMETHEE	preference ranking organisation method for enrichment evaluations	
PS	polystyrene	
psi	pound per square inch	
PTFE	polytetrafluoroethylene	
PVC	polyvinylchloride	
PVdC	polyvinylidene chloride	
Py	pyrolysis	
q	indifference threshold	
REML	restricted maximum likelihood estimate	
rpm	rotations per minute	
s	seconds	
s	Gaussian threshold	
S	sulphur	
SAS	statistical analysis software	
T	temperature	
	T_{max}	maximum degradation temperature
	PT	pyrolysis temperature
	RT	room temperature
TG	thermogravimetry	
TGA	thermogravimetric analysis	
THF	tetrahydrofuran	
TIC	total ion chromatogram	
W	Watt	
w_i	weight	
w/w	weight-to-weight ratio	
3D	three-dimensional	
Δ	a GAIA quality control measure	
Φ	net flow, also called Phi score	
Φ^+	positive flow	
Φ^-	negative flow	
#	the amount of	
$\pi(a,b)$	overall (multi-criteria) preference index	
%	percentage	
	m%	mass percentage

Research objectives and outline

The Kyoto Protocol, which is closely related to the climate change threat, together with the depletion of fossil fuels and materials in general urgently force society to become "renewable". Extensive research and projects dedicated to renewable energy sources such as water, wind, solar and biomass are therefore being carried out worldwide. A final solution satisfying the global demand for energy and raw materials has yet to emerge, however. A diversified portfolio of renewables offers increased potential nonetheless. One such technology able to satisfy a part of the demand for renewable energy and raw materials is the flash pyrolysis of biomass. Flash pyrolysis is defined as heating a material, biomass/waste in most cases, in the absence of oxygen, rather oxygen deficient, in order to produce a liquid, called bio-oil. Besides bio-oil, char (solid residue) and gases are produced as well. The most important features of flash pyrolysis are intermediate high temperatures, high heating rates and rapid cooling of the pyrolytic volatiles. Many commercial reactor configurations, especially designed for flash pyrolysis are available. For this research, the production of valuable bio-oil is put forward. Therefore, constructing a reactor that satisfies all the requirements of flash pyrolysis is defined as the preliminary goal.

Flash pyrolysis breaks biomass, which mainly consists of three basic constituents (cellulose, hemicelluloses and lignin) containing high amounts of oxygen, into smaller molecules with water as an unavoidable reaction product. Generally, water is defined as detrimental for the applicability of bio-oil. The maximum water content of bio-oil is determined to be around 28%, while often higher water contents are reported. The bio-oil, stemming from willow, obtained in this research also shows a higher water content. Therefore, it is intended in this research to reduce the water content or the amount of pyrolytic water by countering its production or by consuming it during pyrolysis. The flash co-pyrolysis of biomass and biopolymers is proposed as an attractive solution. During this process, the biopolymer's ester bonds are supposed to react with the available water resulting in the production of acids and alcohols. For this research, willow has been chosen as the reference biomass material, while polylactic acid (PLA), corn starch, polyhydroxybutyrate (PHB), Biopearls, Eastar, Solanyl and potato starch are selected as the biopolymers under investigation.

In Chapter 1, a general overview of flash pyrolysis is provided. The construction of the semi-continuous home-built pyrolysis reactor is discussed in Chapter 2. In §2.1. the requirements for flash pyrolysis and thus for the dedicated reactor configurations with the goal of producing bio-oil is summarised. Some commercially available reactor types are discussed in §2.2., with a description of the horizontal tubular pyrolysis reactors of the research group in §2.3. In order to handle larger biomass batches and to meet the requirements of flash pyrolysis, a semi-continuous pyrolysis reactor that is closely related to commercially available pyrolysis reactors has been developed and constructed (§2.4.). Chapter 3 describes the experimental approach (§3.1.) of the entire research together with the materials under investigation (§3.2.) and the methods applied (§3.3.).

In Chapter 4, the seven biopolymers are evaluated as potential pyrolysis "enhancers". The evaluation is performed with the multi-criteria decision aid Decision Lab, in which the flash pyrolysis of willow and the flash co-pyrolysis of the willow/biopolymer blends, all with a w/w ratio of 1:1, are evaluated against each other based on five predefined criteria. The two most performant biopolymer blends are investigated more thoroughly in Chapter 5, where the flash (co-)pyrolysis of willow, the biopolymer and 4 willow/biopolymer blends are investigated analytically using Thermogravimetric techniques in combination with Mass Spectrometry and Fourier Transform Infrared Spectroscopy. Similarly, the actual flash (co-) pyrolysis is carried out with the semi-continuous home-built pyrolysis reactor indicating the occurrence of synergetic interactions between willow and the respective biopolymers. The synergy observed during flash co-pyrolysis is further investigated in Chapter 6, to better comprehend the reaction circumstances and to propose an explanation of the observed synergy. Therefore, the analytical Py-GC/MS in combination with statistical data processing, pattern recognition and the identification and quantification of the pyrolytic volatiles prior to condensation is carried out. Finally, the influence of the flash co-pyrolysis on the bio-oil composition, obtained from the reactor experiments, is investigated with complementary techniques (Gel Permeation Chromatography, Fourier Transform Infrared Spectroscopy, High Performance Liquid Chromatography and Gas Chromatography in combination with Mass Spectrometry).

Chapter 1: Introduction

Global Warming, the Kyoto Protocol and the emission of greenhouse gases are the topics of environmental pleadings worldwide. Many countries, both European and non-European, are facing the challenge to reduce their CO_2 emissions. Additionally, the world's energy supply is limited due to the depletion of fossil fuels, which are still the most important energy sources consumed. The Green Paper – 'Towards a European strategy for the security of energy supply' of the European Commission [1] advices the European Union to broaden the spectrum of energy sources available to limit the dependence on one specific energy source and thus to secure its energy supply. With regard to supply, priority must be given to the fight against global warming. The development of new and renewable energy sources (including biofuels) is the key to change. The use of biomass as an energy source is an issue of great importance, as it constitutes part of an alternative solution for the replacement of fossil fuels [2]. Materials in general evolve to become sustainable too (Club of Rome) [3].

Biomass is a renewable resource which implies that it is part of the flow of resources occurring naturally and repeatedly in the environment [4]. Compared with fossil fuel, biomass has a much shorter period of life cycle. Therefore, the application of biomass for energy can lead to zero net CO_2 emissions in a very short life cycle period since carbon in the form of CO_2 and energy are fixed by photosynthesis during biomass growth [5]. The pyrolysis, a thermal degradation process in the absence of oxygen/air, of biomass (as waste) is a promising route for the production of solid, liquid and gaseous products. These products are of interest as they are possible alternate sources of energy or chemical feedstock [6-8]. Flash pyrolysis, in specific, is a high temperature process in which biomass is rapidly heated. As a result, biomass decomposes to generate mostly vapours and aerosols and char. While it is related to the traditional pyrolysis process for making charcoal, flash pyrolysis is an advanced process which is carefully controlled to give high yields of liquid – bio-oil which has a heating value about half that of conventional fuel oil [9]. If the purpose is to maximise the bio-oil yield, process conditions are selected as relatively low temperature, high heating rate and short gas residence time (to minimise secondary reactions) [10].

The potential of being paid to take biomass wastes greatly enhances the economics of power generation. The combined burden of increasing quantities of wastes and environmental legislation in Europe that limits the wastes that can be disposed to landfill has lead to an increase in the number of thermal treatment plants operating on biomass wastes [11].

1.1. Energy production from biomass

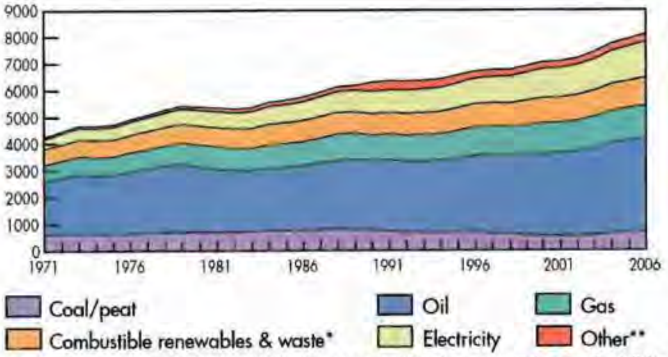

Figure 1.1: Evolution from 1971 to 2006 of world total final consumption by fuel (Mtoe) [12].
*Prior to 1994 combustible renewables and waste final consumption has been estimated.
** Other includes geothermal, solar, wind, heat, etc.

The major energy demand is fulfilled from the conventional energy resources like coal, petroleum (oil) and natural gas (Figure 1.1). These sources are in the verge of getting extinct. Additionally, the process of obtaining energy from these sources causes atmospheric pollution, resulting in problems like global warming, acid rain, etc. In view of such pollution and the continuous increase in energy demand, a shift to non-conventional energy sources like wind, sunlight, water, biomass, etc., is inevitable [13].

Biomass has always been a major source of energy for mankind. Nowadays, the use of renewable energy sources is becoming increasingly necessary, if we have to achieve the changes required to address the impacts of global warming. Biomass is the most common form of renewable energy, widely used in the third world but until recently, less so in the Western world. Biomass is available on a renewable basis and is produced by green plants converting sunlight into plant material through photosynthesis and includes all land- and water-based vegetation, as well as all organic wastes. If biomass is processed efficiently, either chemically or biologically, by extracting the energy stored in the chemical bonds and the subsequent 'energy' product combined with oxygen, the biomass is oxidised to produce CO_2 and water. The process is cyclical, as the CO_2 is then available again to produce new biomass [14-16].

Much attention has been focused on identifying suitable biomass species, which can provide high-energy outputs, to replace conventional fossil fuel energy sources. The type of biomass required is largely determined by the energy conversion process and the form in which the energy is required [15].

In general, the characteristics of the ideal energy crop are:

- high yield (maximum production of dry matter per hectare),
- low energy input to produce,
- low cost,
- composition with the least contaminants, and
- low nutrient requirements [15].

The most important industrial 'biomass-to-energy' application today is the Rankine cycle using solid biomass. Other existing biomass fuelled power plant concepts apply either gas engines or gas turbines fuelled with biologically (landfill gases, anaerobic digestion gases) or thermally (gasification) derived fuel gases. However, decoupling of bulky solid fuel handling from the actual power generating plant would be highly advantageous [17]. As with any energy resource there are limitations on the use and applicability of biomass and it must compete not only with fossil fuels but with other alternative energy sources such as wind, solar and wave power [18].

1.2. Advantages of biomass

The use of biomass fuels provides, compared to fossil fuel usage, substantial benefits as far as the environment is concerned [5, 15, 19, 20]:

- Burning fossil fuels uses "old" biomass and converts it into "new" CO_2; which contributes to the "greenhouse" effect and depletes a non-renewable resource. Burning new biomass contributes no new CO_2 to the atmosphere, because replanting harvested biomass ensures that CO_2 is absorbed and returned for a cycle of new growth.
- Woody biomass contains virtually no sulphur, so SO_2 emissions are also reduced in direct proportion to the coal replacement.
- Biomass is considered to be an indigenous energy source, available in most countries and its application may diversify the fuel-supply in many situations, which in turn may lead to a more secure energy supply.
- If intensive agriculture is replaced by less intensively managed energy crops, there are likely to be environmental benefits, such as reduced leaching of fertilisers and reduced use of pesticides. Moreover, if appropriate crops are selected, restoration of degraded lands may be possible.

1.3. Biomass composition

The chemical structure and major organic components in biomass are extremely important in the development of processes for producing fuels and chemicals. Biomass can generally be defined as any hydrocarbon material which mainly consists of carbon, hydrogen, oxygen and nitrogen. Sulphur is also present in minor proportions [10]. The presence of large amounts of oxygen in plant carbohydrate polymers means that the pyrolytic chemistry differs sharply from fossil feeds [20]. In general, the major constituents of biomass are cellulose, hemicelluloses, lignin, organic extractives, and inorganic minerals [10, 20, 21]. The weight percent of these constituents varies for different biomass species. The typical lignocellulose contents of some plant materials are given in Table 1.1, while the composition of willow (which is the reference biomass material for this research) is shown in Figure 1.2.

Table 1.1: Typical lignocellulose content of some plant materials [20].

	Lignocellulose content (%)		
Plant material	Hemicelluloses	Cellulose	Lignin
orchard grass	40	32	5
rice straw	27	34	14
birch wood	26	40	16

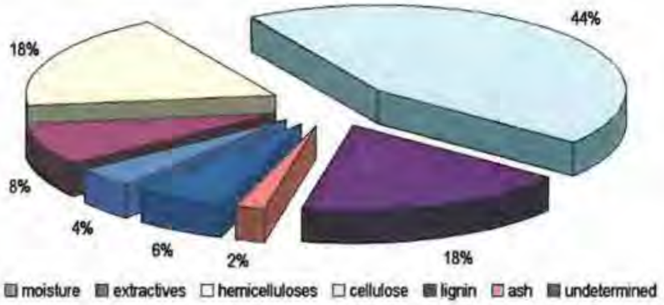

Figure 1.2: The composition of willow (the reference biomass for this research), analysed by Mark Stals (PhD student UH – Research group Applied and Analytical Chemistry – private communication).

1.3.1. Cellulose

Cellulose is a polysaccharide having the general formula $(C_6H_{10}O_5)_r$ and forms the skeletal structure of most terrestrial biomass. Cellulose fibres provide wood's strength and comprise 40 - 50 % of dry wood [10, 15, 16, 20]. Cellulose is a high molecular weight (10^6 Dalton or more) linear polymer of β-

(1→4)-D-glucopyranose units in the ${}^4C_1$ conformation (Figure 1.3). The basic repeating unit of the cellulose polymer consists of two glucose anhydride units, called a cellobiose unit.

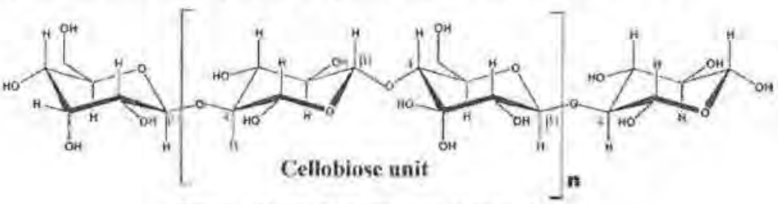

Figure 1.3: Chemical structure of cellulose [20].

1.3.2. Hemicelluloses

A second major wood chemical constituent is hemicelluloses, which is also known as polyose. Hemicelluloses varies considerably among different woody and herbaceous biomass species [10, 15, 16, 20]. Many of them have the general formula $(C_5H_8O_4)_n$ and usually account for 25 - 35% of the mass of dry wood. Hemicelluloses is a mixture of various polymerized monosaccharides (sugars) such as glucose, galactose, mannose, xylose, arabinose, and glucuronic acid (see Figure 1.4).

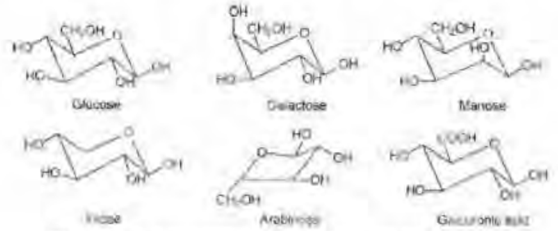

Figure 1.4: Main components of hemicelluloses [20].

Cellulose has only glucose in its structure, whereas hemicelluloses has a heteropolysaccharide make-up of pentosanes and hexosanes, and contains some short side-chain "branches" pendent along the main polymeric chain.

1.3.3. Lignin

The third major component of wood is lignin, which accounts for 16 - 33% of the mass. It is an amorphous three-dimensional cross-linked polyphenolic resin with no exact structure [10, 15, 16, 20, 22]. It is the main binder for the agglomeration of fibrous cellulosic components while also providing a shield against the rapid microbial or fungal destruction of the cellulosic fibers. Lignin consists of an irregular array of variously bonded "hydroxy-" and "methoxy-"substituted phenylpropane units, which exhibit the *p*-coumaryl, coniferyl, and sinapyl structures (Figure 1.5).

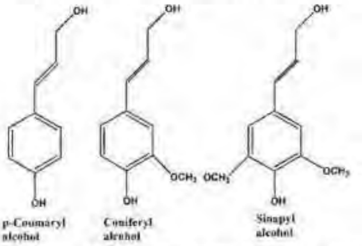

Figure 1.5: *p*-coumaryl, coniferyl and sinapyl structures [20].

In contrast to cellulose and hemicelluloses (carbon content less than 50% and oxygen content about 50%) lignin consists of 60% carbon and 30% oxygen [16]. A small section of a lignin polymer is presented in Figure 1.6, illustrating some typical lignin chemical linkages [20].

Figure 1.6: Example of a partial structure of a lignin molecule [20].

1.3.4. Inorganic material

Biomass also contains a small mineral content. Some typical mineral components in wood are potassium, sodium, phosphorous, calcium, and magnesium. The concentration of mineral ash ranges from less than 1% to 15% (and even more) in biomass and agricultural residues [10, 20].

1.3.5. Organic extractives

A fifth wood component is comprised of organic extractives. These can be extracted from wood with polar solvents (such as water or alcohol) or nonpolar solvents (such as toluene or hexane). Examples of extractives include fats, waxes, alkaloids, proteins, phenolics, simple sugars, pectins, mucilages, gums, resins, terpenes, starches, glycosides, saponins, and essential oils [20].

1.4. Biomass conversion methods

Biomass can be converted into various useful forms of energy using a number of different processes. In contrast to other renewables, biomass represents the only source of liquid, solid and gaseous fuels [9]. Factors that influence the choice of conversion process can be:

- the type and quantity of biomass feedstock,
- the desired form of the energy, i.e. end-use requirements,
- environmental standards,
- economic conditions, etc.

In many situations it is the form in which the energy is required, followed by the available types and quantities of biomass that determines the process route [18]. While particular plant species may have specific benefits for subsequent processing technologies, the amount of energy potentially available from a given biomass source is the same, irrespective of the conversion technology used. What will vary between conversion technologies is the actual amount of energy recovered from the biomass source and the form of that energy [15].

Conversion of biomass to energy is undertaken using two main process technologies (Figure 1.7) [10, 18, 19, 23, 24]:

- thermochemical and
- biochemical/biological.

Mechanical extraction (combined with esterification) is the third technology for producing energy from various biomass crops, e.g. rapeseed methyl ester (RME) bio-diesel [18]. The concept of extracting oil, both for food and fuel practices, by pressure with a screwpress is well known [4]. The extracted oil can be processed further by reacting it with alcohol using a process termed esterification to obtain bio-diesel that can be used as a supplement to transportation fuel. Since a few years, many projects related to this bio-liquid as a fuel have been launched and were heavily promoted. However, these biofuels have recently been widely countered as unethical, because they compete with the basic food supply chain.

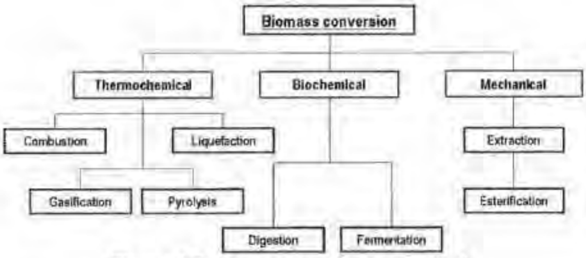

Figure 1.7: Biomass conversion methods.

Biochemical conversion encompasses two process options: anaerobic digestion (biogas) and fermentation (bio-ethanol). Anaerobic digestion is the bacterial conversion of organic material in the absence of oxygen directly to a gas, termed biogas, a mixture of mainly methane and carbon dioxide with small quantities of other gases such as hydrogen sulphide. Anaerobic digestion is widely used for treating organic wastes with high moisture content [18]. Fermentation is also an anaerobic biological process in which sugar and starch crops (e.g. sugar cane, sugar beet, maize, wheat) are converted to bio-ethanol by the action of micro-organisms. Bio-ethanol can be used as a petrol additive/substitute or directly as a liquid biofuel [18, 23]. The main thermochemical conversion processes are described in further detail below.

1.4.1. Thermochemical conversion

The thermochemical conversion of biomass is being considered as one of the most promising non-nuclear forms of future energy [25]. With the aid of thermal degradation processes, biomass (as waste) can be used in a variety of ways to provide energy:

- by direct combustion to provide heat for use in heating, for steam production and hence electricity generation;
- by gasification to provide a fuel gas for combustion for heat, or in an engine or turbine for electricity generation;
- by pyrolysis to provide a solid, gaseous and/or liquid fuel. The liquid can also be used to produce a range of speciality and commodity chemicals [9].

As shown in Figure 1.8, the three thermochemical conversion technologies described above can best be differentiated based on the oxygen demand of each technology: λ, which is representative for the stoechiometric amount of oxygen required. The fourth thermal degradation process, liquefaction, is mainly aimed at obtaining low molecular weight liquid fuels from organic high molecular weight compounds by conversion of biomass in liquid water at high temperature and high pressure in the presence of suitable catalysts, e.g. alkali metal salts, with or without reducing gas, e.g. hydrogen [26-28].

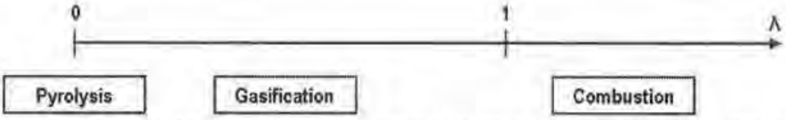

Figure 1.8: Classification of thermochemical conversion technologies based on stoechiometrical oxygen demand (λ).

In general, thermal degradation of biomass can give rise to three different fractions:

- solids (charcoal and mineral ashes),
- liquids (oils, tars), and
- gases (H_2, CO, CO_2, and small hydrocarbons).

Their relative fractions depend on the process operating conditions which are chosen according to the desired final uses of the products [29].

1.4.1.1. Combustion

Direct combustion of biomass has been carried out worldwide since ancient times for cooking and heating [2]. Combustion, e.g. the burning of biomass in air, is used over a wide range of outputs to convert the chemical energy stored in biomass into heat, mechanical power, or electricity using various items of process equipment, e.g. stoves, furnaces, boilers, steam turbines, turbo-generators, etc. Combustion of biomass produces hot gases at temperatures around 1100–1300 K. Net bio-energy conversion efficiencies for biomass combustion power plants range from 20% to 40% [10, 18]. Since biomass usually contains high moisture content and has low density, there are some difficulties and economic limitations related to transportation, storage, and usage of biomass without any pre-treatment. Additionally, high content of moisture results in unstable combustion [2, 10].

One misleading opinion on biomass combustion is that biomass is easy to burn and that the available coal combustion technology can be directly used for biomass. Biomass is a rather difficult fuel due to the lower calorific value, the content of chlorine and alkali metal, and its vast geographical dissemination [30].

1.4.1.2. Gasification

During World War II, the shortages of petroleum products in Europe lead to the need to develop alternative technologies to provide fuel for motor vehicles. The technology chosen was gasification of wood, using a fixed bed gasifier unit attached to the front of the vehicle [11].

Gasification is the conversion of biomass into a combustible gas mixture by the partial oxidation of biomass in a gasification medium at high temperatures, typically in the range 1100 – 1200 K. If air is present, the ratio of oxygen to biomass is typically around 0.3 [19]. The resulting gas is a mixture of carbon monoxide, hydrogen and methane together with carbon dioxide, nitrogen and water vapour.

Technically, gasification is a pyrolysis process, performed at high temperatures in order to optimize gas production. It can be stated that, if the primary pyrolysis product is gas, the process is considered as gasification. If the primary products are condensable vapours, the process is considered as pyrolysis [26]. The overall efficiency of conversion of biomass to energy using pyrolysis/gasification is estimated as 75–80% [11].

High mineral matter can make gasification impossible. The oxidation temperature is often above the melting point of the biomass ash, leading to clinkering/slagging problems and subsequent feed blockages [11].

1.4.1.3. Pyrolysis

Pyrolysis is the decomposition of organic matter in vacuum or inert atmosphere with the effect of heat. The pyrolysis of biomass has been known since the earliest stages of technology and has been applied to vegetable biomass resources for producing gases, liquids and chars. The usage of the pyroligneous acids from wood as an embalming fluid was already known in ancient Egypt [31].

Generally, pyrolysis is the conversion of biomass to liquid, solid and gaseous fractions, by heating the biomass in the absence of air to around 700 – 800 K [6, 7]. The amounts of solid, liquid, and gaseous fractions formed is dependent markedly on the process variables, as are the distribution of products within each solid, liquid, and gas phase produced (see *section 1.5*) [20]. Pyrolysis can be divided into two main categories [18, 20, 29]:

- Slow pyrolysis mainly leads to char.
- Fast or flash pyrolysis mainly yields liquid products.

Decoupling the fuel production from the actual application is an important advantage of flash pyrolysis compared to gasification and combustion.

It should be noted that the evolution towards sustainable materials is an important aspect too. The production of chemical feedstock by biomass conversion can be considered at least as important as the energy production. Processing carbonaceous feedstocks to produce heat, chemicals, or fuels offers an alternative to landfills and provides a supplement to fossil fuel use [20]. Incineration will not be widely accepted due to dioxin exhaust [32]. Pyrolysis, liquefaction, fermentation and mechanical extraction (trans-esterification) all produce liquids suitable for use as (transportation) fuels; while other conversion processes produce energy in a form that is best used at the point of production i.e. hot air/steam or a gas [18]. For this research, flash pyrolysis is considered to provide the most potential.

1.5. Pyrolysis

The word *pyrolysis* is a combination of the Greek words *pyros* (means: fire, heat or warmth) and *lysis* (means dissolving). Since the earliest stage of human civilization, pyrolysis of biomass is well known and has been used extensively. Originally, pyrolysis of biomass was mainly performed to produce gases and char, whereas the liquid products were regarded as undesirable by-products. However, since the oil crises in the nineteen seventies, the general interest in the liquid products of the pyrolysis of biomass is increasing steadily [16].

Pyrolysis is the decomposition of chemical bonds by the use of thermal energy only. The degradation of a molecule is caused by the dissociation of a chemical bond and the production of free radicals. The way in which a molecule fragments during pyrolysis and the identity of the fragments produced depend on the types of chemical bonds involved and the instability of the resulting smaller molecules [33].

The main parameters influencing the pyrolysis reactions are:

- Temperature
- Heating rate
- Residence time
- Particle size
- Biomass species
- Chemical and structural composition of biomass
- Catalyst used [7, 16, 19, 25].

Some parameters will be discussed in further detail.

1.5.1. Parameters

1.5.1.1. Temperature

The pyrolysis temperature is probably the most important parameter under consideration, because it directly influences the devolatilisation degree and the amount of residual char. Low pyrolysis temperatures (partial pyrolysis) can be applied to prepare a solid fuel (e.g. briquettes) with an enhanced calorific value. Intermediate temperatures are required for the highest production of valuable bio-oil, while high temperatures favour the production of noncondensable pyrolytic gases [8, 25, 34-40].

1.5.1.2. Heating rate

If the production of bio-oil is put forward as the pyrolysis objective, the heating rate of the biomass particles is at least as important as the pyrolysis temperature. Low heating rates favour carbonisation and promotes secondary reactions reducing the yield of liquid products and resulting in an increase in noncondensable gases [10, 41]. Employing a sufficiently high heating rate (> 300 K/min) breaks heat and mass transfer limitations in the pyrolysis, resulting in a significant increase in bio-oil yield [8, 39, 42]. At the high heating rates (up to 1000 K/s), temperatures below 923 K and rapid quenching of the products, the high molecular weight products can be condensed before being cracked to gaseous products, while high heating rates and temperatures above 923 K tend to favour the formation of gaseous products at the expense of bio-oil [43, 44].

1.5.1.3. Residence time

The residence time combined with the pyrolysis temperature and heating rate, define the time-temperature profile of the biomass. Based on this time-temperature profile, pyrolysis can be divided into two main pyrolysis categories: conventional (or slow) and fast (or flash) pyrolysis. Many pyrolyses have been performed at rates that are not considered fast nor slow but are conducted in a broad range between these extremes [20, 45]. During the Pyrolysis 2008 Conference in Lanzarote, some researchers opted to introduce a "new" type of pyrolysis: intermediate pyrolysis. This third class of pyrolysis would cover those that lie somewhere in between but is not considered for this research.

The time-temperature envelope that the biomass and the pyrolysis vapours endure affects the composition of the pyrolysis products. Low process temperature and long vapour residence time favour the production of char. High temperature and long residence time increase the biomass conversion to gas. Moderate temperature and short vapour residence time, necessary to minimise secondary cracking, are optimum for producing bio-oil (Table 1.2) [8, 9, 24, 40, 46-49].

Table 1.2: Summary of the influence of the time-temperature profile [6, 10, 20].

	Main pyrolysis product		
Parameter	Char	Bio-oil	Gas
Temperature	Low	Low/Intermediate	High
Heating rate	Low	High	Low
Gas residence time	Long	Short	Long
	Slow pyrolysis	**Flash pyrolysis**	**Gasification**

1.5.1.4. Particle size

Under ideal conditions there is nearly no temperature gradient within the heated sample [50]. However, the particle size of the biomass has an important bearing on the ability of the biomass to be heated quickly in a given heat flux environment and is known to influence the pyrolysis yield. This effect may be related to the heating rate, in that larger particles will heat up more slowly, so the average particle temperatures will be lower, and hence volatile yields may be expected to be less. Secondary reactions can also occur when the particle is too large, resulting in additional char or tar formation. If the particle size is sufficiently small, it will be heated uniformly [8, 35, 39, 44].

Generally, particles have to be very small to fulfil the requirements of rapid heating and to achieve high liquid yields. A particle size < 2 mm ensures rapid heat transfer and reaction and is considered as a good compromise for maximum bio-oil production [4, 20, 35, 50].

1.5.2. Secondary reactions

The primary pyrolysis products participate in secondary interactions, resulting in a modified final product distribution [7, 51]. The time and temperature profile between the formation of pyrolysis vapours and their quenching to bio-oil affects the final composition and quality of the bio-oil. Secondary reactions of the volatiles and further decomposition of the char particles proceeds in the reactor with increasing pyrolysis temperature and favours the formation of noncondensable gases [8, 40, 52]. Char also contributes to vapour cracking by catalysing secondary cracking in the vapour phase. Although secondary reactions become slow around 623 K, some secondary reactions continue down to room temperature in the liquids, which contributes to the instability of the pyrolysis liquid (see *section 1.6.6*).

1.5.3. Modelling and kinetics

Ever since the existence of pyrolysis, part of the research objectives are focussed on the interpretation and in-depth analysis of pyrolysis reaction mechanisms in order to understand how pyrolysis evolves. However, as can be concluded from previous statements, pyrolysis is fairly complex and any model will be confronted with its limitations. Nevertheless, many authors tried to achieve their "model" explaining pyrolysis [7, 42, 53, 54].

Janse et al. [42], for instance, tried to model flash pyrolysis of a single cylindrical wood particle. In general, biomass is mainly composed of cellulose fibres which are hold together by the lignin fraction. In a cylindrical particle, these fibres are aligned in parallel, through which the pyrolysis vapours can escape the particle. This may imply that the direction of heat flux into the particle is perpendicular to the flow direction of the pyrolysis vapours, see Figure 1.9. However, it should be noted that the penetration of heat into the particle can be hampered by outflowing gases [42, 54]. Based on their model, Janse et al. [42] concluded that an extensive description of internal mass transport phenomena in flash-pyrolysis modelling is not necessary, while accurate knowledge of the reaction kinetics and heat transfer parameters is crucial.

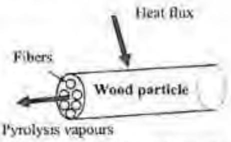

Figure 1.9: Schematic picture of a wood particle with the direction of incoming heat flux perpendicular to the flow direction of pyrolysis vapours (side-way outflow of gases) [42].

Knowledge of the kinetics helps to achieve control of the pyrolysis process and assists in optimising system design. The actual reaction scheme of pyrolysis of biomass is extremely complex because of the formation of over a hundred intermediate products. Pyrolysis of biomass is, therefore, generally modelled on the basis of apparent (simplified) kinetics. The study of kinetics of pyrolysis of biomass is helpful in developing the mechanism of a thermochemical conversion process. Ideally, the chemical kinetics model should account for the primary decomposition reactions as well as the secondary reactions, Figure 1.10 [7, 20, 51, 55]. Various contributions have been made on kinetic modelling: f.i. [7, 29, 46, 51, 54-60].

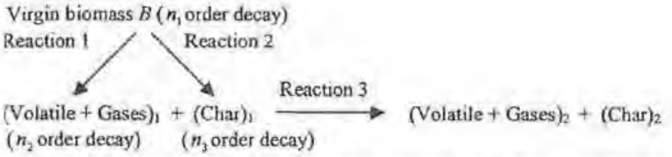

Figure 1.10: A general pyrolysis scheme accounting for primary and secondary decomposition reactions [61].

1.5.4. Flash pyrolysis

If the aim is to produce liquid biofuels (bio-oil), flash pyrolysis is recommended. Biomass is rapidly heated and decomposes to generate vapours, aerosols and char. After cooling and condensation of the vapours and aerosols, a dark brown mobile liquid is formed that has a heating value that is about half that of conventional fuel oil. Flash pyrolysis processes produce 60 - 75 % of bio-oil, 15 - 25 % of solid char, and 10 - 20 % of noncondensable gases, depending on the feedstock used. No waste is generated, because the bio-oil and solid char can each be used as a fuel while the gas can be recycled back into the process [20, 24].

The essential features of a flash pyrolysis process are:

- very high heating rate (> 100 K/min) and heat transfer rates,
- a finely ground biomass feed (< 1-2 mm),
- carefully controlled pyrolysis reaction temperature of around 773 K,
- short vapour residence times of typically less than 2 seconds, and
- rapid cooling (quenching) of the pyrolysis vapours to give the bio-oil product [6, 9, 20, 45, 49].

Biomass flash pyrolysis is of rapidly growing interest in Europe as it is perceived to offer significant logistical and hence economic advantages over other thermal conversion processes. This is because the liquid product can be stored until required, or readily transported to where it can be most effectively utilised. Therefore, it offers the possibility of decoupling (time, place, and scale), easy handling of the liquids and more consistent quality, compared to any solid biomass [20, 24, 62].

There is only little room for improvement in the bio-oil yields being obtained. Improvement of oil quality is now considered more important either through better control of the pyrolysis reaction system including secondary reactions or through modification of the pyrolysis products either catalytically, physically or thermally [24].

1.5.5. Pyrolysis of biomass

Biomass is a general definition of organic material made from plants and animals. Biomass includes agricultural, forestry and even industrial materials, which can differ extensively in composition. It is pure logic that very different biomass species react differently during pyrolysis. Virtually any form of biomass can be considered for (flash) pyrolysis and many types of biomass have already been tested, ranging from agricultural wastes to energy crops. Forestry and other solid wastes have also been studied. Söderman remarks that recovering energy from waste is part of the future energy matrix, since energy recovery from waste is necessary in order to fulfil the ban on landfilling of combustible and organic waste [63].

It is impossible to list all biomass types investigated for pyrolysis and only a "short list" is reported: wood [16, 64], forestry waste [65], spruce wood [25, 66, 67], pine [16, 35, 67-72], beech [16, 60, 73], birch [74], willow [60, 75-78], poplar [76], locust [76], eucalyptus [16], sawdust [5, 26, 79, 80], larch bark [80]; miscanthus [64], hazelnut shell [25], coconut shell [45, 46, 58], cashew nut shell [58, 81], wheat straw [25, 46], rice husk [32, 46, 80, 82], rice straw [36, 45, 80], corn stover [56], corn stalk [80], cotton stalk [46], sugar cane bagasse [32, 45, 80], rapeseed [4, 8, 31, 38, 39, 83], rapeseed cake [14], safflower seed [84], safflower seed press cake [2, 85], linseed [86], pistaccia khinjud seed [87], tobacco stalk [69], oil palm waste [80, 88], olive residu [89]; cow biosolids [32]; sewage sludge [32, 40, 43, 64, 90-97]; and even microalgae [47].

Each kind of biomass has a characteristic pyrolysis behaviour which can be explained based on the individual component characteristics. Direct additive correlations based on biomass component pyrolysis adequately explain both the pyrolysis characteristics and product distribution of biomass. No detectable interaction among the components during pyrolysis is inferred [98]. Nonetheless, it is the goal to specifically invoke non-additive behaviour (synergy) during (flash) co-pyrolysis.

1.5.5.1. Organic fraction of biomass

Biomass is a mixture of hemicelluloses, cellulose, lignin and minor amounts of extractives which each pyrolyse at different rates and by different mechanisms and pathways [23].

- Cellulose decomposes within a narrow temperature range: 573 – 703 K, and shows the highest decomposition rate. Cellulose, additionally, results in the lowest char yield.
- Lignin on the other hand decomposes over a wider temperature range: 523 – 823 K and results in the highest char yield (45 – 50 %).

- Hemicelluloses is the most unstable component, decomposing at much lower temperatures than every other component, and shows to have a char fraction of around 30%.
- Finally, extractives decompose in a similar way to lignin but at a slightly higher rate and at a slightly lower temperature [6, 98].

Pyrolysis mechanisms typically include a superposition of the kinetic mechanisms for the individual components of the biomass materials (Figure 1.11) [99, 100]. The weight loss occurring at temperatures below 373 K mainly represents the evolution of moisture. The relevance of the differences in the decomposition temperature and rate between the constituents is not yet described during fast pyrolysis, which is completed in few seconds at a rapid heating rate (dynamic versus static circumstances) [20].

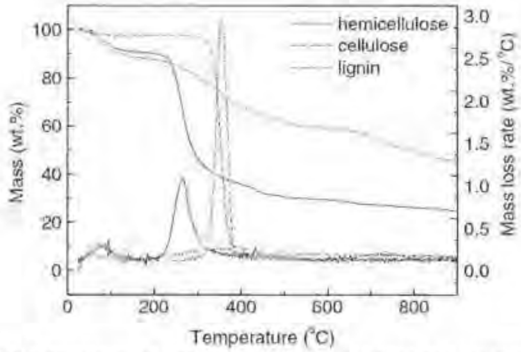

Figure 1.11: Pyrolysis curves of hemicelluloses, cellulose and lignin in TGA [99].

Accordingly, biomass pyrolysis products are a complex combination of the products from the pyrolysis of the individual components. Table 1.3 summarises some typical degradation products of the main constituents of biomass.

Table 1.3: Degradation products of fast pyrolysis of biomass constituents [101].

Biomass constituent	Degradation product
Cellulose	levoglucosan, 5-hydroxymethylfurfural, hydroxyactealdehyde, formaldehyde
Hemicelluloses	acetic acid, furfural, furan
Lignin	small amounts of monomeric phenols: phenols, cresols, guaiacols, syrigols, etc.; and oligomeric phenolic components
Extractives	molecules of waxy components such as fatty acids

1.5.5.2. Inorganic fraction of biomass

Biomass typically contains varying amounts of inorganics (< 1% - 25%). Generally the main elemental constituents of biomass minerals are Si, Ca, K, Na and Mg, with minor amounts of S, P, Fe, Mn and Al. Small amounts of inorganic material, as present in the biomass, are sufficient to alter the pyrolysis behaviour [77, 102, 103]. In general, it can be stated that inorganics catalyse biomass decomposition and char forming reactions during biomass pyrolysis [10]. Another important observation is that during pyrolysis, most alkali and alkali earth metals in the feed are concentrated in char, which enables the easy separation of alkali and alkali earth metals from the product stream [20, 35].

The latter conclusion is of primordial importance for the broad rationale on which this research focuses: pyrolysis can be applied to both derive a useful bio-oil from heavy metal contaminated biomass and fix the possible contaminants in the residual char [9, 104-106].

1.5.5.3. Valorisation of contaminated biomass obtained from phytoremdiation

Phytoremediation involves removing metals from soil or water for environmental and health reasons. Phytomining implies extraction of metals from soils rich in metal content using hyperaccumulators for economic gain. Heavy metals are extracted by plants and accumulated in the shoot (the stem and the leaves). This will slowly result in clean soils if the biomass is removed from these grounds. Large amounts of biomass contaminated with heavy metals are thus obtained, shifting the problem if the biomass cannot be recycled. A future goal is to treat the contaminated biomass by first reducing its volume f.i. with the aid of pyrolysis and to produce bio-oil and pyrolytic gases free of heavy metals. If, accordingly, the contaminants remain in the residual char, as is found for the natural inorganics of biomass, the use of pyrolysis as a first step towards the recovery of heavy metals from hyperaccumulators, used for phytoremediation or phytomining, is assured [107]. Willow, for instance, can be used to remediate heavy metals contaminated soils by phytoextraction [108-112]. Therefore, the utilisation of willow as biomass feed for pyrolysis requires to be investigated in a broader context. Primarily, knowledge on the pyrolysis behaviour of uncontaminated willow and its optimisation are essential and will be discussed in this research.

The rationale for using pyrolysis as the method of choice is:

- reduction in the volume and weight of biomass to be processed,
- energy recovery in the form of valuable bio-oil and/or syngas free from heavy metals,
- achieving on-site processing of the biomass using a portable pyrolysis unit,

- lower temperatures compared to incineration, limiting the amount of pollutants released in the pyrolysis gases, and
- production of a char/ash residue that recovers the metals in the form of a metal concentrate that may be processed using commercially available metallurgical operations [43, 113].

In order to make the complete process viable, the bio-oil produced should be of acceptable quality.

Research on such contaminated biomass is being performed within the research group 'Laboratory of Applied and Analytical Chemistry' of the Hasselt University. Caroline Lievens [104-106] obtained heavy metal free condensable and noncondensable pyrolytic fractions from heavy metal contaminated biomass samples. The amount of contamination was sharply reduced in weight and volume by concentrating the heavy metals in the char residue. By this, the potential of pyrolysis for metal enrichment and the production of valuable pyrolysis products is proven. Other research [113, 114] indicated that more than 99% of the metal in the product stream was concentrated in the char formed by pyrolysing the contaminated biomass. The metal concentration was increased 4 to 6 times in the char compared to the feed. Char with high concentrations of metal can be considered as a rich "ore" or metal concentrate, which can be processed for possible separation of the metal in a conventional ore-processing unit [113]. Sewage sludge and wood impregnated with a preservative such as CCA (chromated copper arsenate) are also waste streams struggling with a heavy metal contamination and their pyrolysis behaviour is being investigated as well [9, 43, 115, 116]. In general, it can be concluded that pyrolysis offers potential for waste treatment by fixing contaminants in the char while also producing a clean liquid fuel [9, 117].

1.6. Bio-oil

A dark brown, free-flowing organic liquid, having a distinctive odour, that is comprised of a complex mixture of highly oxygenated hydrocarbons: bio-oil, is dominantly produced via flash pyrolysis of biomass [94, 118]. Bio-oil shows potential to be applied as a renewable fuel and as a source of value-added chemicals [31]. Generally, liquid biofuels, such as bio-oil, have following advantages:

- possibility to decouple biomass conversion and the generation of energy,
- liquid may be stored and transported,
- use of liquids is less expensive than solids in existing boilers,
- emissions in boilers are less then when firing with solid fuels, and
- potential for intermittent operation [42, 119].

Bio-oil resembles a medium fuel oil in viscosity, although it will not mix with any hydrocarbon liquids. Bio-oils differ a great deal from petroleum-based fuels in both physical properties (Table 1.4) and chemical composition. Pyrolysis liquids contain more water and usually more solids, are often acidic, have a low higher heating value (H.H.V.) of about 17 MJ/kg (as compared to around 40±44 MJ/kg for conventional fuel oil) and are unstable when heated, especially in air [24, 120]. The density of pyrolysis liquids is a function of its water content and is typically 1.2 – 1.3 kg/dm^3 [52].

Bio-oil has several environmental advantages over fossil fuels:

- Bio-oils are CO_2-neutral. Therefore, they can generate carbon dioxide credits.
- No SO_x emissions are generated, because plant biomass contains insignificant amounts of sulphur. Therefore, bio-oil would not be subjected to SO_x taxes.
- Bio-oils generate more than 50% lower NO_x emissions than diesel oil in a gas turbine.
- Renewable and locally produced bio-oil can be produced in countries with large volumes of organic wastes.

Bio-oil also offers the potential to be applied as a feedstock for chemical industries, offering increased economics [20].

Table 1.4: Typical properties of wood pyrolysis bio-oil and heavy fuel oil [118].

Physical property	Bio-oil	Heavy fuel oil
moisture content (wt%)	15 - 30	0.1
pH	2.5	
specific gravity	1.2	0.94
elemental composition		
C	54 - 58	85
H	5.5 - 7.0	11
O	35 - 40	1
N	0 - 0.2	0.3
ash	0 - 0.2	0.1
H.H.V. (MJ/kg)	16 - 19	40
viscosity, at 773 K (cP)	40 - 100	180
solids (wt%)	0.2 - 1.0	1
distillation residue (wt%)	up to 50	1

1.6.1. Bio-oil composition

Chemically, bio-oil is a complex mixture of water, furancarboxaldehydes, carboxylic acids, hydroxyaldehydes, hydroxyketones, sugars, phenolics and oligomeric species. The final composition of bio-oils results form a complex interrelationship of:

- the biomass species used as feedstock,
- the heat transfer rate,
- final pyrolysis temperature,
- the extent of vapour dilution in the reactor,
- the time and temperature history of the vapours,
- whether the vapours pass through accumulated char (i.e. in hot-gas char filtration),
- the efficiency to separate the char from the bio-oil vapours before condensation,
- the efficiency of the condensation equipment,
- the storage time,
- the storage temperature, and
- exposure to air during storage [117].

1.6.2. Oxygen content of bio-oil

The elemental composition of bio-oil resembles that of biomass rather than that of petroleum oils [118]. Proximate analysis of the bio-oil gives a chemical formula of $CH_{1.9}O_{0.7}$. The oxygen content of bio-oils is usually 35 – 40 % and is dominantly present in most of the more than 300 compounds that have been identified in pyrolysis oils. The distribution of these compounds mostly depends on the type of biomass used and on the process severity (temperature, residence time, and heating rate profiles). An increase in pyrolysis severity reduces the organic liquid yield due to cracking of the vapours and formation of gases but leaves the liquid with less oxygen. The C/O atomic ratio of bio-oil thus increases as the pyrolysis temperature and heating rate increase [43].

The high oxygen content results in a low energy density (heating value) (see *1.6.7*) that is less than 50% of that for conventional fuel oils and is immiscible with hydrocarbon fuels (see *1.6.4*). An even more important consequence of the organic oxygen is the instability of bio-oil (see *1.6.6*) [118]. The high oxygen content is indicative of the presence of many highly polar groups leading to relatively poor chemical stability. A significant fraction of the oxygen is present as water (see *1.6.3*) [9].

1.6.3. Water in bio-oil

A main problem when dealing with pyrolysis oil is its high amount of water. Water in bio-oil results from the original moisture in the feedstock and as a product of the pyrolysis reactions and depends on the feedstock and process conditions, including the extent of secondary reaction or cracking. Even from dry biomass, pyrolytic water is produced [17, 24]. Bio-oil has a water content of typically 15–30 %, which cannot be removed by conventional methods like distillation [9]. Typically, phase separations may partially occur when the water content of pyrolysis oil is more than 35 – 40 %. However, water contents below 35 % do not guarantee a single phase bio-oil [16, 17, 24].

The presence of water has both positive and negative effects on the oil properties. It improves bio-oil flow characteristics (reduces the oil viscosity), which is beneficial for combustion (pumping and atomisation). It also leads to a more uniform temperature profile in the cylinder of a diesel engine and to lower NOx emissions. On the other hand, it lowers the heating value, it can lead to premature evaporation of the oil and resultant injection difficulties, it contributes to the increase in ignition delay and in some cases to the decrease of combustion rate compared to diesel fuels [69, 118, 121]. The beneficial effects of the aqueous phase are outbalanced by its negative impact [122]. The effect of water is complex in that it affects stability, viscosity, pH, corrosiveness, and other liquid properties. Selective condensation may reduce the water content of one or more fractions but at the expense of operating problems and a possible loss of low molecular weight volatile components [9].

Water contents of maximum 28% are often hailed as being acceptable to allow bio-oil to be applied as a fuel in static applications [120, 123-125]. Some potential end-users (Fortum/Oilon, Wärtsilä, Ormrod, and Orenda) commented that specifications should even be tighter: water contents should be lower, because of poor ignition properties and high emissions of high-water content bio-oil [125]. However, many biomass streams and pyrolysis reactors result in bio-oils that do not reach such "low" water contents. Water contents of 30 – 50%, and some even > 65% are reported [13, 35, 36, 45, 52, 82] and ask for some serious upgrading, before specific applications can be sought.

1.6.4. Miscibility of bio-oil

Bio-oil can be considered as a mixture of water and water-soluble organic compounds with water-insoluble, mostly oligomeric material. Bio-oils differ to some extent in their ability to dissolve water [52, 120]. Phase separation can take place in higher water and/or lignin-derived material concentration. Here, the heavy, mainly lignin-derived fraction separates out from the aqueous fraction [52].

The solubility of pyrolysis liquids in solvents other than water is significantly affected by the degree of polarity. Good solvents for highly polar bio-oil include alcohols, like ethanol and methanol. These solvents dissolve practically the whole bio-oil. Bio-oil also dissolves in higher alcohols, like isopropanol and polyglycols. Acetone is also a good solvent but not as effective as low alcohols [52, 120].

Typically, bio-oil does not dissolve in hydrocarbons like hexane, diesel fuels and polyolefins. However, some do contain extractives which are soluble in n-hexane [52, 120, 126].

1.6.5. Homogenity of bio-oil

Bio-oil contains a high number of compounds having different chemical functionalities. The homogeneity of the liquids is connected with the complex solubility and reactivity of the various chemical compounds in the liquid. Typically, the pyrolysis liquids are single-phase liquids containing varying amounts of solids. Layering and phase separation may take place already in the fresh liquid product or after a certain storage time.

Even with relatively low water contents a phase separation may also take place. In these cases the reason may be found in an unadvantageous balance of chemical compounds in the liquid, e.g. lack of light dissolving compounds (i.e., alcohols, acids) and a high proportional amount of lignin-derived water-insoluble fraction. The use of this type of liquids as fuels is questionable unless the two- or multi-phase liquid can be emulsified before use [120].

1.6.6. Stability of bio-oil: aging effects

Bio-oil production is made from renewable inhomogeneous feedstocks using an unspecific thermal treatment with short reaction times and rapid quenching which results in a product that is not in thermodynamic equilibrium, even at ambient temperatures. Therefore, reactions in the bio-oil occur after production [117, 127]. During storage, the chemical composition of the bio-oil changes toward thermodynamic equilibrium under storage conditions, resulting in changes in the viscosity, molecular weight, and co-solubility of its compounds [117]. Both the pyrolytic process and storage conditions of the oil influence the stability [50]. Among other parameters, char and ash in the oil is detrimental for the colour, quality and stability. Aging is accelerated by higher temperatures, exposure to oxygen and ultra-violet light. Distillation of pyrolysis oils is not feasible, only to a certain extent. Polymerisation in pyrolysis liquids is strongly accelerated when they are heated to 353 K or more [16, 122]. Stability of pyrolysis oils is additionally influenced by the water content. Aging reactions are fastest in a fresh pyrolysis liquid and retard in time [52].

Diebold [117] provided a very detailed review on the storage stability of bio-oils. Most important reactions that probably occur within bio-oil are listed below of which the main reactive components are mentioned '**in bold**':

1. **Organic acids** with alcohols to form esters and water (esterification),
2. **Organic acids** with olefins to form esters (water is not a by-product),
3. **Aldehydes** (or ketones) and water to form hydrates, also referred to as glycols,
4. **Aldehydes** and alcohols to form hemiacetals (hemiacetal formation), or acetals (acetylation – catalysed by salts) and water,
5. **Aldehydes** to form oligomers and resins (homopolymerisation), water is consumed,
6. **Aldehydes** and phenolics to form resins and water,
7. **Aldehydes** and proteins to form oligomers (dimerisation), in liquid smoke applications (browning),
8. Organic **sulphur** to form oligomers,
9. **Unsaturated** compounds to form polyolefins, and
10. Air oxidation to form more acids and reactive peroxides that catalyse the polymerization of unsaturated compounds, possible co-production of water [117].

In a complex, real bio-oil, the number of possible chemical reactions is very high, especially considering the large number of complex oligomers [117].

Bio-oil's propensity to age is considered as a disadvantage for the bio-oil's applicability. Addition of a light solvent, e.g., methanol or ethanol improves the bio-oil properties as well as the stability of the pyrolysis liquid. Methanol dissolves some structured components of the bio-oil and thus reduces the viscosity increase rate. Moreover, the addition of methanol delays the phase separation process [117, 120, 122]. However, the addition of aqueous phase to the bio-oil lowers the thermal stability significantly.

1.6.7. H.H.V., Density and Viscosity of bio-oil

The H.H.V. of bio-oil is about 17 MJ/kg (at 25 % water content) which is about 40 % that of fuel oil/diesel (at around 42 MJ/kg) in weight terms. When quoting a calorific value, the moisture content needs to be stated as well, as this reduces the available energy from the biomass, because the latent heat contained in water vapour cannot be used effectively [15]. This negative effect of water is considered by the lower heating value (L.H.V.).

The density of pyrolysis liquid is very high at around 1.2 kg/l. Thus, although the energy density is low in weight terms, this corresponds to 20.5 MJ/l compared to about 33.5 MJ/l for fossil fuel oil i.e. 61% of the volumetric energy density. This means that 2.5 kg bio-oil is required for the same energy input as 1 kg fossil fuel oil, but only 1.5 l per litre of fossil fuel oil due to the high density [24]. As presented by Diebold et al. [120] it can be seen that bio-oils with relatively higher densities typically have lower water contents.

Viscosity is a measure of a resistance of a liquid to flow. The viscosity of the fuel is important among others because of its effect on pumping and injecting of fuel [120]. It decreases rapidly at higher temperatures, so that even very viscous bio-oils can be pumped after a moderate preheating. A significant reduction in viscosity can also be achieved by addition of polar solvents such as methanol or acetone [118]. The viscosity of bio-oils can vary over a wide range depending on the water content, feedstock, process conditions, storage conditions, age and especially on the efficiency of collection of low boiling components. Viscosity change is recognised as a major indicator of stability. An undesired effect, especially observed when the oils are stored or handled at higher temperatures, is the viscosity increase with time [24, 118].

1.6.8. Combustion behaviour of bio-oil

Bio-oil properties have an important impact on the behaviour of bio-oils during combustion and consequently on the applications for energy production in standard equipment [118]. Bio-oils are combustible but not flammable, because of the high content of non-volatile components; bio-oil does not spontaneously ignite in a typical compression ignition engine and requires significant energy for ignition, but once ignited, it burns with a stable self-sustaining flame [118, 120]. Despite large differences in fuel properties and combustion mechanisms, the burning times of bio-oils are comparable to petroleum fuel oil under the same conditions [118]. Also the adiabatic flame temperature for bio-oils is relatively high [118].

1.6.9. pH and Corrosiveness of bio-oil

The degradation products from biomass include a wide variety of organic acids such as formic and acetic acid (pKa value of 3.70 and 4.74, resectively) which give the bio-oil its low pH (2 - 3). The oils are corrosive to common construction materials such as carbon steel and aluminium and can effect some sealing materials. The combination of the acids with water are claimed to be the main reasons for the corrosiveness of bio-oils especially at elevated temperatures. The oils are essentially noncorrosive to stainless steel. Many plastics like PTFE (polytetrafluoroethylene), PP (polypropylene), and HDPE (high density polyethylene) are very resistant to pyrolysis liquids. They are excellent materials for containers in storing, transportation and sampling of pyrolysis liquids [24, 52, 118, 120].

1.6.10. Biodegradability of bio-oil

With the increasing interest in bio-oil, the health and safety aspects are of utmost importance, including determination of their environmental impacts in the event of inadvertent problems or leaks during transport, storage or processing. As biodegradation is the dominant pathway for the environmental transformation of most chemicals, biodegradability properties of bio-oils should be known to assess the impact of accidental release [62]. Both the extent of degradation and the rate of this process are important criteria [128]. Bio-oil shows a very fast biological response, indicating that some compounds in pyrolysis oils are immediately degraded by competent degraders. The biodegradability value of bio-oil (± 50% degradation after 28 days) shows that in case of accidental spillages this fuel would be biodegraded better than all fossil fuels, but not as well as vegetables oils [62].

A difference between the biodegradability of slow and fast pyrolysis oils is observed. Fast pyrolysis oils are not as biodegradable as slow pyrolysis oils. However, they do show a very similar biodegradation behaviour. Slow pyrolysis is a more severe reaction for biomass components due to the longer vapour residence time, resulting in a larger fraction of light soluble compounds. The smaller and the simpler the molecules, the better the biodegradability [128].

1.7. Bio-oil applications

Bio-oils have been successfully tested in engines, turbines, and boilers, and have been upgraded to high-quality hydrocarbon fuels (transportation), although at a presently unacceptable energetic and financial cost [24, 118]. Though primarily bio-oils have been expected to become alternative liquid fuels, other potential applications have also emerged [118]. Fast pyrolysis is an accepted, feasible and viable route to renewable liquid fuels, chemicals and derived products. It is also clear that liquid products offer significant advantages in storage and transport over gas and heat. A general scheme on the various applications is given in Figure 1.12. A wide range of applications have been investigated and successfully demonstrated as feasible as summarised in Table 1.5 [129].

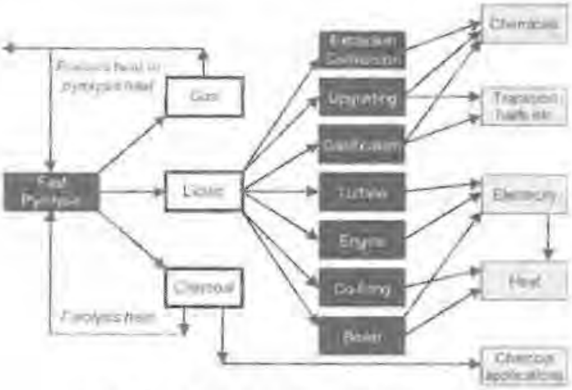

Figure 1.12: Applications of bio-oils [130].

Table 1.5: Examples of applications for bio-oil [129].

Energy	Commodities	Chemicals
Specific energy usage	Emission control reagent - bio-lime	Acetic acid
Fuel for power	Hydrogen	Acetone
Fuel for heat, including co-firing	Fatty acids	Adhesives and resins
Energy carrier	Food flavourings	Alkanes and alkenes
	Glyoxal	Anhydrosugars
Orthodox fuels	Hydroxyacetaldehyde	Anisole
Diesel	Levoglucosan	Aromatics
Fuel oil	Oxychemicals	Aryl ethers
Gasoline	Phenols	Calcium acetate
Reformulated gasoline	Polyphenols	Carboxylic acids
Olefins	Slow release fertiliser	Cresols
Novel fuels e.g. emulsions	Wood preservative	

Within Europe the most promising application is seen as electricity production due to the anticipated ability to use raw bio-oil as produced in an engine or turbine without the need for extensive upgrading. Additionally, there is the ability to decouple fuel production from electricity generation with storage and/or transport of the liquid fuel. The much higher added value of chemicals is, however, deemed to be the most interesting short term commercial opportunity related to pyrolysis [9]. The co-production of chemicals and fuels undoubtedly offers the most interesting opportunities [24, 101]. A summary of the main applications for bio-oil is given below.

1.7.1. Use of bio-oil as a fuel

Significant effort has been spent on research and development directed towards the application of bio-oil for the generation of heat and power, and for use as a transportation fuel [118].
Liquid fuels are of interest for many reasons:

- liquid fuels do not have to be used immediately after production. This allows the decoupling of fuel production from the end-use, and thus decentralised bio-energy production,
- providing base load and peak power,
- the higher energy density of liquid fuels versus that of fuel gases and solid biomass, resulting in reduced storage and transport costs,
- lower costs of retrofitting of existing combustion systems,
- liquid fuel combustion is, in general, much more efficient, controllable and cleaner,
- removal of ash prior to end-use application [17, 131, 132].

Bio-oil is considered to be a suitable boiler fuel [118]. Boilers are common devices used for heat and power generation. Due to the higher added value of electricity compared to heat and its ease of distribution and marketing, electricity production has attracted considerable attention as an application [24]. In power generation diesel engines are applied which can also be adapted to the combined heat and power process (CHP). Besides diesel engines, gas turbines are also capable of firing bio-oils [118].

Interestingly, a comparison between the use of the solid biomass and the use of the liquid bio-oil as feedstock for synthesis gas production encourages serious consideration of the gasification of bio-oil in large-scale syngas generation. Gasification of bio-oil with pure oxygen and further processing of the crude synthesis gas in Fischer-Tropsch processes may become technically and economically feasible. A strong potential exists for making syngas ($CO + H_2$), methane and ethylene, from the pyrolysis of bio-oil derived from biomass. Additionally, it can be used for methanol or hydrogen synthesis for the operation of fuel cells [11, 18-20, 23, 26, 56, 133, 134].

Finally, bio-oil can be applied as a conventional transport fuel but requires extensive upgrading [40]: full deoxygenation, which can be accomplished by two main routes:

- hydrotreating, and
- catalytic vapour cracking [24, 118].

However, both upgrading techniques often result in a decrease in the bio-oil yield and an increase in water content [121].

1.7.2. Bio-oil as a source of chemicals

Chemicals are of significant interest from an economical point of view since they typically have a higher value than fuel products [132]. Several hundred chemical constituents have been identified to date, and increasing attention is being paid to recover individual compounds or families of chemicals. The potentially higher value of speciality chemicals compared to fuels could make recovery of even small concentrations viable [9].

Chemicals that have been reported as recovered include polyphenols for phenol formaldehyde resins, fertilisers, levoglucosan, hydroxyacetaldehyde, and a range of flavourings and essences for the food industry. There are substantial problems to be overcome, such as establishing markets for the less common chemicals and devising low cost and efficient separation and refining techniques. The only currently viable market opportunity is for speciality food flavourings or liquid smoke [9, 24]. Several companies produce these liquids by adding water to the bio-oil. A red-coloured product is obtained that can be used to brown and flavour sausages, bacon, fish, etc. [135]. Another potential application of the water-soluble fraction of bio-oil is the production of calcium salts of carboxylic acids that can be used as environmentally friendly road de-icers [101, 118].

The water-insoluble "lignin-rich" fraction, also called pyrolytic lignin or even natural resin, usually constitutes 25%-30% of the whole bio-oil. It contains monomeric and oligomeric phenolics originating from native lignin degradation. This lignin-rich fraction has not yet been commercialised, but applications such as the use of the lignin as a phenol substitute in synthetic phenol formaldehyde resins has been studied extensively [21, 101, 118, 136]. These resins can primarily be employed in the manufacture of wood panels such as plywood, MDF, particle-board and OSB. The interest in the use of pyrolytic lignin is enhanced by the fact that high lignin content biomass is widely available, often at low cost and in large quantities, while phenol is a relatively expensive bulk chemical that is manufactured from increasingly costly crude oil [21]. Ensyn Technolgies Inc., for instance, already patented in 1998 the application of bio-oil as a preservative [136]. Additionally, several of the monomeric lignin derived products are of significant economic value as synthetic raw materials, flavour chemicals (e.g. vanillin), plant growth inhibitors, plant pathogen control agents and as pharmaceutical precursors [101]. Syringol and guaiacol are also found in significant concentrations in biomass derived pyrolysis oils and are used in the production of biodegradable polyesters and polyethers [41].

Some other promising application of the whole bio-oil exploits its high content of acidic functional groups. Carboxylic acids and phenols of whole or fractionated bio-oil can easily react with lime (calcium hydroxide suspension) to form calcium salts and phenates, cfr. Dynamotive's BioLime^R, which is used for control of SO_x and NO_x in coal combustion systems [24, 118]. By reacting bio-oil with ammonia, urea, or other $-NH_2$ containing materials, various imide and amide bonds are formed between carbonyl carbons and nitrogen, resulting in a biodegradable slow-release nitrogen fertiliser [9, 101, 118].

1.8. Bio-oil upgrading

Tailoring of certain physico-chemical properties of bio-oil already during or immediately after the production process has attracted increasing interest. This improvement of desired properties of the bio-oil is often referred to as 'upgrading'. Different procedures can be envisaged for the upgrading of pyrolysis oils [16]. Physical methods include hot-gas filtration, char removal in the gas phase, liquid filtration, and solvent addition. Chemical methods are, for example, reactive solvent addition and catalytic upgrading of pyrolysis vapours as well as of the crude pyrolysis oil by hydrogenation [16, 94]. In what follows, a very brief overview of some upgrading possibilities will be shared:

- Incompatibility with conventional fuels (~ oxygen content)
    - Emulsification with hydrocarbon fuels with the aid of surfactants improves the ignition characteristics of the oil [94, 126].
    - Heterogeneous catalysts during the pyrolysis process in order to modify the vapour composition of the oil before cooling down (catalytic vapour treatment) [16].
    - Pyrolysis oils can be hydrogenated after the production in order to modify the type and amount of functional groups in the oils [16].

- Stability (~ oxygen content)
  - Low temperature hydrotreatment [10] .
  - Reactive rectification using ethanol and solid acids (SO_4^{2-}/M_xO_y) (catalytic esterification). This treatment additionally results in:
    - lowered dynamic viscosity and enhanced fluidity,
    - a lower density,
    - a higher gross calorific value, and
    - a lower water content [82, 94].
- Odour
  - Esterification, especially of the small fraction of the volatile acids of the bio-oil, with ethanol, which is a renewable resource, and sulphuric acid (as a catalyst) at 323 K for 24 hours. It results in:
    - a non-irritating odour level,
    - reduced viscosity,
    - increased heating value, and
    - improved stability [94].
- High viscosity
  - Solvent (polar) addition to homogenise, reduce the viscosity and improve the bio-oil stability [94, 126].
- Solids content
  - Hot-gas filtration (= filtration over sintered metals or ceramic elements prior to condensation) for char removal. Such filters provide higher char removal efficiencies as compared to cyclones, but a lower bio-oil yield is induced. The advantage of hot-gas filtration lies in a lowering of both the viscosity of the pyrolysis oil and the rate of viscosity increase during storage [16, 94, 126].
- Low heating value
- Water content

As can be seen from previous overview, the oxygen content is problematic in two areas: incompatibility and instability. It also contributes to a lower H.H.V. Deoxygenation can best be obtained by the chemical upgrading techniques: catalytic upgrading and hydrogenation. The catalytic treatment occurs in the vapour phase during production of the bio-oil, while hydrogenation is performed on the pyrolysis oil itself after production [16]. Steam reforming of bio-oil can also be considered in order to produce sustainable hydrogen.

1.9. By-products

1.9.1. Char

The solid product from pyrolysis, called char (residue), actually contains char, mineral ash and unchanged biomass material. The pyrolysis conditions determine the chemical composition of the solid products. The char can be used in the preparation of active carbon when its pore structure and surface area are appropriate [10]. Carbon adsorbents obtained by means of pyrolysis from biomass have hydrophilic surfaces and are suitable for removing metal ions and other pollutants from water. The char can be upgraded to activated carbon with water vapour or carbon dioxide and used in various purification processes, e.g. as filter medium. The char reactivity is very strongly influenced by the treatment conditions and may be significantly increased by using high heating rates, small particle size of the biomass and short residence time at higher temperatures. However, high temperature and fast heating rates are considered to decrease the yield of char [10, 137]. Additionally, the H/C and O/C ratios of the char decrease as the pyrolysis temperature is increased [20]. The solid char has a relatively high H.H.V., which enables the char to be used as an energy source in the form of briquettes or as a char–oil/water slurry [8]. For agriculture, wood charcoal has been used as a soil amender to improve soil physical properties and as filtering agent in fish aquaria. The intrinsic mechanisms involved in its use as a soil amender have yet to be clarified [32, 35]. They can improve soil physical properties but also soil nutritional properties [32]. Char can thus be considered as an eco-material. In other words, valuable potential uses are proposed for these products as opposed to the loss of these uses if the source materials are landfilled or even incinerated [32, 137].

However, the char formed during pyrolysis can serve as a vapour-cracking catalyst and reduces the yield of bio-oil. It can also raise the viscosity of the bio-oil through catalytic reactions during storage, and is likely to be detrimental to most applications. Therefore, char should be separated from the pyrolysis reactor and/or bio-oil produced [36].

1.9.2. Pyrolytic gas

Pyrolysis gas mainly comprises CO, CO_2 and CH_4. The other components present are H_2, ethane, propane, propylene, butane, butenes, C_5, etc. [13]. The content of CO, CH_4, and other gases with high calorific values increases as reaction temperature is increased. Pyrolysis gas containing significant amount of carbon monoxide along with methane might be used as a fuel for industrial combustion purposes [10, 13, 35]. The use of pyrolysis gases as a synthesis gas requires reforming to result in the desired gas composition. The gaseous products can be considered to be a binary mixture of primary (volatilisation during pyrolysis) and secondary (secondary cracking of primary volatiles) gases [44].

The heating value of the gas obtained by pyrolysis yields between 13–15 MJ/Nm^3, much higher than the data reported by conventional air, even oxygen, gasification, approximately two times in value. This means that pyrolytic gas can be applied well to downstream gas turbine/gas engine combustion for power generation or used as a substitute for civil gas for cooking or at least for internal energy recuperation [5].

1.10. Concluding remark

Recently, Dinesh Mohan [20] wrote a critical, but more importantly very extensive review on the pyrolysis of biomass/wood for bio-oil, in which he concluded that the fast pyrolysis of biomass in the absence of oxygen has the potential to contribute to the world's need for liquid fuels and, ultimately, for chemicals production. However, the feed complexity and variability makes it difficult to define standard processes. Bio-oil production within the context of biorefineries is likely to be of greater value than self-standing bio-oil plants in the same way as petroleum refinery economics is dependent on the formation of heavy oils, lubricants, fuel oils, gasoline, kerosene, waxes, and such chemicals as the BTX fraction, ethylene, propylene, etc. Figure 1.13 shows an example of a possible bio-refinery.

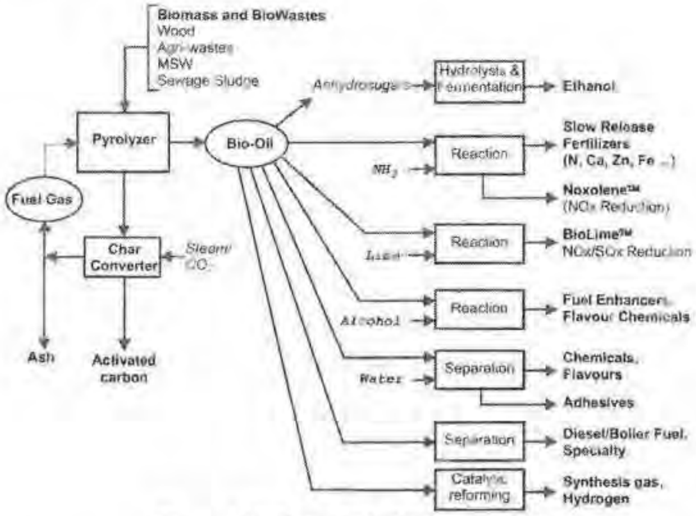

Figure 1.13: Concept of a bio-refinery [101].

Therefore, it is envisioned that pyrolysis processes in which biomass alone, or biomass co-feeds with waxes, petroleum residues, waste plastics, oxidised oils, and/or municipal wastes, can be varied and adapted to produce liquid fuels or gases of designed compositions to supply energy for transportation, heating, or electricity generation. In this way the use of raw biomass as a source of chemicals production should become more attractive within the biorefinery concept. According to Mohan [20], the current situation resembles the early days of the development of a chemicals industry from coal and coke or the later development of the early petrochemical industry.

Major technical opportunities exist to develop catalytic biomass pyrolysis processes and subsequent catalytic transformation of the bio-oils and gases produced. This area is certainly understudied and in its infancy. The applications of novel solid feed mixtures for pyrolysis, catalysts, co-gas feeds, and related approaches have not been explored very much. These topics are open for development. Adapting innovative chemical thinking should lead to major advances [20].

Following this rationale and due to the fact that most upgrading techniques, described up until now, do not result in the expected results and are still confronted with many disadvantages. It is proposed, in this research, to co-pyrolyse two totally different waste streams: (contaminated) biomass – wood and a selectively collected future plastic waste stream – biopolymers, in order to achieve a strongly pronounced win-win situation.

1.11. References

[1] European Commission. Towards a European strategy for the security of energy supply. Green Paper 2000; 1-111.

[2] Sensöz S, Angln D. Pyrolysis of safflower (Charthamus tinctorius L.) seed press cake in a fixed-bed reactor: Part 2. Structural characterization of pyrolysis bio-oils. Bioresource Technology 2008; 99:5498-504.

[3] Pestel E. The limits to growth - A report to The Club of Rome (1972) by Donella H. Meadows, Dennis I. Meadows, Jorgen Randers, William H. Behrens III.

[4] Sensöz S, Angln D, Yorgun S. Influence of particle size on the pyrolysis of rapeseed (Brassica napus L.): fuel properties of bio-oil. 2000; 19:271-9.

[5] Chen G, Andries J, Luo Z, Spliethoff H. Biomass pyrolysis/gasification for product gas production: the overall investigation of parametric effects. 2003; 44:1875-84.

[6] Demirbas A, Arin G. An overview of Biomass pyrolysis. Energy Sources 2002; 24:471-82.

[7] Babu BV, Chaurasia AS. Modeling, simulation and estimation of optimum parameters in pyrolysis of biomass. Energy Conv. Manag. 2003; 44:2135-58.

[8] Onay O, Kockar OM. Slow, fast and flash pyrolysis of rapeseed. Renew. Energy 2003; 28:2417-33.

[9] Bridgwater AV, Meier D, Radlein D. An overview of fast pyrolysis of biomass. Org. Geochem. 1999; 30:1479-93.

[10] Yaman S. Pyrolysis of biomass to produce fuels and chemical feedstocks. Energy Conv. Manag. 2004; 45:651-71.

[11] McKendry P. Energy production from biomass (part 3): gasification technologies. Bioresource Technology 2002; 83:55-63.

[12] IEA. Key world energy statistics. International Energy Agency 2008; 1-83.

[13] Goyal HB, Seal D, Saxena RC. Bio-fuels from thermochemical conversion of renewable resources: A review. Renewable and Sustainable Energy Reviews 2008; 12:504-17.

[14] Özçimen D, Karaosmanoglu F. Production and characterization of bio-oil and biochar from rapeseed cake. 2004; 29:779-87.

[15] McKendry P. Energy production from biomass (part 1): overview of biomass. Bioresource Technology 2002; 83:37-46.

[16] Scholze B. Long-term stability, catalytic upgrading, and application of pyrolysis oils - improving the properties of a potential substitute for fossil fuels. Dissertation Chemie, Universität Hamburg 2002; 1-148.

[17] Chiaramonti D, Oasmaa A, Solantausta Y. Power generation using fast pyrolysis liquids from biomass. Renewable and Sustainable Energy Reviews 2007; 11:1056-86.

[18] McKendry P. Energy production from biomass (part 2): conversion technologies. Bioresource Technology 2002; 83:47-54.

[19] Demirbas A. Sustainable cofiring of biomass with coal. Energy Conversion and Management 2003; 44:1465-79.

[20] Mohan D, Pittman CU, Steele PH. Pyrolysis of wood/biomass for bio-oil: A critical review. Energy Fuels 2006; 20:848-89.

[21] Effendi A, Gerhauser H, Bridgwater AV. Production of renewable phenolic resins by thermochemical conversion of biomass: A review. Renewable and Sustainable Energy Reviews 2008; 12:2092-116.

[22] Amen-Chen C, Pakdel H, Roy C. Production of monomeric phenols by thermochemical conversion of biomass: a review. Bioresource Technology 2001; 79:277-99.

[23] Demirbas A. Progress and recent trends in biofuels. Progress in Energy and Combustion Science 2007; 33:1-18.

[24] Bridgwater AV, Peacocke GVC. Fast pyrolysis processes for biomass. Renew. Sust. Energ. Rev. 2000; 4:1-73.

[25] Demirbas A. Effect of initial moisture content on the yields of oily products from pyrolysis of biomass. 2004; 71:803-15.

[26] Lédé J, Broust F, Ndiaye F-T, Ferrer M. Properties of bio-oils produced by biomass fast pyrolysis in a cyclone reactor. Fuel 2007; 86:1800-10.

[27] Qian Y, Zuo C, Tan J, He J. Structural analysis of bio-oils from sub-and supercritical water liquefaction of woody biomass. Energy 2007; 32:196-202.

[28] Demirbas A. Mechanisms of liquefaction and pyrolysis reactions of biomass. Energy Conv. Manag. 2000; 41:633-46.

[29] Baumlin S, Broust F, Ferrer M, Meunier N, Marty E, Lédé J. The continuous self stirred tank reactor: measurement of the cracking kinetics of biomass pyrolysis vapours. Chemical Engineering Science 2005; 60:41-55.

[30] Lin W, Song W. Power production from biomass in Denmark. J. of Fuel Chem. and Tech. 2005; 33:650-5.

[31] Karaosmanoglu F, Tetik E, Göllü E. Biofuel production using slow pyrolysis of the straw and stalk of the rapeseed plant. 1999; 59:1-12.

[32] Shinogi Y, Kanri Y. Pyrolysis of plant, animal and human waste: physical and chemical characterization of the pyrolytic products. Bioresource Technology 2003; 90:241-7.

[33] Wampler TP, *Analytical pyrolysis: an overview*, in *Applied pyrolysis handbook - second edition*, T.P. Wampler, Editor. 2006, CRC Press. p. 1-27.

[34] Debdoubi A, amarti AE, Colacio E. Production of fuel briquettes from esparto partially pyrolyzed. Energy Conversion and Management 2005; 46:1877-84.

[35] Kang B-S, Lee KH, Park HJ, Park Y-K, Kim J-S. Fast pyrolysis of radiata pine in a bench scale plant with a fluidized bed: Influence of a char separation system and reaction conditions on the production of bio-oil. Journal of Analytical and Applied Pyrolysis 2006; 76:32-7.

[36] Lee K-H, Kang B-S, Park Y-K, Kim J-S. Influence of reaction temperature, pretreatment, and a char removal system on the production of bio-oil from rice straw by fast pyrolysis, using a fluidized bed. Energy and Fuels 2005; 19:2179-84.

[37] Maniatis K. *Flash pyrolysis of wood and dried sewage sludge for liquid fuel production*. in *Biomass for energy and industry - 5th EC conference*. 1990.

[38] Onay O, Koçkar OM. Pyrolysis of rapeseed in a free fall reactor for production of bio-oil. Fuel 2006; 85:1921-8.

[39] Onay Ö, Beis SH, Koçkar ÖM. Fast pyrolysis of rape seed in a well-swept fixed-bed reactor. 2001; 58-59:995-1007.

[40] Shen L, Zhang D-K. An experimental study of oil recovery from sewage sludge by low-temperature pyrolysis in a fluidised-bed. Fuel 2003; 82:465-72.

[41] Horne PA, Williams PT. Influence of temperature on the products from the flash pyrolysis of biomass. Fuel 1996; 75:1051-9.

[42] Janse AMC, Westerhout RWJ, Prins W. Modelling of flash pyrolysis of a single wood particle. Chemical Engineering and Processing 2000; 39:239-52.

[43] Inguanzo M, Domínguez A, Menéndez JA, Blanco CG, Pis JJ. On the pyrolysis of sewage sludge: the influence of pyrolysis conditions on solid, liquid and gas fractions. Journal of Analytical and Applied Pyrolysis 2002; 63:209-22.

[44] Diebold JP, Bridgwater AV, *Overview of fast pyrolysis of biomass for the production of liquid fuels*, in *Fast pyrolysis of biomass: a handbook*, PyNe, Editor. 1999, CPL Press. p. 14-33.

[45] Tsai WT, Lee MK, Chang YM. Fast pyrolysis of rice straw, sugarcane bagasse and coconut shell in an induction-heating reactor. 2006; 76:230-7.

[46] Shuangning X, Zhihe L, Baoming L, Weiming Y, Xueyuan B. Devolatilization characteristics of biomass at flash heating rate. Fuel 2006; 85:664-70.

[47] Miao X, Wu Q, Yang C. Fast pyrolysis of microalgae to produce renewable fuels. Journal of Analytical and Applied Pyrolysis 2004; 71:855-63.

[48] Bridgwater AV, Czernik S, Piskorz J, *The status of biomass fast pyrolysis*, in *Fast pyrolysis of biomass: a handbook Volume 2*, A. Bridgwater, Editor. 2002, CPL Press. p. 1-23.

[49] Bridgwater AV, *An introduction to fast pyrolysis of biomass for fuels and chemicals*, in *Fast pyrolysis of biomass: a handbook*, PyNe, Editor. 1999, CPL Press. p. 1-14.

[50] Meier D, Faix O. State of the art of applied fast pyrolysis of lignocellulosic materials -- a review. Biores. Techn. 1999; 68:71-7.

[51] Srivastava VK, Sushil, Jalan RK. Prediction of concentration in the pyrolysis of biomass material--II. 1996; 37:473-83.

[52] Oasmaa A, Peacoke C, *A guide to physical property characterisation of biomass-derived pyrolysis liquids*. 2001, VTT. p. 1-100.

[53] Feng W, van der Kooi HJ, de Swaan Arons J. Application of the SAFT equation of state to biomass fast pyrolysis liquid. Chemical Engineering Science 2005; 60:617-24.

[54] Babu BV, Chaurasia AS. Pyrolysis of biomass: improved models for simultaneous kinetics and transport of heat, mass and momentum. Energy Conversion and Management 2004; 45:1297-327.

[55] Maiti S, Purakayastha S, Ghosh B. Thermal characterization of mustard straw and stalk in nitrogen at different heating rates. Fuel 2007; 86:1513-8.

[56] Kumar A, Wang L, Dzenis YA, Jones DD, Hanna MA. Thermogravimetric characterization of corn stover as gasification and pyrolysis feedstock. Biomass and Bioenergy 2008; 32:460-7.

[57] Thipkhunthod P, Meeyoo V, Rangsunvigit P, Rirksomboon T. Describing sewage sludge pyrolysis kinetics by a combination of biomass fractions decomposition. Journal of Analytical and Applied Pyrolysis - Pyr06 2007; 79:78-85.

[58] Tsamba AJ, Yang WH, Blasiak W. Pyrolysis characteristics and global kinetics of coconut and cashew nut shells. Fuel Process. Technol. 2006; 87:523-30.

[59] Strezov V, Moghtaderi B, Lucas JA. Computational calorimetric investigation of the reactions during thermal conversion of wood biomass. 2004; 27:459-65.

[60] Prins MJ, Ptasinski KJ, Janssen F. Torrefaction of wood - Part 1. Weight loss kinetics. J. Anal. Appl. Pyrolysis 2006; 77:28-34.

[61] Koufopanos C, Maschio G, Lucchesi A. Kinetic modeling of the pyrolysis of biomass and biomass components. Can. J. Chem. Eng. 1989; 67:75-84.

[62] Blin J, Volle G, Girard P, Bridgwater T, Meier D. Biodegradability of biomass pyrolysis oils: Comparison to conventional petroleum fuels and alternatives fuels in current use. 2007; 86:2679-86.

[63] Söderman ML. Recovering energy from waste in Sweden--a systems engineering study. 2003; 38:89-121.

[64] Barth T. A comparison of product profiles from aqueous pyrolysis of selected biomass and waste materials. Fuel Chem Div Prep 2002; 47:173-4.

[65] Zabanniotou AA. Pyrolysis of forestry biomass by-products in Greece. Energy Sources 1999; 21:395-403.

[66] Adam J, Blazsó M, Mészáros E, Stöcker M, Nilsen MH, Bouzga A, et al. Pyrolysis of biomass in the presence of Al-MCM-41 type catalysts. Fuel 2005; 84:1494-502.

[67] Ingemarsson Å, Nilsson U, Nilsson M, Pedersen JR, Olsson JO. Slow pyrolysis of spruce and pine samples studied with GC/MS and GC/FTIR/FID. Chemosphere 1998; 36:2879-89.

[68] Aho A, Kumar N, Eränen K, Salmi T, Hupa M, Murzin DY. Catalytic pyrolysis of biomass in a fluidised bed reactor. Influence of the acidity of H-Beta zeolite. Process safety and environmental protection 2007; 85:473-80.

[69] Demirbas A. The influence of temperature on the yields of compounds existing in bio-oils obtained from biomass samples via pyrolysis. Fuel Processing Technology 2007; 88:591-7.

[70] Butt DAE. Formation of phenols from the low-temperature fast pyrolysis of Radiata pine (Pinus radiata): Part I. Influence of molecular oxygen. Journal of Analytical and Applied Pyrolysis 2006; 76:38-47.

[71] Butt D. Formation of phenols from the low-temperature fast pyrolysis of radiata pine (Pinus radiata): Part II. Interaction of molecular oxygen and substrate water. Journal of Analytical and Applied Pyrolysis 2006; 76:48-54.

[72] Butt DAE. Formation of phenols from the low-temperature fast pyrolysis of Radiata pine (Pinus radiata): Part III. Influence of fluidised bed parameters. Journal of Analytical and Applied Pyrolysis 2006; 76:55-9.

[73] Branca C, Di Blasi C, Russo C. Devolatilization in the temperature range 300-600 K of liquids derived from wood pyrolysis and gasification. 2005; 84:37-45.

[74] Nilsson M, Ingemarsson Å, Pedersen JR, Olsson JO. Slow pyrolysis of birch (Betula) studied with GC/MS and GC/FTIR/FID. Chemosphere 1999; 38:1469-79.

[75] Ingemarsson A, Nilsson M, Pedersen JR, Olsson JO. Slow pyrolysis of willow (Salix) studied with GC MS and GC/FTIR/FID. Chemosphere 1999; 39:103-12.

[76] Meszaros E, Jakab E, Varhegyi G, Szepesvary P, Marosvolgyi B. Comparative study of the thermal behavior of wood and bark of young shoots obtained from an energy plantation. J. Anal. Appl. Pyrolysis 2004; 72:317-28.

[77] Nowakowski DJ, Jones JM, Brydson RMD, Ross AB. Potassium catalysis in the pyrolysis behaviour of short rotation willow coppice. Fuel 2007; 86:2389-402.

[78] Prins MJ, Ptasinski KJ, Janssen F. Torrefaction of wood - Part 2. Analysis of products. J. Anal. Appl. Pyrolysis 2006; 77:35-40.

[79] Zhang S, Yan Y, Li T, Ren Z. Upgrading of liquid fuel from the pyrolysis of biomass. 2005; 96:545-50.

[80] Gani A, Naruse I. Effect of cellulose and lignin content on pyrolysis and combustion characteristics for several types of biomass. Renewable Energy 2007; 32:649-61.

[81] Das P, Sreelatha T, Ganesh A. Bio oil from pyrolysis of cashew nut shell-characterisation and related properties. Biomass and Bioenergy 2004; 27:265-75.

[82] Junming X, Jianchun J, Yunjuan S, Yanju L. Bio-oil upgrading by means of ethyl ester production in reactive distillation to remove water and to improve storage and fuel characteristics. 2008; 32:1056-61.

[83] Predel M, Kaminsky W. Pyrolysis of rape-seed in a fluidised-bed reactor. Bioresource Technology 1998; 66:113-7.

[84] Onay O. Influence of pyrolysis temperature and heating rate on the production of bio-oil and char from safflower seed by pyrolysis, using a well-swept fixed-bed reactor. Fuel Processing Technology 2007; 88:523-31.

[85] Sensöz S, Angln D. Pyrolysis of safflower (Charthamus tinctorius L.) seed press cake: Part 1. The effects of pyrolysis parameters on the product yields. Bioresource Technology 2008; 99:5492-7.

[86] Acikgoz C, Kockar OM. Flash pyrolysis of linseed (Linum usitatissimum L.) for production of liquid fuels. Journal of Analytical and Applied Pyrolysis 2007; 78:406-12.

[87] Onay O. Fast and catalytic pyrolysis of pistacia khinjuk seed in a well-swept fixed bed reactor. Fuel 2007; 86:1452-60.

[88] Masuda T, Kondo Y, Miwa M, Shimotori T, Mukai SR, Hashimoto K, et al. Recovery of useful hydrocarbons from oil palm waste using ZrO2 supporting FeOOH catalyst. 2001; 56:897-904.

[89] Pütün AE, Uzun BB, Apaydin E, Pütün E. Bio-oil from olive oil industry wastes: Pyrolysis of olive residue under different conditions. Fuel Processing Technology 2005; 87:25-32.

[90] Fullana A, Conesa JA, Font R, Martl[combining acute accent]n-Gullón I. Pyrolysis of sewage sludge: nitrogenated compounds and pretreatment effects. Journal of Analytical and Applied Pyrolysis 2003; 68-69:561-75.

[91] Houillon G, Jolliet O. Life cycle assessment of processes for the treatment of wastewater urban sludge: energy and global warming analysis. Journal of Cleaner Production 2005; 13:287-99.

[92] Lu GQ, Low JCF, Liu CY, Lua AC. Surface area development of sewage sludge during pyrolysis. Fuel 1995; 74:344-8.

[93] Menéndez JA, Inguanzo M, Pis JJ. Microwave-induced pyrolysis of sewage sludge. Water Research 2002; 36:3261-4.

[94] Doshi VA, Vuthaluru HB, Bastow T. Investigations into the control of odour and viscosity of biomass oil derived from pyrolysis of sewage sludge. Fuel Process. Technol. 2005; 86:885-97.

[95] Domínguez A, Menéndez JA, Inguanzo M, Pís JJ. Production of bio-fuels by high temperature pyrolysis of sewage sludge using conventional and microwave heating. Bioresource Technology 2006; 97:1185-93.

[96] Font R, Fullana A, Conesa JA, Llavador F. Analysis of the pyrolysis and combustion of different sewage sludges by TG. Journal of Analytical and Applied Pyrolysis 2001; 58-59:927-41.

[97] Kim Y, Parker W. A technical and economic evaluation of the pyrolysis of sewage sludge for the production of bio-oil. Bioresource Technology 2008; 99:1409-16.

[98] Raveendran K, Ganesh A, Khilar KC. Pyrolysis characteristics of biomass and biomass components. 1996; 75:987-98.

[99] Yang H, Yan R, Chen H, Lee DH, Zheng C. Characteristics of hemicellulose, cellulose and lignin pyrolysis. 2007; 86:1781-8.

[100] Dayton DC, Brown AL, Daily JW. Biomass pyrolysis chemistry an global kinetics at high heating rates. Fuel Chem Div Prepr 2002; 47:404-5.

[101] Radlein D, *The production of chemicals from fast pyrolysis oils*, in *Fast pyrolysis of biomass: a handbook*, PyNe, Editor. 1999, CPL Press. p. 164-88.

[102] Scott DS, Paterson L, Piskorz J, Radlein D. Pretreatment of poplar wood for fast pyrolysis: rate of cation removal. Journal of Analytical and Applied Pyrolysis 2001; 57:169-76.

[103] Raveendran K, Ganesh A, Khilar KC. Influence of mineral matter on biomass pyrolysis characteristics. 1995; 74:1812-22.

[104] Lievens C, *Valorization of heavy metal contaminated biomass by fast pyrolysis*, in *PhD thesis - Research Group: Applied Chemistry*. 2007, Hasselt University: Diepenbeek. p. 221.

[105] Lievens C, Yperman J, Vangronsveld J, Carleer R. Study of the potential valorisation of heavy metal contaminated biomass via phytoremediation by fast pyrolysis: Part I. Influence of temperature, biomass species and solid heat carrier on the behaviour of heavy metals. Fuel 2008; 87:1894-905.

[106] Lievens C, Yperman J, Cornelissen T, Carleer R. Study of the potential valorisation of heavy metal contaminated biomass via phytoremediation by fast pyrolysis: Part II: Characterisation of the liquid and gaseous fraction as a function of the temperature. Fuel 2008; 87:1906-16.

[107] Koppolu L, Clements LD. Pyrolysis as a technique for separating heavy metals from hyperaccumulators. Part I: Preparation of synthetic hyperaccumulator biomass. Biomass and Bioenergy 2003; 24:69-79.

[108] Vassilev A, Schwitzguébel J-P, Thewys T, vanderLelie D, Vangronsveld J. The use of plants for remediation of metal-contaminated soils. The Scientific World Journal 2004; 9-34.

[109] Schwitzguébel J-P, vanderLelie D, Baker A, Glass DJ, Vangronsveld J. Phytoremediation: European and American trends. Journal of Soils and Sediments 2002; 1-9.

[110] Greger M, Landberg T. Use of willow in phytoextraction. International Journal on Phytoremediation 1999; 115-23.

[111] Hammer D, Kayser A, Keller C. Phytoextraction of Cd and Zn with Salix viminalis in field trials. Soil Use and Management 2003; 187-92.

[112] Klang-Westin E, Eriksson J. Potential of salix as phytoextractor for Cd on moderately contaminated soils. Plant and Soil 2003; 127-37.

[113] Koppolu L, Agblevor FA, Clements LD. Pyrolysis as a technique for separating heavy metals from hyperaccumulators. Part II: Lab-scale pyrolysis of synthetic hyperaccumulator biomass. Biomass and Bioenergy 2003; 25:651-63.

[114] Koppolu L, Prasad R, Davis Clements L. Pyrolysis as a technique for separating heavy metals from hyperaccumulators. Part III: pilot-scale pyrolysis of synthetic hyperaccumulator biomass. Biomass and Bioenergy 2004; 26:463-72.

[115] Helsen L, Van den Bulck E, Van den Broeck K, Vandecasteele C. Low-temperature pyrolysis of CCA-treated wood waste: Chemical determination and statistical analysis of metal input and output; mass balances. Waste Management 1997; 17:79-86.

[116] Helsen L, Van den Bulck E, Mullens S, Mullens J. Low-temperature pyrolysis of CCA-treated wood: thermogravimetric analysis. Journal of Analytical and Applied Pyrolysis 1999; 52:65-86.

[117] Diebold JP. A review of the chemical and physical mechanisms of the storage stability of fast pyrolysis bio-oils. NREL 2000; 1-51.

[118] Czernik S, Bridgwater AV. Overview of applications of biomass fast pyrolysis oil. Energy Fuels 2004; 18:590-8.

[119] Solantausta Y, Oasmaa A, Siplilä K, *Fast pyrolysis of forestry residues*, in *Pyrolysis and gasification of biomass and waste*, A.V. Bridgwater, Editor. 2003, CPL Press. p. 271-7.

[120] Oasmaa A, Leppämäki E, Koponen P, Levander J, Tapola E, *Physical characterisation of biomass-derived pyrolysis liquids. Application of standard fuel oil analyses*. 1997, VTT. p. 1-85.

[121] Antonakou E, Lappas A, Nilsen MH, Bouzga A, Stöcker M. Evaluation of various types of Al-MCM-41 materials as catalysts in biomass pyrolysis for the production of bio-fuels and chemicals. Fuel 2006; 85:2202-12.

[122] Boucher ME, Chaala A, Pakdel H, Roy C. Bio-oils obtained by vacuum pyrolysis of softwood bark as a liquid fuel for gas turbines. Part II: Stability and ageing of bio-oil and its blends with methanol and a pyrolytic aqueous phase. Biomass and Bioenergy 2000; 19:351-61.

[123] Oasmaa A, Meier D, *Characterisation, analysis, norms and standards*, in *Fast pyrolysis of biomass: a handbook Volume 3*, A.V. Bridgwater, Editor. 2005, CPL Press. p. 19-59.

[124] Gust S, Mclellan RJ, Meier D, Oasmaa A, Peacocke GVC, *Determination of basic fuel quality standards for biomass-derived pyrolysis liquids*, in *Pyrolysis and gasification of biomass and waste*, A.V. Bridwater, Editor. 2003, CPL Press. p. 161-9.

[125] Gust S, McLellan RJ, Meier D, Oasmaa A, Ormrod D, Peacocke GVC, *Determination of norms and standards for bio-oil as an alternative renewable fuel for electricity and heat production*, in *Fast pyrolysis of biomass: a handbook Volume 3*, A.V. Bridgwater, Editor. 2005, CPL Press. p. 9-19.

[126] Czernik S, Maggi R, Peacocke GVC, *Review of methods for upgrading biomass-derived fast pyrolysis oils*, in *Fast pyrolysis of biomass: a handbook Volume 2*, A.V. Bridgwater, Editor. 2002, CPL Press. p. 141-7.

[127] Meier D, Jesussek G, Radtke S, *Chemical stability of wood fast pyrolysis liquids*, in *Pyrolysis and gasification of biomass and waste*, A.V. Bridgwater, Editor. 2003, CPL Press. p. 221-9.

[128] Blin J, Volle G, Girard P, *Biodegradability of fast pyrolysis oil*, in *Fast pyrolysis of biomass: a handbook Volume 3*, A.V. Bridgwater, Editor. 2005, CPL Press. p. 71-95.

[129] Bridgwater AV, *Fast pyrolysis of biomass: technical requirements for commercialsation*, in *Pyrolysis and gasification of biomass and waste*, A.V. Bridgwater, Editor. 2003, CPL Press. p. 33-40.

[130] Czernik S, Bridgwater AV. Applications of biomass fast pyrolysis oil. In: Bridgwater AV, editor. Fast Pyrolysis of Biomass: A Handbook Volume 3, United Kingdom: CPL Press. 2005; 105-20.

[131] Badger PC, Fransham P. Use of mobile fast pyrolysis plants to densify biomass and reduce biomass handling costs - A preliminary assessment. Biomass and Bioenergy 2006; 30:321-5.

[132] Graham RG, Huffman DR. *Commercial aspects of rapid thermal processing (RTP™)*. in *Power production from biomass II*. 1995. Espoo, Finland.

[133] Hamelinck CN, Faaij AP, *Future prospects for production of methanol and hydrogen from biomass*, in *Pyrolysis and gasification of biomass and waste*, A.V. Bridgwater, Editor. 2003, CPL Press. p. 493-501.

[134] Hamelinck CN, Faaij AP, *Fischer-Tropsch products from biomass: system study and routing to implementation - preliminary results*, in *Pyrolysis and gasification of biomass and waste*, A.V. Bridgwater, Editor. 2003, CPL Press. p. 501-11.

[135] www.btgworld.com.

[136] Freel B, Graham RG, *Bio-oil preservatives*, in *USPTO*. 1998, Ensyn Technolgy, Inc.: US.

[137] David E. Production of eco-materials from organic wastes by pyrolysis process. Journal of Alloys and Compounds 2008; 452:188-93.

Chapter 2: Construction of a lab-scale pyrolysis reactor

Within the research group, four horizontal tubular pyrolysis reactors are available [1-3]. These are, however, not suited in view of continuous biomass processing and are rather intended for fundamental research in which detailed mass balance studies of biomass contaminated with heavy metals are investigated in small batches. Additionally, they are not able to meet the requirements of flash pyrolysis. The maximum heating rate approximates 100 K/min, which is insufficient. Therefore, a new reactor is constructed which resembles the industrial pilot installations, that claim to produce bio-products from biomass (waste) in a continuous manner, closer. In *section 2.4.* the semi-continuous home-built pyrolysis reactor, intended for fundamental research experiments, will be discussed in detail. Preliminary, a general overview of the different types of pyrolysis reactors discussed in literature is given in *section 2.2.* Additionally, the available horizontal tubular pyrolysis reactors will be described as well (*section 2.3*). The requirements to achieve a high bio-oil production will first be summarised in *section 2.1.*

2.1. Requirements

As already stated in Chapter 1, different types of pyrolysis exist. Depending on the goal of the pyrolysis, some important aspects need to be taken into account for the construction of a pyrolysis reactor. For this research, the production of bio-oil that can be applied as a source of renewable energy and as a supplier of value-added chemical feedstock is put forward. A maximum yield of organic liquid product is only met by fast (or flash) pyrolysis and requires (for atmospheric pressure operation) [4-7]:

- Intermediate and carefully controlled pyrolysis temperature,
- High to very high heating rate,
- Rapid heat transfer from the heating medium (gas and/or solid material) to the sample,
- Relatively small particle size (low temperature gradient inside the particles),
- Rapid mass transfer from the inside of the particles to the surface,
- An apparent volatiles residence time of less than a few seconds,
- A minimum amount of char particle attrition, and
- Rapid cooling or quenching of the pyrolysis vapours.

2.2. *Pyrolysis reactors* [4-10]

The centre of a fast pyrolysis process is the reactor and considerable research has focussed on several reactor types. The essential parameters in the reactor design are high heating rates and short vapour residence times.

Seven commercially available continuous reactor designs, that meet the rapid heat-transfer requirements, are briefly discussed. Generally, the reactors can be classified within the following categories:

1. fluidised bed,
2. transported and circulating fluidised bed,
3. ablative (vortex or cyclonic and rotating blade or plate),
4. rotating cone and
5. vacuum reactors.

In addition, auger reactors are briefly considered. Some of these reactor configurations have been shown to achieve liquid product yields up to 70 – 80 %, based on the starting dry biomass weight. Except for vacuum pyrolysis, high heating rates are assured. However, the very short residence time in the reaction zone is guaranteed for all methods.

2.2.1. Bubbling fluidised bed reactors

The most common reactor type suggested and used for the fast pyrolysis of lignocellulosics is the bubbling fluidised bed reactor [5]. Bubbling fluidised beds are usually referred to as fluidised beds, as opposed to circulating fluidised beds. Bubbling fluidised beds provide good temperature control and very efficient heat transfer to biomass particles, because of the high solids density in the bed. Most importantly, they produce good quality bio-oil with a high liquid product yield.

In general, fluidised beds transfer heat from a heat source to the biomass by a mixture of convection and conduction. The heat transfer limitation is within the particle, thus, requiring very small particles to obtain acceptable liquid yields. Substantial carrier gas is needed for fluidisation or transport [8]. The bubbling fluid bed utilises an inert solid, typically sand, as the heat transfer medium for the biomass particles (solid-solid heat transfer) [4]. A fluidised bed of sand arises by blowing gas through nozzles at the bottom of the reactor. The required gas flow depends on the size and mass of the fluidising material. The residence time of solids and vapours is controlled by the fluidising gas flow rate. To prevent blowing out the whirl material from the reactor, a minimum size above the fluidised bed, the so-called freeboard, is required [9]. However, char does not accumulate in the fluidised bed, but it is rapidly eluted. Char has a higher residence time than the gases and acts as an effective vapour cracking catalyst at fast pyrolysis reaction temperatures. Therefore, rapid and effective char separation is important. This is usually achieved by ejection followed by separation in one or more cyclonic separators. Thus, careful design of sand and biomass/char hydrodynamics is important.

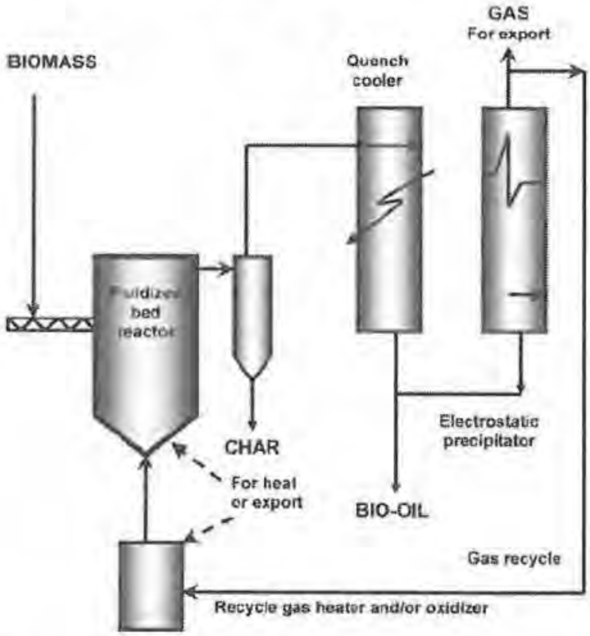

Figure 2.1: Schematic representation of a bubbling fluidised bed reactor [8].

The design of the bubbling fluidised bed type of reactor has the greatest potential for improved performance and economics, while still giving satisfactory product yields and quality [4]. Bubbling fluidised beds are a well-understood technology. They are simple to construct and operate, and they provide good temperature control and very efficient heat transfer to biomass particles, because of the high solids density in the bed.

2.2.2. Circulating fluidised bed and transported bed reactors

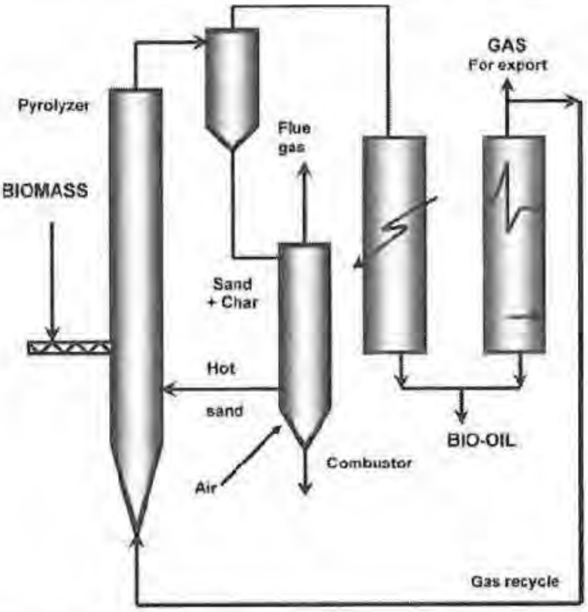

Figure 2.2: Schematic representation of a circulating fluidised bed reactor [8].

Circulating fluidised bed (CFB) and transported bed reactor systems have many of the features of bubbling fluidised beds, except that the residence time for the char is almost the same as that for the vapours [8]. These reactors easily achieve short residence times for volatiles, but biomass particle residence times are not uniform and are only a little greater than the volatiles residence time. So, solid recycling of partially reacted feed is necessary, or very fine particle sizes are required [4]. As with bubbling fluidised beds, the circulating fluidised bed of the solid heat carrier, typically sand, arises by blowing gas through nozzles at the bottom of the reactor. The fluidising material is circulated during the entire operation time. Therefore, the required gas flow is three to four times higher [9]. Because of the higher gas velocities, the char is more attrited which can lead to higher char contents appearing in the condensated bio-oil. Additionally, the heat transfer rates in CFB's are not particularly high, because they are dependent primarily on gas-solid convective transfer. Again, the heat transfer limitation is within the particle, thus, requiring very small particles of typically not more than 3 mm to obtain good liquid yields [6]. An advantage of CFBs is that they are suitable for very large throughputs. In a transported bed reactor, hot recirculated sand is often contacted with biomass in an up-flowing reactor [7].

It is common that a char combustor is employed to reheat the circulating solids. Therefore, ash carryover to the pyrolyser is possible, leading to ash build-up in the circulating solids. Biomass ash is known to be a cracking catalyst for the organic molecules in the volatile pyrolysis products and can cause a loss of volatiles from the bio-oil yield.

In conclusion, it can be stated that the sand (heat transfer medium) stays within the reactor for bubbling fluidised beds and that only char is removed during operation, while both sand and char are removed from the reactor when a circulating fluidised bed is considered. In case of circulating fluidised beds, the combustion of the char heats the sand. The hot sand is recycled back into the reactor.

2.2.3. Vacuum pyrolysis reactors

Vacuum pyrolysis involves the thermal decomposition of biomass under reduced pressure. Different from the other reactor types under consideration, vacuum pyrolysis operates at slow heating rates. The heat transfer rate, both to and through the solid biomass, is much slower than that observed in other reactors. Thus, pyrolysis products evolve from the solid phase over a longer time frame [8]. However, the pyrolytic vapours are quickly withdrawn from the reactor by the vacuum. So, the vapour residence times are comparable to those in fast pyrolysis. Therefore, the residence time of the volatile molecules is not coupled to the residence time of the biomass particles, which continue to decompose in the reactor [4, 8]. Vacuum pyrolysis is actually not a true fast pyrolysis, rather, it simulates fast pyrolysis.

Vacuum pyrolysis of biomass is generally conducted at a temperature of ~ 723 K and a total pressure of 15 kPa. The feedstock is conveyed over two horizontal plates which are heated by a mixture of molten salts. The hot salts are heated by means of a burner which can be supplied with the non-condensable gases produced during the pyrolysis process. An additional heater is optionally used to maintain a constant temperature inside the reactor. When heated, the organic matter in the feedstock decomposes into vapours which are rapidly removed from the reactor by means of a vacuum pump and are quickly condensed [7]. Total liquid yields are typically lower (60 ± 65 %) compared to the previous two methods (75 ± 80 %) [6]. The more-rapid volatilisation under vacuum minimises the extent of secondary decomposition reactions. Thus, the chemical structure of the pyrolysis products more closely resembles the original structures of the complex biomolecules that constitute the original organic material. Finally, it should be noted that larger particles are required for such reactors.

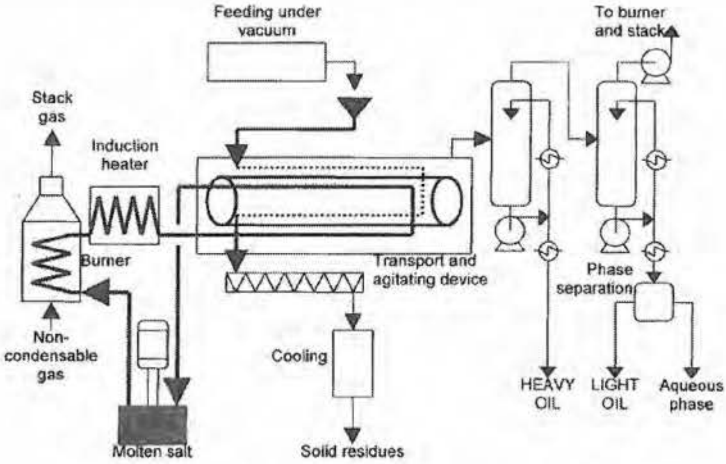

Figure 2.3: The Pyrocycling™ vacuum pyrolysis process of Pyrovac [7].

2.2.4. Ablative pyrolysis reactors [4-10]

Ablative pyrolysis relies on heat transfer occurring when a biomass particle impacts and slides over a solid hot source. The mode of reaction in ablative pyrolysis is analogous to melting butter in a frying pan: pressing down and moving the butter over the heated pan surface can significantly enhance the rate of melting and speed up heat transfer. The shearing action additionally creates more surface area, which can then contact the heat source, further increasing the heat transfer. Therefore, ablative pyrolysis is sometimes defined as 'melting' or 'thermal erosion'.

During ablative pyrolysis of biomass, heat is transferred from the hot reactor wall to "melt" wood/biomass that is in contact with it under pressure. The pyrolysis front moves unidirectionally through the biomass particle. Different from the other reactor configurations, the reaction is limited by the rate of heat supply to the reactor. When wood is pressed against a heated surface and rapidly moved during the heating, the wood melts at the heated surface and leaves a residual oil film behind which provides lubrication for successive biomass particles and also rapidly evaporates to give pyrolysis vapours for condensation and collection in the same way as for other processes.

The mechanical action or centrifugal force causes the particles to pyrolyse (thermally erode) and thus a high speed (> 1.2 m/s) relative to the hot reactor surface (< 873 K) is required. The rate of reaction is strongly influenced by:

- pressure,
- the relative velocity of wood on the heat-exchange surface,

- shear forces that reduce particle size and increase surface area, and
- the reactor's surface temperature.

As for vacuum pyrolysis, larger particles of wood are required.

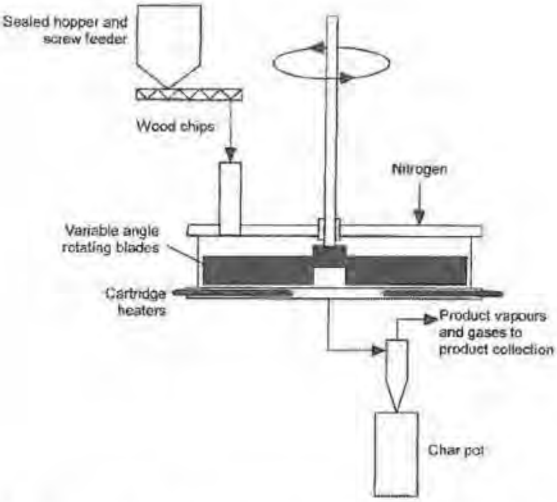

Figure 2.4: Aston University ablative pyrolysis reactor: simplified schematic [7].

Ablative pyrolysis leads to compact and intensive reactors that do not need a carrier gas, but with the penalty of a surface area controlled system combined with moving parts at high temperature. A high degree of char attrition also occurs, with the result that there can be a high carry-over of carbon into the bio-oil product.

2.2.5. Rotating cone reactors [10]

The rotating cone reactor is a compact high intensity reactor in which biomass at ambient temperature is mixed with a heat transfer medium, e.g. sand. The original aim was to achieve ablative pyrolysis where biomass particles slide and are pressing on a heated surface in a rotating cone. However, subsequent development led to a type of transported bed pyrolyser [7]. The ablative character is still under debate, because the ratio of sand and biomass is 20:1 [9].

The principle is based on the rapid heat transfer from the solid surface of a rotating cone to small wood particles, which are mixed with hot sand or a catalytically active material for a better heat transfer [5]. The reactor design consists of two cones: a stationary inner cone is heated while the outer cone is rotating. Biomass and sand are fed to the bottom of the cones. The biomass particles are ablated while they are spirally transported upwards by centrifugal forces to the top of the reactor [9]. The final char/ash residue is ejected from the top of the cone [7]. An important feature of this reactor type is the absence of carrier gas since it is the rotating action of the cone which propels the solids from the reactor entrance to its exit. Because of the absence of carrier gas, the vapour products are not diluted and their flow is minimal.

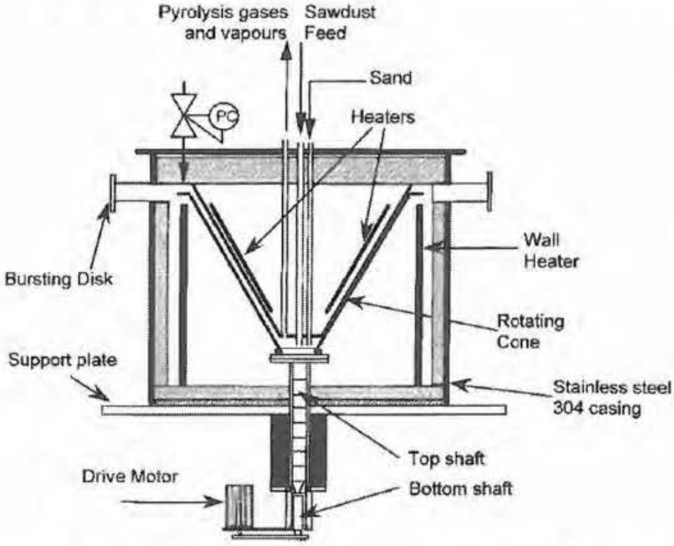

Figure 2.5: University of Twente rotating cone principle [7].

2.2.6. Vortex reactors

During flash pyrolysis in a vortex reactor, small particles are forced by a steam current with high speed (up to 1200 m/s) to rotate on the heated inner wall of a cylindrical reactor inducing ablative pyrolysis. The biomass particles, entrained in the carrier gas, enter the vortex reactor tangentially so that the particles are forced to the hot reactor wall by high centrifugal forces [7]. Accordingly, very high heat transfer rates are obtained by direct contact between the hot reactor wall and biomass particles sliding against it. The wall temperature has to be limited to a maximum of about 898 K to ensure production of a liquid film between the wall of the reactor and the particle. The isolating liquid and solid pyrolysis products arising on the surface during pyrolysis are removed by friction or vaporisation [5, 7].

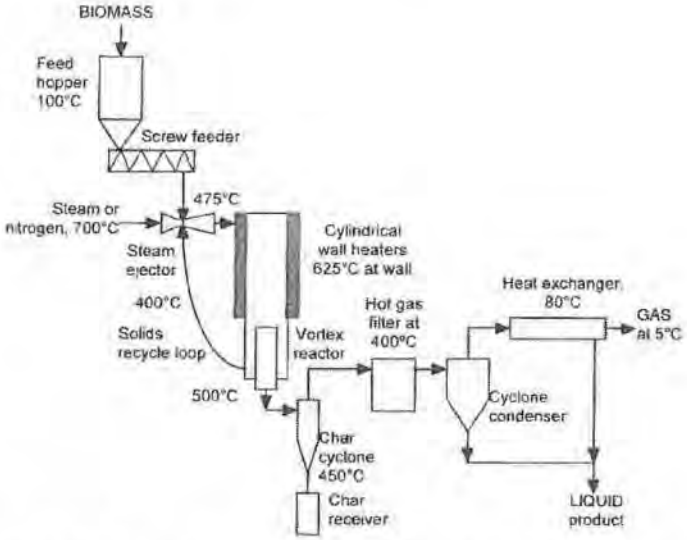

Figure 2.6: The vortex pyrolysis reactor - NREL pilot plant flow diagram [7].

2.2.7. Auger reactors

An auger-feed pyrolysis reactor, in which the "auger" (cfr. Archimedes' screw) plays a crucial role, has the following features: it is compact and does not require any carrier gas, it operates at lower process temperatures (which can be in the range of 673 and 1073 K), and operates as a continuous process. Augers are used to move biomass feedstock through an oxygen-free cylindrical heated tube. A passage through the tube raises the feedstock to the desired pyrolysis temperature, causing it to devolatilise and gasify. Char is produced and gases are condensed as bio-oil, while noncondensables are collected as biogas. The vapour residence time can be modified by increasing the length of the heated zone through which the vapours pass prior to entering the condenser train.

2.2.8. Heat transfer considerations [6]

There are two important features of heat transfer in a pyrolysis reactor:

1. to the heat transfer medium (solid reactor wall in ablative reactors, gas and solid in fluid and transport bed reactors, gas in entrained flow reactors);
2. from the heat transfer medium to the pyrolysing biomass. Additionally, two main ways of heating biomass particles in a fast pyrolysis system can be considered:

a. gas-solid heat transfer where heat is transferred from the hot gas to the pyrolysing biomass particle by primary convection, and
b. solid-solid heat transfer with mostly conductive heat transfer.

It should be noted that some radiation effects occur in all reactors.

Since the thermal conductivity of biomass is very poor (0,1 W/mK along the grain, ca. 0.05 W/mK cross grain), reliance on gas-solid heat transfer means that biomass particles have to be very small to fulfil the requirements of rapid heating to achieve high liquid yields. Claimed temperature increases of 10^4 K/s may be achieved at the thin reaction layer but the low thermal conductivity of wood/biomass will prevent such temperature gradients throughout the whole particle. As particle size increases, liquid yields reduce as secondary reactions within the particle become increasingly significant. Additionally, the low thermal conductivity of biomass gives low heating rates through larger particles and leads to increased char formation. Hot char is known to be catalytically active: it cracks organic vapours to secondary char, water and gas both during primary vapour formation and in the reactor gas environment. Therefore, the rapid char removal from the hot reactor environment (avoiding slow pyrolysis reactions) and minimal contact with the pyrolysis vapour products (secondary char formation) is essential for large particles (> 2 mm).

Remark 1:

- The important feature of ablative heat transfer is that the contact of the biomass and the hot solid abrades the product char off the particle exposing fresh biomass for reaction. This removes particle size limitations in certain ablative reactors, but at the expense of producing micro-carbon which is difficult to remove from the vapour phase and is transferred to the liquid product.

Remark 2:

- Fluidised bed reactors inherently utilise the good solids mixing to transfer approximately 90% of the heat to the biomass by solid-solid heat transfer with a probable small contribution from gas-solid convective heat transfer of up to 10%.
- Circulating fluidised bed and transport reactors also rely on both gas-solid convective heat transfer from the fluidising gas and solid-solid heat transfer from the hot fluidising solid although the latter may be less significant than for fluidised beds due to the lower solids bulk density.

- In general, the fluidised bed reactors are considered as the most popular because of their simple design [9]. Recently, modern heating technologies are being investigated such as microwave and induction heating [11-17].

2.3. Horizontal tubular pyrolysis reactors

Within the research group, small horizontal tubular pyrolysis reactors are available. The tubular reactors are especially designed, after several optimisation experiments, for a horizontal Nabertherm oven and consist of a (1) char/ash, (2) tar, (3) oil and (4) gas collector, see Figure 2.7 [1]. The core of the reactor is a horizontal tube constructed in quartz. There is opted for the use of a solid heat carrier to improve the heat transfer in the reactor [18]. Two different matrices, of different particle sizes, are used: sand (Merck; number 107712) and fumed silica (Sigma, 0.007 µm; number S5130). It can be stated that the silica used does not play any catalytic role during the pyrolysis process [19].

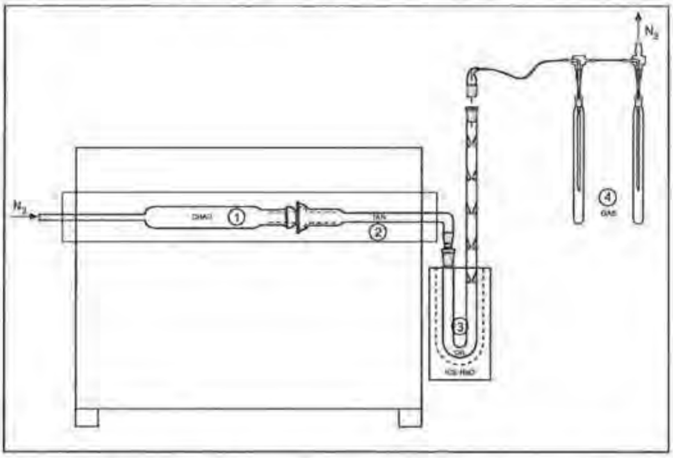

Figure 2.7: Horizontal tubular pyrolysis reactor set-up of the Hasselt University [1].

The pyrolysis experiments are performed with a 3 - 5 g of biomass feedstock, mixed with sand (~ 12 g) or fumed silica (~ 0.5 g). N_2 is used as sweep gas (typically 30 ml/min). Prior to heating, the sample is placed into the pyrolysis reactor together with the sand or fumed silica. The horizontal Nabertherm oven heats the reactor, the solid heat carrier and, therefore, the sample as well with an intermediate heating rate (typically 35 K/min) which does not meet the requirements of flash pyrolysis. Interestingly, a sample drying step is incorporated into the pyrolysis process: the sample retained in (1) can be heated up to, for instance, 423 K and kept isothermally for a certain period, for instance 10 minutes, in order to evaporate the initial moisture of the sample into the gas phase.

Afterwards the temperature is further increased to the final pyrolysis temperature with the same intermediate heating rate, using salty ice ($263 K \leq T < 273 K$) to condense the condensable gases into an oil phase in (3). The noncondensable pyrolytic gases are collected in separate solutions in (4), composed of a mixture of 10 % HNO_3 and 10 % H_2O_2, respectively. Finally, an isothermal period of, for instance, 15 minutes at the actual pyrolysis temperature is implemented [1].

2.4. Semi-continuous home-built pyrolysis reactor

The goal of this research is to produce sufficient amounts of bio-oil with a good quality. The horizontal tubular pyrolysis reactors described above are, however, too small to obtain a sufficient amount of bio-oil. Additionally, the experimental set-up does not meet the requirements of flash pyrolysis, partly caused by the insufficient maximum heating rate (< 100 K/min). In short, these reactors are more suitable for other aspects related to fundamental research of biomass waste streams then for

- the production of high amounts of bio-oil with good quality, or
- upgrading of pyrolysis conditions to obtain bio-oil with improved characteristics, or
- simulating commercially available continuous pyrolysis reactors.

As the horizontal tubular pyrolysis reactors do not satisfy the goal of this research, the construction of a new and bigger reactor capable of ensuring flash pyrolysis: the semi-continuous home-built pyrolysis reactor is executed. Combining basic technological and thermodynamic considerations with expertise concerning biomass pyrolysis within the research group, a first semi-continuous pyrolysis reactor has been constructed (*2.4.1*). After some preliminary tests further improvements have been executed, leading to an equipment (*2.4.2*) suitable to pursue the research goals: exercising fundamental research experiments closely related to industrial pyrolysis plants.

2.4.1. Initial pyrolysis reactor

Based on the known commercially available pyrolysis reactors (*section* 2.2.), the initial reactor has been constructed, Figure 2.8. As for many reactor configurations, a heat transfer medium (sand) is used to induce flash pyrolysis and to enhance the intensity of reaction. Thus, an effective solid-solid heat transfer is applied. The biomass particles are injected when the heat transfer medium has reached the pre-set pyrolysis temperature (PT). During the entire pyrolysis process, an Archimedical screw is used to:

- create optimal semi-continuous flash pyrolysis conditions,

- ensure a homogeneous temperature sand bed,
- provide homogeneous biomass/sand mixture, and
- enhance the impact of the hot sand on the biomass particles.

As for fluidised bed reactors, it is intended to utilise the intense solids mixing to transfer approximately 90% of the heat to the biomass by solid-solid (conductive) heat transfer with a probable small contribution from gas-solid convective heat transfer of up to 10% [6]. The heat transfer limitation is within the biomass particle, thus, requiring very small particles to obtain optimal liquid yields.

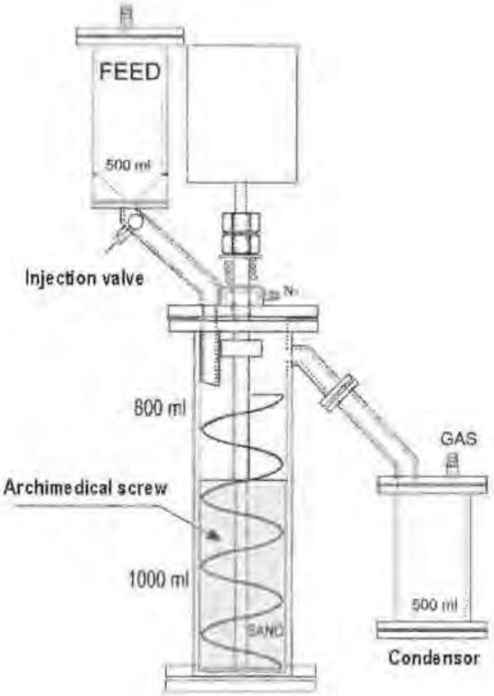

Figure 2.8: The initial semi-continuous pyrolysis reactor.

Unfortunately, a few unexpected anomalies with the initial set-up appeared to occur. First, a free-fall injection system seemed not to be suited for small biomass particles. Apparently "bridges" were formed by the biomass particles, blocking the feeder and inhibiting the free-fall of biomass particles. By inserting a pin in the injection system and moving it manually during pyrolysis, the biomass bridges could be overcome and, if necessary, destroyed. By this, the biomass could partly be injected into the hot reactor zone, but confronted us with a second processing anomaly: complete pyrolysis did not occur (partial pyrolysis). Char, semi-pyrolysed and unpyrolysed material was recuperated in the condensation vessel. The biomass particles seemed to float over the hot sand and were flung to the reactor outlet without actually impacting the biomass particles with the hot sand. Therefore, the injection system has been adapted (see *section* 2.4.2.), which resulted in the improved pyrolysis reactor that is still operative today.

2.4.2. Improved pyrolysis reactor

2.4.2.1. Experimental flash pyrolysis set-up

The improved pyrolysis reactor (360 mm high with a diameter of 88 mm), Figure 2.9 (part a), is manufactured in stainless steel (AISI 304). Within the reactor, the heat transfer medium (white sand, < 1mm, ± 700 g or 450 ml) is inserted providing a high solids density. Before use, this sand is dried at 383 K to ensure that all water is removed. Preliminary, the sand is pre-treated in batch at 873 K to remove all impurities. During the entire process, the sand is in constant motion with the aid of an Archimedical screw, of which the blades are moderately perforated, ensuring a homogeneous temperature sand bed operating system. This Archimedical screw also serves as a pre-heating gas inlet system. The reactor (and the sand) is externally heated by a tailored heating jacket (Horst GmbH, Lorsch, Germany).

The injection system, Figure 2.9 (part b), is manufactured in stainless steel (AISI 304) as well. It consists of a reservoir with a volume of 600 ml and an injector. The injector is a hollow tube connecting the reservoir, which contains the biomass, with the reactor. Via this tube, the biomass is transported into the reactor by means of a second Archimedical screw with a controlled feeding rate (1 – 120 rpm). A second gas inlet is situated inbetween the biomass container and the injector.

The recuperation system, Figure 2.9 (part c), is a stainless steel (AISI 304) collector vessel with a volume of 580 ml and is kept at room temperature. Inbetween the reactor and the collector, a small water cooler is constructed to quench the gases. On top of the collector vessel, a cold trap made out of copper (kept at 77 K with liquid nitrogen) is installed to collect all condensable gases. The non-condensable gases exit the recuperation system via the chimney into a fume hood. In industrial pyrolysis plants, these noncondensable gases can be used for internal energy recuperation (e.g. attaining the pyrolysis temperature and/or biomass drying).

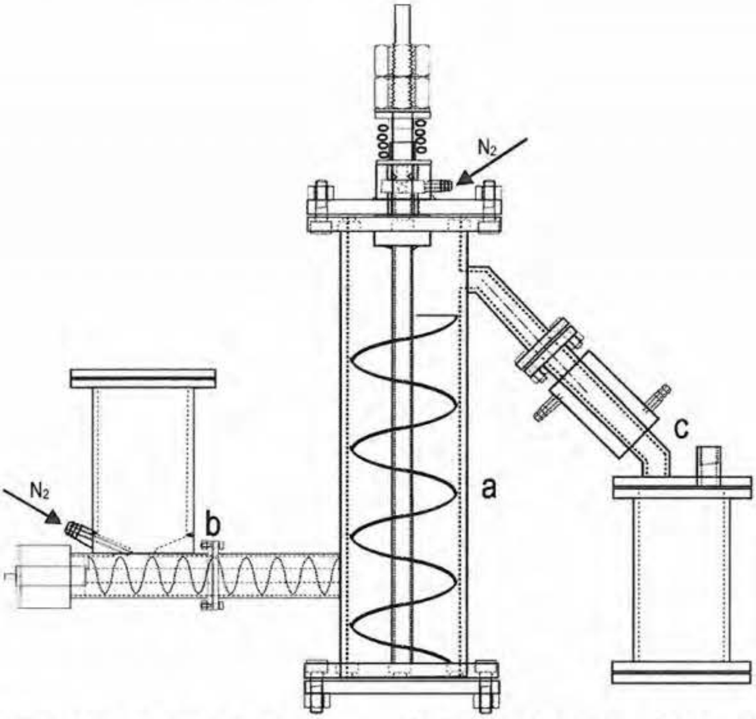

Figure 2.9: The final pyrolysis set-up: a, reactor containing the heat transfer medium (at PT); b, injection system (at RT) with a biomass reservoir; and c, recuperation system (at RT) with an additional water cooler.

2.4.2.2. Procedure

Preliminary, all materials (± 700 g sand and ± 100 g input) are dried at 383 K. When heating has started, nitrogen gas continuously enters the reactor via two ways to guarantee an "oxygen-free", rather oxygen poor, environment:

1. via the hollow shaft of the Archimedical screw in the reactor which also acts as a gas pre-heater (70 ml/min), and
2. via the injection system (70 ml/min).

As soon as the sand inside the reactor reaches the pyrolysis temperature (PT), the nitrogen flow is stopped and the injection system is started. By this, the biomass material is inserted into the reactor at a rate of 20 rpm. In this way, an injection rate of approximately 140 ml per minute is achieved. The biomass subsequently undergoes a flash pyrolysis and is converted into volatiles which mainly condense into the recuperation system as condensables, mostly bio-oil. Figure 2.10 represents a flash pyrolysis flow chart customised to the findings of this research.

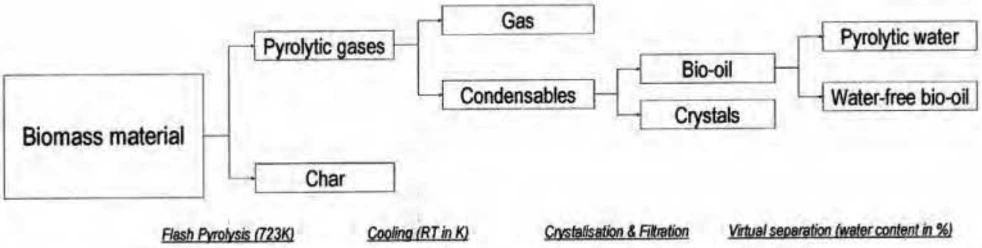

Figure 2.10: Extended schematic representation of the flash pyrolysis flowchart.

During the entire experiment (heating, injection, pyrolysis,…), temperature measurements are taken at the top of the sand bed with a thermocouple type K and are continuously monitored by coupling an ATAL Smart Reader Plus with a PC.

2.4.2.3. Reactor evaluation

The pyrolysis reactor results in a liquid collection that is significantly lower (± 50 %) compared to the bio-oil yields of 60, 70 and even 80 % described in literature. Some possible reasons of the lower bio-oil yield are discussed:

- No 'perfect' flash pyrolysis is induced. The biomass is injected from the storage vessel (Figure 2.9 (part b)) into the heated reactor by a horizontal Archimedical screw rotating at 20 rpm. The time required for injection can amount up to a few seconds. The hollow shaft in which the biomass is transported shows a gradual temperature increase from room temperature to the reactor temperature. This diminishes the temperature shock that the biomass undergoes when impacting with the hot sand while entering the reactor. Only recently, the injection system is further improved by constructing a water cooler around the hollow tube. For the results discussed in this work, the additional water cooler was not installed yet.
- Additionally, an increased chance for secondary reactions might be applicable for the pyrolysis reactor under consideration:
    - A relatively high homogeneous temperature sand bed is present. Gases must pass almost the entire bed upwards before they leave the reactor to be quenched in the condensation system. This might result in an increased gas residence time at the pyrolysis temperature.
    - The biomass char particles stay behind inside the reactor and the homogeneous temperature sand bed. Char is a cracking catalyst for volatiles, and prolonged

contact of bio-oil vapours with char can result in secondary product degradation, which may occur when hot filtration of char dust is practised or when a large circulating load of partially charred biomass particles is involved [4, 5]. Possibly, the negative char effect might be circumvented by the high sand-to-char-ratio applied. Additionally, relatively small amounts of biomass are pyrolysed during the semi-continuous batch pyrolysis experiments.

- Finally, it is well known that the liquid collection after pyrolysis is one of the technical difficulties owing to the aerosol nature of the volatile products. Many systems combine a quencher with an electronic or electrostatic precipitator (ESP) for recovering aerosols. Meier et al. consider the integration of an electrostatic precipitator after the cold traps as the most effective way to separate condensables from the product gases [5, 20]. The pyrolysis reactor under consideration, however, does not consist of such a precipitator.

2.5. References

[1] Lievens C, *Valorization of heavy metal contaminated biomass by fast pyrolysis*, in *PhD thesis - Research Group: Applied Chemistry*. 2007, Hasselt University: Diepenbeek. p. 221.

[2] Lievens C, Yperman J, Vangronsveld J, Carleer R. Study of the potential valorisation of heavy metal contaminated biomass via phytoremediation by fast pyrolysis: Part I. Influence of temperature, biomass species and solid heat carrier on the behaviour of heavy metals. Fuel 2008; 87:1894-905.

[3] Lievens C, Yperman J, Cornelissen T, Carleer R. Study of the potential valorisation of heavy metal contaminated biomass via phytoremediation by fast pyrolysis: Part II: Characterisation of the liquid and gaseous fraction as a function of the temperature. Fuel 2008; 87:1906-16.

[4] Scott DS, Majerski P, Piskorz J, Radlein D. A second look at fast pyrolysis of biomass-the RTI process. J. Anal. Appl. Pyrolysis 1999; 51:23-37.

[5] Meier D, Faix O. State of the art of applied fast pyrolysis of lignocellulosic materials -- a review. Biores. Techn. 1999; 68:71-7.

[6] Bridgwater AV, Meier D, Radlein D. An overview of fast pyrolysis of biomass. Org. Geochem. 1999; 30:1479-93.

[7] Bridgwater AV, Peacocke GVC. Fast pyrolysis processes for biomass. Renew. Sust. Energ. Rev. 2000; 4:1-73.

[8] Mohan D, Pittman CU, Steele PH. Pyrolysis of wood/biomass for bio-oil: A critical review. Energy Fuels 2006; 20:848-89.

[9] Scholze B. Long-term stability, catalytic upgrading, and application of pyrolysis oils - improving the properties of a potential substitute for fossil fuels. Dissertation Chemie, Universität Hamburg 2002; 1-148.

[10] Wagenaar BM, Venderbosch RH, Carrasco J, Strenziok R, vanderAa BJ, *Rotating cone bio-oil production and applications*. Progress in thermochemical biomass conversion, ed. A.V. Bridgwater. Vol. 2. 2001: Blackwell Science.

[11] Chen M-q, Wang J, Zhang M-x, Chen M-g, Zhu X-f, Min F-f, et al. Catalytic effects of eight inorganic additives on pyrolysis of pine wood sawdust by microwave heating. 2008; 82:145-50.

[12] Domínguez A, Menéndez JA, Inguanzo M, Pis JJ. Investigations into the characteristics of oils produced from microwave pyrolysis of sewage sludge. 2005; 86:1007-20.

[13] Domínguez A, Menéndez JA, Inguanzo M, Pís JJ. Production of bio-fuels by high temperature pyrolysis of sewage sludge using conventional and microwave heating. Bioresource Technology 2006; 97:1185-93.

[14] Domínguez A, Menéndez JA, Fernández Y, Pis JJ, Nabais JMV, Carrott PJM, et al. Conventional and microwave induced pyrolysis of coffee hulls for the production of a hydrogen rich fuel gas. 2007; 79:128-35.

[15] Huang YF, Kuan WH, Lo SL, Lin CF. Total recovery of resources and energy from rice straw using microwave-induced pyrolysis. 2008; 99:8252-8.

[16] Tsai WT, Lee MK, Chang YM. Fast pyrolysis of rice straw, sugarcane bagasse and coconut shell in an induction-heating reactor. 2006; 76:230-7.

[17] Tsai W-T, Chang J-H, Hsien K-J, Chang Y-M. Production of pyrolytic liquids from industrial sewage sludges in an induction-heating reactor. In Press, Corrected Proof:

[18] Lappas AA, Samolada MC, Iatridis DK, Voutetakis SS, Vasalos IA. Biomass pyrolysis in a circulating fluid bed reactor for the production of fuels and chemicals. 2002; 81:2087-95.

[19] Raveendran K, Ganesh A, Khilar KC. Pyrolysis characteristics of biomass and biomass components. 1996; 75:987-98.
[20] Oasmaa A, Peacoke C, *A guide to physical property characterisation of biomass-derived pyrolysis liquids*. 2001, VTT. p. 1-100.

Chapter 3: Description of the experimental approach, materials investigated and methods applied

3.1. Experimental approach

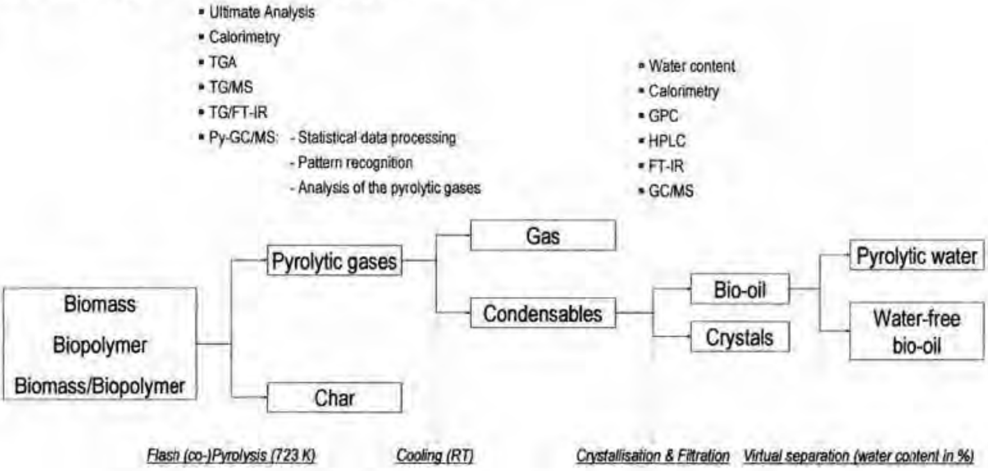

Figure 3.1: Experimental approach projected on the extended pyrolysis flowchart.

The extended pyrolysis flowchart, shown above, summarises the entire experimental approach of this research. As starting material for flash pyrolysis, biomass, biopolymers and biomass/biopolymer blends are put forward. These are investigated with a multitude of complementary analytical techniques (*section 3.4*): ultimate analysis, calorimetry, thermogravimetry (TGA); and hyphenated techniques (*section 3.5*): thermogravimetry/mass spectrometry (TG/MS), thermogravimetry/Fourier transform infrared spectroscopy (TG/FT-IR) and pyrolysis-gas chromatography/mass spectrometry (Py-GC/MS). These analytical techniques are applied on the starting material to analyse the evolving volatile components during slow and flash (co-)pyrolysis. Hyphenated techniques allow the online identification of components, classes of compounds and functional groups of the condensable and noncondensable pyrolytic gases [1]. The actual flash (co-)pyrolysis (*section 3.3*) of the input materials is performed at 723 K with the semi-continuous home-built pyrolysis reactor (discussed in Chapter 2) and results, after condensation, in condensables which includes bio-oil and occasionally crystals. The condensables, on their turn, are also investigated with a myriad of complementary analytical techniques (*section 3.6*): azeotropic distillation, calorimetry, gel permeation chromatography (GPC), liquid chromatography (HPLC), Fourier transform infrared spectroscopy (FT-IR) and gas chromatography/mass spectrometry (GC/MS).

It should be noted that the final separation shown in the extended pyrolysis flowchart (of bio-oil into pyrolytic water and water-free bio-oil – Figure 3.1)) is merely virtual and is only calculated based on the water content of the bio-oil. In practice, no real separation of bio-oil into pyrolytic water and water-free bio-oil is performed, because up until now no such separation method is available. For instance, simple distillation at increased temperature induces an increased instability of the bio-oil and results into a viscous tar-like residue.

No analysis has been performed on the pyrolytic char/ash residue and gas fraction (noncondensable pyrolytic gas fraction after condensation), because they are out of the scope of this research. For biomass contaminated with heavy metals, these fractions become as important as the bio-oil itself. However, for this research, only uncontaminated biomass is investigated.

3.2. Materials

3.2.1 Biomass

The general focus of this research is directed towards the flash pyrolysis and flash co-pyrolysis of uncontaminated biomass waste streams in order to produce bio-oil that can be applied as a source of energy and as a supplier of value-added chemical feedstock. As a reference biomass, willow – Salix, harvested on the university campus, is applied. The willow branches (the leaves are not taken into account in this study) are cut and dried at room temperature before being shredded into small particles (~2mm) by a Retsch SM100 mill. A particle size of < 2mm guarantees a fast inner-heating rate during pyrolysis and thus ensures a flash pyrolysis of the entire particle [2]. Prior to analysis, the biomass is dried at 378 K till constant weight is obtained.

3.2.2. Biopolymers

The conversion of wood biomass residues as well as polymer waste is an important problem of the environmental protection [3]. The use of co-pyrolytic techniques on biomass/plastic ratios has already been investigated on 'traditional' synthetic plastics [3-6]. Co-pyrolytic techniques provide an alternative way to dispose and convert waste (like plastics) and cellulose (or lignine) derived materials into high value feedstock. The specific benefits of this method potentially include:

- the reduction of the volume of the waste,
- the recovery of chemicals (feedstock recycling) and
- the replacement of fossil fuels [4].

Sharypov et al. [3-6] demonstrated that mixtures of different types of biomass wood and polyolefinic polymers (polyethylene (PE), atactic-polypropylene (aPP) and isotactic-polypropylene (iPP)) can be radically converted to liquid products by slow pyrolysis. The studied polyolefins are thermally degraded at a higher temperature than biomass. The optimum temperature for biomass/plastic mixture conversion which corresponds to the maximum yield of light liquids is, however, only 673 K [3]. For the liquid production, the biomass/plastic ratio in the feedstock is the most important parameter. In general, the evolution of products is additive in the range 100 to 50 % biomass (in weight). For the runs with plastic content higher than 50 %, non-additive phenomena (synergy) occur, leading to higher light liquid production. Sharypov et al. conclude that the co-pyrolysis of wood biomass and polyolefins is a process of synthetic polymer depolymerisation assisted by biomass. The free radical degradation mechanism of polymers is a chain reaction involving thermal initiation, depropagation, intramolecular and intermolecular transfer and termination of radicals [3]. Biomass, whatever its origin, leads to solid, liquid (water) and gas at a temperature lower than 673 K, while the polyolefins lead to liquid and gaseous olefins and parrafins [4]. The solids from the biomass provide radicals, enhancing the homolytic scission of the polyolefinic chains and explaining the observed synergy. Marin et al. note that the composition of the liquids is mainly dependent on the origin of the polymer and only slightly connected with the proportion of biomass in the mixture [4].

Zhou et al. studied the thermogravimetric characteristics and kinetics of polyolefins (high density polyethylene (HDPE), low density polyethylene (LDPE) and polypropylene (PP)) and biomass blends co-pyrolysis and indicated a significant synergistic effect on the weight loss at the high-temperature region (800 – 923 K) [7]. Matsuzawa investigated the pyrolysis of pure cellulose, polyethylene (PE), polypropylene (PP), polystyrene (PS), poly(vinyl chloride) (PVC), poly(vinylidene chloride) PVdC and mixtures of cellulose with polymers by thermal analysis to study the pyrolysis of municipal solid waste [8]. Cellulose was shown only to interact with PVC and PVdC during pyrolysis. Co-pyrolysis experiments have also been executed on coal/biomass and coal/polymer blends [9, 10].

Biopolymers, which are a special kind of plastic, originate from renewables and/or are biologically degradable. Despite their biodegradability, however, most biopolymers still have to be considered as waste, since it would be ecologically unacceptable to dispose of them in the environment [11]. The physical and chemical structures of the biopolymers are the basic properties that affect the degradation and the biodegradation [12]. Some basic properties are mentioned informatively:

- Molecular structure,
- Complexity (functional groups),
- Length of the polymer chain, and
- Crystallinity.

Based on their origin, biopolymers can be classified into two main categories:

- Biopolymers produced on the basis of renewable feedstock, and
- Biopolymers with biodegradable characteristics but manufactured from petrochemical resources.

De Schoenmakere [11] notes that not all biodegradable materials are compostable and that not all compostable materials have a biological origin.

The renewable biopolymers, on their turn, can be separated into three groups [11, 13].

- Biopolymers directly obtained from biomass: e.g. cellulose, proteins, fats and polysaccharides.

  Three different biopolymers that belong to the group of polysaccharides, and more specifically the subgroup of starch based biopolymers, are considered for this research: e.g. **corn starch**, **potato starch** and **Solanyl**.
- Biopolymers directly produced by micro-organisms: e.g. cellulose, polysaccharides and polyhydroxyalkanoates (PHA's) .

  Polyhydroxybutyrate (**PHB**), an aliphatic polyester, is the most applied PHA. PHB can be produced by bacteria, yeasts, and/or plants [11, 14]. The production of PHB is, however, often combined with genetic modification. In this research PHB from Biomer – Germany is used.
- Biopolymers formed via chemical synthesis: e.g. polyesters

  For this research **polylactic acid** (**PLA**) is investigated. PLA is obtained by polymerisation of the renewable fermentation product lactic acid. Lactic acid can be synthesised by chemical means, but is generally produced by the microbial fermentation of sugars and starch [11, 15]. PLA shows to be one of the worst biodegradable biopolymers [11, 12, 14]. Technically, PLA can be recycled. The amounts produced are, on this moment, too limited to make the recycling process economically viable.

Biopearls is additionally investigated for this research. Biopearls stems from plant material [16, 17]. However, the exact origin of this biopolymer is unknown to the author.

EastarBio is chosen as a synthetic biopolymer. EastarBio is a polytetramethyleneadipate-terephthalate and belongs to the modified polyethylene terephthalates (PET). Such petrochemical biopolymers can be manufactured via the classical, but slightly modified, synthetic route of crude oil.

In this research, the flash co-pyrolysis of biomass/biopolymer blends is proposed as an alternative waste treatment option and is expected to act as an upgrading step during the pyrolysis of biomass. Therefore, the seven different biopolymers (PLA, corn starch, PHB, Biopearls, Eastar, Solanyl and potato starch) are investigated as potential pyrolysis "enhancers". The flash pyrolysis of biomass (willow) serves as a reference. The biopolymers are shredded with a Retsch ZM1000, because, as for biomass, a particle size < 2mm is required to ensure flash pyrolysis of the entire particle.

3.3. Flash (co-)pyrolysis

Flash (co-)pyrolysis is executed with the semi-continuous home-built pyrolysis reactor, which is discussed in more detail in Chapter 2. Preliminary, all materials (± 700 g sand, which was already pre-treated in batch at 873 K to remove all impurities, and ± 100 g input material (willow, biopolymers, and willow/biopolymer blends)) are dried at 383 K. During the entire process, the sand is in constant motion with the aid of an Archimedical screw, ensuring a homogeneous temperature sand bed operating system. When heating has started, nitrogen gas continuously enters the reactor via two ways to guarantee an "oxygen-free" (rather oxygen poor) environment: firstly, via the hollow shaft of the Archimedical screw in the reactor which also acts as a gas pre-heater (70 ml/min), and secondly via the injection system (70 ml/min). As soon as the sand (heat transfer medium) inside the reactor reaches the pyrolysis temperature (PT), the nitrogen flow is stopped and the injection system is started; inserting the willow, biopolymer or willow/biopolymer blend into the reactor at a rate of 20 rpm. In this way, an injection rate of approximately 140 ml per minute is achieved. The willow, biopolymer or willow/biopolymer blend subsequently undergoes a flash pyrolysis and is converted into volatiles which mainly condense into the recuperation system as condensables, mostly bio-oil and occasionally crystals (Figure 3.1). The non-condensable gases exit the recuperation system via the chimney into a fume hood. The char/ash residue stays behind in the reactor together with the sand.

During the entire experiment (heating, injection, pyrolysis,...), temperature measurements are taken at the top of the sand bed with a thermocouple type K. An ATAL Smart Reader Plus is used to monitor the temperature evolution continuously during heating and pyrolysis on a PC.

After flash (co-)pyrolysis, the pyrolysis yields are immediately calculated:

- The bio-oil is decanted into a storage vessel manufactured from glass and weighed afterwards.
- The amount of char/ash residue is obtained by substraction of the amount of sand present after combustion at 873 K from the amount of sand and char/ash present in the reactor after pyrolysis. This procedure, however, results in some unavoidable measurement errors.
- The gas yield is calculated by difference.

3.4. Characterisation of the input materials

Prior to pyrolysis, the CHNS- and O-content, the higher heating value (H.H.V.) and the thermal degradation behaviour of the biomass and biopolymer samples are investigated.

3.4.1. Ultimate Analysis

The CHNS- and O-content of the biomass and biopolymers are determined via two distinct experiments, using a FlashEA 1112 Elemental Analyser of Thermo Electron Corporation. Approximately 2 – 4 mg of sample is introduced into a container, which is injected by an autosampler. In case of CHNS-determinations, 5 – 10 mg vanadiumpentoxide is added to the sample as a combustion catalyst. 2,5-Bis(5-tert-butyl-benzoxazol-2-yl)thiophene (BBOT – $C_{26}H_{26}N_2O_2S$) and L-cystine ($C_6H_{12}N_2O_4S_2$) are used as standards for the CHNS- and O-determinations, respectively. All measurements have been performed, at least, in twofold.

Ultimate analysis has also been performed on the bio-oil samples, but did not result in valuable information mainly because of the fact that the elemental analyser is only applicable on solids. However, Chromosorb® W/AW (80 - 100 mesh) of ThermoFinnigan can be used as an absorbent for liquids, but did not result in good measurements either due to the volatility of the bio-oils under consideration. The obtained results will therefore not be discussed in this thesis.

3.4.2. Calorimetry

Calorimetric measurements are performed to determine the initial energy content, when burnt in air, (higher heating value – H.H.V.) of the starting materials. These values will be confronted with the H.H.V.'s of the condensables obtained after flash (co-)pyrolysis with the pyrolysis reactor to calculate a simplified energy recuperation ratio for the flash (co-)pyrolysis experiments.

The samples (approximately 1 g) are analysed with an IKA C5003 control calorimeter equipped with an IKA KV 600 Digital water cooler and a Sartorius CP224S analytical balance. Oxygen is connected to the system to pressurise the bomb. Measurements of the H.H.V.'s are executed in dynamic mode and the calibration of the system is performed with benzoic acid (palleted, C723) of IKA with a higher heating value of 26.46 MJ/kg (relative standard deviation of 0.01%). All measurements have been performed, at least, in twofold.

Remark: The calorific values can also be determined with the aid of Equation 3.1. Channiwala et al. presented in 2002 [18] a 'unified correlation' based on the ultimate analysis for estimating the H.H.V. of solid, liquid and gaseous fuels on a dry basis:

$$HHV = 0.3491 \cdot C + 1.1783 \cdot H + 0.1005 \cdot S - 0.1034 \cdot O - 0.0151 \cdot N - 0.0211 \cdot A \; (MJ/kg) \quad (3.1)$$

C, H, O, N, S and A represent carbon, hydrogen, oxygen, nitrogen, sulphur and ash contents of the material respectively, expressed in mass percentages on dry basis. This correlation offers predictions with average absolute error of 1.45 % [18]. Nevertheless, this formula has not been applied for the final calculations.

3.4.3. Thermogravimetric analysis – TGA

Thermogravimetric analysis (TGA) is a thermal analysis method by which the weight loss of a sample is continuously recorded against temperature or time under a controlled heating rate and gas atmosphere. Differential thermogravimetric analysis (DTG) curves are derived from the respective TG curves [19], and plot the weight change as a function of temperature (time). About 20 to 30 mg of sample is weighed into a quartz crucible. The sample is heated with a heating rate of 10 - 20 K/min from room temperature (RT) to a preset temperature (973 - 1173 K) with a DuPont Instruments 951

Thermogravimetric Analyzer. Different gas atmospheres have been used to investigate the thermal degradation behaviour extensively:

- Heating under oxygen (O_2) is performed to mimic the combustion behaviour.
- Nitrogen (N_2) is used to simulate the pyrolysis behaviour.
- A switch in gaseous atmosphere from N_2 to O_2 during an isothermal period of 10 minutes at 873 K has also been induced to obtain some basic characteristics (moisture, volatiles, fixed carbon and char) of the biomass and biopolymers.

An important remark is that only slow heating is applied during these dynamic experiments.

3.5. Characterisation of the pyrolytic gases

The pyrolytic gases are defined as the volatiles (condensable and non-condensable) that are released immediately after pyrolysis prior to condensation. So, no separation of condensables occurred yet. The investigation of the pyrolytic gases gives detailed information on the pyrolysis behaviour because the entire volatilised fraction is considered and analysed.

TG/MS and TG/FT-IR result in information concerning the thermal degradation of the input materials and the evolution of pyrolytic gases as a function of a temperature profile and is related to slow pyrolysis. Py-GC/MS is performed according to flash pyrolytic circumstances, and separates and analyses the flash pyrolytic gases at a fixed and preset temperature. Py-GC/MS is thus the most related to the reactor experiments and has the most resolving power because of chromatographic interfacing pyrolysis with a dedicated mass detector.

3.5.1. Thermogravimetric/Mass spectrometric analysis - TG/MS

A Hi-Res TGA 2950 Thermogravimetric Analyzer and a TGA Q5000 Thermogravimetric Analyzer, both of TA Instruments, are connected with a Pfeiffer Vacuum ThermoStar quadrupole mass spectrometer. Approximately 1 – 2 mg of sample is weighed into a platinum crucible. The sample is pyrolysed under a Helium flow of 100 ml/min at a heating rate of 10 - 20 K/min from RT to 873 K. The quadrupole mass spectrometer is set at the standard ionising voltage of 70 eV with a mass range *m/z* of 5 – 255, a scan rate of 5 scans/min and a split-ratio of 1:500. The fused silica capillary interface is kept at 523K.

3.5.2. Thermogravimetric/Fourier Transform – Infrared analysis - TG/FT-IR

A DuPont Instruments 951 Thermogravimetric Analyzer is coupled with a Bruker Vertex 70 FT-IR spectrometer (resolution: 4 cm^{-1}) containing a gas cell. The temperature of the gas cell inside the FT-IR spectrometer, consisting of KBr windows, and the interface is maintained at 473 K. Approximately 20 mg of sample is weighed into a quartz crucible and pyrolysed at a heating rate of 10 - 20 K/min from RT to 873 K under a constant Helium flow of 100 ml/min.

It should be noted that TG/MS and TG/FT-IR are two complementary techniques:

- TG/MS is specific for water and CO_2, but to a lesser extent for CO, while
- TG/FT-IR is specific for CO and CO_2, but to a lesser extent for water because of interferences.

3.5.3. Pyrolysis–gas chromatography/Mass spectrometry – Py-GC/MS

Py-GC/MS simulates the flash (co-)pyrolysis of biomass and biopolymers with the semi-continuous home-built pyrolysis reactor analytically. A Perkin Elmer AutoSystem XL gas chromatograph, connected to a Perkin Elmer TurboMass quadrupole mass spectrometer, is equipped with a Frontier Lab Double-Shot Pyrolyzer PY - 2020 iD interfaced at 553 K. A DB-WAX capillary fused silica column (30 m x 0.25, d_f = 0.25 μm) is used to analyse the evolving pyrolytic gases. The column temperature is programmed from 308 to 533 K at 13 K/min after an initial 1 minute isothermal period and kept at the final temperature for 12 minutes. The mass spectrometer is set at the standard ionising voltage of 70 eV with a mass range *m/z* of 33 – 500 and a scan rate of 2 scans/second. Sample injection was executed at 723 K during 1 minute in the single shot mode, while the injector temperature is 533 K. A helium carrier flow of 12 psi and a split flow of 50 ml/min is applied.

The Py-GC/MS chromatograms are investigated extensively: statistical data processing, pattern recognition and component identification and quantification are performed to obtain complementary information. The chromatograms obtained are processed statistically in two different manners:

1. based on carefully chosen peaks, and
2. based on a limited number of identical areas.

Pattern recognition is performed on the Total Ion Chromatogram (TIC) and on specific mass fragment ion chromatograms. Finally, the identification of the compounds is accomplished by advising a NIST database containing up to 100.000 data.

3.6. Characterisation of the condensables

3.6.1. Water content

The water content of the different bio-oil samples, containing a high percentage of water, is measured using the Dean-Stark method. Around 5 to 10 ml sample is introduced into a 250 ml flask together with approximately 60 ml toluene. Water is separated from the bio-oil in azeotropic conditions into a calibrated reservoir, indicating the amount of water present in the bio-oil. The evolution of the amount of water collected in the reservoir is followed every minute for the first 15 minutes, afterwards two extra measurements are done: one on 30 minutes and one on 60 minutes (constant water level), indicating the total amount of water in the bio-oil.

Bio-oils with very low water content are analysed by means of a Karl-Fisher titration. A SCHOTT, equipped with a TR85 detector, a 180/10 full-automatic burette and a TM120 reaction vessel, is used on 0.5 ml sample.

3.6.2. Calorimetry

Calorimetric measurements are performed to obtain the energy content (H.H.V.) of the condensables. Accordingly, these values will be confronted with the H.H.V.'s of the starting materials to calculate a simplified energy recuperation ratio for the flash (co-)pyrolysis experiment. The samples (approximately 1 g) are analysed according to the same procedure as the input materials, see *section 3.4.2.*

3.6.3. Gel permeation chromatography – GPC

The molecular weight distribution of the bio-oil samples is obtained by GPC. The GPC module consists out of a Spectraseries P100 pump of Spectra-Physics, equipped with a Shodex RI-71 refractometer and a column oven keeping a PLgel MIXED BLS 10 µm column at 308 K. A flow of 1 ml/min of tetrahydrofuran (THF) is maintained. Polystyrene standards from Polymer Laboratories in the 160 – 11000 g/mol molecular weight range are used for calibration. The molecular size distribution is determined on 50 mg of bio-oil dissolved in 5 ml THF stabilised with 0.025 – 0.040 % BHT (Butylated Hydroxy Toluene – anti-oxidant). Before injection (20 µl), the solution is dried with Na_2SO_4 p.a. and filtered over a 0.45 µm PTFE filter.

3.6.4. High performance liquid chromatography – HPLC

An Agilent 1100 liquid chromatograph containing a Zorbax C8 column (250x4.6mm 1/4" VALCO) of Chrompack is connected to a diode array. Detection is performed at five different wavelengths: 200, 225, 254, 260 and 278 nm. Chromatography is executed on 50 mg of bio-oil dissolved in 5 ml THF. Before injection (20 µl), the solution is dried with Na_2SO_4 p.a. and filtered over a 0.45 µm PTFE filter. Binary solvent gradient elution of a methanol/THF (4:1) and a 1%-solution of acetic acid in water is performed according to the eluent programme summarised in Table 3.1.

Table 3.1: Eluent gradient programme of the HPLC mobile phase

Time *(min)*	MeOH/THF (4:1) *(%)*	1% CH_3COOH in H_2O *(%)*	Flow *(ml/min)*
0	20	80	1.0
11	55	45	1.0
16	75	25	1.0
20	90	10	1.0
23	100	0	1.0
30	100	0	1.0

3.6.5. Fourier transform infrared spectroscopy – FT-IR

FT-IR analysis of the crystals and the water-free air-dried bio-oils is carried out on a Bruker IFS 48 and a Bruker Vertex 70 FT-IR spectrometer. The respective sample is placed as a thin film between two KBr windows. Typically, 32 scans per minute are taken with a resolution of 4 cm^{-1}.

3.6.6. Gas Chromatography/Mass Spectrometry – GC/MS

A Varian 3400 gas chromatograph equipped with a Finnigan TSQ 700 mass selective quadrupole detector and a DB-WAX capillary fused silica column (30 m x 0.25 mm; d_f = 0.25 µm) is used. The column temperature is programmed from 308 to 533 K at 12 K/min after an initial 1 min isothermal period and kept at the final temperature for 6 min. Sample injection of 1 µl of a 1 – 4 % solution in methanol is performed in the split less mode while the injector temperature is 533 K.

The quadrupole mass spectrometer is set at the standard ionising voltage of 70 eV with a mass range *m/z* of 42 – 500 and a scan rate of 2 scans/second. The identification of the compounds is accomplished by advising a NIST database containing up to 100.000 data.

3.7. References

[1] Lievens C, *Valorization of heavy metal contaminated biomass by fast pyrolysis*, in *PhD thesis - Research Group: Applied Chemistry*. 2007, Hasselt University: Diepenbeek. p. 221.

[2] Bridgwater AV, Meier D, Radlein D. An overview of fast pyrolysis of biomass. Org. Geochem. 1999; 30:1479-93.

[3] Sharypov VI, Marin N, Beregovtsova NG, Baryshnikov SV, Kuznetsov BN, Cebolla VL, et al. Co-pyrolysis of wood biomass and synthetic polymer mixtures. Part 1: influence of experimental conditions on the evolution of solids, liquids and gases. J. Anal. Appl. Pyrolysis 2002; 64:15-28.

[4] Marin N, Collura S, Sharypov VI, Beregovtsova NG, Baryshnikov SV, Kutnetzov BN, et al. Copyrolysis of wood biomass and synthetic polymers mixtures. Part II: characterisation of the liquid phases. J. Anal. Appl. Pyrolysis 2002; 65:41-55.

[5] Sharypov VI, Beregovtsova NG, Kuznetsov BN, Membrado L, Cebolla VL, Marin N, et al. Co-pyrolysis of wood biomass and synthetic polymers mixtures. Part III: Characterisation of heavy products. J. Anal. Appl. Pyrolysis 2003; 67:325-40.

[6] Sharypov VI, Beregovtsova NG, Kuznetsov BN, Baryshnikov SV, Cebolla VL, Weber JV, et al. Co-pyrolysis of wood biomass and synthetic polymers mixtures - Part IV: Catalytic pyrolysis of pine wood and polyolefinic polymers mixtures in hydrogen atmosphere. J. Anal. Appl. Pyrolysis 2006; 76:265-70.

[7] Zhou LM, Wang YP, Huang QW, Cai JQ. Thermogravimetric characteristics and kinetic of plastic and biomass blends co-pyrolysis. Fuel Process. Technol. 2006; 87:963-9.

[8] Matsuzawa Y, Ayabe M, Nishino J. Acceleration of cellulose co-pyrolysis with polymer. Polym. Degrad. Stabil. 2001; 71:435-44.

[9] Vuthaluru HB, Brooke RJ, Zhang DK, Yan HM. Effects of moisture and coal blending on Hardgrove Grindability Index of Western Australian coal. 2003; 81:67-76.

[10] Orinák A, Halás L, Amar I, Andersson JT, Ádámová M. Co-pyrolysis of polymethyl methacrylate with brown coal and effect on monomer production. 2006; 85:12-8.

[11] DeSchoenmakere M, *Inventarisatie en analyse van verschillende materiaal- en afvalaspecten van bioplastics*, in *IVPV - mileucoördinator A*. 2007, Ghent University: Gent. p. 131.

[12] Massardier-Nageotte V, Pestre C, Cruard-Pradet T, Bayard R. Aerobic and anaerobic biodegradability of polymer films and physico-chemical characterization. 2006; 91:620-7.

[13] Jans M, *Co-pyrolyse van biomassa met biopolymeren ter reductie van het watergehalte in bio-olie*, in *Dep. IWT*. 2007, Xios: Diepenbeek. p. 190.

[14] www.biomer.de.

[15] www.hycail.com/.

[16] www.biopearls.nl.

[17] www.verpakkingsmanagement.nl/.

[18] Channiwala SA, Parikh PP. A unified correlation for estimating HHV of solid, liquid and gaseous fuels. Fuel 2002; 81:1051-63.

[19] Yaman S. Pyrolysis of biomass to produce fuels and chemical feedstocks. Energy Conv. Manag. 2004; 45:651-71.

Chapter 4: Flash co-pyrolysis of biomass and biopolymers

The observations and conclusions of this chapter have been orally presented on the Pyrolysis2008 conference in Lanzarote – Spain and submitted for publication in The Journal of Analytical and Applied Pyrolysis:

Flash co-pyrolysis of biomass: The influence of biopolymers;
T. Cornelissen, M. Jans, T. Kuppens, T. Thewys, G.K. Janssens, H. Pastijn, J. Yperman, G. Reggers, S. Schreurs, R. Carleer;
Journal of Analytical and Applied Pyrolysis (under revision).

4.1. Introduction

The flash pyrolysis of biomass waste streams is a promising method to obtain both energy and materials (e.g. chemicals), without endangering the basic food supply chain. All obtained pyrolysis products are suitable for use as energy feedstock. Nevertheless, bio-oil shows the most potential. In order to maximise the bio-oil yield, flash pyrolysis should be applied: low temperature, high heating rate and short gas residence time [1, 2]. A major drawback of (flash) pyrolysis of biomass is the inherent production of pyrolytic water, which results in a bio-oil with a relatively high water content. Nevertheless, the presence of water has both positive and negative effects on the bio-oil properties [1, 3]. In view of the applicability of bio-oil in general, water is defined as detrimental [4]. The **reduction of the water content** is one of the few required but essential upgrading steps in order to increase the applicability of bio-oil and to make the production of bio-oil competitive. In this research the flash co-pyrolysis of biomass and biopolymers is proposed to counter the production of pyrolytic water.

The use of co-pyrolytic techniques on biomass/plastic ratios has already been investigated [5-8]. One of the most important parameters is the ratio in the feedstock. However, the flash co-pyrolysis of biomass and biopolymers, which are a special kind of plastic, has never been investigated. Even though biopolymers originate from renewables and/or are biologically degradable, most of them still have to be considered as waste, since it is ecologically unacceptable to dispose of them in the environment. The flash co-pyrolysis of biomass and biopolymers will be proven to be a promising route, not only as a supplier of **renewable energy**, but also as an attractive **upgrading** method for the pyrolysis of biomass, as a supplier of value-added **materials** and as an alternative **waste treatment** option.

The goal of this research is to reduce the amount of pyrolytic water by flash co-pyrolysis of biomass and biopolymers. Willow is applied as the biomass reference material. The co-pyrolytic behaviour of the different willow/biopolymer blends in a w/w ratio of 1:1 is investigated with the pyrolysis reactor (Figure 2.9).

In *section 4.3.* a myriad of biopolymers:

- polylactic acid (PLA),
- corn starch,
- polyhydroxybutyrate (PHB),
- Biopearls,
- Eastar,
- Solanyl, and
- potato starch

are investigated in identical circumstances to evaluate their influence on the flash co-pyrolysis behaviour of uncontaminated willow (target biomass) at 723 K with the pyrolysis reactor. The flash pyrolysis of pure (100%) uncontaminated willow serves as a reference. The main characteristics of willow and the seven biopolymers will be discussed in *section 4.2.*

Based on five predefined criteria, the different flash (co-)pyrolysis experiments are compared with a multi-criteria decision aid (MCDA) methodology 'PROMETHEE', *section 4.4.* PROMETHEE, which belongs to the outranking family of MCDA methodologies, is implemented by the 'Decision Lab' tool. This decision support tool is comparing pairwise the different biopolymer options and ranks them, based on assessments of these options for the different criteria [9-11]. The output obtained by PROMETHEE will be discussed in *section 4.4.4. – 4.4.7.* Prior to the actual multi-criteria decision making (MCDM), the respective importance of the five predefined criteria is expressed by weights in *section 4.4.1.* These weights are computed by means of pairwise comparisons of the criteria and 'MCDM tool', a software that incorporates an eigenvalue method, related to the Analytic Hierarchy Process (AHP) method by Saaty [12].

4.2. Material characterisation

The main characteristics of willow and the seven biopolymers are listed in Table 4.1. All materials have a high C- and O-content, an intermediate H-content, and a very low to negligible N-content. No sulphur is detected. The calorific values of the input materials vary between 17.0 and 26.2 MJ/kg.
For the slow pyrolysis (10 K/min) of the pure materials, the mass loss curves and the derivatives, obtained by TGA, are shown in Figure 4.1. Some basic characteristics, as summarised in Table 4.1, can be deduced. Additionally, a first indication towards the general pyrolysis behaviour of the input materials is obtained. Willow (Figure 4.1a) decomposes within a relatively wide temperature interval. The main decomposition of willow takes place in the range of 473 – 673 K. Some biopolymers on the other hand (PLA, PHB, Eastar and Solanyl; Figure 4.1 b, d, f and g, respectively) decompose in one single and narrow temperature interval, while others show a multi-step decomposition (corn starch, Biopearls and potato starch; Figure 4.1 c, e and h, respectively). As compared with willow (T_{max} = 623 K), the maximum degradation temperature (T_{max}) of some biopolymers (PLA and Eastar) is higher, while for others (PHB, Solanyl and potato starch) T_{max} is lower. In the case of corn starch and Biopearls, however, the comparison of T_{max} is less straightforward.

4.3. Flash co-pyrolysis

4.3.1. Pyrolysis yields and efficiencies

To study the influence of the biopolymers on the pyrolysis behaviour of willow, the flash (co-)pyrolysis of each biopolymer option (pure willow, and 1:1 willow/biopolymer blends) is performed at **723 K** with the pyrolysis reactor. Table 4.2a outlines a brief summary of the pyrolysis yields and efficiencies of the condensables, char and gas productions. The amount of gases is calculated by difference. Besides bio-oil, the flash co-pyrolysis of willow and biopolymers can result in the production of crystals: PHB, for instance, yields crystals of crotonic acid. These crystals appear after a spontaneous phase separation in the recuperation system (Figure 2.9, part c) and offer added value as a source of chemicals. Both bio-oil and crystals are retained in the condensation system of the reactor set-up and are grouped under the term 'condensables'. In Table 4.2b, a subdivision of these condensables in bio-oil and crystals and of bio-oil (virtually) in water-free bio-oil and pyrolytic water, based on the water content, is shown. From both tables, it can be concluded that not all biopolymers react in the same way during flash co-pyrolysis with willow.

Table 4.1: Main characteristics (on dry basis) of willow and the biopolymers.

Characteristics	Willow	PLA	Corn starch	PHB	Biopearls	Eastar	Solanyl	Potato Starch
Proximate analysis (%)								
Moisture	1.88	0.00	0.48	0.17	0.00	0.00	1.05	0.00
Volatile	75.27	98.05	92.78	97.97	94.92	95.02	80.81	87.56
Fixed C	21.14	1.30	4.62	0.80	1.77	3.68	13.00	3.87
Ash	1.71	0.65	2.12	1.06	3.31	1.30	5.14	8.57
Ultimate analysis (%)								
Carbon	46.91	49.84	56.21	55.96	52.85	62.45	43.96	49.76
Hydrogen	5.95	5.63	6.89	7.07	6.01	7.07	7.21	5.65
Nitrogen	0.63	0.15	0.18	0.14	0.00	0.03	0.10	0.10
Oxygen	41.69	44.42	36.77	36.40	33.15	31.85	50.00	39.33
H/C molar ratio	1.52	1.36	1.47	1.52	1.36	1.36	1.97	1.36
O/C molar ratio	0.67	0.67	0.49	0.49	0.47	0.38	0.85	0.59
Calorimetric analysis								
H.H.V. (MJ/kg)	18.7	18.6	22.9	22.8	20.5	26.2	17.0	18.9

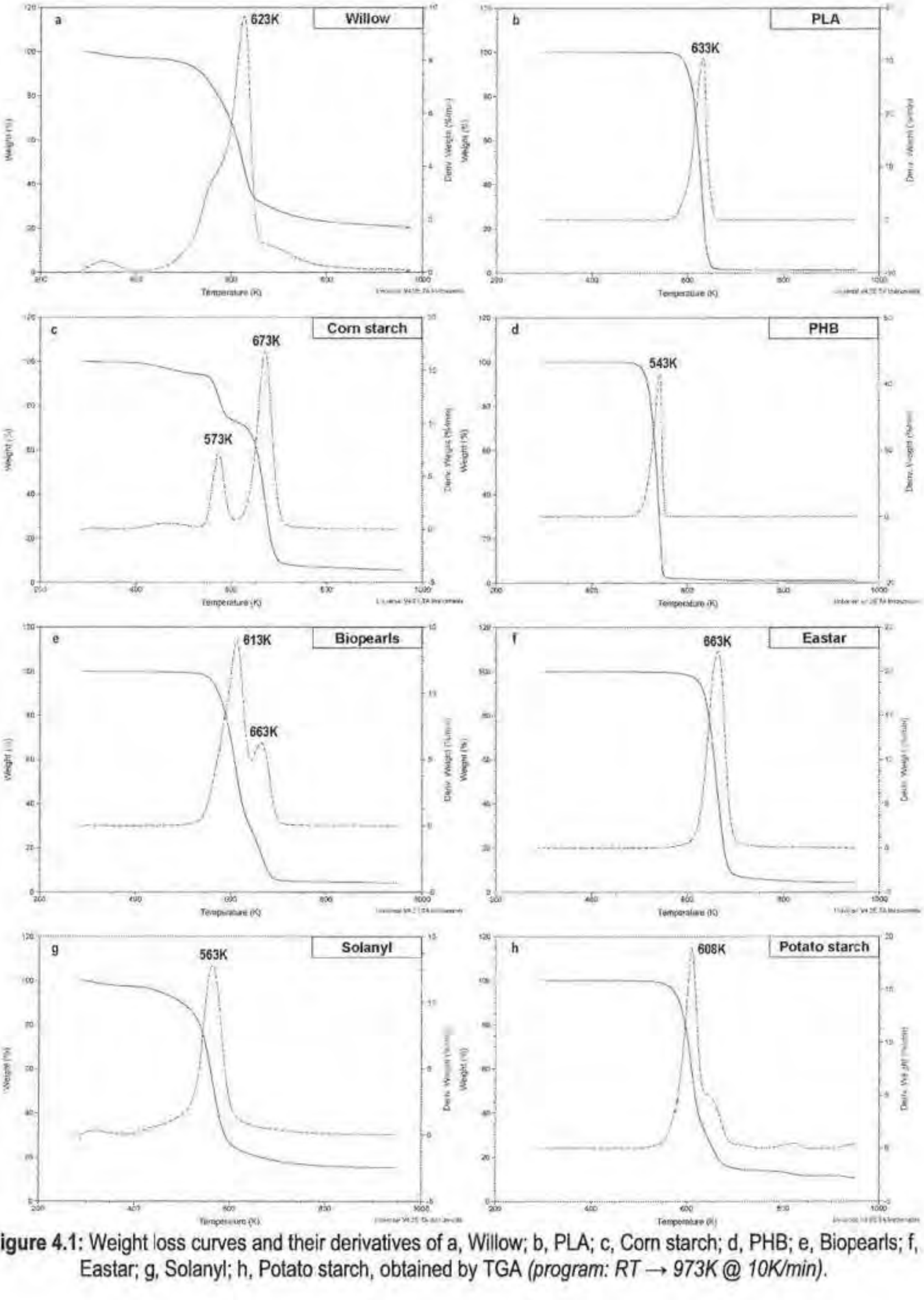

Figure 4.1: Weight loss curves and their derivatives of a, Willow; b, PLA; c, Corn starch; d, PHB; e, Biopearls; f, Eastar; g, Solanyl; h, Potato starch, obtained by TGA *(program: RT → 973K @ 10K/min)*.

Table 4.2: a. Pyrolysis yields and efficiencies of the condensables, char and gas productions for the different biopolymer options. (*Input (m%) is calculated on dry basis); b. Subdivision of condensables into crystals and bio-oil; and of bio-oil (virtually) into water-free bio-oil and pyrolytic water based upon the water content; obtained out of 100 g input; and c. H.H.V.'s of the bio-oils in Mega Joule per kilogram and energy recuperation of the biopolymer options in % (The energy recuperation of willow/PHB = sum of bio-oil and crystals (H.H.V.= 23.1 MJ/kg)).

a.	Willow	Willow/PLA	Willow/Corn starch	Willow/PHB	Willow/Biopearls	Willow/Eastar	Willow/Solanyl	Willow/Potato starch
*Input (m%)**								
Willow	100.00	51.80	50.36	50.06	49.90	49.83	52.57	49.97
Biopolymer	0.00	48.20	49.64	49.94	50.10	50.17	47.43	50.03
Output (m%)								
Condensables	50.10	51.96	43.72	64.24	52.79	50.01	59.24	51.52
Char	22.39	13.46	14.47	9.50	12.92	13.92	15.24	13.49
Gases (by diff.)	27.50	34.58	41.81	26.26	34.29	36.07	25.52	34.99

b.	Willow	Willow/PLA	Willow/Corn starch	Willow/PHB	Willow/Biopearls	Willow/Eastar	Willow/Solanyl	Willow/Potato starch
Cristals (g)	0.00	0.00	0.00	29.70	0.00	0.00	0.00	0.00
Bio-oil (g)	50.10	51.96	43.72	34.54	52.79	50.01	59.24	51.52
Water content (m%)	36.65	15.53	26.94	15.97	16.81	18.96	32.82	16.17
Water-free Bio-oil (g)	31.74	43.89	31.94	29.03	43.92	40.53	39.80	43.19
Pyrolytic Water (g)	18.36	8.07	11.78	5.52	8.87	9.48	19.44	8.33

c.	Willow	Willow/PLA	Willow/Corn starch	Willow/PHB	Willow/Biopearls	Willow/Eastar	Willow/Solanyl	Willow/Potato starch
H.H.V. (MJ/kg)	16.1	18.5	18.5	20.2	19.1	20.8	15.7	19.2
Energy recuperation (%)	43.1	51.5	38.9	66.8	51.5	46.3	52.1	52.6

In Table 4.2a, a first indication of the effect of biopolymers is observed:

- The flash co-pyrolysis of willow and biopolymers results in a reduced char yield compared with the willow reference,
- Except for the biopolymers corn starch and Eastar, a higher yield in condensables is achieved.

Table 4.2b shows that:

- Generally, a significant reduction of the water content is obtained via flash co-pyrolysis of willow with biopolymers.
- Except for Solanyl, a vast reduction of the total amount of pyrolytic water is observed.
- All biopolymer options result in an enhanced yield of valorisable condensables (= water-free bio-oil yield + total amount of crystals): each biopolymer option, with the exception of PHB, induces an increase in the amount of water-free bio-oil yield. Interestingly, PHB results, besides a reasonably high water-free bio-oil yield, in the formation of crystals of crotonic acid, which offer increased economic potential as value-added chemicals.

The averaged experimental H.H.V.'s of the different bio-oils are summarised in Table 4.2c. The addition of biopolymers (except for Solanyl) clearly shows an additional advantage: an increase in the H.H.V. of bio-oil produced from willow/biopolymer blends compared to the bio-oil of pure willow (16.1 MJ/kg to 20.8 MJ/kg). Taking into account the yield in condensables (Table 4.2a and 4.2b) and the experimental H.H.V. of the input materials (Table 4.1), of the respective bio-oil (Table 4.2c) and of the crystals (H.H.V. of crystals = 23.1 MJ/kg), the energy recuperation for each biopolymer option (Table 4.2c) can be calculated:

$$\text{Energy recuperation in condensables} = \frac{[\#\ \text{bio-oil} \times \text{HHV(bio-oil)} + \#\ \text{crystals} \times \text{HHV(crystals)}]}{[\#\ \text{biomass} \times \text{HHV(biomass)} + \#\ \text{biopolymer} \times \text{HHV(biopolymer)}]} \times 100 \qquad (4.1.)$$

For instance, the energy recuperation in condensables for the 1:1 willow/PLA flash co-pyrolysis is :
=[(51.96g x 18.5 kJ/g + 0.00g x 23.1 kJ/g)/(51.80g x 18.7 kJ/g + 48.20g x 18.6 kJ/g)] x 100 = 51.54%.
Except for 1:1 willow/corn starch, all biopolymer options result in an enhanced energy recuperation compared with the willow reference.

4.3.2. Pyrolytic water - Synergy

It should also be emphasised that some biopolymers result in a **synergy** during the flash co-pyrolysis with willow. This synergy is best illustrated by calculating the difference between the actual amount and the minimum **amount of pyrolytic water** produced during the flash co-pyrolysis:

- The actual amount of pyrolytic water is calculated via the bio-oil yield and the respective water content (Table 4.2). It should be noted that the crystals, originating from the flash co-pyrolysis of willow and PHB, do not contain any water.
- The minimum amount of pyrolytic water, for which it is assumed that the biopolymer itself does not result in the formation of pyrolytic water during pyrolysis (= absolute minimum), is calculated by the amount of willow in the respective blend and the pyrolysis results of pure willow (reference): 100 gram willow results in 18.36 gram pyrolytic water (Table 4.2b).

Table 4.3: The influence of biopolymers on the amount of pyrolytic water produced.

	Pyrolytic water (m%)		
Biopolymer option	Actual amount	Absolute minimum	Influence (%)
Willow	18.36	18.36	-
Willow/PLA	*8.07*	*9.51*	*-15*
Willow/corn starch	11.78	9.25	+27
Willow/PHB	*5.52*	*9.19*	*-40*
Willow/Biopearls	*8.87*	*9.16*	*-3*
Willow/Eastar	9.48	9.15	+4
Willow/Solanyl	19.44	9.65	+101
Willow/potato starch	*8.33*	*9.18*	*-9*

The biopolymer options in *italic* result in a synergy.

Table 4.3 summarises the influence of each biopolymer on the production of pyrolytic water during flash co-pyrolysis with willow. Four biopolymer options result in a lower actual amount of pyrolytic water compared with the absolute minimum amount and thus result in a synergy: PLA, PHB, Biopearls and potato starch. The flash co-pyrolysis of 1:1 willow/PHB shows the highest synergy, reaching minus 40% [13]:

- the absolute minimum amount of pyrolytic water for willow/PHB
  = [(50.06g x 18.36m% + 49.94g x 0.00m%)/100] = 9.19 m%,
- the actual yield in pyrolyitc water is 5.52 m% (Table 4.2b),
- thus a decrease of 3.67 m% or [(3.67/9.19) *100] = - 39.93 % is calculated.

The other three biopolymers (corn starch, Eastar and Solanyl) do not provide any straightforward evidence towards the occurrence of such a synergy.

Unfortunately, there is not one specific biopolymer option that is dominant in all areas of interest. For instance, the willow/Solanyl blend results in the highest bio-oil yield, but shows the lowest reduction in water content and results in a bio-oil with the lowest H.H.V. as compared with the other willow/biopolymer blends. Additionally, not all areas of interest are of equal importance, making it ambiguous to decide which biopolymer option is the best one to pursue. This is a typical example of a **multi-criteria decision making (MCDM)** problem.

4.4. Multi-criteria decision making

In order to determine which biopolymer option performs best, the multi-criteria decision aid (MCDA) software 'Decision Lab 2000 – Executive Edition, Version 1.0' of Visual Decision Inc., based on PROMETHEE and GAIA, is applied [11]. **PROMETHEE** and **GAIA** belong to a family of multi-criteria decision aid methods known as outranking methods and are based on the principle of pairwise comparison [9-11]. Some different steps need to be carried out to correctly model and analyse the MCDM problem with Decision Lab:

Step 1: Defining the actions (= biopolymer options),
Step 2: Defining the criteria,
Step 3: Granting each criterion an objective weight,
Step 4: Constructing an evaluation table,
Step 5: Choosing a transformation function and respective thresholds for each criterion, and
Step 6: Analysing the MCDM problem.

Eight different **biopolymer options** are under investigation (*Step 1*):

- the flash pyrolysis of pure willow, which serves as a reference, and
- the flash co-pyrolysis of willow and PLA, corn starch, PHB, Biopearls, Eastar, Solanyl and potato starch, respectively, all in a w/w-ratio of 1:1.

Each biopolymer option is evaluated using five **predefined criteria** (*Step 2*):

1. water-free bio-oil yield,
2. water content,

3. energy recuperation,
4. char yield, and
5. total amount of readily separable chemicals.

4.4.1. Determination of the respective weights

Because all criteria differ in **importance**, the respective weights of the criteria must be taken into account (*Step 3*). To grant each criterion an acceptable weight, a decision support software 'MCDM tool 1.0, beta version', which incorporates an eigenvalue method related to the Analytic Hierarchy Process (**AHP**) method by Saaty, is applied [12, 14]. A 5 x 5 pairwise comparison matrix of the relative importance of the five predefined criteria, interpreted by and based upon the experience and judgment of the author, is constructed (Matrix 4.1). The entry in row *i* and column *j* of Matrix 4.1 indicates how much more important criterion *i* is than criterion *j*. "Importance" is measured on an integer-valued 1 – 9 ratio scale and its respective reciprocals [12]. In *section 4.4.5.* a sensitivity analysis of the weights obtained by 'MCDM tool' will be performed.

Matrix 4.1: Pairwise comparison matrix (5 x 5) to obtain the respective weights of each criterion.

$$\begin{array}{rc|ccccc|}
 & & 1 & 2 & 3 & 4 & 5 \\
\text{Water-free bio-oil yield} & 1 & 1 & 3 & 2 & 4 & 1/2 \\
\text{Water content} & 2 & 1/3 & 1 & 1/2 & 2 & 1/5 \\
\text{Energy recuperation} & 3 & 1/2 & 2 & 1 & 3 & 1/3 \\
\text{Char yield} & 4 & 1/4 & 1/2 & 1/3 & 1 & 1/8 \\
\text{Total amount of readily separable chemicals} & 5 & 2 & 5 & 3 & 8 & 1
\end{array}$$

To obtain Matrix 4.1, the following motivation is applied:

- The amount of readily separable chemicals is fairly the most important criterion because separated chemicals have a much higher chemical and economic importance than energy.
- The water-free bio-oil yield is considered the second most important criterion, because it summarises the valorisable fraction of the bio-oil that has the potential for application as an energy source and, in the future, as a source of value-added chemicals which are still dissolved in the bio-oil.
- The criterion 'Energy recuperation' only focuses on the valorisable fraction of the condensables as energy source, which makes it economically less attractive than the water-free bio-oil yield.

- Even though the water content is a very important aspect of bio-oil, it is conceived as the least but one important criterion under consideration since it only provides an indication towards the applicability and usability of the bio-oil.
- Finally, the char yield, which is only considered as a by-product for this research, is selected as the least important criterion.

With the aid of MCDM tool, the **normalised principal eigenvector** of Matrix 4.1 is calculated, resulting in the respective weights of each criterion. Table 4.4 ranks the criteria according to their relative weights (sum equals '1') obtained by MCDM tool and summarises the motivation applied. Additionally, MCDM tool calculates a consistency ratio (C.R.) of 0.006. In a perfectly consistent comparison matrix, a C.R. of zero would be obtained. This, however, is very unlikely and some inconsistency is allowed (consistent if: C.R. < 0.1). If C.R. is higher than 0.1, a revision of the pairwise comparisons would be required [12].

Table 4.4: Summary of the five predefined criteria ranked according to their relative weights and the motivation applied.

Criterion	Weight	Motivation
Total amount of readily separable chemicals	0.4543	The economic value of separated chemicals is higher than energy
Water-free bio-oil yield	0.2511	The valorisable fraction: energy and dissolved chemicals
Energy recuperation	0.1525	The valorisable fraction: energy only
Water content	0.0887	An indication for the applicability of the bio-oil
Char yield	0.0533	A by-product

4.4.2. Evaluation table

Once all data have been gathered (cfr. Table 4.2, 4.3 and 4.4), an evaluation table is constructed (*Step 4*; Table 4.5). Each criterion corresponds to a column and each biopolymer option to a row. In the top of the evaluation table, some characteristic parameters of the respective criteria are listed. The maximisation or the minimisation requirement for each criterion is one of the crucial criterion qualifiers [11]. It is supposed to be advantageous if the water-free bio-oil yield, the energy recuperation, and the total amount of readily separable chemicals are high; while the water content and the char yield are low.

Table 4.5: The Decision Lab evaluation table, summarising the performance of the biopolymer options in terms of the five predefined criteria, obtained out of 100 g input. The upper rows contain the requested preference parameters, while the lower rows describe the eight biopolymer options. The columns represent the five predefined criteria.

	Water-free bio-oil	Water content	Energy recuperation	Char	Separable chemicals
Min/Max	*Maximise*	*Minimise*	*Maximise*	*Minimise*	*Maximise*
Weight	*0.2511*	*0.0887*	*0.1525*	*0.0533*	*0.4543*
Transformation function	*V-shape*	*V-shape*	*V-shape*	*V-shape*	*Usual*
Indifference threshold q	-	-	-	-	-
Preference threshold p	*14.89*	*21.12*	*27.90*	*12.89*	-
Gaussian threshold s	-	-	-	-	-
Threshold unit	*g*	*m%*	*%*	*g*	*g*
Average performance	*38*	*22.48*	*50.4*	*14.42*	*3.71*
Standard deviation	*6.13*	*8.47*	*8.3*	*3.64*	*10.5*
Unit	*g*	*m%*	*%*	*g*	*g*
Willow (Reference)	31.74	36.65	43.1	22.39	0.00
Willow/PLA 1:1	43.89	15.53	51.5	13.46	0.00
Willow/corn starch 1:1	31.94	26.94	38.9	14.47	0.00
Willow/PHB 1:1	29.03	15.97	66.8	9.5	29.70
Willow/Biopearls 1:1	43.92	16.81	51.5	12.92	0.00
Willow/Eastar 1:1	40.53	18.96	46.3	13.92	0.00
Willow/Solanyl 1:1	39.8	32.82	52.1	15.24	0.00
Willow/potato starch 1:1	43.19	16.17	52.6	13.49	0.00

4.4.3. Transformation functions

PROMETHEE (Decision Lab) offers six transformation functions for six different types of criteria:

1. Usual (e.g. qualitative data),
2. U-shape (e.g. discrete resources),
3. V-shape (e.g. operational criteria),
4. Level (e.g. financial long term),
5. Linear (e.g. financial short term), and
6. Gaussian (e.g. security).

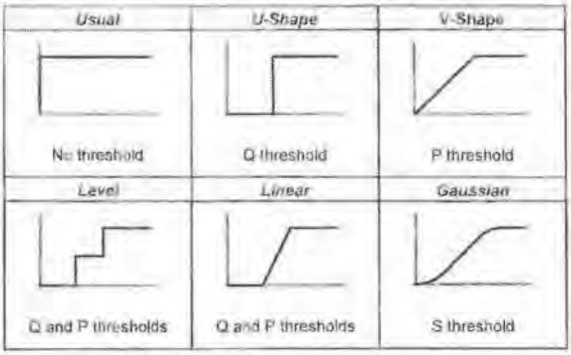

Figure 4.2: The six transformation functions and their respective thresholds available for PROMETHEE [11].

Each function is defined by parameters like an indifference threshold *q*, a preference threshold *p*, and a Gaussian threshold *s*, see Figure 4.2. When a transformation function and the respective threshold values have been defined for each criterion (*Step 5*), the deviations between the evaluations of pairs of biopolymer options on one criterion are translated into a **preference degree $P_i(a,b)$** ranging between 0 and 1 (*a* and *b* represent two different biopolymer options), allowing a comparison of one criterion with another, independently from the scales of measurement. The preference degree is a non-decreasing function of the deviation: smaller deviations will contribute to weaker degrees of preference, and larger ones to stronger degrees of preference. For a detailed description of the transformation functions and the thresholds, consult references [9-11]. The choice of such a transformation function and the respective thresholds is first and foremost directed by the guideline: minimise the loss of information during transformation. This can be translated into the following rule: "the more accurate the data, the more continuous the transformation function".

For this research, the **V-shape** transformation function is applied the most because it fits the characteristics of the accurate quantitative data of the decision problem best. The V-shape transformation function requires accurate quantitative data such as operational and technical data. All measurements performed for this research are considered accurate, even though only one experiment per biopolymer option is executed. Most experiments are not repeated, so that the variability of the measurements are not quantifiable. That is why the measurements and conclusions can only be interpreted as indicative. It should be noted that in the case of the total amount of readily separable chemicals, the **Usual** transformation function is applicable, because only two nominal values exist: '0.00' or '29.70' (Table 4.5).

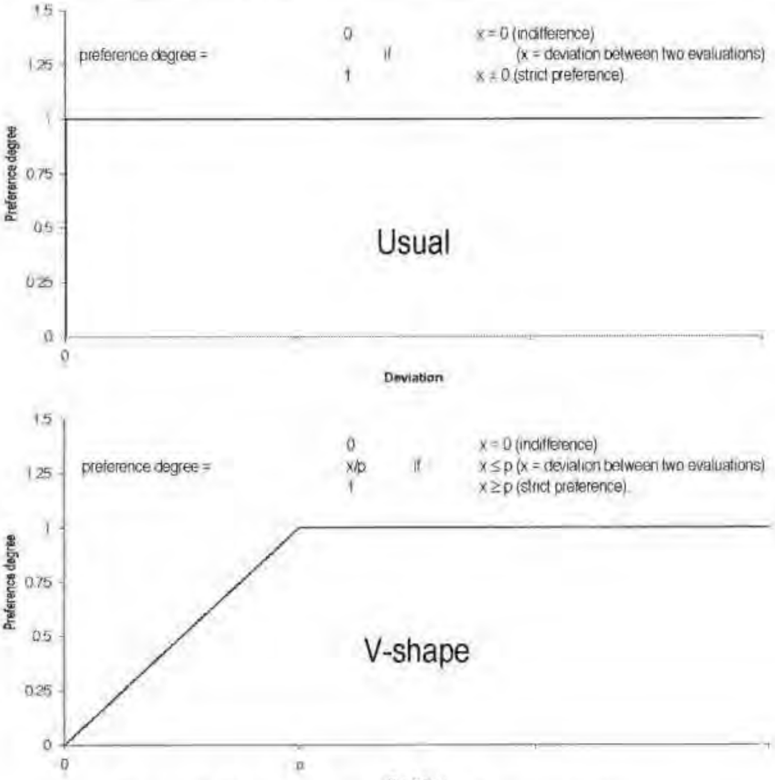

Figure 4.3: The Usual and V-shape transformation functions.

In the case of the V-shape transformation function, the preference degree increases linearly until the deviation between the evaluations of two biopolymer options (*a* and *b*) on a single criterion reaches the preference threshold *p* [9-11], Figure 4.3. In order to minimise the loss of information no indifference threshold *q* is defined. Here, it is assumed that even the smallest difference stimulates some kind of preference over the other. However, a very small preference is achieved. The preference threshold p is considered as the lowest value above which there is strict preference ($P_i(a,b) = 1$) of one of the corresponding biopolymer options over the other. An important remark is that the preference threshold p is defined as a function of the **deviation** between the evaluations on the criteria and not as a function of the evaluation itself. For this research, p is set standard at the maximum deviation of each criterion, which is considered the best in order to minimise the loss of information. At p, the preference degree takes value 1, indicating strict preference.

4.4.4. Analysis of the MCDM problem

Accordingly, the **overall (multi-criteria) preference index $\pi(a,b)$** of a biopolymer option with regard to the other biopolymer options is obtained by calculating the weighted (w_i) average of all preference degrees $P_i(a,b)$ of that specific biopolymer option (Equation 4.2). The closer this value is to 1, the greater the overall preference is [9-11].

$$\pi(a,b) = \frac{\sum_{i=1}^{n} w_i P_i(a,b)}{\sum_{i=1}^{n} w_i}, \qquad \textit{with } n = \textit{the number of criteria.} \tag{4.2}$$

In addition, preference flows (Φ^+, Φ^-, and Φ) are computed in PROMETHEE and Decision Lab to summarise the results of all pairwise comparisons. The **"positive flow" Φ^+** of a biopolymer option is the preference degree with which this biopolymer option is preferred on average over the other biopolymer options. The **"negative flow" Φ^-** of a biopolymer option is the preference degree with which the other biopolymer options are preferred on average to that biopolymer option. Both, Φ^+ and Φ^-, represent positive values. The larger the Φ^+ and the smaller the Φ^-, the better the biopolymer option is. Equation 4.3 and 4.4 represent the mathematical formulation of Φ^+ and Φ^-:

$$\phi^+(a) = \sum_{\substack{b\in K \\ b\neq a}} \pi(a,b), \qquad \textit{with } K \textit{ being the set of biopolymer options.} \tag{4.3}$$

$$\phi^-(a) = \sum_{\substack{b\in K \\ b\neq a}} \pi(b,a). \tag{4.4}$$

Finally, the net flow Φ, also called **Phi score**, of a biopolymer option is the balance between Φ^+ and Φ^- ($\Phi = \Phi^+ - \Phi^-$). The larger the net flow, the better the biopolymer option is. Both Φ^+ and Φ^- are used to rank the biopolymer options partially (PROMETHEE I); while the net flow Φ is used to rank them completely (PROMETHEE II) [9-11].

4.4.4.1. PROMETHEE

The **PROMETHEE I** partial ranking is defined as the intersection of the Φ^+ and Φ^- rankings. It only contains preferences that are confirmed by both preference flows: a biopolymer option is preferred over another only if that biopolymer option has a better (higher) Φ^+ and a better (lower) Φ^-. In case both flows are in conflict, actions are considered incomparable. The preferences that appear in the PROMETHEE I ranking can thus be considered as well established. The **PROMETHEE II** complete ranking ranks all biopolymer options from the best to the worst, leaving no incomparable pair of biopolymer options. It is directly based on the net flow Φ [9-11]. Figure 4.4 shows the PROMETHEE I and II ranking of the decision problem, *Step 6a*.

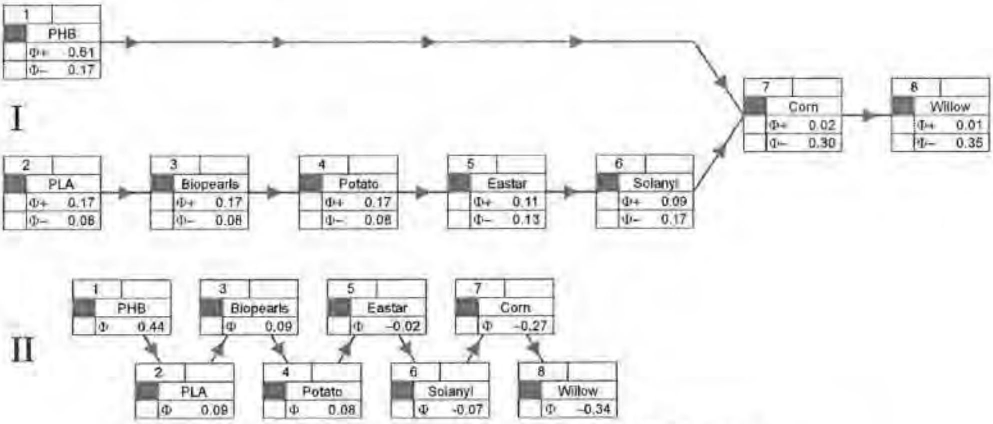

Figure 4.4: PROMETHEE I and II ranking of the MCDM problem.

The PROMETHEE I partial ranking in Figure 4.4 shows that the biopolymer options PHB, PLA, Biopearls, potato starch, Eastar and Solanyl are preferred over corn starch and willow; and that corn starch is preferred over willow. It also indicates that a slight preference of PLA over Biopearls and of Biopearls over potato starch appears, even though the three Φ^+ and Φ^- equal 0.17 and 0.08, respectively, due to rounding errors. Therefore, PLA is preferred over Biopearls, Biopearls over potato starch, potato starch over Eastar, and Eastar over Solanyl. Finally, PHB is in conflict with PLA, Biopearls, potato starch, Eastar, and Solanyl: PHB definitely has the highest Φ^+, but PLA, Biopearls, potato starch and Eastar have a lower (better) Φ^-, while the Φ^- of Solanyl is equal (only slightly lower/better) to the one of PHB. PHB has a relatively high Φ^- because it results in the lowest water-free bio-oil yield (Table 4.2), which is the second most important criterion of the decision problem (Table 4.4). However, PROMETHEE II undoubtedly prefers PHB over all other biopolymer options because it has the highest net flow Φ. PLA, Biopearls and potato starch have a comparable net flow Φ, with PLA having a slightly higher (better) net flow Φ.

4.4.4.2. GAIA

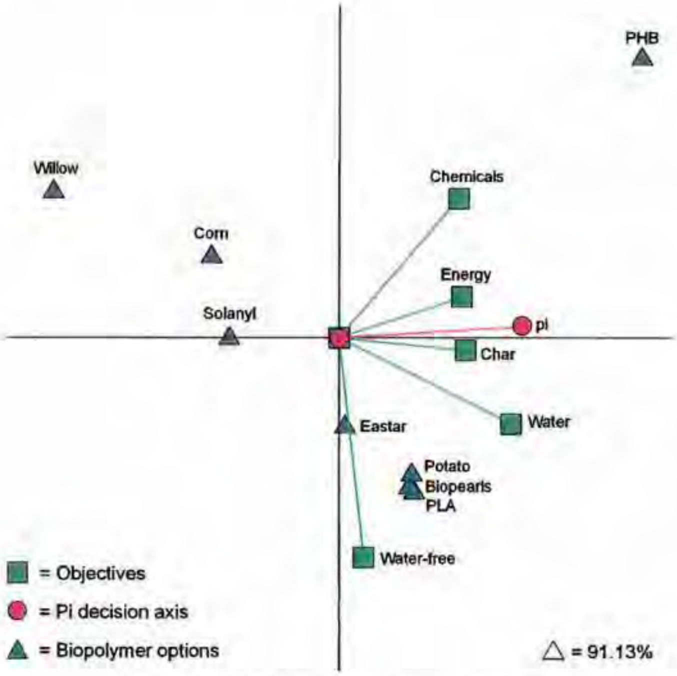

Figure 4.5: The GAIA plane of the decision problem.

Decision Lab provides the **GAIA plane** as a descriptive complement of both PROMETHEE rankings. The information relative to a decision problem including *k* criteria can be represented in a *k*-dimensional space. The GAIA plane is obtained by projection of this information on a plane (two dimensional) such that as few information as possible is lost. GAIA makes use of the Principal Components Analysis (PCA) method and is applied on the net preference flow ($\Phi = \Phi^+ - \Phi^-$). The GAIA plane corresponds to the first two principal components, which ensures that a maximum quantity of information is available in the plane. However, some information usually gets lost in the projection process in the GAIA plane. For this, GAIA generates a Δ value which serves as a quality control measure. It measures the amount of information preserved in the GAIA plane. In practice, Δ values larger than 70% correspond to reliable GAIA planes; Δ values lower than 60% should be considered with care [11]. Figure 4.5 shows the GAIA plane of the decision problem (*Step 6b*) and has a Δ value of over 91%. In the GAIA plane the criteria are presented by axes connected to squares, and the biopolymer options by triangular shapes. The weights of the criteria are represented by a separate axis, called the **Pi decision axis**. This decision axis shows the kind of compromise solution that is proposed by PROMETHEE.

The GAIA plane confirms the observations from the PROMETHEE rankings:

- PHB is the biopolymer option that is in best agreement with the Pi decision axis and is especially supported by the criteria "total amount of readily separable chemicals" and "energy recuperation".
- PLA, Biopearls and potato starch are clustered, indicating that these biopolymer options have similar profiles. Out of these three biopolymer options, PLA is located the furthest in the direction of the Pi decision axis and is thus considered as the best option.
- Eastar seems to "flirt" with the borders.
- Solanyl, corn starch and willow are directed towards the opposite direction of the Pi decision axis, with Solanyl the closest and willow the furthest.

The GAIA plane also indicates that the "total amount of readily separable chemicals" and the "water-free bio-oil yield" are the two most conflicting criteria.

4.4.5. Weight sensitivity analysis

Finally, a weight sensitivity analysis is performed (*Step 6c*). Table 4.6 summarises the range within which the respective weights of each criterion are allowed to deviate (ceteris paribus) without changing the PROMETHEE II ranking of all the biopolymer options. It can be observed that the decision problem is fairly robust: the weights of each criterion can be altered in a relatively wide range, without any further consequence. The char yield presents the most narrow interval. However, even if the char yield would double in importance, which for this research is unlikely, no alterations in the PROMETHEE II ranking are induced.

Table 4.6: Weight sensitivity analysis of the decision problem.

		Absolute values			Relative values (%)		
Objective	Unit	Weight	Min	Max	Weight	Min	Max
Water-free bio-oil yield	g	0.2511	0.1294	0.5536	25.11%	14.73%	42.50%
Water content	m%	0.0887	0.0452	0.2856	8.87%	4.73%	23.86%
Energy recuperation	%	0.1525	0.000	0.3038	15.25%	0.00%	26.39%
Char yield	g	0.0533	0.000	0.1162	5.33%	0.00%	10.94%
Yield in readily separable chemicals	g	0.4543	0.1524	Infinity	45.43%	21.84%	100.00%

4.4.6. Equal weights

Up till now, all conclusions have been based upon a single scenario of the decision problem: the base scenario. In order to investigate the robustness of the methodology applied to a full extent, a second scenario will additionally be discussed: the scenario based on equal weights. In this approach, all criteria are assumed to be of equal importance ($w_i = 0.2$). All other parameters of the base scenario remain unchanged. Figure 4.6 shows that the PROMETHEE II ranking is completely identical to that in Figure 4.4, but clear differences in the net flow *Φ* are observed.

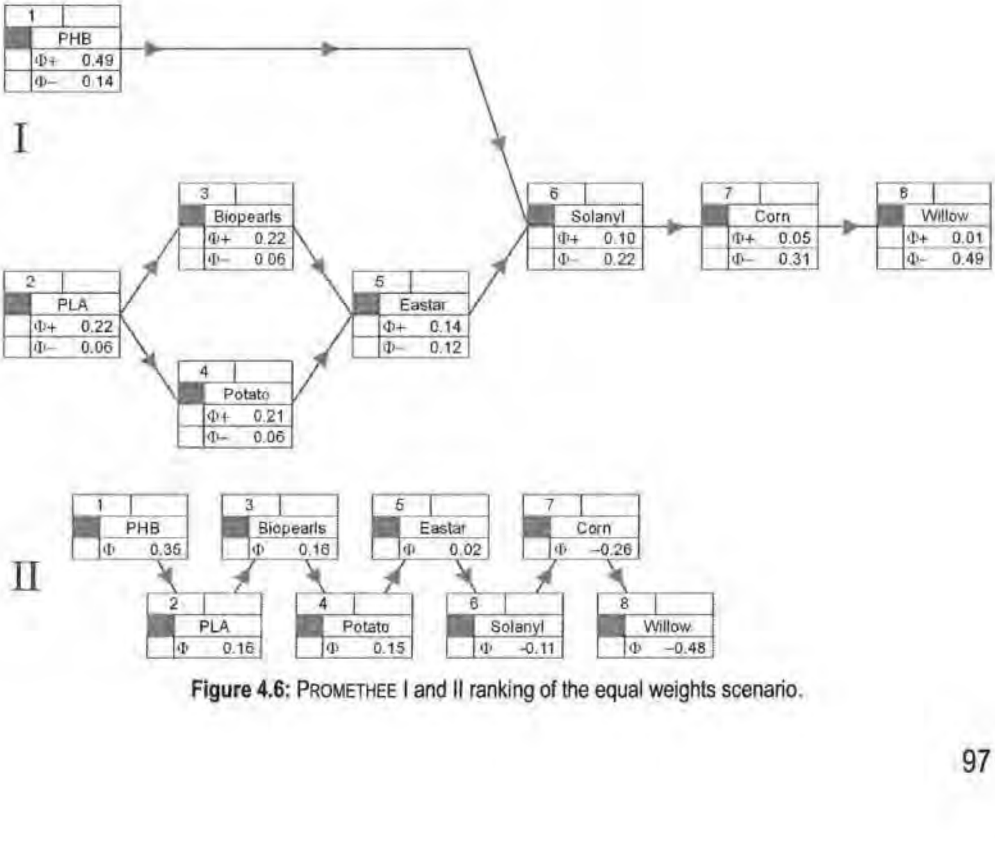

Figure 4.6: PROMETHEE I and II ranking of the equal weights scenario.

The PROMETHEE I ranking in Figure 4.6, however, shows a different pattern as compared to the base scenario shown in Figure 4.4. Here, the biopolymer options PHB, PLA, Biopearls, potato starch and Eastar are preferred over Solanyl, corn starch and willow; and Solanyl is preferred over corn starch, and corn starch over willow. Thus, Solanyl slightly decreased in the level of preference. PLA is still preferred over Biopearls, potato starch and Eastar. But, Biopearls is now considered as incomparable with potato starch: Biopearls has a higher Φ^+, while potato starch has a slightly lower (better) Φ^-. Relatively, potato starch slightly increased in the level of preference. Finally, both Biopearls and potato starch are still preferred over Eastar.

4.4.7. MCDM output

Taking into account the five predefined criteria, it can be concluded that:

- The flash co-pyrolysis of biomass and biopolymers results in improved pyrolysis characteristics.
- PHB is always preferred over PLA, and PLA is preferred over all the other biopolymer options. However, PLA, Biopearls and potato starch are almost identical.
- PHB, PLA, Biopearls, potato starch and Eastar are always preferred over Solanyl, corn starch and willow.
- In both scenarios (respective weights and equal weights), the first four biopolymer options of the PROMETHEE II ranking are similar to the ones that resulted earlier on in a synergy in the amount of pyrolytic water produced (Table 4.3).

4.5. Conclusions

The flash co-pyrolysis of biomass and biopolymers is a promising route to produce energy and materials in a sustainable manner and can be regarded as a win-win situation, which can easily be converted into an economically attractive industrial process. Flash co-pyrolysis of biomass and biopolymers generally results in bio-oil with a reduced water content, an enhanced pyrolysis yield, a reduction of the waste volume, and a more attractive recycling route for biopolymers. This allows the flash co-pyrolysis of willow and biopolymers to be defined as an interesting upgrading step for the pyrolysis of biomass waste streams, a supplier of value-added materials and renewable energy, and as an alternative waste treatment option. Within CMK (centre for environmental sciences) an economical assessments of the flash co-pyrolysis of willow and biopolymers is also being performed.

Even though all 1:1 willow/biopolymer blends result in improved pyrolysis characteristics at 723 K as compared with pure willow, polyhydroxybutyrate (PHB), polylactic acid (PLA), Biopearls and potato starch are the most performant options by taking into account the five predefined criteria (water-free bio-oil yield, water content, energy recuperation, char yield and total amount of readily separable chemicals). These four biopolymers additionally result in a synergy during co-pyrolysis with willow: a decrease in the amount of pyrolytic water, higher than theoretically expected, is observed. The two most performant biopolymer options: willow/PHB and willow/PLA will be discussed in more detail in Chapter 5.

4.6. References

[1] Yaman S. Pyrolysis of biomass to produce fuels and chemical feedstocks. Energy Conv. Manag. 2004; 45:651-71.

[2] Bridgwater AV, Meier D, Radlein D. An overview of fast pyrolysis of biomass. Org. Geochem. 1999; 30:1479-93.

[3] Czernik S, Bridgwater AV. Overview of applications of biomass fast pyrolysis oil. Energy Fuels 2004; 18:590-8.

[4] Oasmaa A, Peacocke C, Gust S, Meier D, McLellan R. Norms and standards for pyrolysis liquids. End-user requirements and specifications. E&F 2005; 19:2155-63.

[5] Sharypov VI, Marin N, Beregovtsova NG, Baryshnikov SV, Kuznetsov BN, Cebolla VL, et al. Co-pyrolysis of wood biomass and synthetic polymer mixtures. Part 1: influence of experimental conditions on the evolution of solids, liquids and gases. J. Anal. Appl. Pyrolysis 2002; 64:15-28.

[6] Marin N, Collura S, Sharypov VI, Beregovtsova NG, Baryshnikov SV, Kutnetzov BN, et al. Copyrolysis of wood biomass and synthetic polymers mixtures. Part II: characterisation of the liquid phases. J. Anal. Appl. Pyrolysis 2002; 65:41-55.

[7] Sharypov VI, Beregovtsova NG, Kuznetsov BN, Membrado L, Cebolla VL, Marin N, et al. Co-pyrolysis of wood biomass and synthetic polymers mixtures. Part III: Characterisation of heavy products. J. Anal. Appl. Pyrolysis 2003; 67:325-40.

[8] Sharypov VI, Beregovtsova NG, Kuznetsov BN, Baryshnikov SV, Cebolla VL, Weber JV, et al. Co-pyrolysis of wood biomass and synthetic polymers mixtures - Part IV: Catalytic pyrolysis of pine wood and polyolefinic polymers mixtures in hydrogen atmosphere. J. Anal. Appl. Pyrolysis 2006; 76:265-70.

[9] Brans JP, Vincke PH. A Preference Ranking Organization Method - (the Promethee Method for Multiple Criteria Decision-Making). Manage. Sci. 1985; 31:647-56.

[10] Brans JP, Vincke P, Mareschal B. How to Select and How to Rank Projects - the Promethee Method. Eur. J. Oper. Res. 1986; 24:228-38.

[11] VisualDecisionInc, *Decision Lab 2000 - Executive Edition, Getting Started Guide*. 1999.

[12] Saaty TL, Alexander JM, *Thinking with Models – Mathematical models in the physical, biological and social sciences*. 1981: Pergamon Press. 148-75.

[13] Cornelissen T, Jans M, Yperman J, Reggers G, Schreurs S, Carleer R. Flash co-pyrolysis of biomass with polyhydroxybutyrate: Part 1. Influence on bio-oil yield, water content, heating value and the production of chemicals. Fuel 2008; 87:2523-32.

[14] DeBeir P, Hallot F, Pastijn H, *MCDM tool 1.0, beta version*. 1998-2005.

Chapter 5: Flash co-pyrolysis of willow/PHB and willow/PLA blends

The observations and conclusions of this chapter have already been published in Fuel:

Flash co-pyrolysis of biomass with polylactic acid. Part 1: Influence on bio-oil yield and heating value;
T. Cornelissen, J. Yperman, G. Reggers, S. Schreurs, R. Carleer; Fuel (87) 2008, p. 1031 – 1041.

Flash co-pyrolysis of biomass with polyhydroxybutyrate. Part 1: Influence on bio-oil yield, water content, heating value and the production of chemicals;
T. Cornelissen, M. Jans, J. Yperman, G. Reggers, S. Schreurs, R. Carleer; Fuel (87) 2008, p. 2523 – 2532.

In Chapter 4 it is proven that the flash co-pyrolysis of biomass and biopolymers is a promising route to produce energy and materials in a sustainable manner and that it can be regarded as an interesting upgrading step for the pyrolysis of biomass waste streams and as an alternative waste treatment option, which can easily be converted into an economically attractive industrial process. Even though all 1:1 willow/biopolymer blends resulted in improved pyrolysis characteristics at 723K as compared with pure willow, polyhydroxybutyrate (PHB) and polylactic acid (PLA) were indicated as the two most performant biopolymer options. Therefore, the flash co-pyrolysis of willow/PHB and willow/PLA blends will be discussed in more detail in *section 5.1.* and *section 5.2.*, respectively. Each section is divided into two subsections:

1. An **analytical study** of the (co-)pyrolysis of willow, one of the two biopolymers and their respective blends. TGA, TG/MS and TG/FT-IR, which all operate under slow pyrolytic circumstances, are the analytical techniques under consideration.
2. The flash (co-)pyrolysis of willow, one of the two biopolymers and their respective blends is performed with the **pyrolysis reactor**. Here, the pyrolysis yields and efficiencies are evaluated and coupled with a simplified energetic valorisation. The obtained results will be used to propose an optimum biomass/biopolymer ratio.

5.1. Flash co-pyrolysis of willow and PHB

PHB is the most commonly occurring polyhydroxyalkanoate (PHA), which are mainly polymers of 3-hydroxyalkanoic acids, in nature, see Figure 5.1 [1]. PHB was the first PHA to be discovered and is also the most widely studied and best characterised PHA. PHB is a naturally occurring biologically degradable polymer, accumulated by many bacteria as carbon and energy reserve material at up to 80% of the dry cell weight [2-4]. It is produced in an aerobic fermentation process in which a sugar carbon source is converted into a biopolymer by means of a micro-organism. The biopolymer stored in the cell as a carbon reserve can then be recovered by an extraction and purification process [1]. PHB can be degraded to water and carbon dioxide under environmental conditions by a variety of bacteria, and shows much potential for its application as an environmentally degradable plastic [5]. PHB is a isotactic, absolutely linear, thermoplastic homopolyester built of 3-hydroxy butyric acid (Figure 5.2).

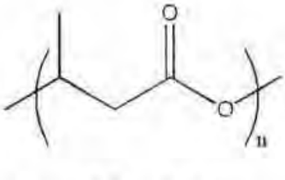

Figure 5.1: PHB structure.

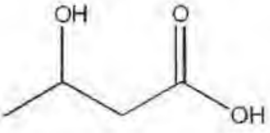

Figure 5.2: Monomer (3-hydroxy butyric acid) structure.

PHB has mechanical properties very similar to conventional plastics like polyethylene (PE) and polypropylene (PP) [1, 2]. It can be processed into pellets that can be handled on machines the same way as classic plastics produced from oil [6]. Thus, it can be processed as a conventional thermoplast in most industrial transformation processes, including extrusion, injection and thermopressing. For instance by extrusion, PHB can be transformed into rigid shapes (for example pipes) and films for packaging. Other important uses of this biomaterial include packaging for cosmetics and food, agrotoxic packaging and tublettes, and medical and veterinary implants [1]. In general, PHB can be used to develop devices including sutures, suture fasteners, meniscus repair devices, rivets, tacks, staples, screws, bone plates and bone plating systems, bulking and filling agents, toys, controlled drug release use and wound dressings, but also packaging films mainly in bags, containers and paper coatings, disposable items such as razors, cutlery, fireworks, clips, utensils, diapers, feminine hygiene products, cosmetic containers, shampoo bottles and cups, to name a few [2, 7, 8].

The thermal decomposition of PHB has already been studied in detail analytically with the aid of TGA, DSC, Py-MS, Py-GC/MS, and Py-GC-FTIR [9-12]. The pyrolysis of PHB followed by a condensation of the volatiles produced, has already been executed as well: the pyrolysis of purified PHB yields 60 to 65% of crotonic acid [13].

Table 5.1: Main characteristics (on dry basis) of willow and PHB.

Characteristics	Willow	PHB
Proximate analysis (%)		
Moisture	1.88	0.17
Volatiles	75.27	97.97
Fixed C	21.14	0.80
Ash	1.71	1.06
Ultimate analysis (%)		
Carbon	46.91	55.96
Hydrogen	5.95	7.07
Nitrogen	0.63	0.14
Oxygen	41.69	36.40
H/C molar ratio	1.52	1.52
O/C molar ratio	0.67	0.49
Calorimetric analysis (MJ/kg)		
Higher Heating Value (H.H.V.)	18.7	22.8

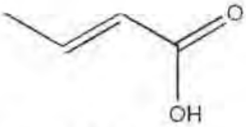

Figure 5.3: Crotonic acid.

In this section, the influence of the flash co-pyrolysis of willow and PHB on the pyrolysis behaviour and the evolving pyrolytic gases, the bio-oil yield, its water content and heating value are discussed in function of the w/w ratio applied in the blend. The main characteristics of willow and PHB are summarised in Table 5.1. As was already observed for 1:1 willow/PHB in Chapter 4, some blends not only result in bio-oil, but additionally produce a pure crystalline phase (crystals of crotonic acid), which is an important next step in the upgrading and separation of bio-oils into chemicals with added value. Crotonic acid (CAS No. 3724-65-0; Figure 5.3) has a reactive double bond and carboxlic group in one molecule. It can, for instance, be applied in the manufacturing of copolymers with vinyl acetate used in lacquers and paper sizing, in the manufacturing of softening agents for synthetic rubber, or in medicinal chemistry, e.g. in the manufacturing of DL-threonine, or vitamine A. It can also function as a first step towards the production of flavouring agents, perfume, internal plasticizers, pesticides, dyes, textile treatment agents, fungicides and pharmaceuticals. The production of these crystals, empowered by a high energy recuperation, are the main reasons why the flash co-pyrolysis of willow and PHB is selected as the most performant option by Decision Lab as discussed in Chapter 4.

5.1.1. Analytical study of the (co-)pyrolysis of willow and PHB

5.1.1.1. TGA analysis

The pyrolysis behaviour of willow, PHB and willow/PHB blends with a w/w ratio of 7:1, 3:1, 2:1 and 1:1 is investigated with the aid of TGA. The mass loss curves and the derivatives of willow, PHB and 1:1 willow/PHB are shown in Figure 5.4. From the thermograms of the pure materials, the moisture content can be approximated: after preliminary drying, willow still contains about 1.9 % moisture, while PHB only contains a negligible amount of 0.2 %.

As most woody biomass, willow mainly exists of the three basic constituents: cellulose, hemicelluloses and lignin. As described in Chapter 1, each of these constituents has a specific influence on the TG and DTG profile of biomass [14-17]. It is known that lignin decomposes within a wide temperature interval (433 – 1173 K) and its DTG peak is not commonly distinguishable [14-17]. Hemicelluloses (the shoulder in the profile of Figure 5.4a) is the second constituent to decompose, followed by cellulose (the main DTG peak centered around 622 K), which decomposes in a narrow temperature interval from about 470 up to 670 K. This is the interval in which the main decomposition takes place and which accounts for the greatest mass loss during the biomass pyrolysis process [14-17]. PHB on the other hand (Figure 5.4b), decomposes in a very narrow temperature interval between 480 and 565 K, resulting in a sharp degradation peak with a maximum at 545 K.

The willow/PHB blends (Figure 5.4c only shows the thermogram of the 1:1 willow/PHB blend) all give very comparable profiles and are almost a superposition of the individual materials: PHB (maximum decomposition at 545 K) and willow (maximum decomposition at 622 K). So, no detectable interaction among willow and PHB during pyrolysis is inferred by TGA. Even though willow and PHB are present in the same amount (1:1), the magnitude of the first peak at 545 K, which represents the decomposition of PHB, is excessively higher as compared to the magnitude of the second peak at 622 K, which represents the decomposition of willow. Figure 5.4 also shows that most of the decomposition reactions are finalised at a temperature of about 670 K, so justifying a flash pyrolysis temperature of 723 K during the reactor pyrolysis experiments, which will be discussed in 5.1.2.

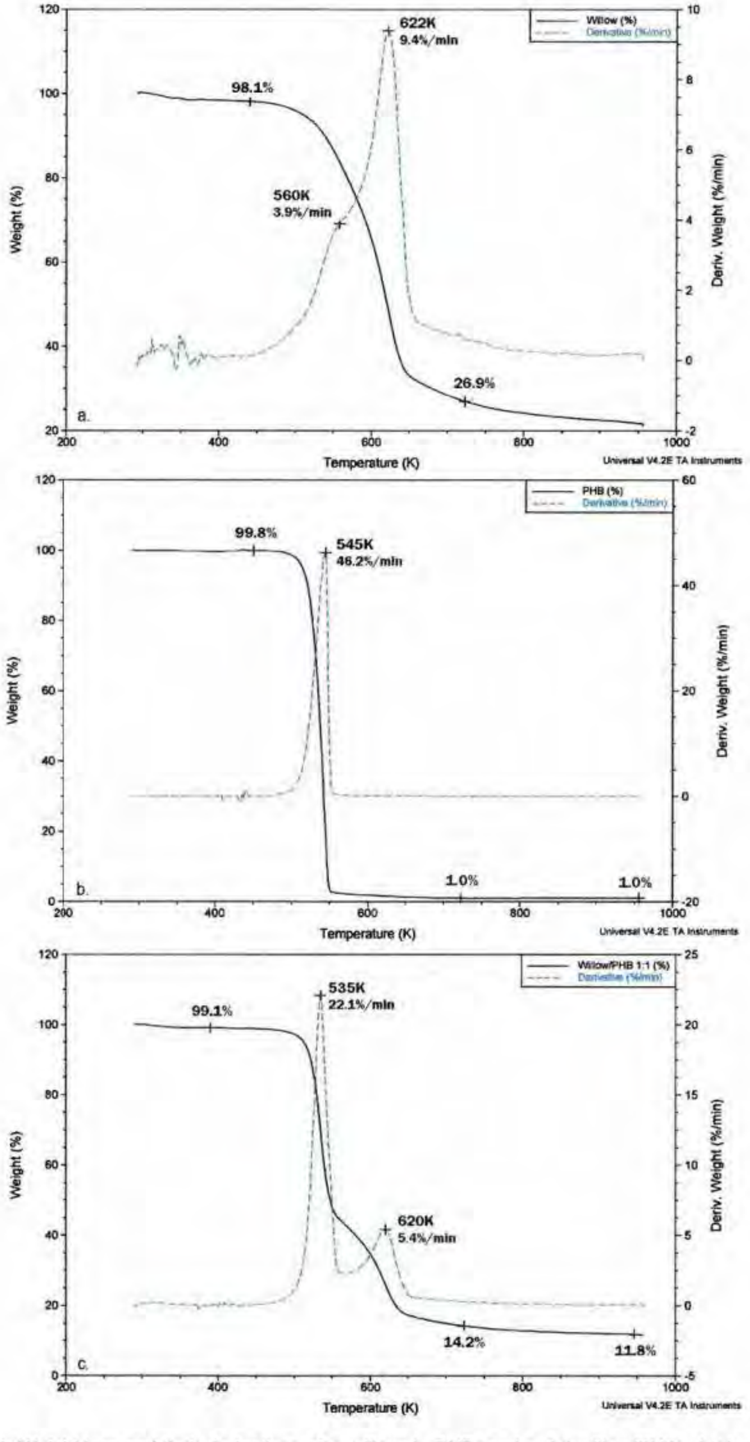

Figure 5.4: Weight loss and their derivatives of a, willow; b, PHB; and c, 1:1 willow/PHB; obtained by TGA.

5.1.1.2. TG/MS analysis

From the TG/MS ion-kinetograms of the mass fragment ion *m/z* 18 (Figure 5.5), it can be concluded that **pyrolytic water** is formed during the intense decomposition of the input materials in the temperature range between 470 and 670 K. Depending on the sample (± 2 mg starting material) being examined, a one- or two-peak pattern similar to the DTG-profile (shown in Figure 5.4) is obtained. A difference in the amount of pyrolytic water produced out of pure willow and pure PHB (reference 1 and 2, respectively) is observed, with the pyrolysis of willow resulting in a higher amount of pyrolytic water.

In the case of the 1:1 willow/PHB blend, a relatively high amount of pyrolytic water is detected: the area under the 1:1 curve is significantly higher as compared to the fractional sum of the individual areas of both references (pure willow and pure PHB) in their ion-kinetograms and can be interpreted as an indication that the co-pyrolysis of willow and PHB does not seem to result in a reduction of the amount of pyrolytic water. Additionally it can be noted that a sharp contrast to the DTG-profile of 1:1 willow/PHB (Figure 5.4c) is observed: the magnitude of the first peak (at 545 K) in the ion-kinetogram of the mass fragment ion *m/z 18* of 1:1 willow/PHB (Figure 5.5) is lower compared to the second peak (at 622 K), which indicates that the influence of PHB on the production of pyrolytic water is fairly lower compared to willow in the blend.

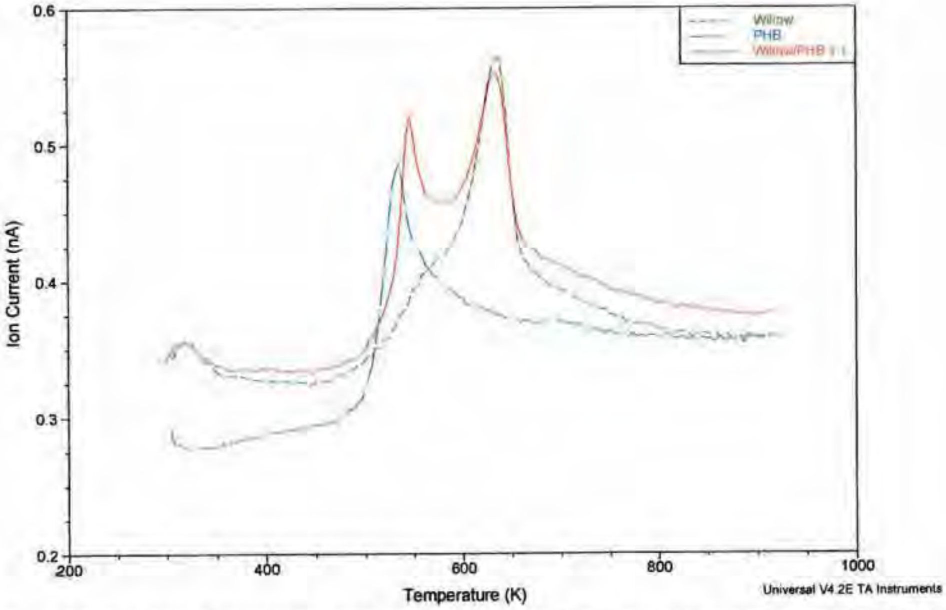

Figure 5.5: Evolution of the mass fragment ion '18' in function of temperature (= ion-kinetogram of *m/z* 18) for willow, PHB, and 1:1 willow/PHB; obtained by TG/MS.

Other mass fragment ions, e.g. *m/z* 16, 28, 29, 44, 45, and 46, potentially representing the release of methane, carbon monoxide, typical fragments of aldehydes and/or ketones, carbon dioxide, typical fragments of alcohols and/or ethers, and typical fragments of acids, respectively, have also been evaluated by TG/MS and show patterns comparable to those of the ion-kinetograms of m/z 18 (Figure 5.5).

Additionally, the formation of a specific component during the decomposition of PHB and the willow/PHB blends at approximately 545 K is exposed by TG/MS: the mass fragment ion *m/z* 86 increases in direct relation with the addition of PHB (Figure 5.6). This trend is also observed for the mass fragment ions *m/z* 39, 41, 68, and 69. These *m/z* values are characteristic signals of crotonic (or butenoic) acid. The formation of **crotonic acid** during the thermal degradation of pure PHB has already been observed in the evolving pyrolytic gases and is discussed in literature [17-20,24].

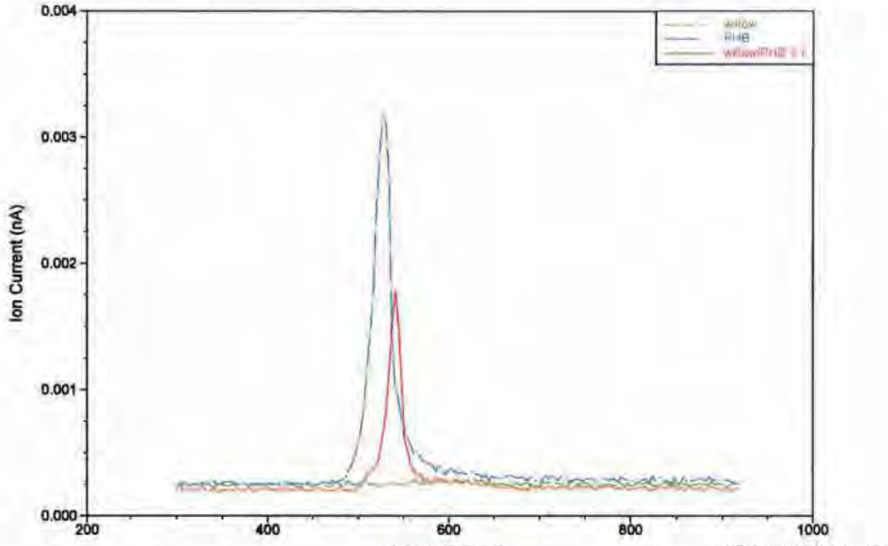

Figure 5.6: The ion-kinetogram of the mass fragment ion *m/z* 86, representing the production of crotonic acid during the (co-)pyrolysis of willow, PHB and 1:1 willow/PHB; obtained by TG/MS.

5.1.1.3. TG/FT-IR analysis

Additionally, TG/FT-IR experiments have also been performed on pure willow, pure PHB and the four willow/PHB blends. The TG/FT-IR spectra extracted at 545 K and 622 K (the main decomposition temperatures of PHB and willow, respectively) of the evolving pyrolytic gases of pure willow, pure PHB and 1:1 willow/PHB are visualised in Figure 5.7, where a comparison between the different FT-

IR spectra at their respective temperature, e.g. 545 K (left) and 622 K (right), is made. One should be aware that these spectra are to be considered as the FT-IR analysis of a mixture of several volatiles evolving at the same time/temperature event.

At **545 K**, the pure PHB and 1:1 willow/PHB FT-IR spectra are very similar. Only a few differences are observed:

- the willow/PHB blend shows a relatively higher response for CO_2 (2300 – 2400 cm^{-1}) compared to pure PHB, and
- the band pattern at 1150 cm^{-1} (most probably referring to C-O vibrations) slightly differs between pure PHB and 1:1 willow/PHB.

The decomposition of the 1:1 willow/PHB blend at 545 K is clearly dominated by and can almost completely be attributed to the degradation of PHB, indicating that yet no significant interactions occur during the analytical co-pyrolysis.

At **622 K**, on the other hand, the FT-IR spectrum of 1:1 willow/PHB resembles the FT-IR spectrum of willow the most. However, the spectrum features are still affected by PHB. This can possibly be explained by tailing of the PHB decomposition (also consult the 3D diagrams in Figure 5.9 where such tailing is also observed). All three FT-IR spectra at 622 K show the presence of CO_2 (and CO), but the actual peak pattern of CO_2 slightly differs for all three inputs. The response for CO_2 is the highest in the 1:1 willow/PHB spectrum. This observation can be an indication towards another degradation mechanism, which results in an increased production of CO_2, occurring during the co-pyrolysis of willow and PHB.

Figure 5.8, which contains some minor artefacts due to background substraction, shows the evolution of CO and CO_2 as a function of temperature for pure willow, pure PHB, and 1:1 willow/PHB. The evolving gases monitored by TG/FT-IR contain much more CO_2 than CO, with PHB (Figure 5.8b) producing only a negligible amount of CO. The CO_2-profile of the 1:1 willow/PHB blend obtained by TG/FT-IR (shown in Figure 5.8c) resembles the profile for water obtained by TG/MS of that same blend (ion-kinetogram of the mass fragment ion *m/z* 18, Figure 5.5): the magnitude of the first peak (at 545 K) of 1:1 willow/PHB is lower compared to the second peak (at 622 K), which is in sharp contrast to the DTG-profile of 1:1 willow/PHB (Figure 5.4c), indicating that, as for the production of pyrolytic water, the influence of PHB on the production of CO_2 is fairly lower compared to willow in the blend.

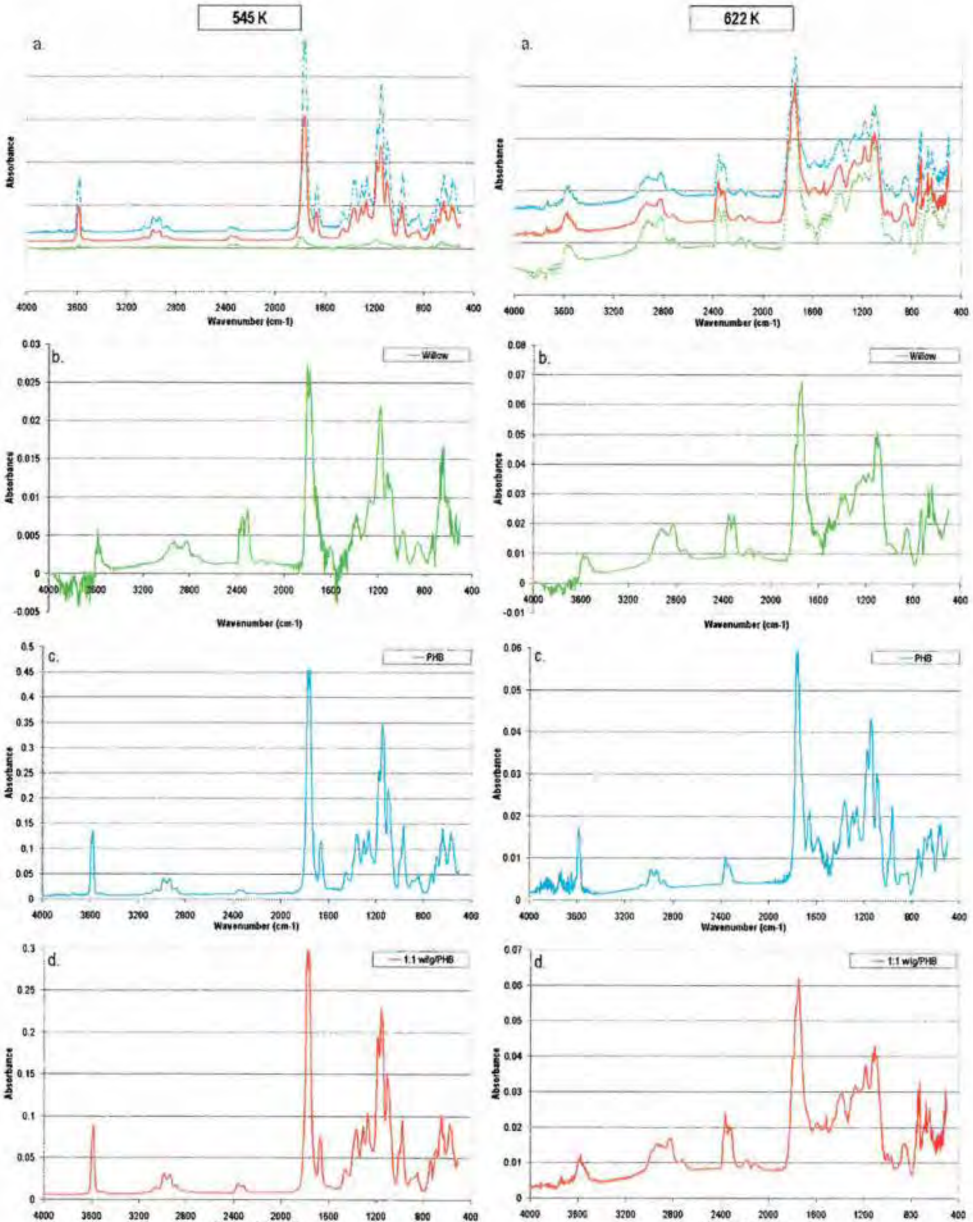

Figure 5.7: FT-IR spectra of the evolving gases at 545 K (left) and 622 K (right); a, overlay; b, for willow; c, PHB; and d, 1:1 willow/PHB; obtained by TG/FT-IR.

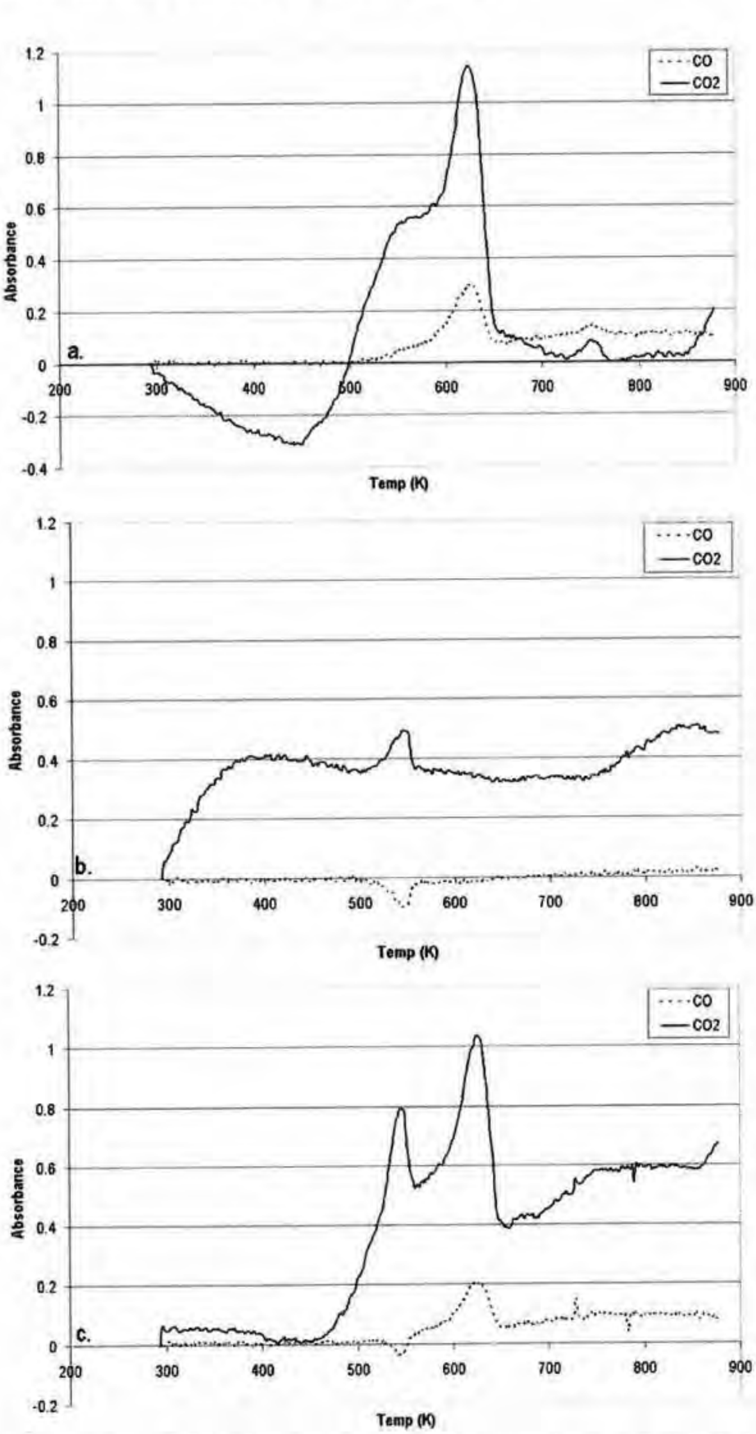

Figure 5.8: The evolution of CO and CO$_2$ during the thermal decomposition of a, willow; b, PHB; and c, 1:1 willow/PHB; obtained by TG/FT-IR.

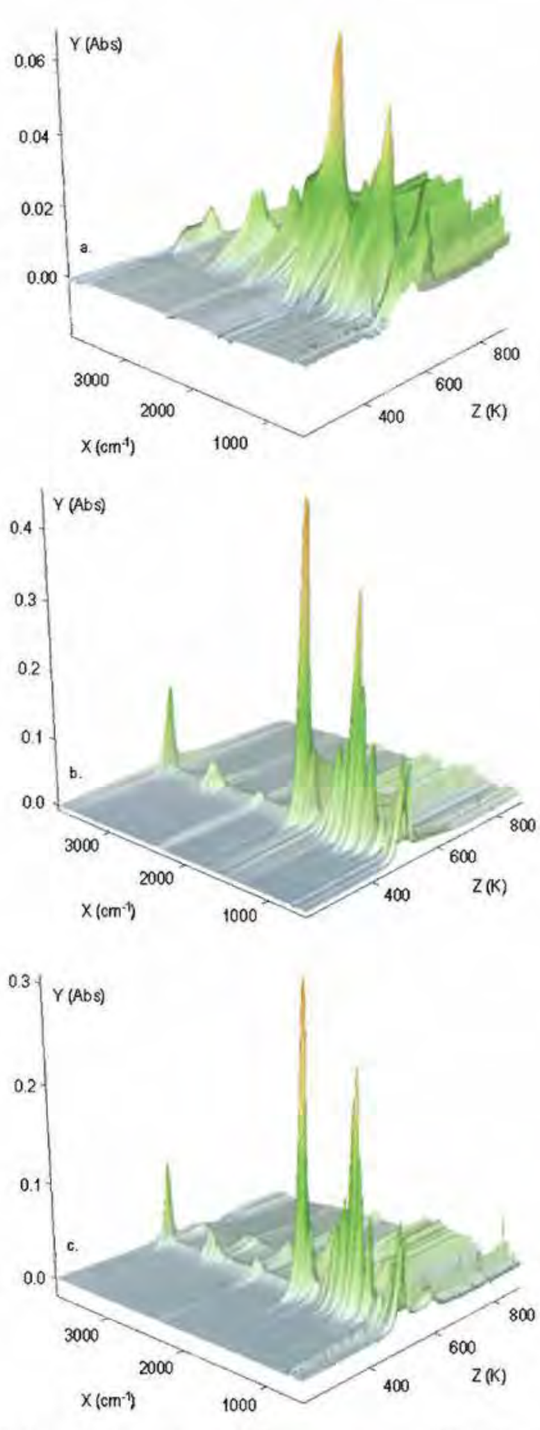

Figure 5.9: 3D TG/FT-IR diagrams of a, willow; b, PHB; and c, 1:1 willow/PHB with X: Wave number (cm^{-1}) ; Y: Absorbance Units (Abs); Z: Temperature (K).

In both the FT-IR spectra at 545 K and 622 K (Figure 5.7) and in the 3D-diagrams (Figure 5.9), obtained by plotting the absorbance (Y) of the evolving gases as a function of the wave number (X) and temperature (Z), the most abundant peaks are represented by the carbonyl functionalities located at 1800 – 1690 cm^{-1}.

Figure 5.10 specifically focuses on the evolution of these carbonyl functionalities, expressed as the overall intensity within a specific spectral window (1876 – 1696 cm^{-1}) as a function of temperature. The most abundant peak is obtained from PHB, and the least one from willow, while the 1:1 willow/PHB blend is located somewhere in between. This trend is observed for almost all functionalities and their respective spectral windows. In general, it can be concluded that the overall evolution of functional groups as a function of temperature (obtained by TG/FT-IR), ignoring the small temperature differences due to the experimental set-up, resembles the DTG-profiles shown in Figure 5.4, indicating that no significant reactions and/or interactions seem to occur during the co-pyrolysis of willow and PHB under these analytical circumstances.

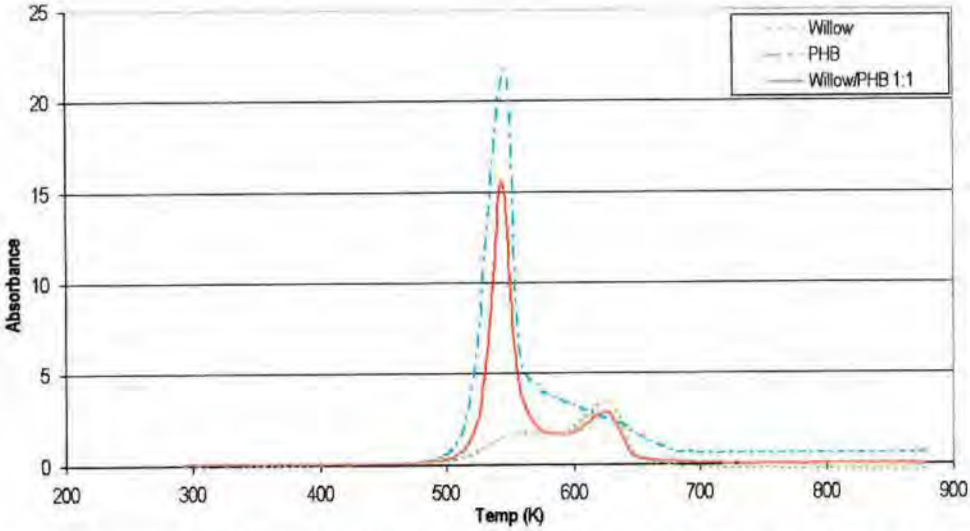

Figure 5.10: Traces of carbonyl functionalities (1876 – 1696 cm^{-1}) for willow, PHB, and 1:1 willow/PHB; obtained by TG/FT-IR.

5.1.2. Flash (co-)pyrolysis of willow and PHB – reactor experiments

So far, different analytical pyrolysis techniques have been performed in order to grasp some ideas on the general pyrolysis mechanisms that might occur during the co-pyrolysis of willow and PHB. However, all experiments have been applied analytically based on slow pyrolysis, while during the semi-continuous (co-)pyrolysis experiments flash pyrolysis is induced. In what follows, the results of the flash (co-)pyrolysis experiments on willow, PHB and their blends, performed with the pyrolysis reactor (Figure 2.9), will be discussed.

5.1.2.1. Pyrolysis yields and efficiencies

The flash pyrolysis of willow and the flash co-pyrolysis of 7:1 and 3:1 willow/PHB, with the pyrolysis reactor, result into a typical brown viscous bio-oil. However, as soon as a sufficient amount of PHB is added (2:1 and 1:1 willow/PHB), crystals are formed in the bio-oil (after condensation; Figure 2.9 part c). After complete crystallisation, the bio-oil is filtered and the crystals are readily separated from the bio-oil. The pyrolysis of pure PHB, on the other hand, only results in the production of such crystals. The crystals contain no water and are characterised with the aid of GC/MS as crotonic acid (or butenoic acid). The presence of crotonic acid in the pyrolytic gases is already observed with the aid of TG/MS (*m/z* 39, 41, 68, 69, and 86), Figure 5.6.

Table 5.2a summarises the pyrolysis yields and efficiencies of the flash (co-)pyrolysis of pure willow, pure PHB and the willow/PHB blends with a w/w-ratio of 7:1, 3:1; 2:1 and 1:1; performed with the pyrolysis reactor. In Table 5.2a, 'condensables' is used to group bio-oil and crystals, while in Table 5.2b a subdivision of 'condensables' into bio-oil and crystals is made. Additionally, Table 5.2b virtually subdivides bio-oil into water-free bio-oil and pyrolytic water based on the water content. Figure 2.10 and Figure 3.1 schematically represent the pyrolysis flowchart.

Table 5.2a: Pyrolysis yields and efficiencies of the condensables, char and gas productions in function of the willow/PHB w/w ratios. The gas yield is calculated by difference.

	Willow	7:1	3:1	2:1	1:1	PHB
Input (m%)						
Willow	100.00	85.80	73.94	64.68	50.06	0.00
PHB	0.00	14.20	26.06	35.32	49.94	100.00
Output (m%)						
Condensables	**50.10**	**53.29**	**57.76**	**59.38**	**64.24**	**68.67**
Char	22.39	22.28	16.20	13.80	9.50	0.49
Gases (by diff.)	27.50	24.43	26.04	26.82	26.26	30.84

'Input (m%) is calculated on dry basis.

Table 5.2b: Subdivision of condensables into crystals and bio-oil; and virtually of bio-oil into water-free bio-oil and pyrolytic water based on the water content; obtained from 100 g input.

	Willow	7:1	3:1	2:1	1:1	PHB
Cristals (g)	0.00	0.00	0.00	9.20	29.70	68.67
Bio-oil (g)	50.10	53.29	57.76	50.18	34.54	0.00
Water content (m% of bio-oil)	36.65	26.87	21.00	20.26	15.95	0.00
Water-free Bio-oil (g)	**31.74**	**38.97**	**45.63**	**40.01**	**29.03**	**0.00**
Pyrolytic Water (g)	18.36	14.32	12.13	10.17	5.51	0.00

Based on these results, some conclusions can be drawn:

- The yield in condensables (Table 5.2a) increases in direct relation to the addition of PHB.
- Additionally, a **synergy** can be calculated, i.e. an increased yield in condensables compared to the sum of the fractional experimental values of both inputs is achieved. The occurrence of synergetic interactions is observed based on a comparison between the actual pyrolysis results of the willow/PHB blends, the theoretical pyrolysis results calculated from the reference pyrolysis experiments (pure willow and pure PHB) and their respective w/w ratio.

  Table 5.3a summarises the synergy (in %) in the total yield in condensables obtained by the flash co-pyrolysis of the 7:1, 3:1, 2:1 and 1:1 blends. The synergy is calculated based on the yield in condensables of the two reference materials (pure willow and pure PHB) and their respective w/w ratio, and the yield in condensables obtained by the actual flash co-pyrolysis of the blends. The synergy in the total yield in condensables culminates in the 1:1 w/w-ratio, and reaches more than plus 8%:

*The theoretical yield in condensables = [(50.06g x 50.10% + 49.94g x 68.67%)/100] = 59.37m%, while the actual yield in condensables is 64.24 m%, thus an increase of 4.87 m% or [(4.87*100)/59.37] = + 8.20 %.*

- The yield in water-free bio-oil also shows a **synergy** for all willow/PHB blends (Table 5.3b). Here, however, the most pronounced synergy is obtained for the 2:1 willow/PHB blend reaching almost + 95%:

  *The theoretical water-free bio-oil yield = [(64.68g x 31.74% + 35.32g x 0.00%)/100] = 20.53m%, while the actual yield in water-free bio-oil is 40.01 m%, thus an increase of 19.48m% or [(19.48*100)/20.53] = + 94.89 %.*

- The maximum yield in water-free bio-oil (in absolute terms (Table 5.2b)), on the contrary, is obtained during the flash co-pyrolysis of 3:1 willow/PHB, representing a yield of 45.63 m%.
- The presence of a **synergy** is also confirmed in Table 5.3c, where the production of pyrolytic water is lower compared to the sum of the fractional experimental values of both inputs. Again, the synergy peaks at the 1:1 w/w-ratio resulting into a decrease of minus 40%:

  *The theoretical yield in pyrolytic water = [(50.06g x 18.36% + 49.94g x 0.00%)/100] = 9.19m%, while the actual yield in pyrolyitc water is 5.51 m%, thus a decrease of 3.68 m% or [(3.68*100)/9.19] = - 40.05 %.*

- On the other hand, it is observed from Table 5.2b that the production of crystals is lower in comparison with the sum of the fractional experiments. However, after a preliminary GC/MS analysis of the different bio-oils, it is worth mentioning that the amount of dissolved crotonic acid in bio-oil increases in accordance with the addition of PHB. This will be discussed in further detail in Chapter 6.

In general, it can be concluded that the flash co-pyrolysis of willow and PHB results in a bio-oil with added value, and that the preferred w/w-ratio of willow/PHB depends on the specific goal of the flash co-pyrolysis.

Table 5.3: Synergy (in %) in a. the total yield in condensables, b. the water-free bio-oil yield and c. the amount of pyrolytic water; calculated by '[(Actual-Theoretical)/Theoretical]•100%'.

a.	Total yield in condensables		
Bio-oil	Theoretical (m%)	Actual (m%)	Synergy (%)
Willow	*50.10*	*50.10*	-
7:1 willow/PHB	52.74	53.29	1.05
3:1 willow/PHB	54.94	57.76	5.13
2:1 willow/PHB	56.66	59.38	4.80
1:1 willow/PHB	59.37	64.24	8.20
PHB	*68.67*	*68.67*	-

b.	Water-free bio-oil yield		
Bio-oil	Theoretical (m%)	Actual (m%)	Synergy (%)
Willow	*31.74*	*31.74*	-
7:1 willow/PHB	27.23	38.97	43.10
3:1 willow/PHB	23.47	45.63	94.43
2:1 willow/PHB	20.53	40.01	94.89
1:1 willow/PHB	15.89	29.03	82.70
PHB	*0.00*	*0.00*	-

c.	Amount of pyrolytic water		
Bio-oil	Theoretical (m%)	Actual (m%)	Synergy (%)
Willow	*18.36*	*18.36*	-
7:1 willow/PHB	15.75	14.32	-9.10
3:1 willow/PHB	13.58	12.13	-10.67
2:1 willow/PHB	11.88	10.17	-14.36
1:1 willow/PHB	9.19	5.51	-40.05
PHB	*0.00*	*0.00*	-

Willow and PHB (*in italic*) are considered as the references. Small differences can be found due to rounding error.

5.1.2.2. Energetic valorisation

The averaged experimental H.H.V.'s obtained by calorimetry of the respective bio-oils are summarised in Table 5.4. The addition of PHB clearly shows an additional advantage, i.e. an increase in H.H.V. of the bio-oil compared with bio-oil of pure willow (16.1 MJ/kg), directly correlated with the addition of PHB. One of the main reasons for the increase in H.H.V. seems to be the decrease of the water content. Even though the crystals are economically more attractive as high value feedstock, they show to have the highest H.H.V., reaching 23.1 MJ/kg.

Table 5.4: H.H.V.'s of bio-oils in Mega Joule per kilogram and the synergetic increase (in %) in the energy recuperation; calculated by '[(Actual-Theoretical)/Theoretical]∗100%'. Willow and PHB (*in italic*) are considered as the references.

		Energy recuperation		
Bio-oil	H.H.V. (MJ/kg)	Theoretical (m%)	Actual (m%)	Synergy (%)
Willow	16.1	*43.14*	*43.14*	-
7:1 willow/PHB	18.0	46.91	49.83	6.21
3:1 willow/PHB	19.0	50.07	55.67	11.18
2:1 willow/PHB	19.1	52.53	58.18	10.77
1:1 willow/PHB	20.2	56.41	66.80	18.41
PHB	-	*69.72*	*69.72*	-

The H.H.V. of the crystals equals 23.1 MJ/kg. Small differences can be found due to rounding error.

Taking into account the pyrolysis yields in condensables (Table 5.2a and b), the H.H.V.'s of the input materials (Table 5.1), of the bio-oil (Table 5.4) and the crystals (H.H.V. = 23.1 MJ/kg), an energy recuperation ranging from 43% to 70% for the pyrolysis of pure willow and pure PHB, respectively, is obtained in Table 5.4. The flash co-pyrolysis of 1:1 willow/PHB approximates the energy recuperation obtained from pure PHB (67% - 70%, respectively):

The energy recuperation in condensables for the 1:1 willow/PHB flash co-pyrolysis = [(34.54g x 20217 J/g + 29.70g x 23104 J/g) x 100/(50.06g x 18699 J/g + 49.94g x 22756 J/g)] = 66.80%. The energy recuperation in condensables for the flash pyrolysis of pure PHB = [(68.67g x 23104 J/g) x 100/(100g x 22756 J/g)] = 69.72 %.

It can be concluded that the flash co-pyrolysis of the different w/w-ratios results in an increased energy recuperation compared to the sum of the fractional experimental values of both references (= **synergy**), and thus makes the flash co-pyrolysis of willow and PHB an energetic and economic attractive route. Table 5.4 summarises the theoretical energy recuperation calculated based on the flash pyrolysis results of the two reference materials (pure willow and pure PHB) and their respective w/w ratio, the actual energy recuperation obtained by the flash co-pyrolysis of the blends, and the synergetic increase in the energy recuperation for the 7:1, 3:1, 2:1 and 1:1 willow/PHB blends (in %). Again, the synergy culminates for the 1:1 willow/PHB blend and reaches plus 18.4%:

*The theoretical energy recuperation = [(50.06g x 43.14% + 49.94g x 69.72%)/100] = 56.41 %, while the actual energy recuperation is 66.80 %, thus an increase of 10.39 % or [(10.39*100)/56.41] = +18.41 %.*

5.1.2.3. PHB optima

It can be stated that the flash co-pyrolysis of the 3:1 willow/PHB blend results in the highest bio-oil and water-free bio-oil yield (57.76 m% and 45.63 m%, respectively), while the 1:1 willow/PHB blend results in the highest synergetic decrease (minus 40%) in the amount of pyrolytic water, the highest synergetic increase of the yield in condensables (plus 8%) and the highest synergetic increase in energy recuperation (plus 18%).

Even though the explorative analysis (TGA, TG/MS and TG/FT-IR) did not result in any conclusive evidence regarding interactions between willow and PHB during (slow) co-pyrolysis, nor regarding a decrease in the amount of pyrolytic water in the evolving gases, a synergetic reduction of the water content and of the amount of pyrolytic water produced during the flash co-pyrolysis of willow and PHB with the pyrolysis reactor is achieved. Additionally, a synergetic increase in pyrolysis yield, water-free bio-oil yield and energy recuperation is observed. The obtained synergy points out that the (flash) co-pyrolysis of willow and PHB results in synergetic (non-additive) observations. Therefore, the synergy can only be explained by additional reactions (and different reaction circumstances) during flash co-pyrolysis in the pyrolysis reactor. In Chapter 6, additional experiments will be executed to further explain the observed synergy.

5.2. Flash co-pyrolysis of willow and PLA

Polylactic acid, PLA (Figure 5.11), is produced principally via microbial fermentation of sugar feedstock and of carbohydrates from other renewable resources, such as corn, potato and diverse agricultural products [18-20]. Starch and/or cellulose is extracted and broken down into sugars. These sugars are hydrolysed to form dextrose, which is further fermented to lactic acid (Figure 5.12). Although the major use of lactic acid is in food and related industries, it can subsequently be polymerised via its cyclic dimer (lactide) to polylactic acid via a ring opening process [8, 21, 22]. PLA is possibly the most commonly applied biopolymer and has the most potential for widespread use, but does not have the best biodegradability properties amongst biopolymers. PLA is a biocompatible and biodegradable synthetic polymer with many good properties such as mechanical strength, transparency, and compostability and is being used in many biomedical applications such as controlled drug delivery, implants and vascular prosthesis [19, 20, 23-26].

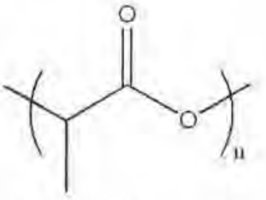

Figure 5.11: PLA strucure.

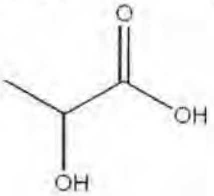

Figure 5.12: PLA monomer – lactic acid.

Recently, interest in polylactic acid has moved beyond its traditional areas of biomedical and pharmaceutical applications to the area of commodity applications such as packaging plastics that will biodegrade upon disposal [25, 27, 28]. Similar to many other plastics, the main techniques for processing PLA into varied products are injection moulding, compression moulding, extrusion and other melt processing methods [26, 27]. PLA is a unique polymer that in many ways looks like PET, also a polyester, but also performs much like polypropylene (PP), a polyolefin. Life-cycle assessment (LCA) indicated that PLA polymers are more energy efficient than PP, which is mainly because PLA consumes almost no feedstock energy [26, 29]. It may eventually be the polymer with the broadest range of applications because of its ability to be stress crystallised, thermally crystallised, impact modified, filled, co-polymerised, and processed in most polymer processing equipment [21]. For instance, PLA can be formed into transparent films or injection moulded into blow-mouldable pre-forms for bottles, similar to PET. It is also excellent for food contact and related packaging applications [21, 26]. Additionally, it is of particular significance for agricultural or gardening applications [21]. Other applications are thermoformed packaging, fiber and fibrefill applications, cold drinking cups, containers, sundae and salad cups, takeaway food trays, overwrap and lamination films, blister packages, bottles, clothes, chewing gum, floor coverage, and many more [8, 18, 26, 30, 31]. Real-life examples of PLA usage today are for instance packaging foods such as Biota™ PLA bottled water, Noble™ PLA bottled juices, and Dannon™ yoghurts [32].

However, whilst the biodegradability of PLA is excellent in terms of its ability to be bioabsorbed, its microbial degradation is limited to a few species of micro-organisms. Any large-scale consumption of PLA products will bring the associated problem of an excess of PLA waste, which will be difficult to treat by biodegradation either in composting plants or in the natural environment [28]. Therefore, an alternative technique, such as flash (co-)pyrolysis, to treat such specific waste is required. The thermal decomposition of PLA has already been studied in detail [10, 33-35].

In this section, the influence of the flash co-pyrolysis of willow and PLA on the pyrolysis behaviour and the evolving pyrolytic gases, the bio-oil yield, its water content and heating value are discussed in function of the w/w ratio applied in the blend. The main characteristics of willow and PLA are listed in Table 5.5. The second highest reduction in the amount of pyrolytic water (after 1:1 willow/PHB), the second highest water-free bio-oil yield and the production of the bio-oil with the lowest water content are the main reasons why the flash co-pyrolysis of willow and PLA is selected by Decision Lab as the second most performant biopolymer option as discussed in Chapter 4.

Table 5.5: Main characteristics (on dry basis) of willow and PLA.

Characteristics	Willow	PLA
Proximate analysis (%)		
Moisture	1.88	0.00
Volatiles	75.27	98.05
Fixed C	21.14	1.30
Ash	1.71	0.65
Ultimate analysis (%)		
Carbon	46.91	49.84
Hydrogen	5.95	5.63
Nitrogen	0.63	0.15
Oxygen	41.69	44.42
H/C molar ratio	1.52	1.36
O/C molar ratio	0.67	0.67
Calorific value (MJ/kg)		
Calorimetric analysis	18.7	18.6

5.2.1. Analytical study of the (co-)pyrolysis of willow and PLA

5.2.1.1. TGA analysis

TGA is executed to obtain an overview of the basic characteristics (Table 5.5) and insight in the pyrolysis behaviour of willow, PLA and their blends. For the pyrolysis of the pure materials and the 1:2 blend, the mass loss curves and the derivatives are shown in Figure 5.13. The thermogram of willow points out that willow still contains approximately 2% moisture, while for PLA a negligible amount is measured.

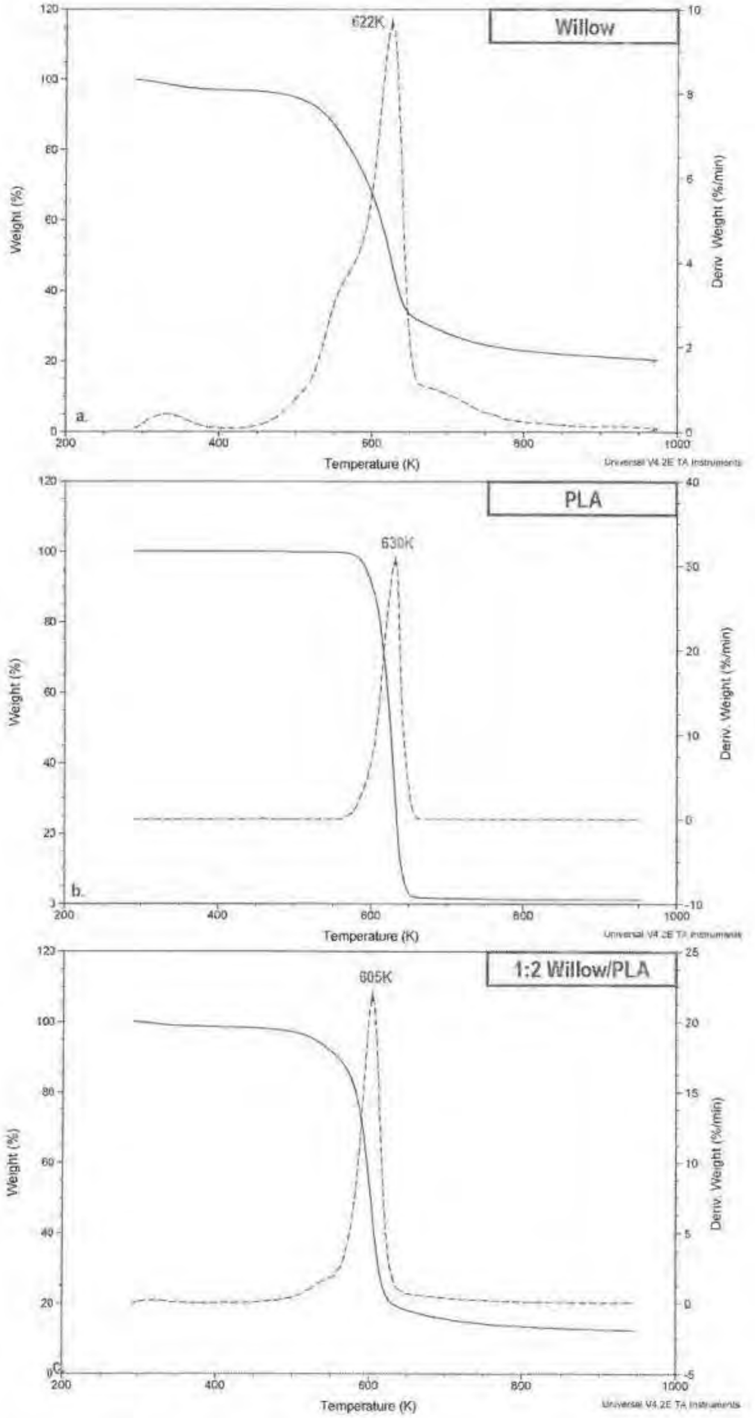

Figure 5.13: Weight loss and their derivatives of a, willow; b, PLA; and c, 1:2 willow/PLA, obtained by TGA.

As previously mentioned, the main decomposition of willow takes place in a temperature range from about 470 up to 670 K, with a maximum decomposition temperature of 622 K (Figure 5.13a). PLA on the other hand (Figure 5.13b) decomposes in one single and narrow temperature interval that ranges from 563 to 663 K, with a maximum at 630 K. Important to note is that the maximum decomposition temperature of willow and PLA coincide.

The triple stage decomposition of willow is observed in all blends, however, in reduced form directly correlated with the addition of PLA. The thermogram of the 1:2 willow/PLA blend (Figure 5.13c) gives a profile that is very comparable to that of pure PLA. The peak maxima of the derivatives of the pure materials and their blends ranges between 603 K and 633 K. As was already observed for PHB, Figure 5.13 shows that most of the decomposition reactions are finalised at a temperature of about 673 K, again justifying a maximum flash pyrolysis temperature of 723 K during the reactor experiments.

5.2.1.2. TG/MS analysis

Based on the TG/MS ion-kinetograms of the mass fragment ion *m/z* 18 (Figure 5.14), it can be concluded that pyrolytic water is formed during the intense decomposition at the temperature range between 473 and 673 K. More specifically, the pattern of the DTG-curves in the thermogram (Figure 5.13) are also visible for the evolution of the mass fragment ion '18' (water) in function of time during the pyrolysis of willow, PLA, and their blends (Figure 5.14). A difference in the amount of pyrolytic water produced from pure willow (1 g of starting material) and pure PLA (also 1 g of starting material) is observed, predicting a high and a low water content for willow and PLA bio-oil, respectively. Additionally, an intermediate production of pyrolytic water for the 1:2 willow/PLA blend (2 g of starting material) is indicated.

Other mass fragment ions, e.g. *m/z* 16, 28, 29, 44, 45, and 46, potentially representing the release of methane, carbon monoxide, typical fragments of aldehydes and/or ketones, carbon dioxide, typical fragments of alcohols and/or ethers, and typical fragments of acids, respectively, have additionally been detected by means of TG/MS. Here, no extra conclusions could be drawn besides the fact that the evolution of the ion-kinetograms resembles the pyrolysis DTG-curves (Figure 5.13), as is shown for water in Figure 5.14.

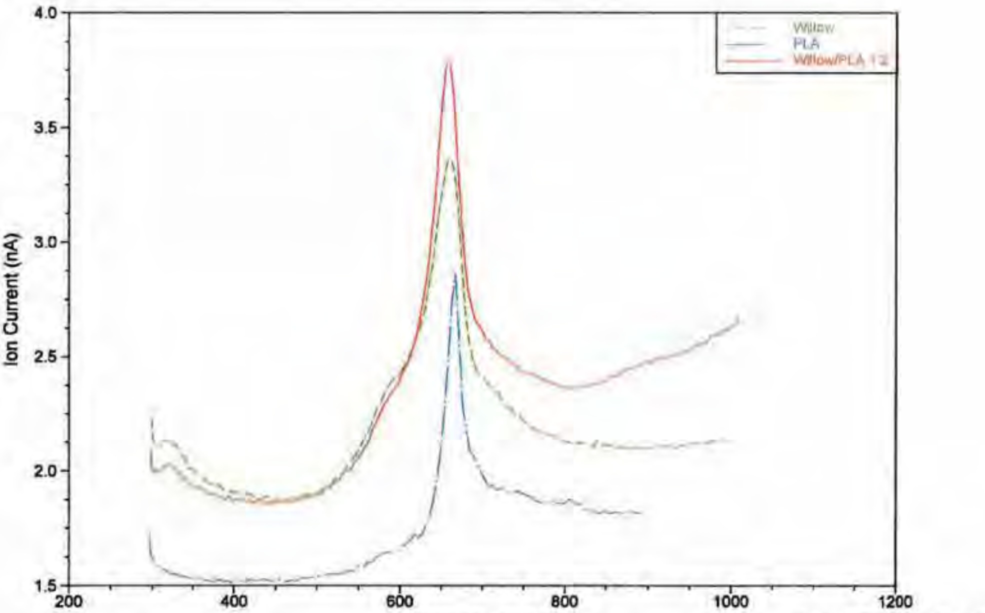

Figure 5.14: Evolution of the mass fragment ion '18' in function of temperature (= ion-kinetogram of *m/z* 18) for willow, PLA, and 1:2 willow/PLA, obtained by TG/MS.

5.2.1.3. TG/FT-IR analysis

TG/FTIR analysis shows some interesting evolutions during co-pyrolysis. For comparison, the FT-IR spectra for willow, PLA and 1:2 willow/PLA extracted at the highest pyrolysis decomposition rate (T = 603 – 633 K) are visualised in Figure 5.15.

- First, a shift in the most abundant band at 1650 – 1860 cm^{-1}, which represents the carbonyl functionalities, is observed. Here, a shift of band position towards a higher wavenumber is shown: 1745 cm^{-1} for willow, 1766 cm^{-1} for PLA and 1793 cm^{-1} for 1:2 willow/PLA, reflecting the presence of increased ester functionalities.
- Additionally, an intense peak at 1200 – 1250 cm^{-1} for 1:2 willow/PLA is formed and cannot be explained by the reference materials according to the ratio applied.

Such differences in pattern can only be explained by additional reactions occurring during co-pyrolysis, resulting in an altered gas composition (both condensable and non-condensable).

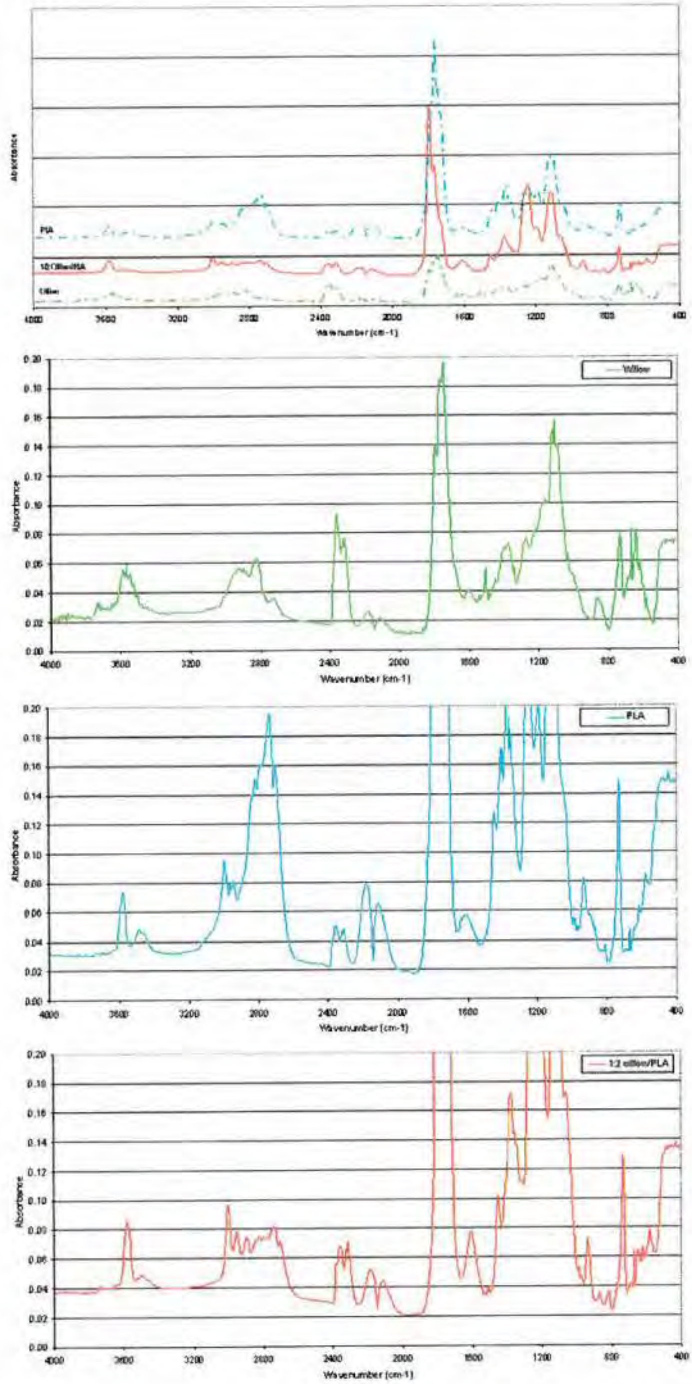

Figure 5.15: FT-IR spectra of the evolving gases at the maximum decomposition rate during pyrolysis; a, overlay; b, for willow; c, PLA (scaled up); and d, 1:2 willow/PLA (scaled up), obtained by TG/FT-IR.

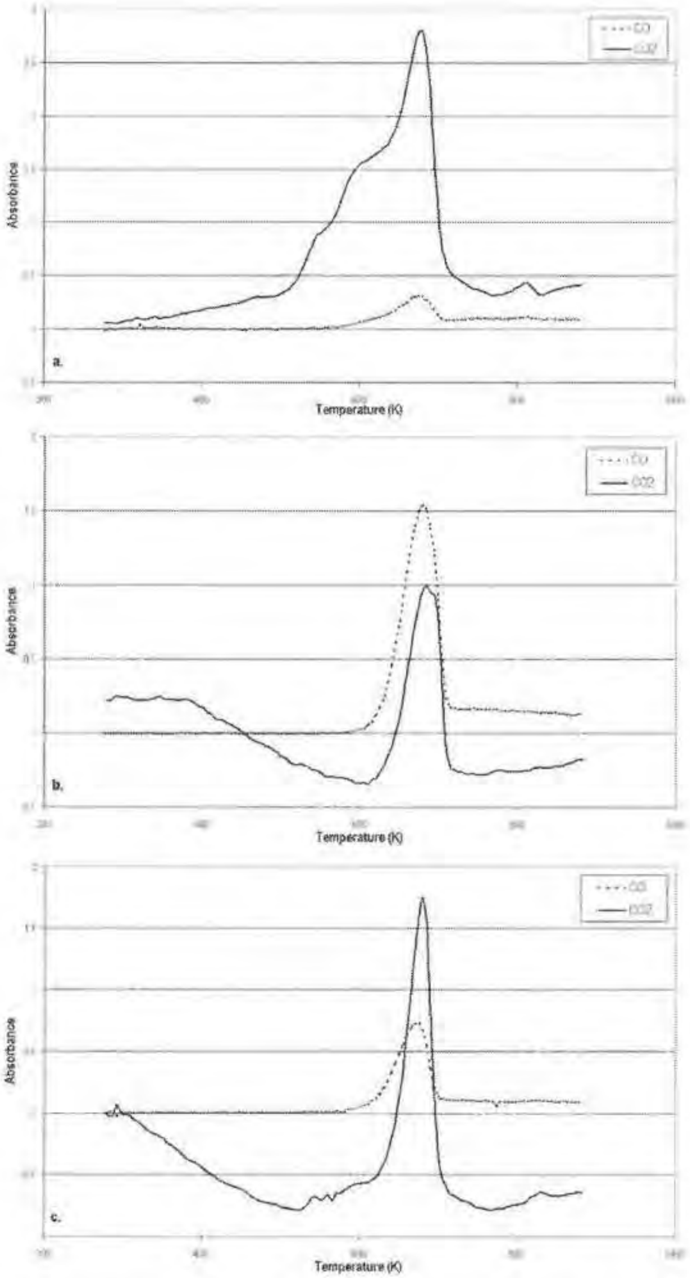

Figure 5.16: The evolution of CO and CO₂ during the thermal decomposition of a, willow; b, PLA; and c, 1:2 willow/PLA, obtained by TG/FT-IR.

Finally, the ratio between the CO and the CO_2 bands for willow, PLA and 1:2 willow/PLA in Figure 5.15 varies: in the case of PLA, the CO band (2000 – 2200 cm^{-1}) is larger compared with the CO_2 band (2300 – 2400 cm^{-1}), while the CO band is clearly less intense for willow and for 1:2 willow/PLA compared with their CO_2 band, although the 1:2 blend is dominated by PLA.

Figure 5.16 shows the evolution of CO and CO_2 during the thermal decomposition of willow, PLA and 1:2 willow/PLA in more detail. The response for CO_2 between 473 and 623 K varies in importance relative to the maximum decomposition temperature (> 623 K): PLA shows almost no response before 623 K, while willow shows an important shoulder in this temperature interval. Even though the proportion between CO and CO_2 of the 1:2 blend resembles willow the most ($CO_2 >> CO$), the evolution of CO_2 obviously differs from that of willow showing only a negligible shoulder between 473 and 623 K. This indicates that another degradation mechanism takes place and confirms the occurrence of additional reactions during co-pyrolysis. It seems that the degradation of 1:2 willow/PLA is shifted towards higher temperatures in comparison with pure willow.

The 3D diagrams in Figure 5.17, which plot the absorbance (Y) in function of wave number (X) and temperature (Z), obtained by TG/FTIR show that carbonyl functionalities (1650 – 1860 cm^{-1}) are the most important functionalities in the evolving pyrolytic gases of all three samples during pyrolysis, representing the most abundant peak in the diagrams.

Additionally, the evolution of functional groups, expressed as the overall intensity within a specific spectral window, as a function of temperature, has been investigated. Figure 5.18 shows the evolution of carbonyl functionalities within the 1650 – 1860 cm^{-1} range, and of –C–O– stretching within the 950 – 1500 cm^{-1} range. With regard to the carbonyl functionalities (Figure 5.18a), the most abundant peak is obtained from PLA, and the least abundant from willow, while the 1:2 blend is situated somewhere in between. The same observation is made for methane and is expected to occur for all functionalities. However, in case of the spectral window of –C–O– stretching range the 1:2 willow/PLA blend seems to represent the most abundant peak (Figure 5.18b). This observation confirms that additional reactions take place during co-pyrolysis of willow and PLA, resulting in an altered gas composition. Moreover, Figure 5.18 also indicates that the start of the decomposition of the blend is shifted towards higher temperatures compared to pure willow.

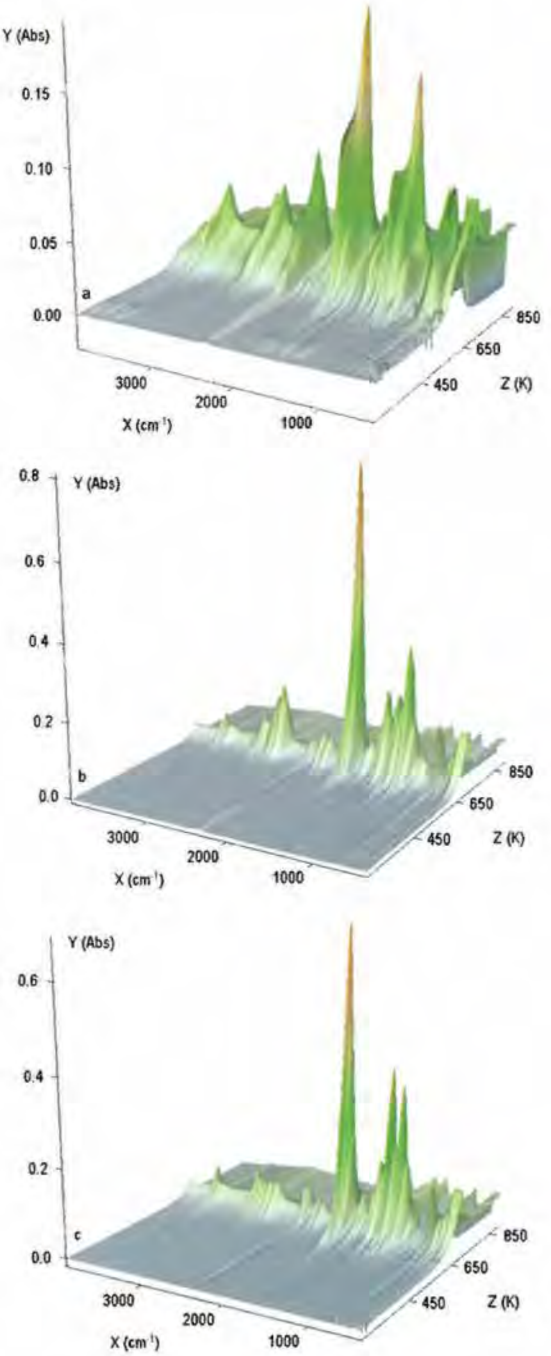

Figure 5.17: 3D diagrams of a, willow; b, PLA; and c, 1:2 willow/PLA with X: Wave number (cm^{-1}) ; Y: Absorbance Units (Abs); Z: Temperature (K), obtained by TG/FT-IR.

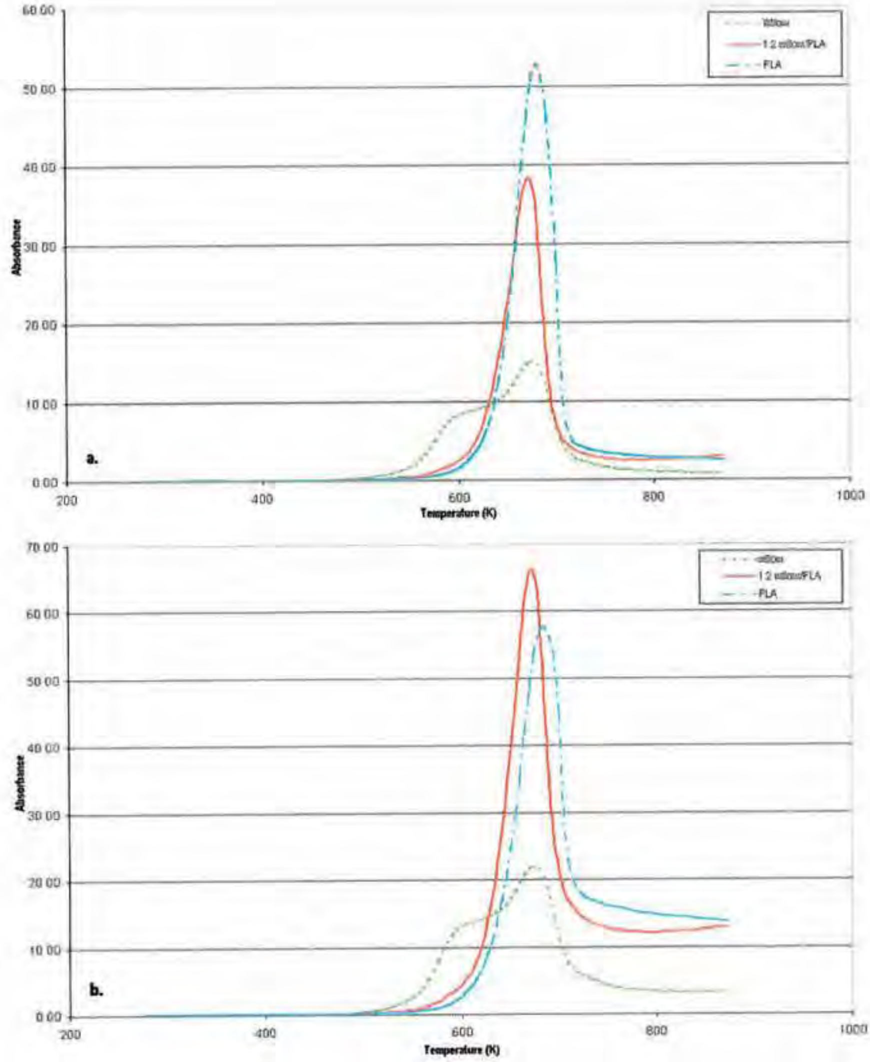

Figure 5.18: Traces of a, carbonyl functionalities; and b, –C–O– stretching; for willow, PLA, and 1:2 willow/PLA, obtained by TG/FT-IR.

5.2.1.4. Comparison of PHB and PLA

During the analytical study, the co-pyrolysis of willow and both biopolymers is performed under slow pyrolytic circumstances. Interestingly, the thermal decomposition of PLA coincides with willow (mainly with cellulose), while the thermal degradation of PHB comes earlier, partly overlapping the decomposition of hemicelluloses. In case of willow/PHB blends, no indications towards interactions between willow and PHB are detected. However, the analytical study of the co-pyrolysis, more specifically TG/FT-IR, of willow and PLA did provide some indications towards the occurrence of interactions between willow and PLA and its influence on the pyrolytic gases. The decomposition of the willow/PLA blend seems to be shifted towards higher temperatures compared to pure willow.

5.2.2. Flash (co-)pyrolysis of willow and PLA – reactor experiments

So far, different analytical pyrolysis techniques have been performed in order to grasp some ideas on the general pyrolysis mechanisms that might occur during the co-pyrolysis of willow and PLA. As for all analytical experiments, TG/FT-IR has been performed as slow pyrolysis and indicated the occurrence of synergetic interactions. In this section, flash (co-)pyrolysis experiments are executed. The results of the flash (co-)pyrolysis experiments on willow, PLA and their blends, performed with the pyrolysis reactor (Figure 2.9), will be discussed.

5.2.2.1. Pyrolysis yields and efficiencies

As for willow and PHB, the flash (co-)pyrolysis on pure willow, pure PLA, and 4 different w/w ratios (10:1, 3:1, 1:1 and 1:2) of willow/PLA-blends is performed at **723 K** with the pyrolysis reactor. Table 5.6a gives a brief summary of the pyrolysis yields and efficiencies of the condensables, char and gas productions. The amount of gases is calculated by difference. In Table 5.6b a subdivision, virtually, of bio-oil into water-free bio-oil and pyrolytic water is made. In contrast to PHB, no crystals are produced, therefore, the bio-oil yield equals the yield in condensables.

In Table 5.6a and b, a first indication towards **synergy** is observed: the flash co-pyrolysis of PLA and willow systematically results in a higher yield in condensables, and thus a higher bio-oil yield too, compared to the sum of the fractional experimental values of both inputs. The synergy seems to increase in direct proportion to the addition of PLA.

The clear synergistic effect is confirmed in Table 5.6b, where the production of water-free bio-oil is higher and that of pyrolytic water lower compared to the sum of the fractional experimental values of both inputs.

Table 5.6a: Pyrolysis yields and efficiencies of the condensables, char and gas productions in function of the willow/PLA w/w ratios.

	Willow	10:1	3:1	1:1	1:2	PLA
Input (m%)*						
Willow	100.00	91.3	75.4	51.8	34.6	0.0
PLA	0.00	8.7	24.6	48.2	65.4	100.0
Output (m%)						
Condensables (only bio-oil)	**50.10**	**51.38**	**53.61**	**51.96**	**55.85**	**43.59**
Char	22.39	20.2	17.3	13.5	n.a.**	1.7
Gases (by diff.)	27.50	28.4	29.1	34.6	n.a.**	54.8

*Input (m%) is calculated on dry basis.

**The amounts of char and gases are unknown due to a failure during sample preparation.

Table 5.6b: Bio-oil yield; and subdivision, virtually, of bio-oil into water-free bio-oil and pyrolytic water based upon the water content; obtained out of 100 g input.

	Willow	10:1	3:1	1:1	1:2	PLA
Bio-oil (g)	50.10	51.38	53.61	51.96	55.85	43.59
Water content (m% of bio-oil)	36.65	34.1	25.6	15.5	8.3	0.8
Water-free Bio-oil (g)	**31.74**	**33.86**	**39.91**	**43.89**	**51.23**	**43.25**
Pyrolytic Water (g)	18.36	17.52	13.70	8.07	4.62	0.34

Table 5.7 summarises the observed synergy (in %) in the total yield in condensables, the water-free bio-oil yield and the amount of pyrolytic water obtained by the flash co-pyrolysis of the 10:1, 3:1, 1:1 and 1:2 willow/PLA blends. The following conclusions can be drawn:

- Table 5.7a shows that the synergy in the yield in condensables culminates in the 1:2 w/w-ratio, and reaches almost +22%:

  *The theoretical yield in condensables = [(34.6g x 50.10% + 65.4g x 43.59%)/100] = 45.84m%, while the actual yield in condensables is 55.85 m%, thus an increase of 10.00m% or [(10.00*100)/45.84] = + 21.83 %.*

- Due to the fact that no crystals are produced, the same synergy can be calculated for the bio-oil yield.
- The yield in water-free bio-oil also shows a synergy for all willow/PLA blends (Table 5.7b). Similarly, the most pronounced synergy is obtained for the 1:2 willow/PLA blend reaching +30%:

  *The theoretical yield in water-free bio-oil = [(34.6g x 31.74% + 65.4g x 43.25%)/100] = 39.27 m%, while the actual yield in water-free bio-oil is 51.23 m%, thus an increase of 11.96 m% or [(11.96*100)/39.27] = + 30.46 %.*

Table 5.7: Synergy (in %) in a. the total yield in condensables, b. the water-free bio-oil yield and c. the amount of pyrolytic water; calculated by '[(Actual-Theoretical)/Theoretical]•100%'.

a.	Total yield in condensables		
Bio-oil	Theoretical (m%)	Actual (m%)	Synergy (%)
Willow	*50.10*	*50.10*	-
10:1 willow/PLA	49.53	51.38	3.73
3:1 willow/PLA	48.50	53.61	10.54
1:1 willow/PLA	46.96	51.96	10.64
1:2 willow/PLA	45.84	55.85	21.83
PLA	*43.59*	*43.59*	-

b.	Water-free bio-oil yield		
Bio-oil	Theoretical (m%)	Actual (m%)	Synergy (%)
Willow	*31.74*	*31.74*	-
10:1 willow/PLA	32.74	33.86	3.40
3:1 willow/PLA	34.57	39.91	15.44
1:1 willow/PLA	37.29	43.89	17.71
1:2 willow/PLA	39.27	51.23	30.46
PLA	*43.25*	*43.25*	-

c.	Amount of pyrolytic water		
Bio-oil	Theoretical (m%)	Actual (m%)	Synergy (%)
Willow	*18.36*	*18.36*	-
10:1 willow/PLA	16.79	17.52	4.36
3:1 willow/PLA	13.93	13.70	-1.62
1:1 willow/PLA	9.67	8.07	-16.60
1:2 willow/PLA	6.57	4.62	-29.70
PLA	*0.34*	*0.34*	-

Willow and PLA (*in italic*) are considered as the references. Small differences can be found due to rounding error.

- The presence of a synergy is also confirmed in Table 5.7c, where the production of pyrolytic water is lower compared to the sum of the fractional experimental values of both inputs. Again, the synergy peaks at the 1:2 w/w-ratio resulting into a decrease of almost minus 30%:

  *The theoretical yield in pyrolytic water = [(34.6g x 18.36% + 65.4g x 0.34%)/100] = 6.57m%, while the actual yield in pyrolyitc water is 4.62 m%, thus a decrease of 1.95 m% or [(1.95*100)/6.57] = - 29.73 %.*

So, the addition of PLA results into an enhanced bio-oil and water-free bio-oil yield, and a lower water content. The reduction of the water content is more pronounced than theoretically would be expected (except for the 10:1 blend). The synergy always reaches its maximum for the 1:2 willow/PLA blend and is observed in two distinct areas (Table 5.6):

- A higher bio-oil yield, i.e. plus 22 % more bio-oil versus the theoretical value (cfr. condensables):
  *The theoretical bio-oil yield = [(34.6g x 50.10% + 65.4g x 43.59%)/100] = 45.84 m%, while the actual bio-oil yield is 55.85 m%, thus an increase of 10.0 m% or [(10.00*100)/45.84] = +21.83%.*
- A lower water content, i.e. minus 37 % less water versus the theoretical value:
  *The theoretical water content = [(34.6g x 36.65% + 65.4g x 0.8%)/100%] = 13.2m%, while the actual water content of the bio-oil is 8.3 m%, thus a decrease of 4.9 m% or [(-4.9*100)/13.2] = - 37.1 %.*
- Incorporating both observations in view of the water-free bio-oil yield, the increase of 30 % is obtained as a synergetic effect (see higher), which is clearly substantial both quantitatively and qualitatively.

In general, it can be concluded that the flash co-pyrolysis of willow and PLA results in a bio-oil with added value.

5.2.2.2. Energetic valorisation

Table 5.8: H.H.V.'s of bio-oils in Mega Joule per kilogram and the synergetic increase (in %) in the energy recuperation; calculated by '[(Actual-Theoretical)/Theoretical]*100%'.

		Energy recuperation		
Bio-oil	H.H.V. (MJ/kg)	Theoretical (m%)	Actual (m%)	Synergy (%)
Willow	16.1	*43.14*	*43.14*	-
10:1 willow/PLA	16.8	43.92	46.27	5.36
3:1 willow/PLA	17.7	45.34	50.77	11.97
1:1 willow/PLA	18.5	47.46	51.53	8.57
1:2 willow/PLA	19.7	49.00	59.06	20.53
PLA	22.2	*52.10*	*52.10*	-

Willow and PLA (*in italic*) are considered as the references. Small differences can be found due to rounding error.

The averaged experimental H.H.V.'s obtained by calorimetry of the respective bio-oils are summarised in Table 5.8 and show a relative standard deviation of maximum 1 %. As previously observed for willow/PHB blends, an increase in the H.H.V. of the bio-oil produced from willow/PLA blends compared to bio-oil of pure willow (16.1 MJ/kg to 19.7 MJ/kg), directly correlated with the addition of PLA is observed. However, bio-oil of pure PLA has the highest H.H.V. (22.2 MJ/kg). The main reason for the increase in H.H.V. seems to be the decrease of the water content.

Table 5.8 summarises the theoretical energy recuperation calculated based on the flash pyrolysis results of the two reference materials (pure willow and pure PLA) and their respective w/w ratio, the actual energy recuperation obtained by the flash co-pyrolysis of the blends with the pyrolysis reactor, and the **synergetic increase** in the energy recuperation for the 10:1, 3:1, 1:1 and 1:2 willow/PLA blends (in %). From Table 5.8 it can be concluded that:

- By taking into account the bio-oil yield (Table 5.6) and the H.H.V.'s of the input materials (Table 5.5), the experimental H.H.V. of the 1:2 willow/PLA bio-oil can be translated into an energy recuperation of 59%:

  The energy recuperation in bio-oil for the 1:2 willow/PLA co-pyrolysis =
  [(55.85g x 19697J/g) x 100/(34.6g x 18699J/g + 65.4g x 18588J/g)]= 59.06%.

  However, bio-oils from pure willow and pure PLA only show an energy recuperation of 43 % and 52 %, respectively.
- In this case, a synergy of plus 20% is calculated, making the flash co-pyrolysis of willow and PLA an energetically and economically attractive route to pursue:

  *The theoretical energy recuperation = [(34.6g x 43.14% + 65.4g x 52.10%)/100] = 49.00 %, while the actual energy recuperation is 59.06 %, thus an increase of 10.06 % or [(10.06*100)/49.00] = + 20.53 %.*

Therefore, it can be stated that the flash co-pyrolysis of the 1:2 willow/PLA blend is the most performant willow/PLA blend.

5.2.2.3. PLA Optima

It can be stated that the flash co-pyrolysis of the 1:2 willow/PLA blend results in the highest bio-oil (condensables) and water-free bio-oil yield (55.85 m% and 51.23 m%, respectively). It additionally results in the highest synergetic decrease in the amount of pyrolytic water (minus 30%), the highest synergetic increase of the bio-oil (condensables) yield (plus 22%) and the highest synergetic increase in energy recuperation (plus 21%).

5.2.2.4. Comparison of PHB and PLA

In order to compare the influence of PHB and PLA on the flash pyrolysis of biomass, it is of primordial importance that the same blends are taken into account. Therefore, only the w/w ratios 3:1 and 1:1 will be considered for comparison.

- The highest yield in condensables is obtained from 1:1 willow/PHB and reaches almost 65%.
- However, 1:1 willow/PLA results in the highest synergetic increase for the total yield in condensables: almost + 11%.
- The highest bio-oil yield, on the contrary, is obtained from 1:1 willow/PLA (51.96%); mainly because PHB does not only result in bio-oil (34.54%) as condensable fraction, but also in crystals (29.70%). It should be noted that 3:1 willow/PHB does not result in the formation of crystals. Therefore, the PHB blend with a w/w ratio of 3:1 results in a higher bio-oil yield (57.76%) as compared to 3:1 willow/PLA (53.61%).
- Likewise, 1:1 willow/PLA scores best on the criteria of water-free bio-oil yield (43.89%). Again, it is 3:1 willow/PHB that beats 3:1 willow/PLA, with a water-free bio-oil yield of 45.63% against 39.91%, respectively.
- Due to the fact that PLA does not result in the formation of any crystals, it is 1:1 willow/PHB that scores best on this criteria (29.70%).
- The lowest production of pyrolytic water is assigned to 1:1 willow/PHB (5.51 g from 100 g input). In case of the w/w ratios 3:1, it is also willow/PHB that performs best with 12.13 g water from 100 g input.
- Additionally, 1:1 willow/PHB results in the highest synergetic decrease in the amount of pyrolytic water: - 40%.
- Finally, the highest energy recuperation is obtained from the flash co-pyrolysis of 1:1 willow/PHB (66.80%) and the second highest from 3:1 willow/PHB (55.67%), followed by 1:1 and 3:1 willow/PLA (respectively, 51.53% and 50.77%).

5.3. Conclusions

1. Even though the explorative analysis did not result in any conclusive evidence regarding interactions between willow and PHB during analytical slow co-pyrolysis (TGA, TG/MS and TG/FT-IR), nor regarding a decrease in the amount of pyrolytic water in the evolving gases, a synergetic reduction of the water content and of the amount of pyrolytic water produced during the flash co-pyrolysis of willow and PHB at 723 K with the pyrolysis reactor is achieved. Besides the difference in heat transfer rates, the difference in heat transfer medium (TGA: none; reactor: sand) can be part of the explanation. The synergistic effect is observed to increase along with the addition of PHB, with a maximum for the 1:1 w/w ratio. Additionally, a synergetic increase in pyrolysis yield, water-free bio-oil yield and energy recuperation is observed. The obtained synergy points out that the flash co-pyrolysis of willow and PHB results in unexpected (non-linear) observations. Therefore, the synergy can only be explained by additional reactions (and different reaction circumstances) during flash co-pyrolysis with the pyrolysis reactor.

The flash co-pyrolysis of the 3:1 willow/PHB blend results in the highest bio-oil and water-free bio-oil yield (57.76 m% and 45.63 m%, respectively), while the 1:1 willow/PHB blend results in the highest synergetic decrease (minus 40%) in the amount of pyrolytic water, the highest synergetic increase of the yield in condensables (plus 8%) and the highest synergetic increase in energy recuperation (plus 18%).

The flash co-pyrolysis of willow and PHB additionally results in an uninitiated phase-separation between bio-oil and crystals (crotonic acid), which are a potential source of value-added speciality chemicals. From the flash co-pyrolysis of 1:1 willow/PHB, almost 30% of crystals were formed.

2. On the contrary, a synergy is observed during the explorative analysis (TG, TG/MS and TG/FTIR) of willow and PLA. Here, (slow) co-pyrolysis of willow and PLA already results in unexpected (non-additive) evolutions. This observation confirms that additional reactions and/or another degradation mechanism take place during co-pyrolysis of willow and PLA, resulting in an altered gas composition. The synergetic behaviour of willow and PLA is confirmed by flash co-pyrolysis at 723 K with the pyrolysis reactor, where an enhanced bio-oil yield with a lower water content and a higher calorific value is obtained. Again, the synergetic effects are observed to increase along with the addition of PLA. The flash co-pyrolysis of 1:2 willow/PLA results in the most pronounced synergy: an increase of

22 % in bio-oil yield, a decrease of 37 % in water content, and an increase of 21 % in energy recuperation.

3. It is less straightforward to define an absolute optimum for both willow/biopolymer blends, because a few aspects need to be considered:

- ► Initial goal of pyrolysis:
    - o Production of chemicals
    - o Production of bio-oil: as a renewable energy source and/or as a source of chemicals
    - o Highest pyrolytic efficiency: energetic and/or economic
    - o Waste treatment: biomass or biopolymers
- ► Available amount of biomass
- ► Available amount of biopolymers
- ► ...

Most probably, the optimum w/w ratio of biomass/biopolymer is a compromise solution dependent on the former aspects.

4. Due to the fact that biomass, and more specifically willow, decomposes in three stages, some possible general reactions can be proposed:

1. the decomposition of lignin and/or hemicelluloses results in volatiles which react with the biopolymer, followed by subsequent reactions with cellulose;
2. the decomposition of the biopolymer results in volatiles which react with willow (cellulose, hemicelluloses and/or lignin);
3. lignin and/or hemicelluloses and the biopolymer interact during the decomposition and result in altered volatiles, which in turn can additionally react with cellulose.

The proposed reactions and interactions can occur:

1. during the decomposition and/or
2. between the volatiles after decomposition and/or
3. between the condensables of willow and the biopolymer.

For PHB, TG/FT-IR explicitly showed that the decomposition of the blends at 545 K is almost completely attributable to the degradation of PHB, indicating that the first proposed reaction is unlikely to occur. However, no straightforward conclusions towards the mechanism of the synergy can be drawn and ask for additional research.

5.4. References

[1] Rossel CEV, Mantelatto PE, Agnelli JAM, Nascimento J, *Sugar-based biorefinery technology for integrated production of poly(3-hydroxybutyrate), sugar, and ethanol*, in *Biorefineries - industrial processes and products. Status quo and future directions. Vol. 1*, B. Kamm, P.R. Gruber, and M. Kamm, Editors. 2006, Wiley-VCH: Weinheim. p. 209-26.

[2] Khanna S, Srivastava VK. Recet advances in microbial polyhydroxyalkanoates. Process Biochemistry 2005; 40:607-19.

[3] Kalnins M, Oics I, Savenkova L, Viesturs U. *Environmentally Degradable Polymeric Composite Materials*. in *Recovery, Recycling, Re-integration 1999 Congress*. 1999.

[4] Weihua K, He Y, Asakawa N, Inoue Y. Effect of Lignin Particles as a Nucleating Agent on Crystallization of Poly(3-hydroxybutyrate). J. Appl. Polym. Sci. 2004; 94:2466-74.

[5] Zhang LL, Deng XM, Zhao SJ, Huang ZT. Biodegradable polymer blends of Poly(3-hydroxybutyrate) and starch acetate. Polym. Int. 1997; 44:104-10.

[6] www.biomer.de.

[7] Chen G-Q, Wu Q. The application of polyhydroxyalkanoates as tissue engineering materials. Biomaterials 2005; 26:6565-78.

[8] DeSchoenmakere M, *Inventarisatie en analyse van verschillende materiaal- en afvalaspecten van bioplastics*, in *IVPV - mileucoördinator A*. 2007, Ghent University: Gent. p. 131.

[9] Kopinke FD, Remmler M, Mackenzie K. Thermal decomposition of biodegradable polyesters .1. Poly(beta-hydroxybutyric acid). Polym. Degrad. Stabil. 1996; 52:25-38.

[10] Kopinke FD, Mackenzie K. Mechanistic aspects of the thermal degradation of poly(lactic acid) and poly(beta-hydroxybutyric acid). J. Anal. Appl. Pyrolysis 1997; 40-1:43-53.

[11] Aoyagi Y, Yamashita K, Doi Y. Thermal degradation of poly (R)-3-hydroxybutyrate , poly epsilon-caprolactone , and poly (S)-lactide. Polym. Degrad. Stabil. 2002; 76:53-9.

[12] Gonzalez A, Irusta L, Fernandez-Berridi MJ, Iriarte M, Iruin JJ. Application of pyrolysis/gas chromatography/Fourier transform infrared spectroscopy and TGA techniques in the study of thermal degradation of poly (3-hydroxybutyrate). Polym. Degrad. Stabil. 2005; 87:347-54.

[13] Morikawa H, Marchessault RH. Pyrolysis of bacterial alkanoates. Can. J. Chem. 1981; 59:2306-13.

[14] Meszaros E, Jakab E, Varhegyi G, Szepesvary P, Marosvolgyi B. Comparative study of the thermal behavior of wood and bark of young shoots obtained from an energy plantation. J. Anal. Appl. Pyrolysis 2004; 72:317-28.

[15] Prins MJ, Ptasinski KJ, Janssen F. Torrefaction of wood - Part 1. Weight loss kinetics. J. Anal. Appl. Pyrolysis 2006; 77:28-34.

[16] Tsamba AJ, Yang WH, Blasiak W. Pyrolysis characteristics and global kinetics of coconut and cashew nut shells. Fuel Process. Technol. 2006; 87:523-30.

[17] Yang H, Yan R, Chen H, Lee DH, Zheng C. Characteristics of hemicellulose, cellulose and lignin pyrolysis. 2007; 86:1781-8.

[18] Petrie EM. Biodegradable polymers in adhesive systems. Adhesives & Sealants 2006; 1-5.

[19] Fan Y, Nishida H, Hoshihara S, Shirai Y, Tokiwa Y, Endo T. Pyrolysis kinetics of poly(-lactide) with carboxyl and calcium salt end structures. 2003; 79:547-62.

[20] Mori T, Nishida H, Shirai Y, Endo T. Effects of chain end structures on pyrolysis of poly(-lactic acid) containing tin atoms. 2004; 84:243-51.

[21] Gruber P, Henton DE, Starr J, *Polylactic acid from renewable resources*, in *Biorefineries - industral processes and products. Status quo and future directions. Vol. 2*, B. Kamm, P.R. Gruber, and M. Kamm, Editors. 2006, Wiley-VCH: Weinheim.

[22] Kijchavengkul T, Auras R. Perspective compostability of polymers. Polymer International 2008; 57:793-804.

[23] Prins MJ, Ptasinski KJ, Janssen F. Torrefaction of wood - Part 2. Analysis of products. J. Anal. Appl. Pyrolysis 2006; 77:35-40.

[24] Fan Y, Nishida H, Shirai Y, Tokiwa Y, Endo T. Thermal degradation behaviour of poly(lactic acid) stereocomplex. 2004; 86:197-208.

[25] Khabbaz F, Karlsson S, Albertsson A-C. PY-GC/MS an effective technique to characterizing of degradation mechanism of poly (L-lactide) in the different environment. Journal of Applied Polymer Science 2000; 78:2369-78.

[26] Kale G, Auras R, Singh SP. Compaision of the degradability of poly(lactide) packages in composting and ambient exposure conditions. Packaging technology and science 2007; 20:49-70.

[27] Fan Y, Nishida H, Shirai Y, Endo T. Thermal stability of poly (-lactide): influence of end protection by acetyl group. 2004; 84:143-9.

[28] Fan Y, Nishida H, Mori T, Shirai Y, Endo T. Thermal degradation of poly(-lactide): effect of alkali earth metal oxides for selective ,-lactide formation. 2004; 45:1197-205.

[29] Bohlmann GM. Biodegradable packaging life-cysle assessment. Environmental Progress 2004; 23:342-6.

[30] Energetics, *Industrial bioproducts: today and tomorrow*. 2003, Energetics, incorporated for the U.S. department of energy, office of energy efficiency and renewable energy, office of the biomass program. p. 1-93.

[31] http://www.hycail.com/.

[32] Jin T, Zhang H. Biodegradable polylactic acid polymer with nisin for use in antimicrobial food packaging. Journal of Food Science 2008; 73:127-34.

[33] McNeill IC, Leiper HA. Degradation Studies of Some Polyesters and Polycarbonates .2. Polylactide - Degradation under Isothermal Conditions, Thermal-Degradation Mechanism and Photolysis of the Polymer. Polym. Degrad. Stabil. 1985; 11:309-26.

[34] Kopinke FD, Remmler M, Mackenzie K, Moder M, Wachsen O. Thermal decomposition of biodegradable polyesters .2. Poly(lactic acid). Polym. Degrad. Stabil. 1996; 53:329-42.

[35] Westphal C, Perrot C, Karlsson S. Py-GC/MS as a means to predict degree of degradation by giving microstructural changes modelled on LDPE and PLA. Polym. Degrad. Stabil. 2001; 73:281-7.

Chapter 6: Statistical and comparative analytical investigation - explanation of the observed synergy

The observations and conclusions of this chapter have been submitted for publication in Fuel:

Flash co-pyrolysis of biomass with polyhydroxybutyrate: Part 2. Statistical and comparative investigation of the observed synergy;
T. Cornelissen, G. Molenberghs, M. Jans, J. Yperman, S. Schreurs, R. Carleer; Fuel (under revision).

Flash co-pyrolysis of biomass with polylactic acid: Part 2. Statistical and comparative investigation of the observed synergy;
T. Cornelissen, G. Molenberghs, J. Yperman, S. Schreurs, R. Carleer; Fuel (submitted).

In chapter 4 it is concluded that, in general, the flash co-pyrolysis of biomass and biopolymers shows the potential to produce bio-oils with a reduced water content. Polyhydroxybutyrate (PHB) and polylactic acid (PLA) showed to be the most promising biopolymers to be co-pyrolysed with biomass. Therefore, the flash co-pyrolysis of biomass/PHB and biomass/PLA blends at 723 K with the pyrolysis reactor is discussed in further detail in Chapter 5. Here, both blends resulted in a pronounced synergetic decrease in the amount of pyrolytic water, and a synergetic increase in pyrolysis yield and in energy recuperation [1, 2]. Besides bio-oil, the flash co-pyrolysis of willow/PHB blends with a high PHB fraction (w/w-ratio 2:1 and 1:1) resulted in the production of crystals of crotonic acid, which offers added value as a source of chemicals [1].

In this part of the research, the synergy observed during the flash co-pyrolysis of willow/PHB (*section 6.2*) and willow/PLA (*section 6.3*) blends is further investigated to better comprehend the reaction circumstances. The analytical Py-GC/MS technique in combination with

1. statistical data processing,
2. pattern recognition and
3. analysis of the condensable and noncondensable pyrolytic gases

is performed on the input materials:

a. pure willow, pure PHB and willow/PHB blends with a w/w ratio of 7:1, 3:1, 2:1 and 1:1; and
b. pure willow, pure PLA and willow/PLA blends with a w/w ratio of 10:1, 3:1, 1:1 and 1:2.

Additionally, the influence of the flash co-pyrolysis of the respective blends on the bio-oil composition, obtained from the reactor experiments, is investigated with complementary techniques: GPC, FT-IR, HPLC and GC/MS. The entire experimental set-up of this research is summarised by the extended pyrolysis flowchart, shown in Figure 3.1, while the analytical strategy applied in this chapter is described in *section 6.1*. The results obtained for 100% pure willow, 100% pure PHB and 100% pure PLA are considered as reference values so as to evaluate the influence of the flash co-pyrolysis experiments on the pyrolytic gas and bio-oil composition and to detect the occurrence of additional reactions (synergy). Finally, an evaluation of the observed synergy is discussed and a potential explanation proposed.

6.1. Statistical and comparative analytical investigation of the observed synergy - Strategy

The experimental focus of this chapter is directed towards two separate but interrelated pyrolytic fractions: 1. the condensable and noncondensable pyrolytic gases and 2. the bio-oil (combined with crystals in case of PHB, summarised as condensables).

1. The pyrolytic gases are investigated by Py-GC/MS, which tries to simulate the flash (co-) pyrolysis of the starting materials with the pyrolysis reactor analytically. The Py-GC/MS chromatograms are investigated thoroughly: statistical data processing, pattern recognition and component analysis and quantification are performed to obtain complementary information.
2. The composition of the bio-oil (bio-oil and crystals in case of PHB), obtained by the flash (co-)pyrolysis of the starting materials with the pyrolysis reactor, is investigated with complementary analytical techniques such as GPC, FT-IR, HPLC and GC/MS.

In this part of the research, all experiments are performed in flash pyrolytic circumstances. However, it should be noted that Py-GC/MS does not employ any heat transfer medium, while the reactor experiments use sand to enhance the impact of the flash pyrolysis.

6.1.1. Condensable and noncondensable pyrolytic gases - Strategy

6.1.1.1. Py-GC/MS – Statistical approach

Even though the occurrence of a synergy during the flash co-pyrolysis of willow/PHB and willow/PLA blends has already been observed during the former reactor experiments discussed in Chapter 5 [1, 2], it is practically extremely difficult to collect observations following a fully sound statistical design, typically encompassing a high number of repetitions, of an intensive and elaborate experimental procedure. This notwithstanding, such experiments can be simulated by Py-GC/MS, thereby saving an appreciable amount of time and effort.

The flash (co-)pyrolysis behaviour of the starting materials is investigated by Py-GC/MS at 723 K in the single shot mode. Each sample is injected and analysed sevenfold. The 2 x 42 injections in total (42 injections for PHB and PLA each – 7 repetitions of 6 different inputs: willow, biopolymer, and 4 willow/biopolymer blends) are performed ad random to exclude systematic measurement errors. The chromatograms obtained, producing data of the form of longitudinal profiles, are processed statistically in two different manners:

a. Peaks in chromatogram and

b. Areas of chromatogram.

a. Peaks in chromatogram

First, 38 carefully chosen peaks are selected of which the response is investigated over all chromatograms. The 38 peaks selected for willow, PHB and the four willow/PHB blends differ from those selected for willow, PLA, and the four willow/PLA blends because of chromatogram specific features, although some might be similar.

Owing to the fact that peaks can sometimes be shifted in terms of retention time, and that some peaks are simply not present in all chromatograms (= time-varying covariate), a general linear mixed-effects model of the form $Y_i = X_i\beta + Z_ib_i + \varepsilon_i$, which can handle repeated measurements in the face of such imbalance, is applied [3, 4]. Y_i is the n_i dimensional response vector for chromatogram i, containing the responses at the different peak retention times, $1 \leq i \leq N$, N is the number of chromatograms and equals 42 (7 x 6) for each biopolymer, X_i and Z_i are $(n_i \times p)$ and $(n_i \times q)$ dimensional matrices of known covariates, and β is the p dimensional vector containing the fixed effects and is related to X_i, while $b_i \sim N(0,D)$ is the q dimensional vector containing the random or subject-specific effects and is related to Z_i. Finally, $\varepsilon_i \sim N(0,\Sigma_i)$ is a n_i dimensional vector of residual components, combining measurement error and serial correlation, with σ^2 the variance of the measurement errors ε_{ij}. It is assumed that the vector of repeated measurements on each subject follows a linear regression model where some of the regression parameters are population-specific (β), i.e. the same for all subjects, whereas other parameters are subject-specific (b_i) and assumed to be random [4]. The random effects in a linear mixed model thus represent the variability in subject-specific intercepts and slopes, not explained by the covariates included in the model. Conditional on these random effects b_i, Y_i is normally distributed with mean vector $X_i\beta + Z_ib_i$ and with covariance matrix Σ_i. Additionally, b_i is also assumed to be normally distributed, but with mean vector zero '0' and covariance matrix D. Consequently, Y_i is normally distributed with mean vector $X_i\beta$ with covariance matrix $V_i = Z_iDZ_i' + \Sigma_i$. For parameter estimation, restricted maximum likelihood (REML) is employed. Generally, it is the goal to reduce the original linear mixed model to a more parsimonious model – the 'less is better' concept. Classically, this is done in a hierarchical way, starting with the highest-order interaction terms, deleting non-significant terms and combining parameters which do not differ significantly, resulting in a reduced final model. More details of this methodology can be found in Verbeke and Molenberghs [4].

Taking into account polynomial-model hierarchies, and applying the conventional backward model selection strategy, the final model states that the response Y_{ij} can be described by means of a full third-order polynomial function in peak retention time (p_{ij} ; 0 → 30 and 35 min for PHB and PLA, respectively; with chromatogram i : 1 → 42; and peak j : 1 → 38) and willow fraction (w_i : 0 → 1). In addition, chromatogram-specific evolutions (random effects, b_i), so as to accommodate the repeated-measures nature of the data, is allowed. The modelling framework envisaged is very flexible in the sense that the set of peaks p_{ij} is allowed to be chromatogram-specific and even the number of repetitions per chromatogram is free to vary. The following initial model for the response Y_{ij} is considered:

$$\begin{aligned} Y_{ij} = \quad & (\beta_0 + b_{0i}) \\ & + (\beta_p + b_{1i})\, p_{ij} + \beta_w w_i \\ & + (\beta_{pp} + b_{2i})\, p_{ij}^2 + \beta_{pw} p_{ij} w_i + \beta_{ww} w_i^2 \\ & + (\beta_{ppp} + b_{3i})\, p_{ij}^3 + \beta_{ppw} p_{ij}^2 w_i + \beta_{pww} p_{ij} w_i^2 + \beta_{www} w_i^3 \\ & + \varepsilon_{ij}. \end{aligned} \tag{6.1}$$

In equation 6.1 it is assumed that the matrix X_i , which is related to the <u>fixed</u> effects (β) of the general linear mixed-effects model, contains the parameters: intercept and the linear, quadratic and cubic term of peak retention time and willow fraction. The matrix Z_i is related to the random or <u>chromatogram-specific</u> effects (b_i) and contains the parameters: intercept and the linear, quadratic and cubic term of peak retention time only. The β parameters (intercept: β_0; first-order: β_p and β_w; second-order: β_{pp}, β_{pw} and β_{ww}; and third-order: β_{ppp}, β_{ppw}, β_{pww} and β_{www}) are the <u>conventional regression</u> effects (also termed fixed effects) describing the mean profile of the response in terms of peak retention time and willow fraction. In addition, the chromatogram-specific vector $b_i = (b_{0i}, b_{1i}, b_{2i}, b_{3i})'$, where $(b_{0i}, b_{1i}, b_{2i}, b_{3i})'$ denotes a transposed vector, is assumed to follow a zero-mean normal distribution with variance-covariance matrix D, where $b_i \sim N(0,D)$.

$$D = \begin{pmatrix} d_{00} & d_{01} & d_{02} & d_{03} \\ d_{10} & d_{11} & d_{12} & d_{13} \\ d_{20} & d_{21} & d_{22} & d_{23} \\ d_{30} & d_{31} & d_{32} & d_{33} \end{pmatrix} \quad (6.2)$$

Finally, parameter estimation takes place using conventional maximum likelihood. For *F* tests, the well-performing Kenward-Roger denominator degrees-of-freedom method [5] is employed, as implemented in the SAS (statistical analysis software) procedure MIXED; the method is considered the gold standard in repeated-measures analysis.

b. Areas of chromatogram

As an alternative way to process the longitudinal Py-GC/MS data, each of the 2 x 42 chromatograms is split into identical areas based on the specific chromatogram features. Therefore, the selected areas for PHB differ from the areas selected for PLA. In each case the zones are common and equal in number across all chromatograms, resulting in a balanced design, for which a different modelling strategy is within reach. Now, the full multivariate model for the area A_{ij} of the form:

$$A_{ij} = \beta_{0j} + \beta_{1j} w_i + \beta_{2j} w_i^2 + \varepsilon_{ij} \quad (6.3)$$

is proposed.

Rather than accommodating within-chromatogram correlation through random effects (b_i), this is now done by assuming that the error vector $\varepsilon_i = (\varepsilon_{i1}, \ldots, \varepsilon_{i7})'$ is correlated. A so-called heterogeneous first-order autoregressive structure, where the variance function is left unstructured and the correlation is modelled as $\mathrm{Corr}(\varepsilon_{ij}, \varepsilon_{ik}) = \rho^{|j-k|}$, is selected. This may be a simplification of reality, and to offset the effects of such misspecification, inferences are made in what is termed a 'robust' fashion [4]. Again, parameter estimation took place using conventional maximum likelihood, and for *F* tests, the Kenward-Roger denominator degrees-of-freedom method [5] is employed.

6.1.1.2. Py-GC/MS – Pattern recognition

To investigate which peaks specifically are/can be responsible for the possible observed synergy, a directed search towards the occurrence of additional reactions during Py-GC/MS of the willow/PHB and willow/PLA blends, resulting in the formation of new components and in unexpected (non-additive) evolutions of some others, is performed by pattern recognition. Besides the Total Ion Chromatogram (TIC), specific mass fragment ions and their respective chromatograms obtained by Py-GC/MS are used as criteria to enhance the resolution of the pattern recognition process. Some of the mass fragment ions are indicative for the PHB and PLA degradation, respectively, while some others are chosen specifically because they were abundantly present during data processing and asked for additional investigation.

6.1.1.3. Py-GC/MS – Analysis of the gaseous pyrolytic components

Finally, the actual analysis of the condensable and noncondensable gaseous pyrolytic components is performed.

6.1.2. Condensables

The focus of this chapter will also be directed towards the investigation of the respective bio-oils (and crystals in case of PHB; cfr. the condensable fraction of the pyrolytic gases), obtained by the flash (co-)pyrolysis of the starting materials with the pyrolysis reactor. The bio-oils are analysed with the aid of complementary analytical techniques (GPC, FT-IR, HPLC and GC/MS) to obtain more detailed information on their composition and to investigate the effect of the previously observed interactions (Chapter 5) during the flash co-pyrolysis of willow/PHB and willow/PLA blends [1, 2].

Additionally, the GC/MS results of the bio-oil (and crystals) obtained from the reactor experiments will be compared with the analytical Py-GC/MS results of the respective pyrolytic gases. This comparison is performed dually:

1. by comparing the 10 most important components of each fraction, and
2. by classifying each fraction into four general classes based on the oxidation number (reactivity) of the respective functionalities. The reactivity is related to the number of bonds that the hetero atoms form with a carbon atom.
    - Class 0: alkenes and aromatics;
    - Class 1: ethers, alcohols and phenols;
    - Class 2: aldehydes and ketones;
    - Class 3: carboxylic acids and esters;

If molecules contain more than one functionality, these molecules are classified according to the highest class of its functionalities. An additional class containing the peaks representing the oligomers of crotonic acid and lactic acid, respectively, is added.

6.2. Flash co-pyrolysis of biomass with PHB

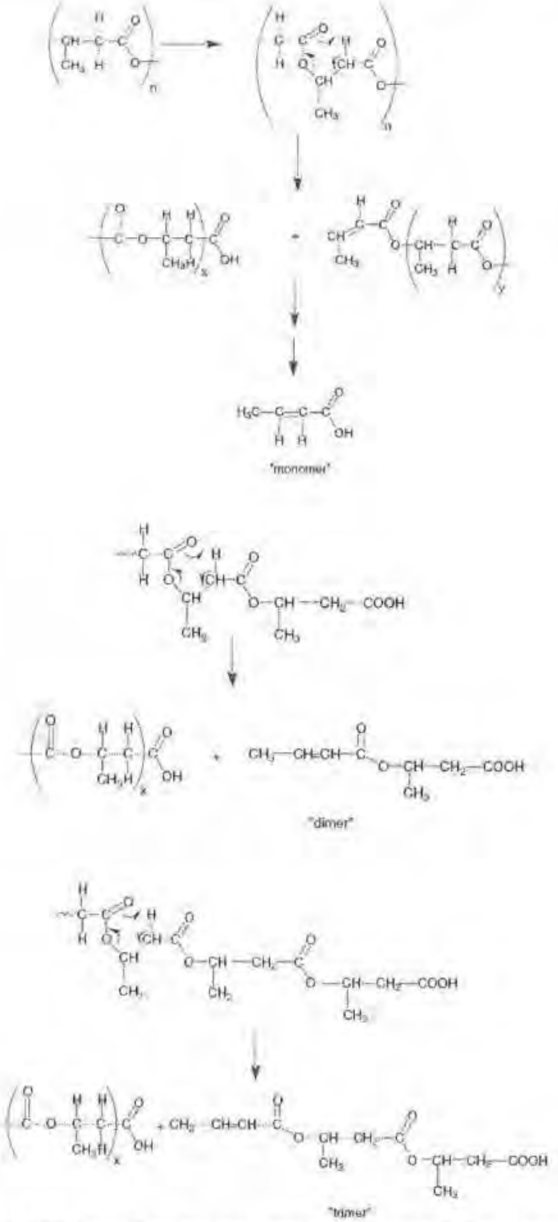

Figure 6.1: PHB degradation into monomer (crotonic acid), dimer and trimer [6].

As mentioned in Chapter 5, the thermal decomposition of the biopolymer polyhydroxybutyrate (PHB), a bacterial alkanoate, is already investigated by means of several thermo-analytical techniques (TGA, DSC, Py-MS, Py-GC/MS, and Py-GC/FT-IR) and is described in earlier literature [6-9]. PHB decomposes according to the *cis*-elimination mechanism and yields crotonic acid as well as some linear oligomers (Figure 6.1).

In addition to the characteristic mass fragment ions of crotonic acid (*m/z* 39, 41, 68, 69 and 86 – Figure 6.2) the averaged mass spectra obtained by Py-MS of PHB reveals additional mass fragment ions (*m/z* 69, 87, 103, 154, 155, 171, 172 and 173), which can be attributed to oligomers of crotonic acid, some of which exhibiting the homologues series $m/z = 87 + n{*}86$ ($n \geq 0$) [7, 9]. The formation of monomeric (crotonic acid) and oligomeric volatile products have also been observed by Py-GC/FT-IR [6]. Kopinke et al. [7, 8] observed a significant difference between the thermal stability of pure PHB and that of PHB still embedded in its crude biomass, although both arise from the same fermentation process. Pure PHB seemed to be much more stable. Thus, matrix effects appear to play a significant role. The pyrolysis of PHB followed by a condensation of the volatiles produced, has already been executed as well. The pyrolysis of purified PHB yields 60 to 65% of crotonic acid [10].

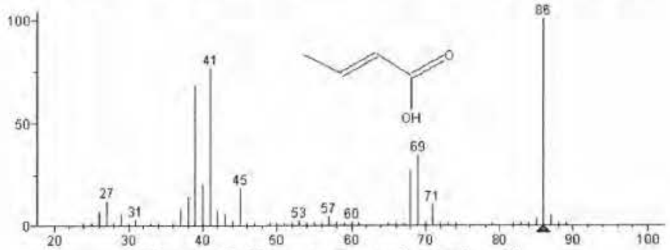

Figure 6.2: Mass spectrum of crotonic acid.

In Chapter 5, a synergetic decrease in the amount of pyrolytic water, together with a synergetic increase in pyrolysis yield and in energy recuperation is observed for willow/PHB blends. Besides bio-oil, the flash co-pyrolysis of willow/PHB blends with a high PHB fraction (w/w-ratio 2:1 and 1:1) resulted in the production of crystals of crotonic acid, which offers added value as a source of chemicals [1]. In *section 6.2.1.* and *6.2.2.*, the condensable and noncondensable pyrolytic gases obtained by Py-GC/MS and the bio-oil and crystals obtained from the reactor experiments, respectively, will be investigated. In *section 6.2.3.* the observed synergy is discussed.

6.2.1. Condensable and noncondensable pyrolytic gases - PHB

6.2.1.1. Py-GC/MS – Statistical approach

a. Peaks in chromatogram

The model fit for the response Y_{ij} in function of peak retention time and willow fraction (see equation 6.1) for PHB is summarised in Table 6.1. Based on the magnitude of the estimates of the ten random-effects-related variance components ($d_{00} \rightarrow d_{33}$; elements of covariance matrix *D*, see equation 6.2) and their standard error, it is observed that all four random or chromatogram-specific effects in the vector b_i (b_{0i}, b_{1i}, b_{2i}, b_{3i}) are necessary, a fact confirmed by likelihood-ratio tests ($p < 0.0001$). Additionally, all terms related to the conventional regression or fixed effects, except for $\beta_{ppw} p_{ij}^2 w_i$ ($p = 0.1270 > 0.05$ = minimal level of significance), are considered statistically significant ($p < 0.05$). Taking into account polynomial-model hierarchies and applying the conventional backward model selection strategy, all lower order terms ($0 \rightarrow n\text{-}1$) are incorporated in the model when at least one term of the n^{th} order is considered significant in that model. Put differently, even though some of the lower order terms ($0 \rightarrow n\text{-}1$: β_0, β_p, β_w , β_{pp}, β_{pw} and β_{ww}) show to be insignificant (p-value > 0.05), these cannot be removed from the model because the third (n^{th}) order terms β_{ppp}, β_{pww}, and β_{www} are necessary for the model under consideration.

Each of the willow effects (β_w, β_{pw}, β_{ww} , β_{pww}, and β_{www}) captures one aspect of the effect of willow on the chromatogram. However, this provides a fragmented picture, and it is therefore instructive to consider the overall hypothesis of no willow effect (equation 6.4):

$$H_{0,\,\text{willow}} : \beta_w = \beta_{pw} = \beta_{ww} = \beta_{pww} = \beta_{www} = 0. \tag{6.4}$$

Testing hypothesis $H_{0,\,\text{willow}}$ (equation 6.4) can be done using an *F* test of which the realised value ($F = 74.25$) is compared to an $F_{5,50.3}$ reference distribution. Note that there are 5 numerator degrees of freedom because $H_{0,\,\text{willow}}$ is compound and involves 5 comparisons; and there are 50.3 denominator degrees of freedom, as derived by the approximate but accurate method of Kenward and Roger [5]. Fractional denominator degrees of freedom are a result of the unbalancedness in the design. The willow effect (and therefore the PHB effect as well) is, as expected, found to be highly significant ($p < 0.0001$) in the model described.

Table 6.1: Parameter estimates and standard error for the linear mixed-effects model for response Y_{ij} for PHB.

Effect	Parameter	Estimate	Standard Error	p
Mean structure (fixed effects)				
Intercept	β_0	0.63	0.09	< 0.0001
Peak linear	β_p	-0.9	0.18	< 0.0001
Willow linear	β_w	0.12	0.26	0.6602
Peak squared	β_{pp}	0.83	0.14	< 0.0001
Peak-by-willow	β_{pw}	-0.19	0.19	0.3180
Willow squared	β_{ww}	1.68	0.51	0.0020
Peak cubed	β_{ppp}	-0.08	0.03	0.0168
Peak squared-by-willow	β_{ppw}	-	-	0.1270
Peak-by-willow squared	β_{pww}	-0.83	0.18	< 0.0001
Willow cubed	β_{www}	-0.75	0.3	0.0185
Random effects Variance components				
	d_{00}	-3.46	0.15	< 0.0001
	d_{01}	7.11	0.31	< 0.0001
	d_{11}	-17.4	0.75	< 0.0001
	d_{02}	-4.4	0.2	< 0.0001
	d_{12}	12.06	0.52	< 0.0001
	d_{22}	-8.96	0.4	< 0.0001
	d_{03}	0.84	0.04	< 0.0001
	d_{13}	-2.47	0.11	< 0.0001
	d_{23}	1.92	0.09	< 0.0001
	d_{33}	-0.43	0.02	< 0.0001
Residual Variance Structure				
Residual variance	σ^2	2.46	0.09	< 0.0001

For the purpose of this research, the higher-order terms in the willow effect are of crucial importance since these specifically indicate that there is a complex interaction (non-linear) between willow and PHB during flash co-pyrolysis, superimposed onto simple additive (linear) aspects. The hypothesis of complex interaction (equation 6.5) is formulated as follows:

$$H_{0,\,\text{interaction}} : \beta_{pw} = \beta_{ww} = \beta_{pww} = \beta_{www} = 0. \qquad (6.5)$$

Testing composite hypothesis $H_{0,\,\text{interaction}}$ (equation 6.5) can be done, likewise, using an *F* test of which the realised value ($F = 87.32$) is compared to an $F_{4,51.9}$ reference distribution. The higher order terms appear to be highly significant ($p < 0.0001$) too.

So, Py-GC/MS and statistical data processing of the 38 carefully chosen peaks confirm the occurrence of synergetic interactions between willow and PHB during analytical flash co-pyrolysis as observed with the former reactor experiments discussed in Chapter 5 [1]. However, no information about which peak(s) is (are) responsible for these findings, nor an indication towards the actual consequences of the observed synergy on the pyrolytic gases is obtained.

b. Areas of chromatogram

Based on the specific chromatogram features of willow, PHB and the four willow/PHB blends, seven areas have been selected which are summarised in Table 6.2.

Table 6.2: Summary for PHB of the seven areas, identical for each chromatogram.

Zone	Start (min)	End (min)
1	0	6
2	6	11
3	11	12.5
4	12.5	17.5
5	17.5	20
6	20	25
7	25	30

Table 6.3 summarises the model fit for area A_{ij} in function of willow fraction (w_i) for PHB. Taking into account polynomial-model hierarchies and applying the conventional backward model selection strategy, all lower order terms ($0 \rightarrow n-1$) are incorporated in the model when the n^{th} order term is considered significant in at least one zone. Additionally, the n^{th} order term is considered significant in all zones considered in the model. Therefore, all regression terms ($\beta_{01} \rightarrow \beta_{27}$) are found to be highly significant. Likelihood-ratio tests on the seven residual variances ($\sigma_1^2 \rightarrow \sigma_7^2$) indicate that the seven random effects in the error vector $\varepsilon_i = (\varepsilon_{i1}, \ldots, \varepsilon_{i7})$ are considered highly significant ($p < 0.0001$) too.

Table 6.3: Robust parameter estimates for the model for area A_{ij} for PHB.

	Intercept				Willow				Willow squared			
Zone	Par.	Estimate	robust std. error	p	Par.	Estimate	robust std. error	p	Par.	Estimate	robust std. error	p
Mean Structure												
1	β_{01}	3	0.1	< 0.0001	β_{11}	6.1	1.4	< 0.0001	β_{21}	-1.2	1.6	0.4363
2	β_{02}	1.6	0.1	< 0.0001	β_{12}	22.7	3.5	< 0.0001	β_{22}	-7.7	4.1	0.0597
3	β_{03}	8.9	0.4	< 0.0001	β_{13}	3.5	1.4	0.0126	β_{23}	-7.2	1.2	< 0.0001
4	β_{04}	7	0.5	< 0.0001	β_{14}	18.3	3.5	< 0.0001	β_{24}	-4.7	4.1	0.2454
5	β_{05}	26.9	0.7	< 0.0001	β_{15}	1.2	2.7	0.6507	β_{25}	-14.2	2.4	< 0.0001
6	β_{06}	21.7	0.9	< 0.0001	β_{16}	-22.4	3.9	< 0.0001	β_{26}	19.3	4.1	< 0.0001
7	β_{07}	30.9	0.6	< 0.0001	β_{17}	-29.4	4.8	< 0.0001	β_{27}	15.7	5.4	0.0042
Residual Variances												
1	σ_1^2	1.1	0.2	< 0.0001								
2	σ_2^2	5.6	1.2	< 0.0001								
3	σ_3^2	0.5	0.1	< 0.0001								
4	σ_4^2	6.5	1.5	< 0.0001								
5	σ_5^2	3.6	0.9	< 0.0001								
6	σ_6^2	5.5	1.1	< 0.0001								
7	σ_7^2	8.6	1.8	< 0.0001								
AR(1) Correlation												
	ρ	0.34	0.07	< 0.0001								

Again, each of the parameters provides only partial information about the effects under consideration and it is therefore of interest to conduct well targeted hypothesis tests. Three sets are considered.

The first set is directed at the entire willow effect across all zones (equation 6.6), hence there are two: for the linear and squared effects of willow fraction, respectively. The corresponding hypotheses are:

$$\begin{aligned} &H_{0,\text{ all zones, linear}}: && \beta_{11} = \beta_{12} = \beta_{13} = \beta_{14} = \beta_{15} = \beta_{16} = \beta_{17} = 0, \\ &H_{0,\text{ all zones, squared}}: && \beta_{21} = \beta_{22} = \beta_{23} = \beta_{24} = \beta_{25} = \beta_{26} = \beta_{27} = 0. \end{aligned} \tag{6.6}$$

The second set is directed at the effect of willow fraction in a specific zone (equation 6.7). This produces seven null hypotheses, one for each zone, with two effects each (linear (β_{1i}) and quadratic (β_{2i})):

$$\begin{aligned} &H_{0,\text{ zone 1}}: \beta_{11} = \beta_{21} = 0, \\ &H_{0,\text{ zone 2}}: \beta_{12} = \beta_{22} = 0, \\ &H_{0,\text{ zone 3}}: \beta_{13} = \beta_{23} = 0, \\ &H_{0,\text{ zone 4}}: \beta_{14} = \beta_{24} = 0, \\ &H_{0,\text{ zone 5}}: \beta_{15} = \beta_{25} = 0, \\ &H_{0,\text{ zone 6}}: \beta_{16} = \beta_{26} = 0, \\ &H_{0,\text{ zone 7}}: \beta_{17} = \beta_{27} = 0. \end{aligned} \tag{6.7}$$

Finally, the overall effect (equation 6.8) of willow is ascertained by the following hypothesis test:

$$H_{0,\text{ overall}}: \beta_{11} = \ldots = \beta_{17} = \beta_{21} = \ldots = \beta_{27} = 0. \tag{6.8}$$

The entire output of all these tests is summarised in Table 6.4. It can be concluded that no matter which hypothesis is considered, they all result in a very high significance ($p < 0.0001$) and confirm the linear willow effect (and thus the PHB effect as well) and the occurrence of interactions (synergy or non-linear) between willow and PHB during flash co-pyrolysis. Again, it should be noted that no indication towards the actual impact of the observed synergy on the pyrolytic gases is obtained.

Table 6.4: Robust hypothesis testing results for areas in chromatogram for PHB.

H_0	Num. d.f.	Den. d. f.	F	p
$H_{0,\text{ all zones, linear}}$	7	231	7.7	< 0.0001
$H_{0,\text{ all zones, squared}}$	7	231	10.0	< 0.0001
$H_{0,\text{ zone 1}}$	2	231	137.0	< 0.0001
$H_{0,\text{ zone 2}}$	2	231	382.5	< 0.0001
$H_{0,\text{ zone 3}}$	2	231	58.2	< 0.0001
$H_{0,\text{ zone 4}}$	2	231	160.5	< 0.0001
$H_{0,\text{ zone 5}}$	2	231	195.1	< 0.0001
$H_{0,\text{ zone 6}}$	2	231	19.5	< 0.0001
$H_{0,\text{ zone 7}}$	2	231	133.7	< 0.0001
$H_{0,\text{ overall}}$	14	231	133.5	< 0.0001

So, with the aid of analytical Py-GC/MS and statistical analysis of the pyrolysis GC-chromatograms, it can be concluded that interactions do occur during flash co-pyrolysis of willow and PHB, resulting into an altered gas (condensable and noncondensable) composition. However, which interactions and where specifically these occur, has not yet been determined and require further research.

In Chapter 5 no straightforward indication towards interactions between willow and PHB was observed with the aid of TG/FT-IR and TG/MS [1]. Nevertheless, a synergy in the amount of pyrolytic water, the pyrolysis yield and the energy recuperation during flash co-pyrolysis experiments of willow and PHB with the pyrolysis reactor was observed. Py-GC/MS clearly confirms the occurrence of such a synergy for willow/PHB blends. An acceptable explanation of these conflicting observations is that thermogravimetric analysis (TGA) has been performed in slow pyrolytic circumstances. The pyrolysis reactor and analytical Py-GC/MS, on the contrary, are performed in flash pyrolysis mode. This indicates that the observed synergy is more pronounced during flash pyrolytic circumstances.

6.2.1.2. Py-GC/MS – Pattern recognition

To investigate which peaks specifically are/can be responsible for the former conclusions, a directed search towards the occurrence of additional reactions during Py-GC/MS of willow/PHB blends, resulting in the formation of new components and in unexpected evolutions of some others, is performed by pattern recognition. Besides the Total Ion Chromatogram (TIC), specific mass fragment ions and their respective chromatograms obtained by Py-GC/MS are used as criteria to enhance the resolution of the pattern recognition process. For this research, the following mass fragment ions have been investigated separately: *m/z* 69, 86, 89, 98, 100, 102, 103, 112, 114, 121, 126, 128, 154, 173, 259, 345 and 431, resulting in seventeen individual mass fragment ion chromatograms. Some of these mass fragment ions are indicative for the PHB degradation, while some others are chosen specifically because they were abundantly present during data processing and asked for additional investigation.

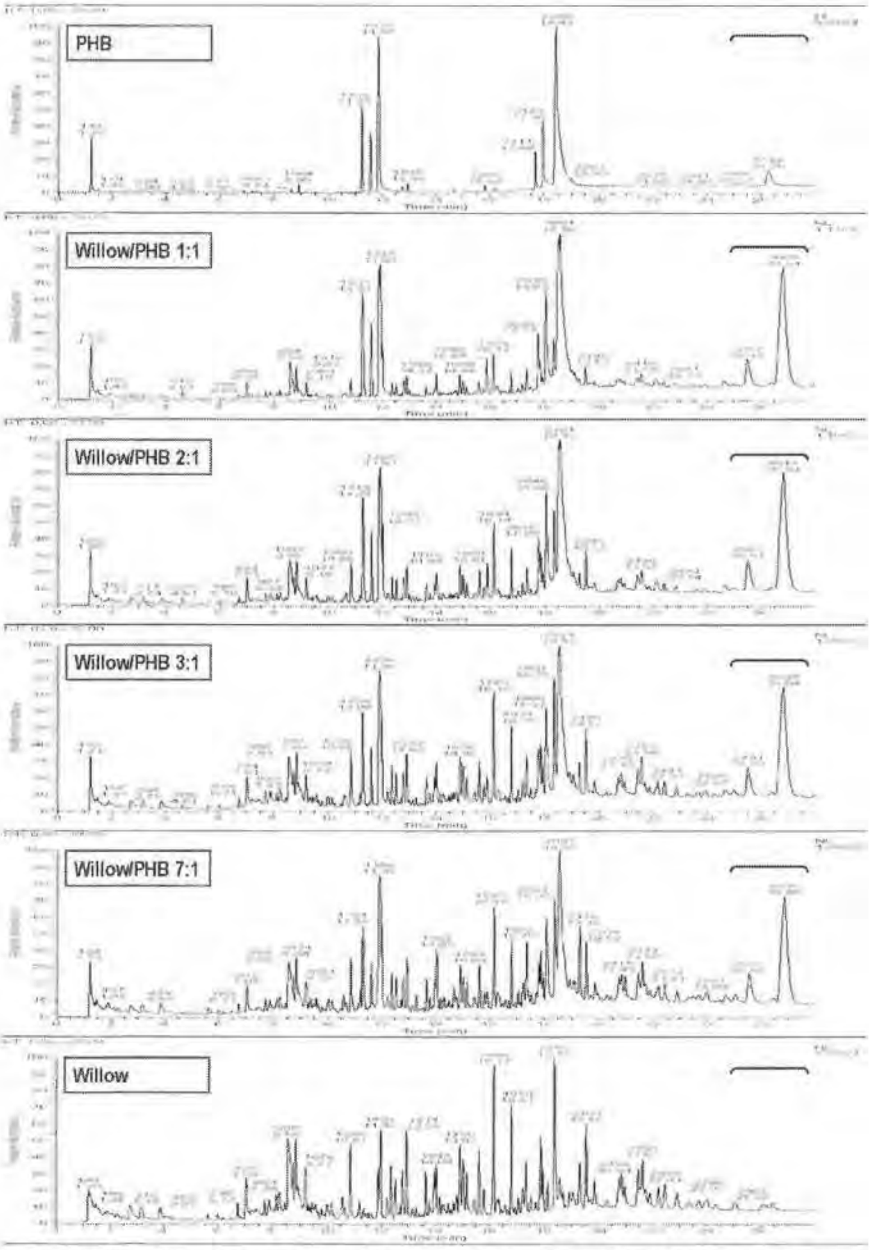

Figure 6.3: Total Ion Chromatograms (TIC) of pure PHB, 1:1, 2:1, 3:1 and 7:1 Willow/PHB, and pure willow, obtained by Py-GC/MS.

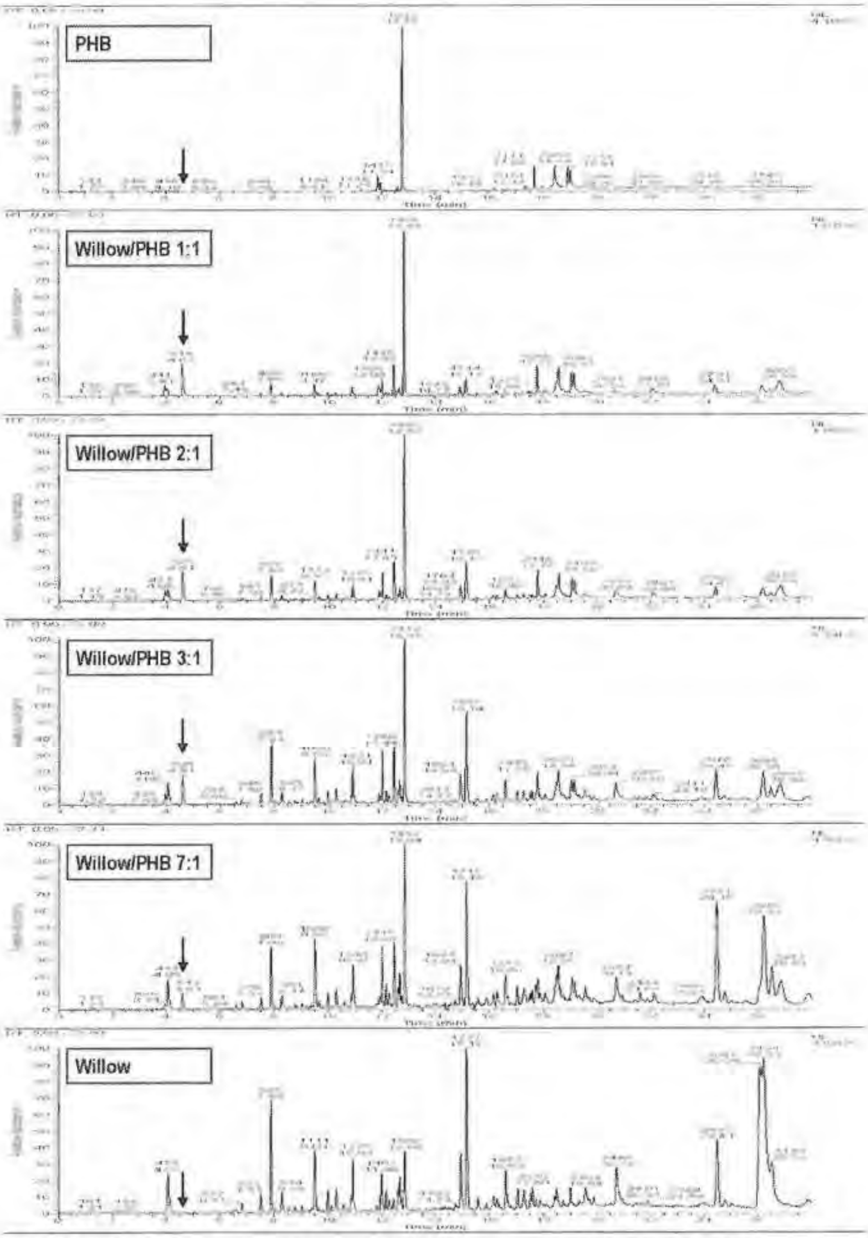

Figure 6.4: Mass fragment ion chromatogram of *m/z* 100 for pure PHB, 1:1, 2:1, 3:1 and 7:1 willow/PHB, and pure willow, obtained by Py-GC/MS.

Comparison of the TIC's, shown in Figure 6.3, immediately reveals that the peaks at 25.5 and 26.8 minutes, representing oligomers of crotonic acid, increase significantly for the willow/PHB blends. The TIC of willow does not contain these peaks at all, while the TIC of PHB shows two similar but much smaller peaks at relatively similar retention times. This increase is already strongly pronounced for the 7:1 willow/PHB blend, indicating that synergetic interactions occur when 'co-pyrolysis' is executed and that the amount of willow or PHB is not the decisive parameter. These observations are confirmed by the mass fragment ion chromatograms of *m/z* 69, 86, 103, 121, 126, 128, 154, 173, 259, 345 and 431, of which some seem to belong to the homologous series of $m/z = 87 + n{*}86$, representing oligomers of crotonic acid.

Additionally, the formation of a new component is visualised for the willow/PHB blends. Both the mass fragment ion chromatograms of *m/z* 69 and 100 show the production of the methyl ester of 2-butenoic acid at 4.61 minutes. Figure 6.4 shows the comparison of the mass fragment ion chromatograms of *m/z* 100. The abundance of this methyl ester increases with increasing PHB fraction in the blend and is not detected when pure willow nor pure PHB is pyrolysed separately.

The changes observed by pattern recognition support the conclusions obtained by the statistical data processing. However, other changes in the pyrolytic gas composition are most likely, even though they are visually not observed. Therefore, the pyrolytic gas composition will be investigated in further detail in the next subsection.

6.2.1.3. Py-GC/MS – Analysis of the gaseous pyrolytic components

Finally, the actual analysis (identification and quantification) of the condensable and noncondensable pyrolytic gases is carried out. Table 6.5 summarises the 10 most important components obtained by Py-GC/MS of pure willow, pure PHB and the four willow/PHB blends. It is observed that:

- The only common component for willow and PHB is CO_2, which is an important component for all chromatograms. However, the amount of CO_2 is always lower for the blends as compared to the references pure willow and pure PHB.
- In general, most components seem to behave more or less linear in function of the ratio applied, e.g. furfural and 2,6-dimethoxyphenol, both originating from the willow fraction. Additionally some components originating from PHB also behave linearly, e.g. both the oligomers of crotonic acid with a mass fragment ion of *m/z* 154 (oligomer 1 and 2).
- Crotonic acid, for instance, behaves linearly over the entire range except for willow/PHB 7:1 where it immediately takes an important share of the pyrolytic gases detected by Py-GC/MS, even though only a small amount of PHB is added.

Table 6.5: Summary of the 10 most important components of the respective pyrolytic gases (condensable and noncondensable) for PHB obtained by Py-GC/MS, with oligomer 1: *m/z* 41, 55, 68, 86, 103, 113, 130, 154; oligomer 2: *m/z* 39, 45, 58, 69, 86, 103, 113, 126, 136, 154; oligomer 3: *m/z* 41, 58, 69, 87, 103, 131, 155; and oligomer 4: *m/z* 41, 58, 69, 87, 103, 113, 128, 155, 171, 189.

	Willow	%		Willow/PHB 7:1	%
1	acetic acid	5.00	1	oligomer 4	10.38
2	2,6-dimethoxy-phenol	4.69	2	oligomer 2	9.00
3	CO_2	3.77	3	crotonic acid	8.57
4	2,6-dimethoxy-4-(2-propenyl)-phenol	3.53	4	acetic acid	3.29
5	furfural	3.37	5	2,6-dimethoxy-4-(2-propenyl)-phenol	3.19
6	1-(3,4-dimethoxyphenol)-ethanone	2.97	6	2,6-dimethoxyphenol	3.10
7	1,2-cyclopentanedione	2.91	7	phenol	2.16
8	4-hydroxy-3,5-dimethoxy-benzaldehyde	2.46	8	furfural	2.14
9	5-(hydroxymethyl)-2-furancarboxaldehyde	2.19	9	oligomer 3	2.11
10	4-(3-hydroxy-1-propenyl)-2-methoxyphenol	2.00	10	CO_2	2.09

	Willow/PHB 3:1	%		Willow/PHB 2:1	%
1	oligomer 4	10.97	1	oligomer 4	14.74
2	oligomer 2	9.50	2	oligomer 2	13.90
3	crotonic acid	8.00	3	crotonic acid	11.70
4	2,6-dimethoxy-4-(2-propenyl)-phenol	4.55	4	oligomer 1	3.00
5	acetic acid	3.39	5	oligomer 3	2.80
6	2,6-dimethoxyphenol	3.00	6	CO_2	2.57
7	CO_2	2.31	7	2,6-dimethoxy-4-(2-propenyl)-phenol	2.08
8	furfural	2.30	8	3-methyl-2(5H)-furanone	2.00
9	oligomer 1	2.12	9	2,6-dimethoxyphenol	1.96
10	oligomer 3	2.08	10	furfural	1.94

	Willow/PHB 1:1	%		PHB	%
1	oligomer 4	17.68	1	oligomer 2	38.88
2	oligomer 2	16.95	2	crotonic acid	28.16
3	crotonic acid	14.70	3	oligomer 1	7.64
4	oligomer 1	4.00	4	oligomer 4	4.89
5	oligomer 3	3.05	5	CO_2	4.30
6	CO_2	3.04	6	3-butenoic acid	3.90
7	3-butenoic acid	2.54	7	2-butenoic acid, 1-methylethylester	3.17
8	acetic acid	2.00	8	oligomer 3	0.70
9	2-butenoic acid, 1-methylethylester	1.81	9	3-methyl-3-cyclohexen-1-one	0.58
10	furfural	1.40	10	*m/z* 39,41,69,126	0.53

- The yield of some components is synergetically increased for the willow/PHB blends: e.g. both oligomers of crotonic acid with the mass fragment ion *m/z* 155 (Oligomer 3 and 4). This synergy results in an altered oligomer distribution. Originally, PHB shows the following distribution of oligomers: oligomer 2 > 1 > 4 > 3. However, oligomer 4 sharply increased in abundance for the willow/PHB blends, while oligomer 3 only shows a moderate increase, resulting in the altered distribution: oligomer 4 > 2 > 1 > 3. Oligomer 3 and 4 have already been observed to behave synergetically by pattern recognition (Figure 6.3).
- Besides small amounts of the methyl ester of 2-butenoic acid, 2-butanone and 2-methyl-butanal are indicated as new components for the willow/PHB blends.

Generally, it can be stated that the pyrolytic gas (condensable and noncondensable) composition alters due to the occurrence of synergetic interactions during the Py-GC/MS experiments of willow/PHB blends. These interactions are strongly pronounced when statistical data processing is applied. Pattern recognition and the actual analysis of the pyrolytic gases are complementary to the statistical approach. By this, the formation of e.g. the methyl ester of 2-butenoic acid, and the synergetic evolution of the oligomers 3 and 4 is indicated.

Py-GC/MS additionally indicates that the pyrolytic gases of the willow/PHB blends contain less carbon dioxide as compared to the willow and PHB separately. It is also observed that the amount of some oligomers of crotonic acid increases synergetically during the Py-GC/MS experiments on willow/PHB blends. This indicates that the ratio of "high molecular weight" pyrolytic gases against "low molecular weight" pyrolytic gases is significantly increased, which can be the result of a lower degree of pyrolytic cracking of willow/PHB blends.

6.2.2. Condensables - PHB

6.2.2.1. Gel permeation chromatography - GPC

In Figure 6.5, the molecular weight distribution, obtained by GPC, of the bio-oils of pure willow and the 7:1, 3:1, 2:1, and 1:1 willow/PHB blends are visualised and confronted with the molecular weight distribution of the crystals of crotonic acid originating from pure PHB. Even though GPC is less suited for the determination of low molecular weights, the retention time of crotonic acid is experimentally confirmed in the GPC-chromatograms. Comparison of the profiles of the respective bio-oils, indicates that the amount of crotonic acid increases in direct relation with the amount of PHB added to the blend: willow → willow/PHB 7:1 → willow/PHB 3:1. However, willow/PHB 2:1 and 1:1 do not show a further increase of the amount of crotonic acid dissolved in the bio-oil, because both blends result in the production of both bio-oil and crystals, which are readily separated by a simple filtration [1]. Apparently, the concentration of crotonic acid in the bio-oil of willow/PHB 3:1 is close to its maximum solubility degree in bio-oil. If higher amounts of PHB are added, a higher amount of crotonic acid is produced of which only a fraction stays dissolved in the bio-oil while the rest crystallises and precipitates as crystals.

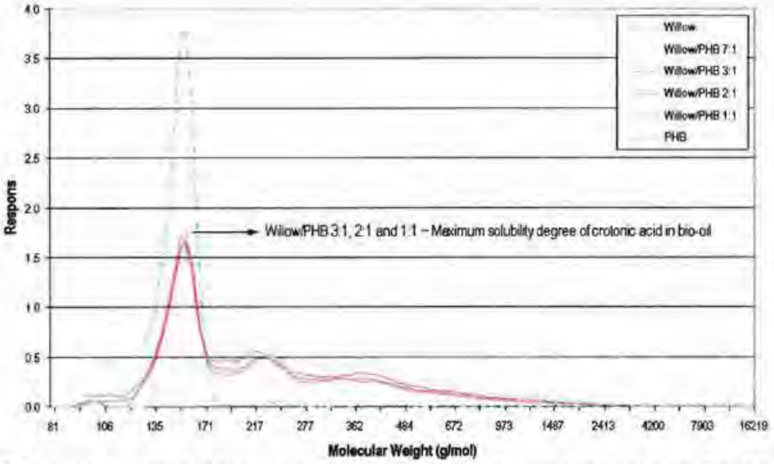

Figure 6.5: Molecular weight distribution (g/mol) of the respective bio-oils (willow and 7:1, 3:1, 2:1, and 1:1 willow/PHB) and of the crystals of crotonic acid (PHB), obtained by GPC.

6.2.2.2. Fourier transform Infrared spectroscopy – FT-IR

The FT-IR-spectra of the crystals of crotonic acid (pure PHB) and of the water-free bio-oils (pure willow, 3:1 and 1:1 willow/PHB) are shown in Figure 6.6. Even though there is a vast difference in the willow/PHB ratio, the FT-IR spectra of 3:1 and 1:1 willow/PHB are almost identical and show features of both input materials (willow and PHB). This confirms the previous observations that the solubility degree of crotonic acid in bio-oil is close to its maximum for the willow/PHB 3:1 blend. In case of 1:1 willow/PHB most of the crotonic acid crystallises and is separated from the bio-oil. This explains why the sharp peaks at 516 cm^{-1}, 538 cm^{-1}, 699 cm^{-1}, 844 cm^{-1} and 922 cm^{-1} in the spectrum of the crystals of crotonic acid are less pronounced in both the willow/PHB blends and that their intensities do not seem to be affected by the initial PHB fraction in the blend.

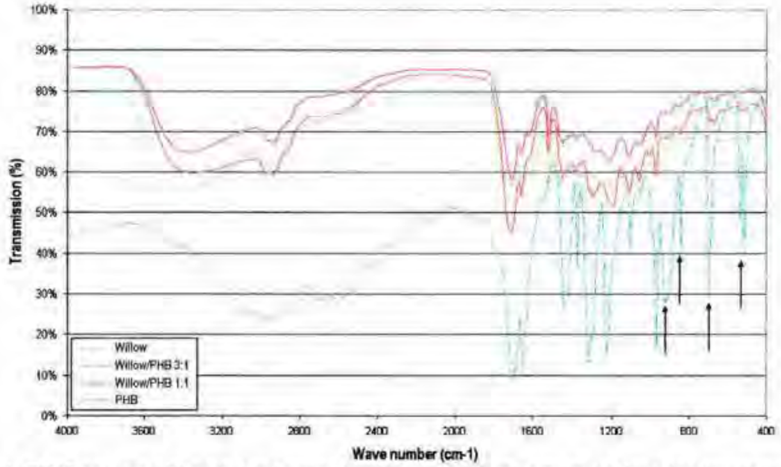

Figure 6.6: FT-IR spectra of the air-dried water-free bio-oils originating from the flash (co-)pyrolysis of pure willow, 3:1 and 1:1 willow/PHB and of the crystals of crotonic acid originating from the flash pyrolysis of pure PHB with the reactor.

6.2.2.3. Gas chromatography/Mass spectrometry – GC/MS

Finally, GC/MS analysis is performed on the respective bio-oils and crystals obtained from the reactor experiments. The ten most important components of each bio-oil are summarised in Table 6.6. As is reported in Chapter 5, the flash pyrolysis of PHB with the pyrolysis reactor does not result in any bio-oil, but only results in the production of crystals of crotonic acid [1]. The methyl ester of 2-butenoic acid, which has been detected as a new component by Py-GC/MS, is synergetically produced in the bio-oils of the blends. Additionally, an oligomer, most probably a dimer, of crotonic acid [9], different from those observed by Py-GC/MS, is only detected in the bio-oil of the willow/PHB blends.

Crotonic acid and the butyl ester of 2-methyl-propanoic acid are more abundantly present in the bio-oils of the blends as compared to the references. It should also be noted that, even though willow/PHB 2:1 and 1:1 result in the formation of crystals of crotonic acid, these blends still have a high amount of crotonic acid dissolved in their respective bio-oil. By combining both fractions of crotonic acid, Table 6.7, it seems that a synergetic increase of crotonic acid might be achieved during flash co-pyrolysis of willow and PHB with the pyrolysis reactor. However, it should also be taken into consideration that bio-oil can only be analysed partly by GC/MS and that a simple addition of the crotonic acid dissolved in the bio-oil with the previously separated crystals is not valid quantitatively.

Table 6.6: Summary of the 10 most important components of the respective bio-oils, obtained by the reactor experiments for PHB, analysed by GC/MS, with the oligomer: *m/z* 41, 69, 87, 103 and 154, different from the oligomers observed by Py-GC/MS.

	Willow	%
1	acetic acid	13.82
2	2,6-dimethoxy-4-(2-propenyl)-phenol	6.40
3	2-(2-ethoxy-1-methoxyethyl)-furan	4.11
4	2-methyl-propanoic acid, butyl ester	3.49
5	1-hydroxy-2-propanone	3.16
6	2-methoxy-4-(1-propenyl)-phenol	3.08
7	dimethoxyphenyl-ethanone	2.35
8	tetrahydro-2,5-dimethoxyfuraan	2.10
9	phenol	2.07
10	4-methoxy-3-(methoxymethyl)-phenol	1.97

	Willow/PHB 7:1	%
1	crotonic acid	25.71
2	acetic acid	6.77
3	1,1-dimethoxy-hexane	5.94
4	2-methyl-propanoic acid, butyl ester	4.86
5	tetrahydro-2,5-dimethoxyfuraan	2.55
6	2,6-dimethoxyphenol	2.46
7	oligomer	2.20
8	2-methoxy-4-(1-propenyl)-phenol	1.79
9	2,6-dimethoxy-4-(2-propenyl)-phenol	1.71
10	butanoic acid, anhydride	1.65

	Willow/PHB 3:1	%
1	crotonic acid	37.81
2	acetic acid	5.50
3	1,1-dimethoxy-hexane	5.21
4	2-methyl-propanoic acid, butyl ester	4.15
5	3-butenoic acid	2.59
6	oligomer	1.99
7	2-(2-ethoxy-1-methoxyethyl)-furan	1.98
8	tetrahydro-2,5-dimethoxyfuraan	1.81
9	1,1,1-trimethoxy-methane	1.65
10	2-hydroxy-3-methyl-2-cyclopenten-1-one	1.40

	Willow/PHB 2:1	%
1	crotonic acid	40.77
2	oligomer	5.51
3	acetic acid	4.78
4	1,1-dimethoxy-hexane	4.10
5	2-methyl-propanoic acid, butyl ester	4.08
6	3-butenoic acid	2.82
7	2-(2-ethoxy-1-methoxyethyl)-furan	1.80
8	2,6-dimethoxy-4-(2-propenyl)-phenol	1.62
9	tetrahydro-2,5-dimethoxyfuraan	1.46
10	dimethylsulfoxide	1.40

	Willow/PHB 1:1	%
1	crotonic acid	43.31
2	oligomer	4.89
3	acetic acid	4.65
4	3-butenoic acid	4.52
5	1,1-dimethoxy-hexane	3.50
6	2-methyl-propanoic acid, butyl ester	2.96
7	butenoic acid, methyl ester	1.68
8	1,1,1-trimethoxymethane	1.48
9	2-(2-ethoxy-1-methoxyethyl)-furan	1.40
10	2,6-dimethoxyphenol	1.26

	PHB*	%
1	-	-
2	-	-
3	-	-
4	-	-
5	-	-
6	-	-
7	-	-
8	-	-
9	-	-
10	-	-

*PHB only results in the formation of crystals of crotonic acid.

Table 6.7: Production of crotonic acid, both as crystals and dissolved in bio-oil, during the flash (co-)pyrolysis reactor experiments of willow and PHB.

	Willow	7:1	3:1	2:1	1:1	PHB
Crystals of crotonic acid (m%)	-	-	-	9.20	29.70	68.67
Bio-oil (m%)	49.71	53.29	57.76	50.18	34.54	-
Crotonic acid dissolved in bio-oil (%)	-	25.71	37.81	40.77	43.31	-

Nevertheless, based on the GC/MS analyses of the bio-oils obtained from the reactor experiments and the fact that for willow/PHB 3:1 crotonic acid is close to its maximum solubility degree in bio-oil, it can be concluded that, besides the synergetic reduction of the water content and the synergetic increase in energy recuperation [1], the flash co-pyrolysis of willow and PHB results in an increased yield of chemicals with added value: crotonic acid.

6.2.2.4. Py-GC/MS versus GC/MS

By comparing the 10 most important components of the pyrolytic gases (condensable and noncondensable) obtained by Py-GC/MS and of the bio-oil (GC/MS) obtained from the reactor experiments (Table 6.5 and Table 6.6, respectively), additional information can be extracted. First and for all, the amount of oligomers are drastically decreased and the amount of crotonic acid increased in the bio-oil. Both observations indicate that much more secondary reactions seem to occur during flash co-pyrolysis of willow and PHB with the pyrolysis reactor compared to the analytical experimental set-up of Py-GC/MS. Possibly, the longer residence times during the reactor experiments and the difference in heat transfer medium (Py-GC/MS: none; reactor: sand) can be part of the explanation. However, the amount of acetic acid, which most importantly originates from willow, behaves more or less "linearly" and contradicts the observations made for components stemming from pure PHB. This indicates that the additional secondary reactions in the willow/PHB blends have more impact on PHB.

The components identified by Py-GC/MS and GC/MS can also be classified into four general classes based on the oxidation number (reactivity) of the respective functionalities, as reported in Table 6.8. A fifth class containing the peaks representing the oligomers of crotonic acid is added. It is observed that the amount of carboxylic acids, esters and ethers in the bio-oil (reactor experiment) is higher than in the pyrolytic gases (Py-GC/MS experiment). The amount of oligomers, aldehydes and alcohols in the bio-oil seems to be decreased as compared to the pyrolytic gases. In case of the oligomers the decrease is strongly pronounced. This indicates that alcohols, aldehydes and oligomers of crotonic acid, present in the pyrolytic gases, mainly decompose in carboxylic acids and esters due to secondary cracking in the pyrolysis reactor.

Table 6.8: Classification of Py-GC/MS and GC/MS results, obtained from PHB, according to the oxidation number or reactivity.

Py-GC/MS

Class	Functionality	Willow	Willow/PHB 7:1	Willow/PHB 3:1	Willow/PHB 2:1	Willow/PHB 1:1	PHB
0	Alkene	-	-	-	-	-	0.03
	Aromatic	-	0.52	0.04	0.04	0.04	0.03
1	Ether	1.75	1.65	1.66	1.5	1.3	0.08
	Alcohol	6.16	5.35	4.98	3.64	2.13	-
	Phenol	21.63	16.79	13.75	10.61	5.54	0.38
2	Aldehyde	11.48	6.85	9.31	5.49	4.2	0.2
	Keton	17.23	10.51	11.52	7.53	5.73	1.24
3	Carboxylic acid	8.63	17.24	15.47	18.52	22.3	33.57
	Ester	8.52	4.76	4.63	6.66	4.41	0.24
-	Oligomers	-	23.75	27.79	38.83	47.12	56.24
	Total	75.4	87.42	89.15	92.82	92.77	92.01

GC/MS

Class	Functionality	Willow	Willow/PHB 7:1	Willow/PHB 3:1	Willow/PHB 2:1	Willow/PHB 1:1	PHB
0	Alkene	-	-	-	-	-	-
	Aromatic	0.93	-	-	-	-	-
1	Ether	11.78	14.74	13.70	9.85	8.26	-
	Alcohol	2.42	0.78	0.37	2.00	1.60	-
	Phenol	23.92	13.52	10.37	8.82	8.13	-
2	Aldehyde	3.19	1.69	1.46	1.68	1.30	-
	Keton	17.13	7.63	6.67	4.74	4.49	0.04
3	Carboxylic acid	15.19	35.28	46.53	48.77	53.42	87.25
	Ester	7.15	12.16	9.31	9.56	8.13	0.22
-	Oligomers	-	2.20	2.46	5.91	5.66	-
	Total	81.71	88.01	90.87	91.33	90.99	87.51

As already observed, the amount of oligomers synergetically increases when willow/PHB blends are considered for Py-GC/MS. The carboxylic acids also show such a synergetic increase, however, this increase is the most pronounced when only small amounts of PHB are added to the blend. The synergetic increase of carboxylic acids (e.g. crotonic acid) in the respective bio-oil is confirmed by GC/MS. Table 6.8 additionally indicates that the amount of esters in the bio-oil of the willow/PHB blends increase synergetically as compared to the bio-oils of pure willow and pure PHB. The methyl ester of 2-butenoic acid for instance has been determined as a new component by Py-GC/MS and has also been observed to behave synergetically by GC/MS of the bio-oil.

6.2.3. Discussion of the observed synergy - PHB

In Chapter 5, a synergetic decrease in the amount of pyrolytic water (-40%), and a synergetic increase in pyrolysis yield (+8%) and in energy recuperation (+18%) is observed by the reactor experiments [1]. Py-GC/MS and statistical data processing confirm the occurrence of synergetic interactions for the willow/PHB blends. It is concluded that the observed synergy only occurs, or at least is more pronounced, when co-pyrolysis is applied in flash pyrolytic circumstances.

Py-GC/MS indicates that the pyrolytic gases of the willow/PHB blends contain less carbon dioxide as compared to willow and PHB separately. Additionally, it is observed that the amount of oligomers of crotonic acid increases synergetically for the willow/PHB blends. This indicates that the ratio of "high molecular weight" pyrolytic gases against "low molecular weight" pyrolytic gases is increased and thus a lower degree of pyrolytic cracking for the willow/PHB blends occurred.

However, the amount of oligomers are drastically reduced and a synergetic increase of crotonic acid seems to be achieved when flash co-pyrolysis of willow and PHB is performed with the pyrolysis reactor. Both these observations indicate that much more secondary reactions seem to occur during the reactor experiments as compared to the analytical experimental set-up of Py-GC/MS. Additionally it is observed that PHB and its oligomers are more sensitive to these secondary reactions as compared to willow. These observations are partly strengthened by earlier research on the pyrolysis of PHB by TGA, DSC, Py-MS and Py-GC/MS performed by Kopinke et al. [7, 8]. Kopinke et al. proposed an alternative explanation for the decomposition kinetics of PHB based on intermediate products of the decomposition process, which can be supposed to have a higher reactivity than PHB itself [7, 8].

According to Kopinke et al. three different substrates have to be considered during the PHB degradation:

(i) the saturated ester in the original PHB molecule,

(ii) an ester chain with an α,β-unsaturated ester as end group, and

(iii) an ester chain with a carboxylic acid as end group (see Figure 6.7).

Kopinke et al. concluded that if (iii) decomposes much faster than (i), the result would be equivalent to a chain reaction [7, 8]. These more reactive intermediates might be the reason for the increased sensitivity of PHB towards secondary cracking observed in this research.

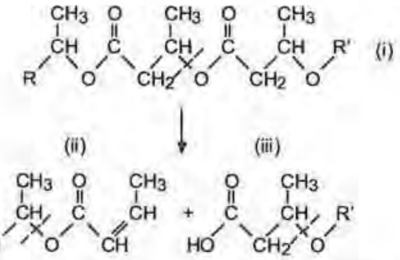

Figure 6.7: Different substrates of cis-elimination during PHB decomposition [7].

Additionally Kopinke et al. observed a matrix effect in the case of PHB embedded in its crude biomass, but concluded that the matrix effect of biomass is not understood [7, 8]. Crude PHB embedded in the original biomass is significantly less stable than the purified polymer, but the decomposition products are essentially identical. However, the main difference lies in the ratio of crotonic acid to oligomers, which is higher for pure PHB [7, 8]. This is in strong agreement with the observations made from this research, where a synergetic increase of oligomers of crotonic acid is detected by Py-GC/MS of the willow/PHB blends.

Finally, it should be noted that the amount of esters in the bio-oil obtained by flash co-pyrolysis of willow and PHB with the pyrolysis reactor increase synergetically as compared to the bio-oils obtained by the flash pyrolysis of pure willow and pure PHB. This however might indicate that the formation of water would be increased and is in conflict with the earlier observations that the amount of pyrolytic water is synergetically reduced.

6.3. Flash co-pyrolysis of biomass with PLA

The thermal decomposition of PLA has already been studied in detail too [8, 9, 11-20]. According to literature, it involves more than two degradation mechanisms. Intra- and inter-molecular transesterifications, *cis*-elimination, and other radical and non-radical reactions occur concurrently resulting in a very complex degradation (Figure 6.8). As prominent degradation products CO, CO_2, acetaldehyde, acrylic acid, two lactide isomers and cyclic oligomers up to the hexamers were detected [8, 13]. During Py-GC/MS, cyclic oligomers appear with at least two peaks, which have almost identical mass spectra, representing diastereomers, derived from the asymmetric C atom in the lactic acid [8, 13]. The mass spectra exhibit a dominant series of signals with $m/z = n*72 - 88$ ($n \geq 3$) or put differently $m/z = 128 + n*72$ ($n \geq 0$) [8, 11-13]. Lactide and cyclic oligomers are obtained from the intramolecular transesterification, while acrylic acid (or 2-propenoic acid) and acyclic oligomers are formed by *cis*-elimination [8, 9, 13, 21]. The acyclic oligomers are represented by the series of homologues with $m/z = n*72$ ($n \geq 2$). Additional mass fragment ions at 1 or 2 mass units above or below each of the strongest peaks have been observed for the acyclic oligomers, explaining the series of signals at $m/z = n*72 - 73$ ($n \geq 3$) and $m/z = 73 + n*72$ ($n \geq 0$) [8, 11-13]. McNeill proposed that the main thermal degradation process in PLA is a non-radical, backbiting ester interchange reaction involving the OH chain ends. Depending on the point in the backbone at which this reaction occurs, the product can be a lactide molecule, an oligomeric ring with more than two repeat units, or acetaldehyde plus carbon monoxide [12]. Recent investigations are focussing on the selective recycling of lactide, converting PLA into a possible candidate for feedstock recycling plastics [15-20].

As discussed in Chapter 5, flash co-pyrolysis of biomass/PLA blends proves to be an alternative waste treatment option and an attractive upgrading method for bio-oil. At 723 K a synergetic decrease in the amount of pyrolytic water, a synergetic increase in bio-oil yield and in energy recuperation is observed for willow/PLA blends [2]. In *section 6.3.1.* and *6.3.2.*, the condensable and noncondensable pyrolytic gases obtained by Py-GC/MS and the bio-oil obtained from the reactor experiments, respectively, will be investigated. In *section 6.3.3.* the observed synergy is discussed.

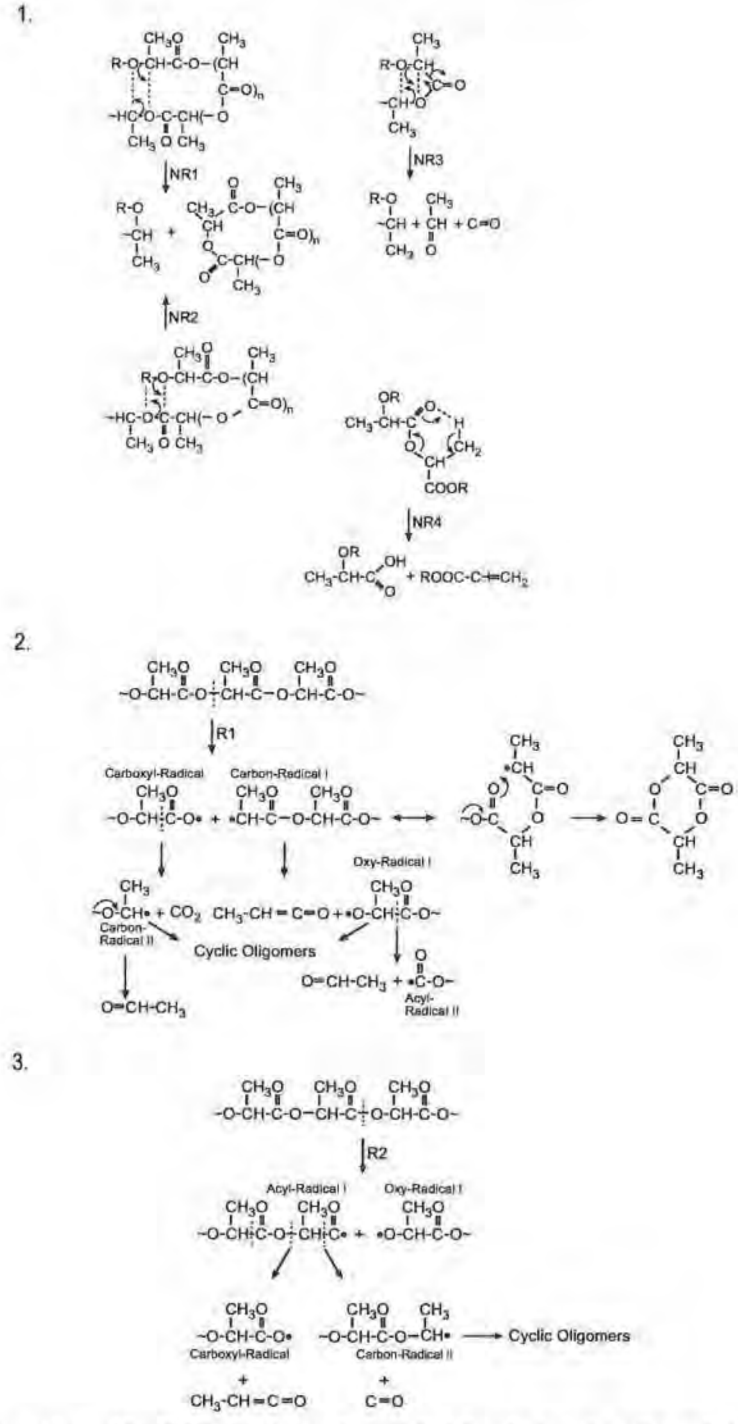

Figure 6.8: Possible reactions of the PLA decomposition: 1. nonradical; 2. radical, starting with an alkyl-oxygen homolysis; 3. radical, starting with an acyl-oxygen homolysis [13].

6.3.1. Condensable and noncondensable pyrolytic gases - PLA

6.3.1.1. Py-GC/MS – Statistical approach

a. Peaks in chromatogram

For the specific PLA data set and the general linear mixed-effects model under consideration (equation 6.1), it is observed that only a constant (b_{0i}) and a linear (b_{1i}) random or chromatogram-specific effect are necessary and that the higher-order random effects are not required. The second- and third-order random effects in b_i (b_{2i} and b_{3i}) can thus be removed from the model for response Y_{ij}. This implies that only three random-effects-related variance components (variance of the first and second random effect and the covariance between both - d_{00}, d_{11} and d_{01}, respectively; elements of covariance matrix *D*, see equation 6.2) have to be taken into account. Based on the magnitude of their estimates and standard errors (Table 6.9), it is observed that both random effects in the vector b_i (b_{0i} and b_{1i}) are necessary, a fact confirmed by likelihood-ratio tests ($p < 0.0001$).

Table 6.9: Parameter estimates and standard error for the linear mixed-effects model for response Y_{ij} for PLA.

Effect	Parameter	Estimate	Standard Error	p
Mean structure (fixed effects)				
Intercept	β_0	0.17	0.08	0.0317
Peak linear	β_p	0.59	0.09	< 0.0001
Willow linear	β_w	0.85	0.39	0.0339
Peak squared	β_{pp}	-0.2	0.02	< 0.0001
Peak-by-willow	β_{pw}	0.11	0.03	0.0003
Willow squared	β_{ww}	-2.38	1	0.0219
Peak cubed	β_{ppp}	-	-	0.0912
Peak squared-by-willow	β_{ppw}	-	-	0.6483
Peak-by-willow squared	β_{pww}	-	-	0.2771
Willow cubed	β_{www}	1.49	0.67	0.0317
Random effects Variance components				
	d_{00}	-0.036	0.006	< 0.0001
	d_{01}	0.025	0.002	< 0.0001
	d_{11}	-0.017	0.001	< 0.0001
Residual Variance Structure				
Residual variance	σ^2	0.38	0.01	< 0.0001

Turning to the conventional regression or fixed effects, the following terms are removed from the model: $\beta_{ppw} p_{ij}^2 w_i$ ($p = 0.6483 > 0.05$ = minimum level of significance), $\beta_{pww} p_{ij} w_i^2$ ($p = 0.2771 > 0.05$), and $\beta_{ppp} p_{ij}^3 w_i$ ($p = 0.0912 > 0.05$). Taking into account polynomial-model hierarchies and applying the conventional backward model selection strategy, all lower order terms ($0 \rightarrow n\text{-}1$) are incorporated in the model when at least one term of the n^th^ order is considered significant in that model. No further terms can be removed from the model because they are considered statistically significant ($p < 0.05$). The model fit for the response Y_{ij} is summarised in Table 6.9.

Each of the willow effects in the final model (β_w, β_{pw}, β_{ww}, and β_{www}) captures one aspect of the effect of willow on the chromatogram. However, this provides a fragmented picture, and it is therefore instructive to consider the overall hypothesis of no willow effect (equation 6.9):

$$H_{0,\,\text{willow}} : \beta_w = \beta_{pw} = \beta_{ww} = \beta_{www} = 0. \qquad (6.9)$$

Testing hypothesis $H_{0,\,\text{willow}}$ (equation 6.9) can be done using an F test of which the realised value ($F = 6.20$) is compared to an $F_{4,50.2}$ reference distribution. Note that there are 4 numerator degrees of freedom because $H_{0,\,\text{willow}}$ is compound and involves 4 comparisons; there are 50.2 denominator degrees of freedom, as derived by the approximate but accurate method of Kenward and Roger [5]. Fractional denominator degrees of freedom are a result of the unbalancedness in the design. The willow effect (and therefore the PLA effect as well) is, as expected, found to be highly significant ($p = 0.0004$) in the model described.

For the purpose of this research, the higher-order terms in the willow effect are of crucial importance since these specifically indicate that there is a complex interaction (non-linear) between willow and PLA during flash co-pyrolysis, superimposed onto simple additive (linear) aspects. The hypothesis of complex interaction (equation 6.10) is formulated as follows:

$$H_{0,\,\text{interaction}} : \beta_{pw} = \beta_{ww} = \beta_{www} = 0. \qquad (6.10)$$

Testing the composite hypothesis $H_{0,\,\text{interaction}}$ (equation 6.10) can be done, likewise, using an F test of which the realised value ($F = 7.08$) is compared to an $F_{3,60.5}$ reference distribution. The higher-order terms appear to be highly significant ($p = 0.0004$) too.

Similar to PHB, Py-GC/MS and statistical data processing of the 38 carefully chosen peaks confirm the occurrence of synergetic interactions between willow and PLA during analytical flash co-pyrolysis as observed with the former reactor experiments discussed in Chapter 5 [2]. However, no information about which peak(s), each representing a component of the (condensable and noncondensable) pyrolytic gases, is (are) responsible for these findings, nor an indication towards the actual consequences of the observed synergy on the pyrolytic gases is obtained.

b. Areas of chromatogram

The ranges of the identical areas are selected based on the specific chromatogram features of willow, PLA and the four willow/PLA blends and are summarised in Table 6.10. In contradiction to PHB, the chromatograms are split into eight areas.

Table 6.10: Summary for PLA of the eight areas, identical for each chromatogram.

Zone	Start (min)	End (min)
1	0	5
2	5	10
3	10	14
4	14	17
5	17	20
6	20	25
7	25	30
8	30	35

Table 6.11 summarises the model fit for A_{ij} (equation 6.3) for PLA. Taking into account polynomial-model hierarchies and applying the conventional backward model selection strategy, all lower order terms ($0 \rightarrow n-1$) are incorporated in the model when the n^{th} order term is considered significant ($p < 0.05$) in at least one zone. Additionally, the n^{th} order term is considered significant in all zones considered in the model. Therefore, all regression terms ($\beta_{01} \rightarrow \beta_{28}$) are found to be highly significant. Likelihood-ratio tests on the eight residual variances ($\sigma_1^2 \rightarrow \sigma_8^2$) indicate that the eight random effects in the error vector $\varepsilon_i = (\varepsilon_{i1}, \ldots, \varepsilon_{i8})$ are considered highly significant ($p < 0.0001$) too.

Table 6.11: Robust parameter estimates for the model for area A_{ij} for PLA.

	Intercept				Willow				Willow squared			
Zone	Par.	Estimate	robust std. error	p	Par.	Estimate	robust std. error	p	Par.	Estimate	robust std. error	p
Mean Structure												
1	β_{01}	10.1	1.1	< 0.0001	β_{11}	-3.9	3.8	0.3113	β_{21}	2	3.1	0.5176
2	β_{02}	9.1	0.7	< 0.0001	β_{12}	10.4	3.4	0.0026	β_{22}	-3.1	3.3	0.346
3	β_{03}	11.1	0.9	< 0.0001	β_{13}	8.1	3.1	0.0089	β_{23}	-7.4	2.5	0.003
4	β_{04}	16.5	1.1	< 0.0001	β_{14}	13.9	3.9	0.0005	β_{24}	-16.7	3.1	< 0.0001
5	β_{05}	11.9	0.6	< 0.0001	β_{15}	4.8	2.9	0.0996	β_{25}	-1.8	2.8	0.5259
6	β_{06}	18	0.9	< 0.0001	β_{16}	-13.8	3.7	0.0002	β_{26}	10.9	3.4	0.0013
7	β_{07}	13.1	1.3	< 0.0001	β_{17}	-9.7	4.8	0.0428	β_{27}	8	4.1	0.0513
8	β_{08}	10.1	1.4	< 0.0001	β_{18}	-9.9	4.9	0.0452	β_{28}	8.1	4	0.0446
Residual Variances												
1	σ_1^2	3.3	0.7	< 0.0001								
2	σ_2^2	4.5	0.9	< 0.0001								
3	σ_3^2	1.8	0.4	< 0.0001								
4	σ_4^2	4.1	0.9	< 0.0001								
5	σ_5^2	7.7	2.1	0.0001								
6	σ_6^2	6.2	1.4	< 0.0001								
7	σ_7^2	4.1	0.7	< 0.0001								
8	σ_8^2	3.9	0.7	< 0.0001								
AR(1) Correlation												
	ρ	0.66	0.05	< 0.0001								

Again, each of the parameters provides only partial information about the effects under consideration and it is therefore of interest to conduct well targeted hypothesis tests. Three sets are considered.

The first set is directed at the entire willow effect across all zones (equation 6.11), hence there are two: for the linear and squared effects of willow fraction, respectively. The corresponding hypotheses are:

$$\begin{aligned} &H_{0,\,\text{all zones, linear}}: && \beta_{11} = \beta_{12} = \beta_{13} = \beta_{14} = \beta_{15} = \beta_{16} = \beta_{17} = \beta_{18} = 0, \\ &H_{0,\,\text{all zones, squared}}: && \beta_{21} = \beta_{22} = \beta_{23} = \beta_{24} = \beta_{25} = \beta_{26} = \beta_{27} = \beta_{28} = 0. \end{aligned} \quad (6.11)$$

The second set is directed at the effect of willow fraction in a specific zone (equation 6.12). This produces eight null hypotheses with two effects each (linear (β_{1i}) and quadratic (β_{2i})):

$$\begin{aligned} &H_{0,\,\text{zone 1}}: \beta_{11} = \beta_{21} = 0, \\ &H_{0,\,\text{zone 2}}: \beta_{12} = \beta_{22} = 0, \\ &H_{0,\,\text{zone 3}}: \beta_{13} = \beta_{23} = 0, \\ &H_{0,\,\text{zone 4}}: \beta_{14} = \beta_{24} = 0, \\ &H_{0,\,\text{zone 5}}: \beta_{15} = \beta_{25} = 0, \\ &H_{0,\,\text{zone 6}}: \beta_{16} = \beta_{26} = 0, \\ &H_{0,\,\text{zone 7}}: \beta_{17} = \beta_{27} = 0, \\ &H_{0,\,\text{zone 8}}: \beta_{18} = \beta_{28} = 0. \end{aligned} \quad (6.12)$$

Finally, the overall effect (equation 6.13) of willow is ascertained by the following hypothesis test:

$$H_{0,\,\text{overall}}: \beta_{11} = \ldots = \beta_{18} = \beta_{21} = \ldots = \beta_{28} = 0. \quad (6.13)$$

The entire output of the eleven hypothesis tests is summarised in Table 6.12. It can be concluded that the effect, both linear and quadratic, of willow fraction in zone 1 ($H_{0,\,\text{zone 1}}$: $p = 0.2181 > 0.05$), zone 7 ($H_{0,\,\text{zone 7}}$: $p = 0.1279 > 0.05$) and zone 8 ($H_{0,\,\text{zone 8}}$: $p = 0.1294 > 0.05$) is not proven. All the other hypotheses considered, however, result in a high ($p < 0.01$) to very high ($p < 0.001$) significance, and confirm the linear willow effect (and thus the linear PLA effect as well) and the occurrence of interactions (synergy or non-linear) between willow and PLA during the analytical flash co-pyrolysis by Py-GC/MS. Again, it should be noted that no indication towards the actual impact of the observed synergy on the pyrolytic gases is obtained.

Table 6.12: Robust hypothesis testing results for areas in chromatogram for PLA.

H_0	Num. d.f.	Den. d. f.	F	p
$H_{0,\text{ all zones, linear}}$	7	270	8.6	< 0.0001
$H_{0,\text{ all zones, squared}}$	7	270	10.3	< 0.0001
$H_{0,\text{ zone 1}}$	2	270	1.5	0.2181
$H_{0,\text{ zone 2}}$	2	270	30.5	< 0.0001
$H_{0,\text{ zone 3}}$	2	270	5.3	0.0054
$H_{0,\text{ zone 4}}$	2	270	40.9	< 0.0001
$H_{0,\text{ zone 5}}$	2	270	7.7	0.0006
$H_{0,\text{ zone 6}}$	2	270	7.5	0.0007
$H_{0,\text{ zone 7}}$	2	270	2.1	0.1279
$H_{0,\text{ zone 8}}$	2	270	2.1	0.1294
$H_{0,\text{ overall}}$	14	270	52.5	< 0.0001

So, with the aid of Py-GC/MS and statistical analysis of the pyrolysis GC-chromatograms, it can be concluded that interactions do occur during analytical flash co-pyrolysis of willow/PLA blends, resulting into an altered gas (condensable and noncondensable) composition. However, which interactions and where specifically these occur, has not yet been determined and requires further research. Additionally, it is shown that statistical data processing executed on the carefully chosen peaks in each chromatogram results in more significant results as compared to the eight identical areas of each chromatogram.

Here, it is worth mentioning that PLA results in less pronounced significance as compared to PHB:

- Peaks in chromatogram:
    - For PHB (Table 6.1) only one third-order term (β_{ppw}) can be removed, while for PLA (Table 6.9) three (β_{ppp}, β_{ppw}, and β_{pww}). This difference does not give any information on the significance of the output, only an indication towards the model itself is obtained.
    - Additionally, the output of the hypotheses tests shows that PLA results in slightly less significant results ($p = 0.0004$) compared to PHB ($p < 0.0001$). However, for both very high significance is observed.

- Areas of chromatogram:
  - Only one regression effect, related to zone 4, of the model for PLA is considered as highly significant (Table 6.11), while PHB shows to have 3: zone 3, 5 and 6 (Table 6.3). Again, this observation does not give any information on the significance of the output, only an indication towards the model itself is obtained.
  - The output of the different hypotheses tests shows obvious differences. For PHB (Table 6.4), no matter which hypotheses is considered, they all result in very high significance ($p < 0.0001$), while for PLA (Table 6.12) only five of the eleven hypotheses result in such high significance. Even for three zones (zone 1, 7 and 8), the effect, both linear and quadratic, of the willow fraction is not proven.

An explanation of these differences can be the particle size of the respective biopolymers. PHB is received as a powder and is mixed with willow as such, while PLA is received as pellets and is milled with a Retsch ZM1000 prior to analysis. Nevertheless, the particle size of the milled PLA is still much larger as compared to the PHB powder. This causes differences in the homogeneity and reproducibility of the blends, especially for small sample sizes as required for Py-GC/MS.

6.3.1.2. Py-GC/MS – Pattern recognition

Specific mass fragment ions and their respective chromatograms obtained by Py-GC/MS are used as criteria to enhance the resolution of the pattern recognition process. For PLA, the following mass fragment ions have been investigated separately: *m/z* 72, 100, 127, 128, 144, 154, 200, 216, 217, 272, 288, 344, 416, 433 and 488, resulting in fifteen individual mass fragment ion chromatograms. Some of these mass fragment ions are indicative for the PLA degradation, while some others are chosen specifically because they were abundantly present during data processing and asked for additional investigation. Kopinke et al. for instance already defined m/z 72, 100 and 200 as marker ions representing acrylic acid (2-propenoic acid), 2,3-pentanedione and the homologues series of cyclic oligomers, respectively [8, 13]. The unambiguous formation of new components is best visualised by the mass fragment ion chromatograms of *m/z* 344 shown in Figure 6.9, where a large number of peaks appear between 15 and 25 minutes for the willow/PLA blends. These peaks are also observed in the mass fragment ion chromatograms (not shown here) of *m/z* 128, 200, 272 and 416 for the willow/PLA blends, and can be attributed to the series of homologues $m/z = n*72 - 88$ ($n \geq 3$) representing the cyclic oligomers of lactic acid (Figure 6.10) [8, 11-13]. In general, cyclic oligomers are also detected by the pattern recognition process for PLA separately. Nevertheless, the willow/PLA blends show to result in far more cyclic oligomers of which most are not detected when pure willow nor pure PLA are pyrolysed separately. Apparently, Py-GC/MS of willow/PLA blends results in the production of newly formed oligomers and thus confirms the occurrence of a synergy.

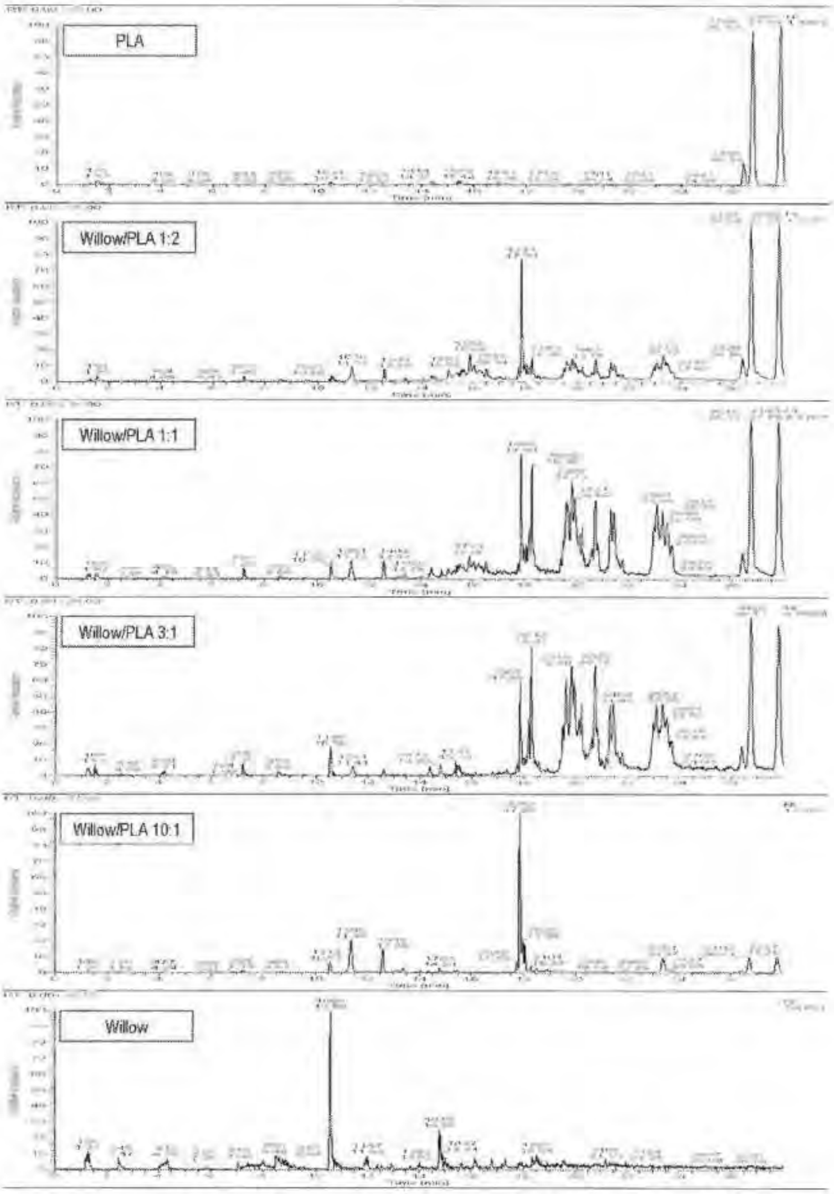

Figure 6.9: Mass fragment ion chromatogram of *m/z* 344 for pure PLA, 1:2, 1:1, 3:1 and 10:1 willow/PLA, and pure willow, obtained by Py-GC/MS.

It should be noted that the newly formed oligomers seemingly behave relatively non-linear. In case of willow/PLA 10:1 only a few peaks are identified as new, with the peak at 17.85 minutes representing by far the most abundant peak. This peak is, however, sharply reduced in relative importance for willow/PLA 3:1 and 1:1, promoting the formation of a wide variety of peaks with almost identical mass spectra. These are assigned to higher cyclic oligomers and their diastereomers derived from the asymmetric C atom in the lactic acid. Surprisingly, the higher oligomers decrease again for willow/PLA 1:2 and lose an important share as compared to the peak at 17.85 minutes.

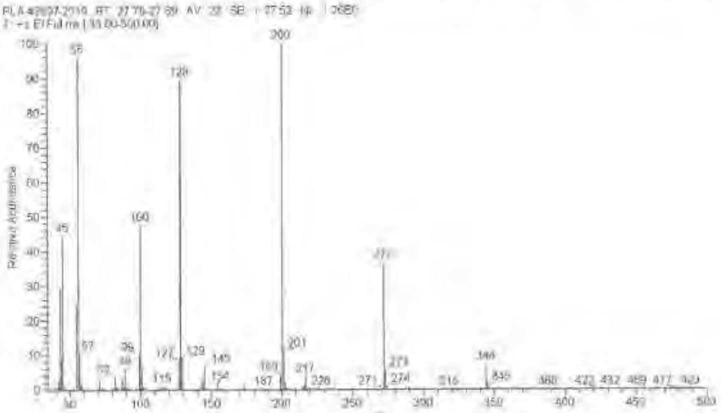

Figure 6.10: Mass spectra of a cyclic oligomer of lactic acid.

The changes observed by pattern recognition support the conclusions obtained by the statistical data processing. However, other changes in the pyrolytic gas composition are most likely, even though they are not observed by pattern recognition. The pyrolytic gas composition will therefore be investigated in further detail in the next subsection.

6.3.1.3. Py-GC/MS – Analysis of the gaseous pyrolytic components

The actual analysis of the condensable and noncondensable pyrolytic gases is performed. Table 6.13 summarises the 10 most important components detected by Py-GC/MS of pure willow, pure PLA and the four willow/PLA blends. It is observed that:

- Except for willow, repeating series of cyclic oligomers ($m/z = n \ast 72 - 88$ ($n \geq 3$)), originating from the degradation of PLA, are always detected and represent an important share in the pyrolytic gases, even when only minor fractions of PLA (e.g. 10:1 willow/PLA) are co-pyrolysed with willow. Even though pure PLA results in the following distribution of oligomers: cyclic hexamer > cyclic pentamer > cyclic heptamer > cyclic tetramer, the cyclic heptamer and tetramer are switched in abundance for the willow/PLA blends, and result in the altered distribution: cyclic hexamer > cyclic pentamer > cyclic tetramer > cyclic heptamer. Such non-linear behaviour indicates the occurrence of interactions.

- For 1:1 and 1:2 willow/PLA a new component, containing the characteristic mass fragment ions *m/z* 43, 44, 45, 55, 56, 57, 72, 73, 88, 99, 100, 120, 145, 174, 217 (Figure 6.11), is identified as the eighth, respectively tenth, most important component. The series of signals can be attributed to acyclic oligomers with a hydroxyl end group generated by an ester cleavage ($m/z = n*72 + 73$) [8, 13] and is defined as '*acyclic oligomer x*' for this research.

  The acyclic oligomer x has been detected for all willow/PLA blends, while pure willow and pure PLA do not result in the formation of this specific oligomer. The acyclic oligomer x can thus be defined as a newly formed component in the pyrolytic gases and confirms the occurrence of interactions during Py-GC/MS of willow/PLA blends.

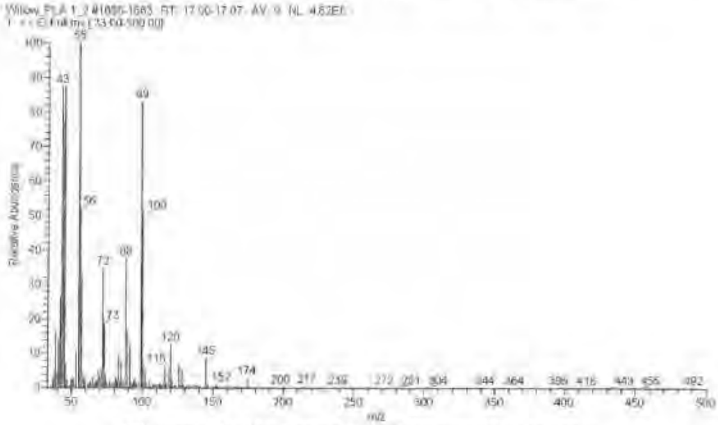

Figure 6.11: Mass spectrum of the acyclic oligomer x.

- After further investigation, it is shown that more newly formed components are obtained for the blends, such as the methyl esters of propanoic, 2-propenoic and 2-hydroxy-propanoic acid. These are, however, present in relatively minor amounts.
- Table 6.13 additionally shows that lactide, which is the cyclic dimer of lactic acid, also behaves non-linear. Interestingly, lactide is already observed to be the most abundant component for willow/PLA 10:1, indicating that some synergetic interactions occur immediately and extensively when 'co-pyrolysis' is executed.
- Finally, it seems that most components originating from the willow fraction, e.g. the phenolic components, behave more or less linear in function to the ratio applied. This observation indicates that the thermal decomposition mechanism of willow is less affected by the

observed synergetic effects between willow and PLA as compared to the thermal degradation mechanism of PLA.

Table 6.13: Summary of the 10 most important components of the respective pyrolytic gases (condensable and noncondensable) analysed by Py-GC/MS, with the acyclic oligomer x: *m/z* 44, 55, 57, 72, 73, 88, 99, 120, 145, 174, 217.

	Willow	%		Willow/PLA 10:1	%
1	2,6-dimethoxy-4-(2-propenyl)-phenol	4.94	1	lactide	4.98
2	2,6-dimethoxyphenol	3.20	2	2,6-dimethoxy-4-(2-propenyl)-phenol	3.49
3	acetic acid	3.00	3	acetic acid	3.30
4	4-(3-hydroxy-1-propenyl)-2-methoxyphenol	3.00	4	2,6-dimethoxyphenol	2.60
5	1,2-cyclopentanedione	2.18	5	cyclic hexamer	2.50
6	pentanal	2.00	6	2-propenoic acid	2.10
7	2-methoxy-4-vinylphenol	1.99	7	2-methoxy-4-vinylphenol	1.96
8	furanmethanol	1.78	8	CO_2	1.93
9	5-(hydroxymethyl)-2-furancarboxaldehyde	1.75	9	1,2-cyclopentanedione	1.92
10	2-methoxy-4-(1-propenyl)-phenol	1.58	10	cyclic pentamer	1.92

	Willow/PLA 3:1	%		Willow/PLA 1:1	%
1	lactide	8.43	1	lactide	9.47
2	cyclic hexamer	4.45	2	cyclic hexamer	5.28
3	acetaldehyde	3.19	3	cyclic pentamer	4.27
4	2-propenoic acid	3.00	4	2-propenoic acid	4.00
5	2,6-dimethoxy-4-(2-propenyl)-phenol	2.88	5	acetaldehyde	3.12
6	cyclic pentamer	2.87	6	2,6-dimethoxy-4-(2-propenyl)-phenol	2.80
7	cyclic tetramer	2.83	7	acetic acid	2.60
8	acetic acid	2.36	8	acyclic oligomer x	2.60
9	propanoic acid	2.00	9	cyclic tetramer	2.58
10	2,6-dimethoxyphenol	1.80	10	propanoic acid	2.40

	Willow/PLA 1:2	%		PLA	%
1	lactide	11.72	1	lactide	11.10
2	cyclic hexamer	6.25	2	cyclic hexamer	9.59
3	cyclic pentamer	5.14	3	2-propenoic acid	6.37
4	2-propenoic acid	5.12	4	cyclic pentamer	6.10
5	acetaldehyde	3.20	5	acetaldehyde	4.18
6	3-methyl-1,2,4-cyclopentanetrione	3.12	6	cyclic heptamer	3.59
7	cyclic tetramer	3.10	7	cyclic tetramer	3.11
8	propanoic acid	2.84	8	3-methyl-1,2,4-cyclopentanetrione	3.09
9	acetic acid	2.60	9	2,4,5-trimethyl-1,3-dioxolane	2.72
10	acyclic oligomer x	2.50	10	propanoic acid	2.70

Generally, it can be stated that the pyrolytic gas (condensable and noncondensable) composition alters due to the occurrence of synergetic interactions during the Py-GC/MS experiments of willow/PLA blends. These interactions are more strongly pronounced when statistical data processing is applied, especially when the peaks in the chromatogram are considered. Pattern recognition and the actual analysis of the pyrolytic gases are complementary to the statistical approach. By this, the formation of the new cyclic and acyclic oligomers and some esters, and the synergetic evolution of some other oligomers is indicated.

6.3.2. Condensables - PLA

6.3.2.1. Fourier transform infrared spectroscopy – FT-IR

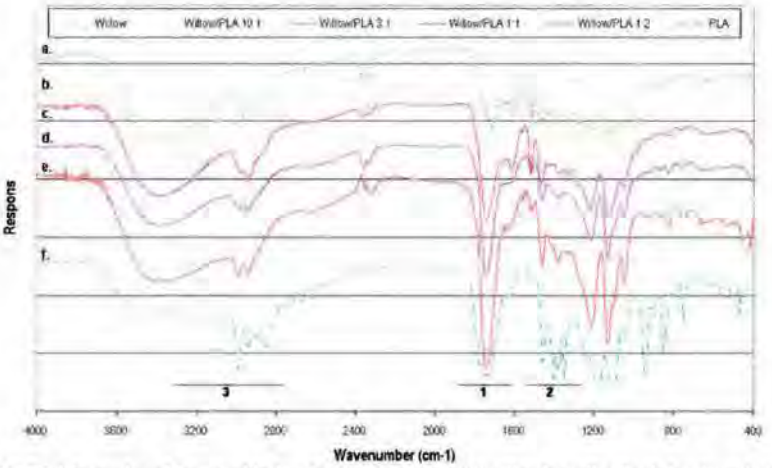

Figure 6.12: FT-IR spectra of the air-dried water-free bio-oils originating from the flash (co-)pyrolysis of pure willow (a); 10:1, 3:1, 1:1 and 1:2 willow/PLA blends (b, c, d and e, respectively); and f. pure PLA.

The FT-IR-spectra of the six air-dried bio-oils of pure willow, pure PLA and the four willow/PLA blends are shown in Figure 6.12. In general, a gradual evolution of the spectral features from willow towards PLA is observed. However, the absorption band centered between 1700 – 1750 cm^{-1} (spectral region 1), representing carbonyl functionalities, increases in relative abundance and is indicated as the most important functionality for the willow/PLA blends. This observation indicates that the fraction of components having one or more carbonyl functionalities, present in the bio-oil, is synergetically increased when willow and PLA are co-pyrolysed and is the most pronounced for the 1:2 willow/PLA blend. Additionally, the absorption bands between 1300 and 1500 cm^{-1} (spectral region 2) and 2500 and 3300 cm^{-1} (spectral region 3), representing O-H bending and the broad band related to O-H stretching of the carboxylic acid functionality 'COOH' of the oligomers, respectively, are sharply reduced in intensity or even not detected. These non-linear evolutions confirm the synergetic interactions and indicate their effect on the bio-oil composition.

6.3.2.2. High performance liquid chromatography - HPLC

Figure 6.13 summarises the HPLC-chromatograms of the bio-oils stemming from willow, PLA and the four willow/PLA blends. Again a gradual evolution from willow to PLA is mainly observed, but some unexpected (non-additive) evolutions also occur: the peaks at 3.6, 3.9 and 25.5 minutes are only detected for the bio-oil originating from pure willow. These peaks, and therefore the respective components, disappear once PLA is co-pyrolysed with willow. Even a high willow fraction mixed with only small amounts of PLA (e.g. willow/PLA 10:1) does not show these peaks in its HPLC chromatogram. This confirms the fact that the bio-oil composition is altered due to interactions between willow and PLA during co-pyrolysis. Detailed information concerning which components in specific are new, disappear or behave synergetically can be obtained from GC/MS-analysis of the respective bio-oils.

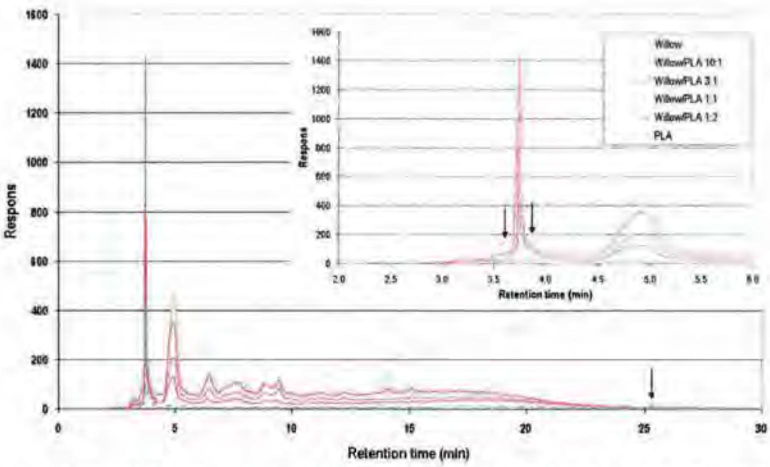

Figure 6.13: HPLC chromatograms for willow, PLA and 10:1, 3:1, 1:1 and 1:2 willow/PLA.

6.3.2.3. Gas chromatography/Mass spectrometry – GC/MS

The ten most important components of each bio-oil, analysed by GC/MS, are summarised in Table 6.14. It is readily observed that both the amount of paraldehyde and the substituted ester of 2-substituted-propanoic acid are sharply reduced for the willow/PLA blends as compared to pure PLA, indicating that the production of these two components is inhibited or that they are consumed when flash co-pyrolysis is applied. Both components make up 40% of the analysable fraction of PLA bio-oil, but amount to less than 10% for 1:2 willow/PLA while approximately 25% would be expected.

It should be noted that the substituted ester of 2-substituted-propanoic acid could not be identified with the aid of a NIST library. GC/MS resulted in the mass fragment ions *m/z* 45, 57 and 88 when electron impact is applied (Figure 6.14a). In order to obtain the molecular ion of the component, chemical ionisation with iso-butane is additionally applied, showing the mass fragment ions m/z 105, 131, 149 and 177 (Figure 6.14b). Here, the characteristic mass loss of '72' is noticed. A substituted ester of 2-substituted-propanoic acid, with a molecular weight of 176 g/mol and chemical formula $C_7H_{12}O_5$, which can explain the major fragment ions, is suggested.

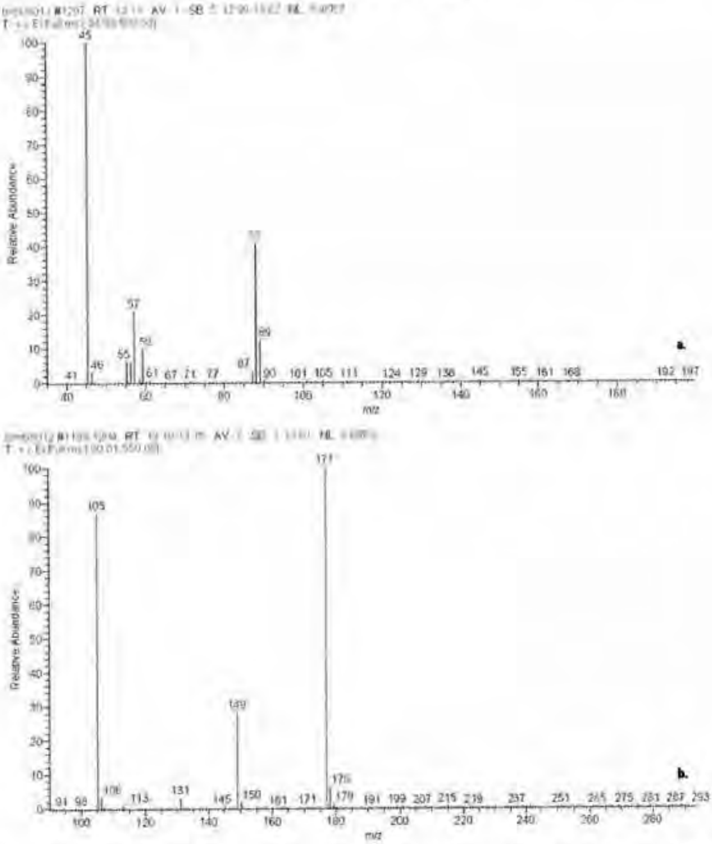

Figure 6.14: Mass spectra of the substituted ester of 2-substituted-propanoic acid obtained by a. electron impact and b. chemical ionisation.

Table 6.14: Summary of the 10 most important components of the respective bio-oils, obtained by flash (co-) pyrolysis of willow, PLA and 10:1, 3:1, 1:1 and 1:2 willow/PLA with the pyrolysis reactor, analysed by GC/MS.

	Willow	%
1	acetic acid	8.14
2	2,6-dimethoxy-4-(1-propenyl)-phenol	7.62
3	2,6-dimethoxyphenol	4.53
4	1-(2,6-dihydroxy-4-methoxyphenyl)-ethanone	4.60
5	3-furaldehyde	2.89
6	1,2,4-trimethoxybenzene	2.89
7	1-hydroxy-2-propanone	2.64
8	4-hydroxy-3,5-dimethoxy-benzaldehyde	2.21
9	phenol	2.10
10	1,2-benzenediol	2.02

	Willow/PLA 10:1	%
1	acetic acid	9.83
2	2,6-dimethoxy-4-(1-propenyl)-phenol	6.69
3	2,6-dimethoxyphenol	4.69
4	3-furaldehyde	3.26
5	1,2,4-trimethoxybenzene	3.09
6	1-hydroxy-2-propanone	2.58
7	1-(2,6-dihydroxy-4-methoxyphenyl)-ethanone	2.28
8	2-hydroxy-3-methyl-2-cyclopenten-1-one	2.22
9	1,2-benzenediol	2.14
10	phenol	2.12

	Willow/PLA 3:1	%
1	acetic acid	7.77
2	2,6-dimethoxy-4-(1-propenyl)-phenol	6.83
3	2,6-dimethoxyphenol	3.95
4	propanoic acid	3.13
5	2-propenoic acid	2.78
6	3-furaldehyde	2.71
7	1,2,4-trimethoxybenzene	2.51
8	2,4,5-trimethyl-1,3-dioxolane	2.25
9	DL-methyltartronic acid	2.12
10	1-hydroxy-2-propanone	2.08

	Willow/PLA 1:1	%
1	acetic acid	6.50
2	2,4,5-trimethyl-1,3-dioxolane	5.45
3	2,6-dimethoxy-4-(1-propenyl)-phenol	5.45
4	DL-methyltartronic acid	4.75
5	2-propenoic acid	4.73
6	propanoic acid	4.31
7	paraldehyde	3.26
8	2,6-dimethoxyphenol	2.94
9	3-furaldehyde	1.97
10	*m/z* 45,56,100,128,200,272	1.82

	Willow/PLA 1:2	%
1	2-propenoic acid	9.92
2	acetic acid	8.40
3	2,4,5-trimethyl-1,3-dioxolane	7.95
4	DL-methyltartronic acid	6.11
5	propanoic acid	4.93
6	substituted ester of 2-substituted-propanoic acid	4.64
7	paraldehyde	4.16
8	2,6-dimethoxy-4-(1-propenyl)-phenol	3.48
9	lactide	2.89
10	*m/z* 45,56,100,128,200,272	2.45

	PLA	%
1	paraldehyde	23.25
2	substituted ester of 2-substituted-propanoic acid	17.00
3	2-propenoic acid	5.32
4	2,4,5-trimethyl-1,3-dioxolane	4.69
5	lactide	3.73
6	propanoic acid	3.40
7	2-methyl-pentanedioic acid, monomethylester	3.07
8	acetic acid	2.69
9	*m/z* 45,56,100,128,200,272	2.21
10	pentanedioic acid, monomethyl ester	0.88

The formation of 2-propenoic acid, propanoic acid and 2,4,5-trimethyl-dioxolane, on the contrary, is promoted during flash co-pyrolysis. Two to three times more 2-propenoic acid is obtained by flash co-pyrolysis, see Table 6.15 and Figure 6.15. DL-methyltartronic acid, of which only a negligible fraction is detected in PLA bio-oil and not at all for willow bio-oil, is additionally observed to be synergetically produced for the willow/PLA blends (see Table 6.14 and Figure 6.15). Acids take an important share of the bio-oil composition of the blends as compared to pure willow and pure PLA and are thus synergetically produced during flash co-pyrolysis (Table 6.15). New components are, however, not detected.

Table 6.15: Summary of the actual and linear amount of 2-propenoic acid and all acids in the Top 10 of most important components present in the bio-oil and the observed synergy for PLA. (*The references are in italic*)

	2-propenoic acid (%)			Acids in 'Top 10' (%)		
Bio-oil	Actual	Linear	Synergy	Actual	Linear	Synergy
Willow	-	-	-	*8.14*	*8.14*	-
Willow/PLA 10:1	1.34	0.46	+ 190.60	9.83	8.42	+ 16.68
Willow/PLA 3:1	2.78	1.31	+ 112.41	15.80	8.94	+ 76.65
Willow/PLA 1:1	4.73	2.56	+ 84.54	20.29	9.72	+ 108.83
Willow/PLA 1:2	9.92	3.48	+ 185.39	29.36	10.28	+ 185.64
PLA	*5.32*	*5.32*	-	*11.41*	*11.41*	-

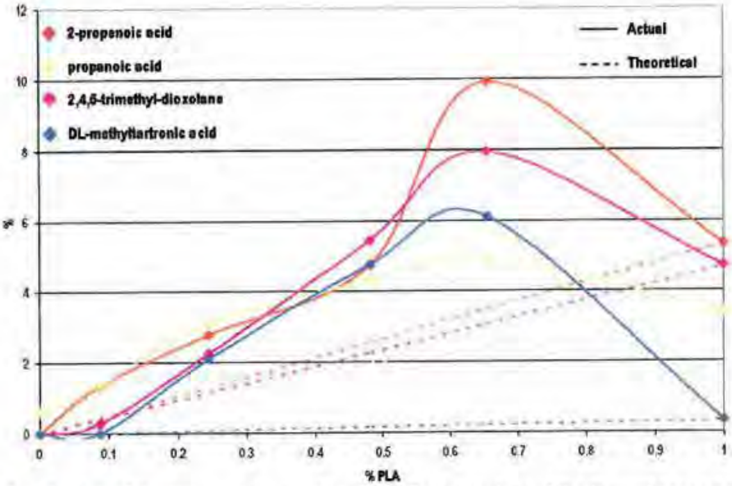

Figure 6.15: Visualisation of the synergy observed by GC/MS: comparison of the theoretical and actual amount of 2-propenoic acid, propanoic acid, 2,4,5-trimethyl-dioxolane and DL-methyltartronic acid in function of the w/w-ratio applied.

6.3.2.4. Py-GC/MS versus GC/MS

By comparing the 10 most important components of the pyrolytic gases (condensable and noncondensable) obtained by Py-GC/MS and of the bio-oil, obtained from the reactor experiments and analysed by GC/MS, (Table 6.13 and Table 6.14, respectively) additional information can be extracted:

- First and for all, the amount of lactide, which is the cyclic dimer of lactic acid, and the other (higher) cyclic oligomers are drastically decreased in the bio-oil.
- Additionally, it can be noted that GC/MS only detects cyclic oligomers inside the bio-oils, while Py-GC/MS indicates both cyclic and acyclic oligomers for the (condensable and noncondensable) pyrolytic gases.
- Paraldehyde on the other hand is not detected by Py-GC/MS, nevertheless, it is an important component of the bio-oils.
- As compared to Py-GC/MS, acids in general seem to increase heavily in their relative importance in the bio-oil (GC/MS). Some of these acids, such as 2-propenoic acid, behave synergetically in case of GC/MS, while more or less additive or linear behaviour is observed for Py-GC/MS.
- It should also be noted that during Py-GC/MS the influence of co-pyrolysis is observed to be instantly significant with lactide becoming the most important component of the pyrolytic gases of willow/PLA 10:1. Such an instant effect is, however, not observed for the reactor experiment of willow/PLA 10:1 as is indicated by GC/MS of the respective bio-oil.
- Additionally, some important components (paraldehyde, the substituted ester of 2-substituted-propanoic acid and DL-methyltartronic acid) inside the bio-oil are not detected by Py-GC/MS, indicating that these are formed due to different reaction circumstances, such as longer residence time and thus increased secondary cracking during and/or a difference in heat transfer medium (Py-GC/MS: none, reactor: sand) for the flash co-pyrolysis with the pyrolysis reactor.

The components identified by Py-GC/MS and GC/MS can also be classified into four general classes based on the oxidation number (reactivity) of the respective functionalities, as is shown in Table 6.16. A fifth class containing the peaks representing the oligomers of lactic acid is added. In case of Py-GC/MS, the quantitative response of most functionalities behave more or less linearly. The amount of phenols, alcohols and ethers might slightly be decreased, while that of acids, ketones and aldehydes is increased for the willow/PLA blends. Only the production of esters is obviously promoted during Py-GC/MS of the blends. Additionally, the amount of oligomers is increased, especially when only a small amount of PLA is added to the blend.

Table 6.16: Classification of Py-GC/MS and GC/MS results, obtained from PLA, according to the oxidation number or reactivity.

Py-GC/MS

Class	Functionality	Willow	Willow/PLA 10:1	Willow/PLA 3:1	Willow/PLA 1:1	Willow/PLA 1:2	PLA
0	Alkene	-	-	-	0.02	-	-
	Aromatic	0.32	0.22	0.2	0.04	0.05	-
1	Ether	3.69	2.08	2.35	2.64	3.46	4.66
	Alcohol	8.28	5.44	4.14	3.35	2.82	0.8
	Phenol	24.25	17.42	13.26	10.99	6.35	0.26
2	Aldehyde	7.84	7.58	9.49	8.72	8.29	6.65
	Keton	14.9	15.11	15.48	13.57	12.45	8.09
3	Carboxylic acid	6.73	10.78	11.89	11.79	13.6	16.41
	Ester	8.3	9.92	15.95	18.05	20.63	18.63
-	Oligomers	-	11.51	16.91	20.46	27.27	36.03
	Total	74.31	80.06	89.67	89.63	94.92	91.53

GC/MS

Class	Functionality	Willow	Willow/PLA 10:1	Willow/PLA 3:1	Willow/PLA 1:1	Willow/PLA 1:2	PLA
0	Alkene	-	-	-	-	-	-
	Aromatic	-	0.05	0.05	0.06	-	-
1	Ether	4.18	3.91	6.41	12.35	14.60	29.00
	Alcohol	1.35	1.01	1.05	0.70	0.69	0.03
	Phenol	25.56	24.64	21.88	15.92	8.81	-
2	Aldehyde	8.28	8.56	8.69	5.31	2.09	-
	Keton	17.99	16.28	16.35	11.75	11.80	1.47
3	Carboxylic acid	9.70	14.69	19.36	21.94	30.62	14.25
	Ester	2.00	3.50	4.30	4.57	9.40	27.38
-	Oligomers	-	-	1.05	3.60	6.63	6.08
	Total	69.05	72.64	79.14	76.21	84.64	78.21

In case of the reactor experiments and the corresponding GC/MS analysis of the respective bio-oils, other observations can be made. Here, the amount of esters and ethers are inhibited, while that of acids and ketones are synergetically increased during co-pyrolysis of willow/PLA blends. Seemingly, esters and ethers are consumed by the previously observed synergetic interactions between willow and PLA during flash co-pyrolysis to produce acids and ketones.

By direct comparison of the Py-GC/MS and the GC/MS results, it is observed that the amount of carboxylic acids and ethers in the bio-oil (condensables) is higher compared to the pyrolytic gases (condensable and noncondensable). The amount of alcohols in the bio-oil, on the contrary, seem to be decreased as compared to the pyrolytic gases. This is also observed for the oligomers of lactic acid, where the amount of oligomers inside the bio-oil is sharply reduced as compared to the pyrolytic gases. Both cyclic and acyclic oligomers are detected by Py-GC/MS and represent the most important class of components of the pyrolytic gases. For the bio-oils, only a relatively small amount of cyclic oligomers is detected. The amount of ketones and aldehydes is more or less comparable for Py-GC/MS and GC/MS. A difference in the amount of aldehydes slowly arises as the PLA fraction increases. Finally, it can be observed that the amount of esters are slightly but synergetically produced in the pyrolytic gases of the blends. Nevertheless, the amount of esters in the bio-oil of the blends is synergetically decreased.

6.3.3. Discussion of the observed synergy - PLA

In Chapter 5, a synergetic decrease in the amount of pyrolytic water (-30%) together with a synergetic increase in bio-oil yield (+22%) and energy recuperation (+21%) is observed [2]. Here, Py-GC/MS and statistical data processing confirm the occurrence of synergetic interactions between willow and PLA during analytical flash co-pyrolysis. It is concluded that the observed synergy occurs when co-pyrolysis is applied and that the heating rate is not a limiting factor. The synergy, however, appears to be the most pronounced when flash pyrolytic circumstances are guaranteed.

Py-GC/MS indicates that the amount of oligomers, in general, increases synergetically for the willow/PLA blends as compared to willow and PLA separately. This observation is the most pronounced when only small amounts of PLA are added to the blend. The increase of oligomers can be interpreted as an increase in the ratio of "high molecular weight" pyrolytic gases, which can be the result of a lower degree of pyrolytic cracking of the willow/PLA blends. Additionally, it is observed that the amount of oligomers of lactic acid, which are relatively long chain esters, is sharply reduced when the bio-oil, obtained from the reactor experiments, is under consideration. This can be explained by increased secondary cracking inside the pyrolysis reactor as compared to the analytical experimental set-up of Py-GC/MS. The increased secondary cracking is primarily the result of longer residence times of the pyrolytic gases at increased temperature inside the pyrolysis reactor. The difference in heat transfer medium can be an additional cause. During the flash pyrolysis of PLA with the pyrolysis reactor, the secondary cracking of the oligomers seems to result in an increased amount of smaller esters. Interestingly, these esters are progressively transformed into carboxylic acids during flash co-pyrolysis of willow/PLA blends. As observed for PHB, it is concluded that PLA and its intermediates, obtained via *cis*-elimination, are more sensitive to these secondary reactions as compared to willow.

6.4. Conclusion

Even though the slow co-pyrolysis of willow/PHB blends did not give straightforward indications towards the occurrence of synergetic interactions, an obvious synergy is observed when flash co-pyrolysis is applied. In case of PLA, synergetic interactions are always observed, independent of the heating rate applied. The synergetic interactions occur immediately and extensively when 'co-pyrolysis' is executed even when the respective blends only contain minor fractions of one of the biopolymers.

Statistical data processing of the Py-GC/MS chromatograms results in less pronounced significance for PLA as compared to PHB. This observation is the most pronounced when the areas in a chromatogram are considered. An explanation of this difference can be the particle size of the respective biopolymers which causes differences in the homogeneity and reproducibility of the blends, especially for small sample sizes as required for Py-GC/MS. However, the linear and complex interaction of willow and both biopolymers is proven.

Py-GC/MS, which focuses on the condensable and noncondensable pyrolytic gases, indicates that the pyrolytic gases of the willow/PHB and willow/PLA blends result in a synergetically increased amount of oligomers of crotonic acid and lactic acid, respectively, which are both long chain esters. This indicates that the ratio of "high molecular weight" pyrolytic gases is significantly increased, which is the result of a lower degree of pyrolytic cracking of the blends.

On the other hand, GC/MS, which focuses on the bio-oil and crystals (condensable fraction), shows that the amount of oligomers is drastically decreased, while the amount of acids is synergetically increased in the bio-oil (condensable fraction). Flash co-pyrolysis with the pyrolysis reactor thus induces much more secondary reactions. The increased secondary reactions is primarily the result of longer residence times of the pyrolytic gases at increased temperature inside the pyrolysis reactor.

The difference in heat transfer medium can be an additional cause. Moreover, PHB and PLA are deemed to be more sensitive towards these secondary reactions as compared to willow. The formation of more reactive intermediates originating from the *cis*-elimination of PHB and PLA, respectively, might be the reason for their increased sensitivity. The fact that PHB decomposes entirely according to the *cis*-elimination mechanism, while PLA shows a more complex degradation mechanism and only partly decomposes according to *cis*-elimination explains the observation that willow/PHB blends result in a higher synergetic decrease in the amount of pyrolytic water as compared to similar willow/PLA blends.

It should be noted that the amount of esters in the bio-oil obtained by flash co-pyrolysis of willow and PHB with the pyrolysis reactor increase synergetically as compared to the bio-oils obtained by the flash pyrolysis of pure willow and pure PHB. However, esters are seemingly consumed by the observed synergetic interactions between willow and PLA resulting in a synergetic decrease of esters in the respective bio-oil of the blends. Additionally, the flash co-pyrolysis of willow and PHB results in an increased yield of easily separable chemicals with added value. Crotonic acid precipitates as crystals once a sufficient amount of PHB is added to the blend. GPC and FT-IR indicate that crotonic acid shows to have a maximum solubility degree within bio-oil. Higher amounts of PHB would result in the production of such easily separable chemicals, while lower amounts result in a one-phase bio-oil.

Initially it was intended to reduce the amount of pyrolytic water by initiating the hydrolysis of the ester bonds of the biopolymer. The pyrolytic water obtained by the flash pyrolysis of biomass would then be consumed during the ester degradation and result in the formation of carboxylic acids and alcohols. However, out of the experimental set-up it can be concluded that water is not consumed during flash co-pyrolysis, e.g. no increase of alcohols is observed. Rather, flash co-pyrolysis results in interactions that inhibit the formation of such pyrolytic water.

It is therefore proposed that the initial degree of pyrolytic cracking is reduced during flash co-pyrolysis of willow/PHB and willow/PLA blends. This is offset by a more pronounced secondary cracking induced by the pyrolysis reactor. However, the secondary reactions of willow and PHB and of willow and PLA, respectively, are in competition. Due to the fact that PHB, PLA and their respective intermediates are more sensitive to secondary cracking, the secondary cracking of the willow fraction is hindered and by this the elimination of pyrolytic water is reduced.

6.5. References

[1] Cornelissen T, Jans M, Yperman J, Reggers G, Schreurs S, Carleer R. Flash co-pyrolysis of biomass with polyhydroxybutyrate: Part 1. Influence on bio-oil yield, water content, heating value and the production of chemicals. Fuel 2008; 87:2523-32.

[2] Cornelissen T, Yperman J, Reggers G, Schreurs S, Carleer R. Flash co-pyrolysis of biomass with polylactic acid. Part 1: Influence on bio-oil yield and heating value. Fuel 2008; 87:1031-41.

[3] Laird NM, Ware JH. Random effects models for longitudinal data. Biometrics 1982; 38:963-74.

[4] Verbeke G, Molenberghs G. Linear Mixed Models for Longitudinal Data. Springer 2000; 1-120.

[5] Kenward MG, Roger JH. Small sample inference for fixed effects from restricted maximum likelihood. Biometrics 1997; 53:983-97.

[6] Gonzalez A, Irusta L, Fernandez-Berridi MJ, Iriarte M, Iruin JJ. Application of pyrolysis/gas chromatography/Fourier transform infrared spectroscopy and TGA techniques in the study of thermal degradation of poly (3-hydroxybutyrate). Polym. Degrad. Stabil. 2005; 87:347-54.

[7] Kopinke FD, Remmler M, Mackenzie K. Thermal decomposition of biodegradable polyesters .1. Poly(beta-hydroxybutyric acid). Polym. Degrad. Stabil. 1996; 52:25-38.

[8] Kopinke FD, Mackenzie K. Mechanistic aspects of the thermal degradation of poly(lactic acid) and poly(beta-hydroxybutyric acid). J. Anal. Appl. Pyrolysis 1997; 40-1:43-53.

[9] Aoyagi Y, Yamashita K, Doi Y. Thermal degradation of poly (R)-3-hydroxybutyrate , poly epsilon-caprolactone , and poly (S)-lactide. Polym. Degrad. Stabil. 2002; 76:53-9.

[10] Morikawa H, Marchessault RH. Pyrolysis of bacterial alkanoates. Can. J. Chem. 1981; 59:2306-13.

[11] McNeill IC, Leiper HA. Degradation Studies of Some Polyesters and Polycarbonates. 1. Polylactide - General Features of the Degradation Under Programmed Heating Conditions. Polym. Degrad. Stabil. 1985; 11:267-85.

[12] McNeill IC, Leiper HA. Degradation Studies of Some Polyesters and Polycarbonates .2. Polylactide - Degradation under Isothermal Conditions, Thermal-Degradation Mechanism and Photolysis of the Polymer. Polym. Degrad. Stabil. 1985; 11:309-26.

[13] Kopinke FD, Remmler M, Mackenzie K, Moder M, Wachsen O. Thermal decomposition of biodegradable polyesters .2. Poly(lactic acid). Polym. Degrad. Stabil. 1996; 53:329-42.

[14] Westphal C, Perrot C, Karlsson S. Py-GC/MS as a means to predict degree of degradation by giving microstructural changes modelled on LDPE and PLA. Polym. Degrad. Stabil. 2001; 73:281-7.

[15] Fan Y, Nishida H, Hoshihara S, Shirai Y, Tokiwa Y, Endo T. Pyrolysis kinetics of poly(-lactide) with carboxyl and calcium salt end structures. 2003; 79:547-62.

[16] Fan Y, Nishida H, Shirai Y, Endo T. Racemization on thermal degradation of poly(-lactide) with calcium salt end structure. 2003; 80:503-11.

[17] Fan Y, Nishida H, Shirai Y, Endo T. Thermal stability of poly (-lactide): influence of end protection by acetyl group. 2004; 84:143-9.

[18] Mori T, Nishida H, Shirai Y, Endo T. Effects of chain end structures on pyrolysis of poly(-lactic acid) containing tin atoms. 2004; 84:243-51.

[19] Fan Y, Nishida H, Shirai Y, Tokiwa Y, Endo T. Thermal degradation behaviour of poly(lactic acid) stereocomplex. 2004; 86:197-208.

[20] Fan Y, Nishida H, Mori T, Shirai Y, Endo T. Thermal degradation of poly(-lactide): effect of alkali earth metal oxides for selective ,-lactide formation. 2004; 45:1197-205.

[21] Khabbaz F, Karlsson S, Albertsson A-C. PY-GC/MS an effective technique to characterizing of degradation mechanism of poly (L-lactide) in the different environment. Journal of Applied Polymer Science 2000; 78:2369-78.

Summary and general conclusions

Global warming, the Kyoto Protocol and the emission of greenhouse gases nowadays hold a prominent place in environmental pleadings worldwide. Many countries, both European and non-European, are facing the challenge to reduce their CO_2 emissions. Additionally, the world's energy supply has become limited due to the depletion of fossil fuels, which remain the most important energy sources consumed. Another important issue is restricting Europe's dependence on one particular energy source and thus to secure its energy supply. The development of new and renewable energy sources (including biofuels) is the key turning point. Materials in general should evolve to become sustainable too.

Biomass is such a renewable resource and is considered to be CO_2 neutral. The pyrolysis, a thermal degradation process, of biomass shows to be a promising route for the production of solid, liquid and gaseous products. These are of great interest since they provide possible alternative energy sources. Flash pyrolysis, in particular, is a process in which biomass is rapidly heated in the absence of oxygen/air (rather oxygen deficient). It is an advanced process which is carefully controlled to render high yields of liquid – bio-oil. A few commercially available pyrolysis reactors, especially designed for a high bio-oil yield, exist. For this research, a semi-continuous home-built pyrolysis reactor, that closely relates to the commercially available pyrolysis reactors, is constructed.

One major problem when dealing with bio-oil is its high water content. Increased amounts of water reduce its heating value and, moreover, significantly change its combustion characteristics. The water in bio-oil originates from the original moisture in the feedstock and is a product of the dehydration reactions occurring during pyrolysis. It therefore depends on the feedstock and the process conditions applied. Water contents of maximum 28% are often considered acceptable in order to allow bio-oil to be applied as a fuel. However, many biomass streams and pyrolysis reactors result in bio-oils that do not reach such "low" water contents. In this research, a water content of 36% is obtained when the flash pyrolysis of the reference biomass material (willow) is carried out with the semi-continuous home-built pyrolysis reactor. Therefore, the aim of this work is to reduce the water content of bio-oil. The flash co-pyrolysis of biomass and biopolymers is proposed as an attractive solution.

Seven different biopolymers are investigated: polylactic acid (PLA), corn starch, polyhydroxybutyrate (PHB), Biopearls, Eastar, Solanyl and potato starch. The flash pyrolysis of willow and the flash co-pyrolysis of the seven willow/biopolymer blends, all with a w/w ratio of 1:1, are evaluated against each other based on five predefined criteria (water-free bio-oil yield, water content, energy recuperation, char yield and total amount of readily separable chemicals), resulting in a multi-criteria decision making problem. With the aid of Decision Lab, a multi-criteria decision aid, an objective ranking of the different biopolymer options is obtained. It should be noted that even though biopolymers are generally regarded as renewable and/or biologically degradable, they are still considered as waste. The flash co-pyrolysis of biomass and biopolymers not only results in bio-oil with a reduced water content, but also in an increased pyrolysis yield, a reduction of the waste volume and a more attractive recycling route for biopolymers. This allows the flash co-pyrolysis of biomass and biopolymers to be defined as an interesting upgrading step for the pyrolysis of biomass waste streams, as a supplier of value-added materials and renewable energy and as an alternative waste treatment option. Simultaneously with this rather technical evaluation, the obtained results will also be evaluated on their economical capacity. This study fits within the framework of the institute of environmental research (CMK) and is still in progress.

Even though all 1:1 willow/biopolymer blends show improved pyrolysis characteristics at 723 K in comparison to pure willow, PHB, PLA, Biopearls and potato starch are evaluated by Decision Lab as the most performant options. These four biopolymers additionally cause a synergy during the co-pyrolysis with willow: a decrease in the amount of pyrolytic water higher than theoretically expected is observed. The production of easily separable chemicals, empowered by the highest energy recuperation, is the main reason for which the flash co-pyrolysis of willow and PHB is selected as the most performant option by Decision Lab. The second highest reduction in the amount of pyrolytic water (after 1:1 willow/PHB), the second highest water-free bio-oil yield and the production of the bio-oil with the lowest water content are the main reasons for which the flash co-pyrolysis of willow and PLA is selected by Decision Lab as the second most performant biopolymer option. Therefore, the flash co-pyrolysis of willow/PHB and willow/PLA blends is investigated more extensively. For PHB, 7:1, 3:1, 2:1 and 1:1 willow/PHB are evaluated against the references of pure willow and pure PHB, while for PLA, 10:1, 3:1, 1:1 and 1:2 willow/PLA blends are compared to pure willow and pure PLA.

First, an analytical study of the (co-)pyrolysis is carried out. TGA, TG/MS and TG/FT-IR, which all operate under slow pyrolytic circumstances, are the analytical techniques under consideration. The analytical slow co-pyrolysis does not indicate synergetic interactions between willow and PHB, while a synergy is observed for willow/PLA blends.

Accordingly, the flash (co-)pyrolysis is performed with the semi-continuous home-built pyrolysis reactor. Here, the pyrolysis yields and efficiencies are evaluated and a simplified energetic valorisation is calculated. A pronounced synergetic decrease in the amount of pyrolytic water and water content, and a synergetic increase in pyrolysis yield and in energy recuperation during the flash co-pyrolysis of willow/PHB and willow/PLA blends at 723 K with the pyrolysis reactor is achieved. The obtained synergy indicates that the (flash) co-pyrolysis of both blends results in unexpected (non-linear) observations. Besides bio-oil, the flash co-pyrolysis of willow/PHB blends with a high PHB fraction (w/w-ratio 2:1 and 1:1) results in the production of crystals of crotonic acid, which offer added value as a source of chemicals. If lower amounts of PHB are added, the co-pyrolysis produces a lower amount of crotonic acid, the entire fraction of which stays dissolved in the bio-oil for as long as the maximum solubility degree of crotonic acid in bio-oil is not reached.

For PHB, the flash co-pyrolysis of the 3:1 willow/PHB blend results in the highest bio-oil and water-free bio-oil yield (57.76 m% and 45.63 m%, respectively), while the 1:1 willow/PHB blend results in the highest synergetic decrease in the amount of pyrolytic water (minus 40%), the highest synergetic increase of the yield in condensables (plus 8%) and the highest synergetic increase in energy recuperation (plus 18%). For the flash co-pyrolysis of 1:1 willow/PHB, almost 30% of crystals are also produced.

In the case of willow/PLA blends, the flash co-pyrolysis of 1:2 willow/PLA results in the most pronounced synergy: a 22% increase in bio-oil yield, a 37% decrease in water content, and a 21% increase in energy recuperation.

Defining an absolute optimal w/w ratio for both willow/biopolymer blends is, however, less straightforward, because a few aspects need to be taken into consideration, such as the initial goal of the pyrolysis (the production of bio-oil and/or chemicals, required water content, pyrolytic efficiency, waste treatment), the available amount of biomass/biopolymers, ... The optimum w/w ratio of biomass/biopolymer is a compromise solution depending on the abovementioned aspects.

The synergy observed during the flash co-pyrolysis of willow/PHB and willow/PLA blends is further investigated in order to better comprehend the reaction circumstances and to propose an explanation for it. Therefore, the analytical Py-GC/MS technique, in combination with statistical data processing, pattern recognition and analysis (identification and quantification) of the condensable and noncondensable pyrolytic gases is performed on the input materials (pure willow, pure PHB, and the willow/PHB blends; and pure willow, pure PLA and the willow/PLA blends).

With the aid of Py-GC/MS and statistical analysis of the pyrolysis GC-chromatograms, it can be concluded that interactions do occur during the analytical flash co-pyrolysis of willow/PHB and willow/PLA blends, resulting in an altered gas composition (condensable and noncondensable). Interestingly, statistical data processing of the Py-GC/MS chromatograms shows a less pronounced significance for PLA as compared to PHB. This can be clarified by the particle size of the respective biopolymers which causes differences in the homogeneity and reproducibility of the blends, especially for small sample sizes as required for Py-GC/MS. Nonetheless, the linear (additive) and complex (synergetic) interaction of willow and both biopolymers is always proven. Precisely which interactions and where specifically these occur, cannot be determined, however. Further in-depth analysis is therefore required.

Pattern recognition of the GC-chromatograms and analysis of the condensable and noncondensable pyrolytic gases obtained by Py-GC/MS, indicate that the pyrolytic gases of the willow/PHB and willow/PLA blends entail a synergetically increased amount of oligomers of crotonic acid and lactic acid, respectively, which both are long chain esters. This indicates that the ratio of "high molecular weight" pyrolytic gases is significantly increased during co-pyrolysis, which is due to a lower degree of pyrolytic cracking of the blends.

Finally, the influence of the flash co-pyrolysis on the bio-oil composition, obtained from the reactor experiments, is investigated using complementary analytical techniques (GPC, FT-IR, HPLC and GC/MS). The results obtained for pure willow, pure PHB and pure PLA are considered reference values so as to evaluate the influence of the flash co-pyrolysis experiments on the bio-oil composition and to detect the occurrence of additional reactions. An obvious synergy is generally observed when flash co-pyrolysis is applied. The synergetic interactions occur immediately and extensively when co-pyrolysis is carried out, even when the respective blends only contain minor fractions of one of the biopolymers.

GC/MS, which focuses on the bio-oil and crystals (condensable fraction), shows that in the bio-oil (condensable fraction) the amount of oligomers is drastically decreased, while the amount of acids is synergetically increased compared to the pyrolytic gases obtained and analysed by Py-GC/MS. Flash co-pyrolysis with the pyrolysis reactor thus induces much more secondary reactions as compared to Py-GC/MS. The increased secondary reactions are primarily the result of longer residence times of the pyrolytic gases at an increased temperature inside the pyrolysis reactor. The difference in used heat transfer medium can be an additional cause. Additionally, PHB and PLA are more sensitive to these secondary reactions as compared to willow. The formation of more reactive intermediates originating from PHB and PLA causes their increased sensitivity.

Initially, it was intended to reduce the amount of pyrolytic water by initiating the hydrolysis of the ester bonds of the biopolymer. The pyrolytic water resulting from the flash pyrolysis of biomass would then be consumed during the ester degradation, which would result in the formation of carboxylic acids and alcohols. However, out of the experimental set-up it can be concluded that water is not consumed during flash co-pyrolysis, e.g. no increase of alcohols is observed. Rather, flash co-pyrolysis results in interactions that inhibit the formation of pyrolytic water.

It is therefore proposed that the initial degree of pyrolytic cracking is reduced during flash co-pyrolysis of willow/PHB and willow/PLA blends. This is partly offset by a more pronounced secondary cracking induced by the pyrolysis reactor. However, the secondary reactions of willow and PHB, and of willow and PLA, respectively, are in competition. Due to the fact that PHB, PLA and their respective intermediates are more sensitive to secondary cracking, the secondary cracking of the willow fraction is obstructed, reducing the elimination of pyrolytic water.

This reasoning also explains why a synergy for willow/PLA blends is observed during both slow and flash co-pyrolysis, while for willow/PHB blends a synergy is only detected during flash co-pyrolysis: the maximum degradation temperatures (T_{max}) of willow and PLA coincide (622 K and 630 K, respectively), while PHB (T_{max} = 545 K) is degraded almost entirely even before willow starts decomposing. Therefore, the intermediates of PHB are already removed prior to the decomposition of willow, preventing any competition between willow and PHB to undergo secondary reactions. During flash pyrolysis, the differences in T_{max} are circumvented, inducing simultaneous degradation and thereby invoking competition and allowing for synergetic interactions.

Future research should be focused towards the flash co-pyrolysis of alternative biomass waste streams and biopolymers or other relevant waste streams. The effect of temperature should also be thoroughly investigated: do the same synergetic interactions occur at reduced/increased temperature? A need towards the valorisation of all the pyrolytic fractions and subsequent upgrading of the bio-oil arises. Additionally, potential biomass pre-treatment steps should be assessed. All these experiments will contribute to the general need for predictive pyrolysis. Finally, the comparison of the semi-continuous home-built pyrolysis reactor and commercially available pyrolysis reactors is of primordial importance in order to extrapolate the findings of applied but fundamental research into real-life industrial processes.

Samenvatting en algemeen besluit

De opwarming van de aarde, het Kyoto Protocol en de uitstoot van broeikasgassen vormen wereldwijd de hoofdthema's van (milieugerelateerde) pleidooien en debatten. Vele landen, zowel Europese als niet-Europese, worden geconfronteerd met de uitdaging van de eeuw: het terugdringen van de wereldwijde CO_2-emissies binnen een redelijke tijdspanne. Bovendien wordt de wereldwijde energiebevoorrading geteisterd door de uitputting van de fossiele brandstoffen, die tot op heden de voornaamste energiebron uitmaken. Tenslotte is de Europese Unie, net als heel wat andere landen, in zeer grote mate afhankelijk van geïmporteerde energie. Voor de Europese Unie is het dan ook van uitermate groot belang om haar energieafhankelijkheid drastisch terug te schroeven en op die manier haar energievoorziening veilig te stellen. De ontwikkeling van nieuwe en vooral hernieuwbare energiebronnen, waaronder biobrandstoffen, speelt hierin een cruciale rol. Dit past eveneens in de filosofie van duurzame materialen en de evolutie naar duurzame productieprocessen.

Biomassa, een van de voornaamste en meest bekende hernieuwbare energiebronnen, wordt beschouwd als CO_2-neutraal. De pyrolyse, een thermisch degradatieproces, van biomassa is een veelbelovende piste voor de productie van vaste, vloeibare en gasvormige bioproducten. Deze producten zijn voornamelijk van belang als potentiële alternatieve energiebronnen. Flash, oftewel snelle, pyrolyse, in het bijzonder, is een procédé waarbij biomassa in de (quasi) afwezigheid van zuurstof/lucht zeer snel verwarmd wordt tot middelmatig hoge temperaturen met als voornaamste doel de efficiënte productie van een vloeistof: bio-olie. Er zijn momenteel enkele pyrolysereactoren, die specifiek ontwikkeld zijn voor de productie van bio-olie, commercieel verkrijgbaar. Voor dit onderzoek is er een in de onderzoeksgroep ontworpen semi-continue pyrolysereactor ontwikkeld.

Een van de voornaamste problemen van bio-olie is het relatief hoge watergehalte. Verhoogde hoeveelheden water verlagen namelijk de verbrandingswaarde van bio-olie en hebben voornamelijk een negatieve invloed op de verbrandingskenmerken. Water in bio-olie is zowel het gevolg van het originele vochtgehalte aanwezig in de biomassa als van dehydratatiereacties die tijdens de pyrolyse optreden. Maximale watergehaltes van 28% worden vaak vooropgesteld, vooral wat betreft energetische toepassingen. Niettemin worden bio-oliën met beduidend hogere watergehaltes regelmatig gerapporteerd. Zo wordt ook in dit onderzoek vanuit de referentiebiomassa (wilg) een bio-olie bekomen met een watergehalte van 36%. Het doel van deze thesis is daarom toegespitst op de reductie van het watergehalte van bio-olie. De flash co-pyrolyse van biomassa en biopolymeren wordt beschouwd als een aantrekkelijke oplossing.

Zeven verschillende biopolymeren worden initieel onderzocht: polymelkzuur (PLA), maïszetmeel, polyhydroxybutyraat (PHB), Biopearls, Eastar, Solanyl en aardappelzetmeel. De flash pyrolyse van wilg en de flash co-pyrolyse van de zeven wilg/biopolymeermengsels, elk in een w/w ratio van 1:1, wordt op basis van vijf vooraf gedefinieerde criteria (opbrengst aan watervrije bio-olie, watergehalte, energierecuperatie, opbrengst aan char en totale opbrengst aan gemakkelijk te scheiden chemicaliën) ten opzichte van elkaar geëvalueerd en kan beschouwd worden als een typisch multi-criteria beslissingsprobleem. Met behulp van Decision Lab, een multi-criteria beslissingshulpmiddel, wordt een objectieve rangschikking van de verschillende biopolymeeropties gemaakt. Hierbij moet vermeld worden dat ondanks het feit dat biopolymeren beschouwd worden als hernieuwbaar en/of biodegradeerbaar, ze nog steeds als afval gezien worden. In het algemeen kan er besloten worden dat de flash co-pyrolyse van biomassa en biopolymeren bij 450°C niet alleen resulteert in bio-olie met een verlaagd watergehalte, maar ook in een verbeterde pyrolyseopbrengst, een daling van het afvalvolume en een aantrekkelijkere verwerking van biopolymeren. Hierdoor kan de flash co-pyrolyse van wilg en biopolymeren gedefinieerd worden als een interessante opwaardering voor de pyrolyse van biomassa-afvalstromen, als een bron van hernieuwbare energie en producten met toegevoegde waarde en als een alternatieve afvalverwerkingtechniek. PHB, PLA, Biopearls en aardappelzetmeel zijn de meest performante biopolymeeropties en resulteren ook in een synergetisch effect tijdens hun co-pyrolyse met wilg: een daling van de hoeveelheid pyrolytisch water, hoger dan theoretisch verwacht, wordt geobserveerd. Hiernaast worden de bekomen resultaten op hun economische draagkracht geëvalueerd. Deze lopende studie past in het kader van het Centrum voor Milieukunde (CMK).

De flash co-pyrolyses van wilg/PHB- en wilg/PLA-mengsels worden in dit proefschrift nader onderzocht. Voor PHB worden 7:1, 3:1, 2:1 en 1:1 wilg/PHB bestudeerd ten opzichte van de referentiematerialen puur wilg en puur PHB, terwijl voor PLA 10:1, 3:1, 1:1 en 1:2 wilg/PLA-mengsels vergeleken worden met puur wilg en puur PLA.

In een eerste benadering wordt er een chemisch-analytische studie van de (co-)pyrolyses uitgevoerd. TGA, TG/MS en TG/FT-IR worden via trage (co-)pyrolyse uitgevoerd op de verschillende uitgangsmaterialen. Voor wilg en PHB worden er geen synergetische interacties gedetecteerd, terwijl er een beperkte synergie vastgesteld wordt tijdens de trage co-pyrolyse van wilg en PLA.

Vervolgens wordt de flash co-pyrolyse uitgevoerd met behulp van de semi-continue pyrolysereactor, waarbij de pyrolyseopbrengsten en -efficiënties geëvalueerd worden en een gesimplificeerde energetische valorisatie berekend wordt. Beide mengsels (wilg/PHB en wilg/PLA) geven aanleiding tot synergetisch verbeterde pyrolyse-efficiënties: een uitgesproken synergetische daling van de hoeveelheid pyrolytisch water en het watergehalte, in combinatie met een synergetische stijging van de pyrolyse-opbrengst en energierecuperatie tijdens de flash co-pyrolyse van de twee wilg/biopolymeermengsels met de pyrolysereactor worden bekomen bij 450°C. De resulterende synergie wijst er op dat de (flash)(co-)pyrolyse van deze mengsels aanleiding geeft tot onverwachte, niet-lineaire waarnemingen. De flash co-pyrolyse van wilg/PHB-mengsels met een grote PHB-fractie (w/w ratio 2:1 en 1:1) resulteert niet alleen in bio-olie, maar ook in de vorming van kristallen van crotonzuur, een product met toegevoegde waarde.

Om de reactieomstandigheden beter te doorgronden, is de flash co-pyrolyse van beide blends verder onderzocht door middel van Py-GC/MS. Deze analytische techniek wordt in combinatie met statistische dataverwerking, patroonherkenning en analyse (identificatie en quantificatie) van de condenseerbare en niet-condenseerbare pyrolytische gassen uitgevoerd op de verschillende uitgangsmaterialen.

Met behulp van Py-GC/MS en statistische dataverwerking van de bekomen GC-chromatogrammen kan er geconcludeerd worden dat er effectief interacties plaatsgrijpen tussen respectievelijk wilg en PHB en tussen wilg en PLA tijdens de analytische flash co-pyrolyse. Deze interacties resulteren in een gewijzigde gassamenstelling (zowel condenseerbare als niet-condenseerbare fractie). Uitgebreidere informatie over de aard van de interacties of de gewijzigde gassamenstelling blijft uit en vereist een aanvullende gegevensverwerking.

Deze aanvullende verwerking van de Py-GC/MS data toont aan dat de condenseerbare en niet-condenseerbare pyrolytische gassen van de wilg/PHB- en wilg/PLA-mengsels een synergetische stijging van de hoeveelheid oligomeren van respectievelijk crotonzuur en melkzuur vertonen. Hieruit kan besloten worden dat het aandeel van "hoogmoleculaire" pyrolytische gassen significant stijgt. Dit kan geïnterpreteerd worden als een verlaagde graad van pyrolytisch kraken tijdens de co-pyrolyse van de mengsels.

De gecondenseerde fractie (bio-olie en eventueel kristallen), verkregen via de reactorexperimenten, wordt eveneens geanalyseerd met behulp van complementaire instrumentele analysetechnieken (GPC, FT-IR, HPLC en GC/MS), voornamelijk om de invloed van de flash co-pyrolyse op de bio-olie samenstelling te onderzoeken en zo bijkomende reacties op te sporen. Algemeen manifesteert zich duidelijk een synergie tussen wilg en beide biopolymeren. Bovendien worden de synergetische interacties onmiddellijk en zeer uitgesproken waargenomen, zelfs als de respectievelijke mengsels slechts een beperkte fractie van biopolymeren bevatten.

In tegenstelling tot Py-GC/MS wordt er in de gecondenseerde fractie een sterke daling van de hoeveelheid oligomeren gedetecteerd via GC/MS, terwijl de hoeveelheid aan zuren synergetisch toeneemt. Flash co-pyrolyse met behulp van de semi-continue pyrolysereactor resulteert met andere woorden in een verhoogd aandeel van secundaire reacties. Dit verhoogd aandeel is voornamelijk te wijten aan de langere verblijftijden van de pyrolytische gassen bij een verhoogde temperatuur in de pyrolysereactor. Ook het verschil in warmteoverdrachtsmedium (Py-GC/MS: geen; reactor: zand) kan een deel van de oorzaak zijn. Daarnaast worden PHB en PLA beschouwd als zijnde gevoeliger voor zulke secundaire reacties in vergelijking met wilg. De vorming van meer reactieve tussenproducten afkomstig van PHB en PLA kan de voornaamste reden zijn voor deze hogere gevoeligheid.

Initieel was het de bedoeling om de hoeveelheid pyrolytisch water te reduceren door de hydrolyse van de esterverbindingen van de biopolymeren te promoten. Het pyrolytische water dat verkregen wordt uit de flash pyrolyse van biomassa zou dan aangewend worden om de esterverbindingen van de biopolymeren om te zetten in zuren en alcoholen. Uit de experimentele set-up blijkt nochtans dat er geen water verbruikt wordt tijdens de flash co-pyrolyse. Het lijkt er eerder op dat de flash co-pyrolyse bepaalde interacties inhibeert die instaan voor de vorming van pyrolytisch water. Dit is de reden waarom er voorgesteld wordt dat de initiële graad van pyrolytische kraking daalt tijdens de co-pyrolyse van wilg/PHB- en wilg/PLA-mengsels. Deze daling wordt deels tenietgedaan door een verhoogd aantal secundaire reacties tijdens de flash co-pyrolyse in de semi-continue pyrolysereactor. Het optreden van secundaire reacties tussen respectievelijk wilg en PHB en tussen wilg en PLA is in competitie. Omwille van het feit dat PHB en PLA, en vooral hun respectievelijke tussenproducten, gevoeliger zijn voor secundaire kraking, wordt de secundaire kraking van wilg geremd, waardoor de vorming van pyrolytisch water afneemt. Deze redenering verklaart op zijn beurt waarom er in het geval van PLA zowel tijdens trage als flash co-pyrolyse synergetische reacties geobserveerd worden, terwijl voor PHB er enkel synergie gedetecteerd wordt tijdens flash co-pyrolyse.

Ten slotte werd er in deze uitgebreide studie duidelijk dat de optimale w/w ratio van biomassa/biopolymeer een compromis is tussen verschillende aspecten, zoals het doel van de pyrolyse (de productie van bio-olie of chemicaliën, het gewenste watergehalte, pyrolyse-efficiëntie, afvalbehandeling) en de beschikbare hoeveelheid biomassa en biopolymeren.

Verder onderzoek naar de co-pyrolyse van verscheidene afvalstromen en het effect van de pyrolysetemperatuur op de mogelijke interacties is noodzakelijk, evenals de valorisatie van de verschillende pyrolytische fracties en de mogelijkheid tot de opwaardering van bio-olie. De koppeling van de semi-continue pyrolysereactor met commerciële reactoren is van cruciaal belang om extrapolaties tussen fundamenteel onderzoek en industriële processen mogelijk te maken.

Publications and conference participation

Publications

First author

Flash co-pyrolysis of biomass with polylactic acid. Part 1: Influence on bio-oil yield and heating value; T. Cornelissen, J. Yperman, G. Reggers, S. Schreurs, R. Carleer; Fuel (87) 2008, p. 1031 – 1041.

Flash co-pyrolysis of biomass with polyhydroxybutyrate:. Part 1. Influence on bio-oil yield, water content, heating value and the production of chemicals; T. Cornelissen, M. Jans, J. Yperman, G. Reggers, S. Schreurs, R. Carleer; Fuel (87) 2008, p. 2523 – 2532.

Flash co-pyrolysis of biomass: The influence of biopolymers; T. Cornelissen, M. Jans, T. Kuppens, T. Thewys, G.K. Janssens, H. Pastijn, J. Yperman, G. Reggers, S. Schreurs, R. Carleer; Journal of Analytical and Applied Pyrolysis (under revision).

Flash co-pyrolysis of biomass with polyhydroxybutyrate: Part 2. Statistical and comparative investigation of the observed synergy; T. Cornelissen, G. Molenberghs, M. Jans, J. Yperman, S. Schreurs, R. Carleer; Fuel (under revision).

Flash co-pyrolysis of biomass with polylactic acid: Part 2. Statistical and comparative investigation of the observed synergy; T. Cornelissen, G. Molenberghs, J. Yperman, S. Schreurs, R. Carleer; Fuel (submitted).

Co-author

Study of the potential valorisation of heavy metal contaminated biomass via phytoremediation by flash pyrolysis: Part II. Characterisation of the liquid and gaseous fraction as a function of the temperature; C. Lievens, J. Yperman, T. Cornelissen, R. Carleer; Fuel (87) 2008, p. 1906 - 1916.

Fast pyrolysis of heavy metal contaminated willow: influence of the plant part; C. Lievens, R. Carleer, T. Cornelissen, J. Yperman; Fuel (under revision).

Conference participation

Oral

Eco-tech2007, International conference on technologies for waste and wastewater treatment, energy from waste, remediation of contaminated sites and emissions related to climate, 2007, Kalmar – Sweden; Flash co-pyrolysis of biomass with biopolymers: a preliminary evaluation.

Pyrolysis2008, 18th International symposium on analytical and applied pyrolysis, 2008, Lanzarote – Spain; Flash co-pyrolysis of biomass: The influence of biopolymers.

Poster

ICCS&T2007, International conference on coal science and technology, Nottingham – United Kingdom; Flash co-pyrolysis of biomass with plastic waste.

International conference on bioremediation of soil and groundwater, 2004, Cracow – Poland; Characterisation and optimisation of the thermal treatment of biomass.

Predoctoral assignment

Thesis

Thermische behandeling van biomassa: Analysestrategie voor de karakterisatie en valorisatie van bio-oliën, 2005.

Courses

Milieu-economie, prof. S. Proost, KUL.
Industry and environment, prof. C. Vandecasteele, KUL.
Energy management, prof. W. D'Haeseleer, L. Helsen, KUL.
Safety and environmental aspects energy engineering, prof. E. Van den Bulck, F. Verplaetsen, KUL.
Gevorderde methoden van de analytische chemie, prof. K. Binnemans, KUL.